Copyright © National Academy of Forensic Engineers (NAFE). Redistribution or resale is illegal.
Originally published in the Journal of the NAFE volume indicated below.

Journal of the National Academy of Forensic Engineers®

http://www.nafe.org
ISSN: 2379-3252
DOI: 10.51501/jotnafe.v37i1

Vol. 37 No. 1 December 2020

National Academy of Forensic Engineers®

Journal Staff

Technical Review Committee Chair:

Martin Gordon, PE, DFE

Managing Editor:

Ellen Parson

Technical Review Process

The Technical Review Committee Chair chooses the reviewers for each Journal manuscript from amongst the members and affiliates of the NAFE according to their competence and the subject of the paper, and then arbitrates (as necessary) during the review process. External reviewers may also be utilized when necessary. This confidential process concludes with the acceptance of the finished paper for publication or its rejection/withdrawal. The name(s) of authors are included with their published works. However, unpublished drafts together with the names and comments of reviewers are entirely confidential during the review process and are excised upon publication of the finished paper.

National Academy of Forensic Engineers®

Board of Directors

President
James Petersen, PE
Fellow

President-Elect
Liberty Janson, PE
Senior Member

Senior Vice President
Samuel Sudler, PE
Senior Member

Vice President
Bart Kemper, PE
Senior Member

Treasurer
Bruce Wiers, PE
Senior Member

Secretary
Richard Rice, PE
Fellow

Past Presidents
John Certuse, PE
Fellow

Martin Gordon, PE
Fellow

Michael Leshner, PE
Fellow

Directors at Large
Joseph Leane, PE
Fellow

Daniel Couture, PEng
Member

Executive Director
Arthur E. Schwartz, Esq.

Journal of the National Academy of Forensic Engineers®

Editorial Board

Editor-in-Chief
Martin Gordon, PE, DFE
Fellow

Managing Editor
Ellen Parson
Affiliate

Senior Associate Editor
James Green, PE, DFE
Life Member

Senior Associate Editor
Joseph Leane, PE, DFE
Fellow

Senior Associate Editor
William Lee, PE, DFE
Senior Member

Senior Associate Editor
John Schwartzberg, PE, DFE
Fellow

Associate Editor
Paul Carr, PhD, PE, DFE
Senior Member

Associate Editor
David Icove, PhD, PE, DFE
Fellow

Associate Editor
Bart Kemper, PE, DFE
Senior Member

Associate Editor
Robert Peruzzi, PhD, PE, DFE
Member

Associate Editor
Steven Pietropaolo, PE, DFE
Senior Member

Associate Editor
Michael Plick, PE, DFE
Fellow

Associate Editor
Richard Rice, PE, DFE
Fellow

Associate Editor
Paul Stephens, PE, DFE
Fellow

Associate Editor
Paul Swanson, PE, DFE
Life Member

OJS Technical Editor
Mitchell Maifeld, PE, DFE
Member

Consulting Editor
Marilyn Dyrud, PhD

Submitting Proposed Papers to NAFE for Consideration

Please visit the Journal's author page at
http://journal.nafe.org/ojs/index.php/nafe/information/authors for submission details.

We are looking for forensic engineers who are interested in giving presentations on technical topics that will further the advancement and understanding of forensic engineering at one of the academy's biannual meetings and then developing those presentations into written manuscripts/papers, which will go through a single-blind peer review process before publication. Only papers presented at a NAFE regular technical seminar and have received oral critique at the seminar will be accepted for review and publication. We recommend that you review the About the Journal page at https://journal.nafe.org/ojs/nafe/about for the journal's section policies, as well as the Author Guidelines at https://journal.nafe.org/ojs/nafe/about/submissions listed on the Submissions page. Authors need to register with the journal prior to submitting or, if already registered, can simply log in and begin the process. The first step is for potential authors to submit a 100- to 150-word maximum abstract for consideration at an upcoming conference into the online journal management system.

Copies of the Journal

The Journal of the National Academy of Forensic Engineers® contains papers that have been accepted by NAFE. Members and Affiliates receive a PDF download of the Journal as part of their annual dues. All Journal papers may be individually downloaded from the NAFE website at http://journal.nafe.org. There is no charge to NAFE Members & Affiliates. A limited supply of Volume 33 and earlier hardcopy Journals (black & white) are available. The costs are as follows: $15.00 for NAFE Members and Affiliates; $30.00 for members of the NSPE not included in NAFE membership; $45.00 for all others. Requests should be sent to Mary Ann Cannon, NAFE, 1420 King St., Alexandria, VA 22314-2794.

Comments by Readers

Comments by readers are invited, and, if deemed appropriate, will be published. Send to: Ellen Parson, Journal Editor, 3780 SW Boulder Dr, Lee's Summit, MO 64082. Comments can also be sent via email to journal@nafe.org.

Material published in this Journal, including all interpretations and conclusions contained in papers, articles, and presentations, are those of the specific author or authors and do not necessarily represent the view of the National Academy of Forensic Engineers® (NAFE) or its members.

© 2020 National Academy of Forensic Engineers® (NAFE). ISSN: 2379-3252

Table of Contents

‡ Paper presented at the NAFE seminar held in January 2018 in Phoenix.

* Paper presented at the NAFE seminar held in July 2018 in Buffalo.

† Paper presented at the NAFE seminar held in July 2019 in Denver.

Table of Contents

† Paper presented at the NAFE seminar held in July 2019 in Denver.

§ Paper presented at the NAFE seminar held in January 2020 in San Diego.

Forensic Engineering Analysis of Projectile Thrown from Phantom Vehicle

By Richard M. Ziernicki, PhD, PE (NAFE 308F), William H. Pierce, PE (NAFE 846C), and Angelos G. Leiloglou, M Arch., (NAFE 956C)

Abstract

This paper presents a case study involving an 8-lb "projectile" piece of concrete thrown from a phantom vehicle into the windshield of a semi-tractor truck, subsequently striking the driver's (plaintiff's) head. A witness told the investigating officer that the phantom vehicle was a white-rear dump truck similar to the trucks he'd seen coming in and out of a construction entrance at a nearby park. However, no follow-up investigation was conducted by investigative officers. The lead author was retained by the plaintiff's attorney to follow up and investigate the witness' observation of the phantom white-rear dump truck in an attempt to identify the probable source of the concrete projectile, locate the phantom vehicle, reconstruct the incident, and determine the probable cause of the incident. Several forensic engineering techniques were used during the forensic engineering investigation, including evidence analysis, photography, high-definition scanning, photogrammetry, evaluation of the accident timeline, physical testing, case study analysis, projectile analysis, and application of the process of elimination methodology. Through the forensic engineering analysis, the probable source of the projectile concrete was identified, the white-rear dump truck and driver were identified, the accident was reconstructed, and the probable cause of the accident was determined.

Keywords

Phantom vehicle, photogrammetry, projectile analysis, high-definition scanning, point cloud, windshield damage, forensic engineering

Introduction

The plaintiff was driving a semi-tractor truck, hauling a load of various manufactured steel product on a flatbed trailer, and traveling southbound on a county road in a rural, rocky area. According to the police report, an 8-lb piece of concrete came off the load of an oncoming, phantom northbound white rear-dump truck, and unexpectedly went through the plaintiff's windshield, striking him in the head. The plaintiff lost control of the semi, and it drifted off the right side of the roadway, struck an electrical pole, and continued traveling to the southwest through an empty field prior to coming to rest. The chain of events, as depicted by the police report, is shown in **Figure 1**. The phantom white rear-dump truck did not stop after the collision.

There was one reported witness to the accident. The witness was initially standing by his shed, approximately 300 ft to the east of the county road. The witness described hearing a thumping sound from a phantom white rear-dump truck he saw traveling northbound on the county road.

After hearing the thumping sound and looking up at the phantom white rear-dump truck for two seconds, the witness continued walking into the shed. Shortly thereafter, lights in the shed went out, the witness looked out the window, and he saw the power pole falling. The witness stated that approximately seven to 10 seconds had elapsed from initially seeing the northbound phantom white rear-dump truck until the power went out. After witnessing the electrical pole falling through his shed window, the witness observed the plaintiff's truck traveling southwest into the field. He got into his truck, and drove to the plaintiff across the street.

When the witness opened the truck's driver-side door, the 8-lb piece of concrete (concrete projectile) that struck the plaintiff fell out of the truck. The witness told investigating officers that he had observed several white dump trucks going into and out of a construction entrance of a park approximately a half-mile to the south of the accident site.

Richard M. Ziernicki, PhD, PE, 7185 S. Tucson Way, Centennial, CO 80112, 303-925-1900, rziernicki@knottlab.com

The witness suggested to an investigating officer that there was similar concrete to the concrete projectile used on the construction entrance's vehicle tracking pad — and that the projectile may have been picked up by a white rear-dump truck's dual tires while leaving the construction site. However, the investigating officers ceased any further investigation to the origin of the concrete.

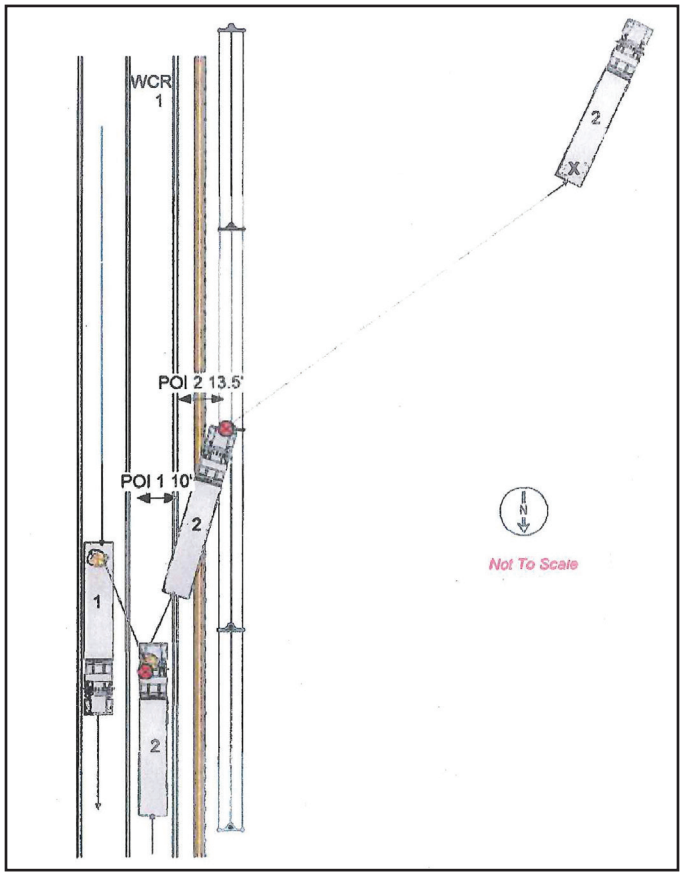

Figure 1
Police diagram of the accident (north facing down). Northbound vehicle one is the phantom semi, and southbound vehicle two is the plaintiff's semi.

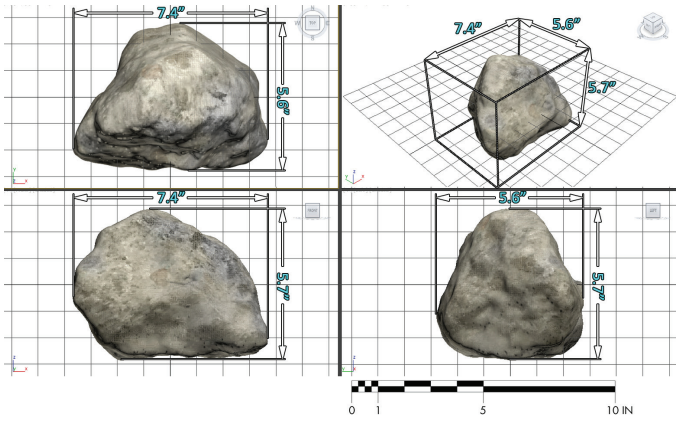

Figure 2
General envelope of the concrete projectile based on HD scans.

Suspected Truck Involved

The plaintiff's counsel identified that there was an active landscaping project at the park identified by the witness at the time of the incident. Through the discovery process, the plaintiff's counsel discovered that there were two white dump trucks traveling to and from the park, delivering loads of compost on the day of the incident. One of the dump trucks was a white side-dump truck; the other was a white rear-dump truck. The white rear-dump truck generally matched the witness' description of the truck heard making the thumping sound prior to the incident.

Engineering Analysis

The lead author was retained by the plaintiff's attorney to follow up and investigate the witness' observation of the phantom white rear-dump truck in an attempt to identify the probable source of the projectile, identify the phantom vehicle, reconstruct the incident, and determine the probable cause of the incident.

Concrete Projectile

The concrete projectile was documented using photography and high-definition (HD) 3D scanning. Six HD scans were taken around the entire surface of the concrete projectile. A virtual model of the concrete with textures was created with a high degree of engineering precision from the HD scans and photographs[1]. **Figure 2** shows the virtual model generated from the HD scans and the general envelope (or overall dimensions) of the concrete. The concrete was, at its widest extents, 7.4 in. by 5.6 in. by 5.7 in. and weighed approximately 8 lb.

Generally, the concrete is elongated and prismatic. One side had soil embedded in several spots (**Figure 3**).

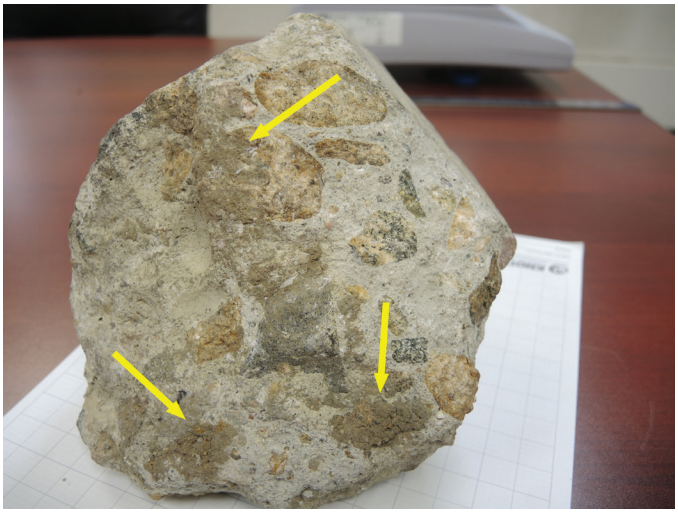

Figure 3
Soil embedded on the face of the projectile concrete.

The presence of soil on only one of the concrete's faces is evidence that the face had initially been resting on soil, and a force was applied on the projectile to embed the soil onto the surface of the concrete. Black residue was also observed on two sides of the concrete. The black residue was primarily found on the two faces that formed a wedge shape opposite of the soil (**Figure 4**).

During inspection of the concrete, a sample of the black material was taken from a section with a heavier concentration of the material. The sample was sent for material identification testing.

A digital microscopy image of the black material is shown in **Figure 5**. The lab analyst visually observed "black material, semi-translucent crystal, and fibers." The lab determined the black material likely contained styrene butadiene rubber, which is a typical elastomer used in the manufacture of tires[2]. The lab also determined that the fibrous material displayed chemical similarities with a compost sample, which was the same type of compost delivered to the park by the two dump trucks on the day of the incident. Therefore, the lab testing showed that there was material that had chemical similarities to tires, and the compost that had been delivered on the day of the incident to the park via dump trucks. A geometric analysis was performed.

Photogrammetry Analysis of Recycled Concrete on Vehicle Tracking Pad

The suspected source of concrete was the construction entrance at a nearby park described by the witness.

Figure 4
Black material observed primarily on two faces of concrete projectile opposite of soil (yellow arrow points to general side of embedded soil).

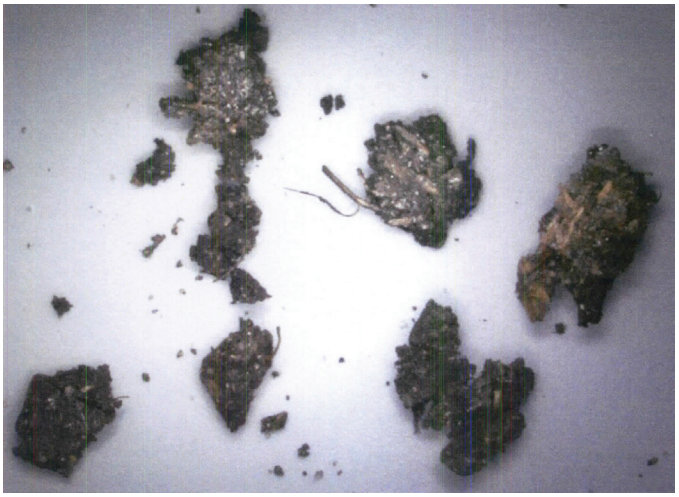

Figure 5
Digital microscopy of the material.

The construction entrance had a vehicle tracking pad comprised of 3-in. aggregate. Next to the vehicle tracking pad was the stabilized staging area, consisting of much larger recycled concrete. **Figures 6** and **7** are photographs of the vehicle tracking pad (VTC) and stabilized staging area (SSA) approximately two weeks before the incident.

The photographs show that, in general, the recycled concrete in the SSA is larger than the material installed on the VTC. However, the photographs also show that recycled concrete from the stabilized staging area overlapped a large portion of the VTC. Therefore, as trucks entered and exited the site, they would have likely run over the larger pieces of recycled concrete from the stabilized staging area that overlapped the VTC.

Figure 6
Photograph of vehicle tracking pad (VTC) and stabilized staging area (SSA) at the park taken by city inspectors, approximately two weeks prior to incident. Yellow arrow shows material in concrete washout area; blue arrow shows material on VTC.

Figure 7
Photograph of concrete washout/SSA and VTC taken by city inspectors on April 22, 2014, approximately two weeks prior to incident. Yellow arrow shows material in concrete washout area; blue arrow shows material on VTC.

The process of photogrammetry was applied to the photographs of the VTC and SSA[3,4,5,6,7]. First, the make, model, and general properties of the camera used to capture the photographs were obtained from each of the image's metadata. After identifying the camera, an exemplar camera was purchased and calibrated. The calibration process was used to correct the digital photographs for lens distortion.

After lens distortion was corrected, control points seen in both photographs and reference points from HD scanning of the park's construction entrance were input into photogrammetry software (**Figures 8** and **9**). Through the photogrammetry process, virtual cameras were created, matching the properties, location, and orientation of the cameras that captured each of the VTC photographs. After solving for the virtual cameras, the modeled virtual concrete projectile was placed within the virtual scene through the perspective of each virtual camera, essentially overlaying the modeled concrete projectile (to-scale) within the photographs over two of the pieces of recycled concrete installed on the VTC prior to the incident.

The virtual concrete projectile overlaid (to-scale) on the photographs is shown in **Figures 10** and **11**. The Figures show that concrete projectile was similar in both size and shape to the recycled concrete installed on the VTC prior to the incident.

Inspection of the Park

During the park inspection, the previous construction entrance was documented using photography and HD scanning. Seven high-definition scans were taken near the entrance. **Figure 12** shows the HD scan of the park.

The construction project had long been completed prior to the inspection, and the vehicle tracking pad was no longer in place. The recycled concrete that had been spread over the VTC during the construction project had been removed prior to the inspection, and most of the inspection area was covered in grass (**Figure 13**).

Near the entrance, there were some protruding sections of recycled concrete embedded within the soil. Our firm observed one piece of recycled concrete above soil level. The aggregates observed on the surface of the recycled concrete sample were of various colors. The authors visually compared the aggregate within the sample piece of recycled concrete and the aggregate within the projectile concrete using inspection photographs. **Figure 14** shows that the aggregate found on the sample's surface was visually similar to the aggregate found on the concrete projectile's surface. Therefore, the recycled concrete found at the accident site had visual similarities to the concrete projectile.

Figure 8
Control points between the two photographs and reference points used to solve for the cameras.

Figure 9
Control points between the two photographs and reference points used to solve for the cameras with the point cloud of the scene.

Figure 10
Projectile concrete overlay (to-scale) on photograph.

Figure 11
Projectile concrete overlay (to-scale) on photograph.

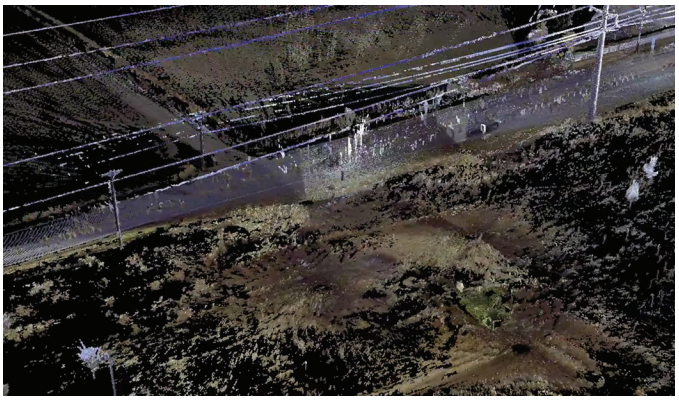

Figure 12
High-definition scanning of the park.

Figure 13
The area where VTC was previously installed is shown here. The circle represents general area that sample concrete was collected during inspection.

Concrete Projectile Fit in Dual Tires

The defendant's dump trailer was documented using photography and HD scanning. At the time of the inspection, for demonstration purposes, a concrete of similar size and shape to the projectile concrete that was obtained at the park was embedded in the trailer's rear left set of dual tires to show that the concrete fit very well in the set of dual tires (**Figure 15**).

Geometrical analysis with a virtual model of the trailer tires and concrete projectile was done to determine how the projectile concrete would have fit within the set of dual tires, matching the areas where the black material was observed on the concrete with where the concrete made contact with the tires (**Figure 16** and **Figure 17**). The analysis also showed how the concrete would have been pressed fit into the set of dual tires (**Figure 18**).

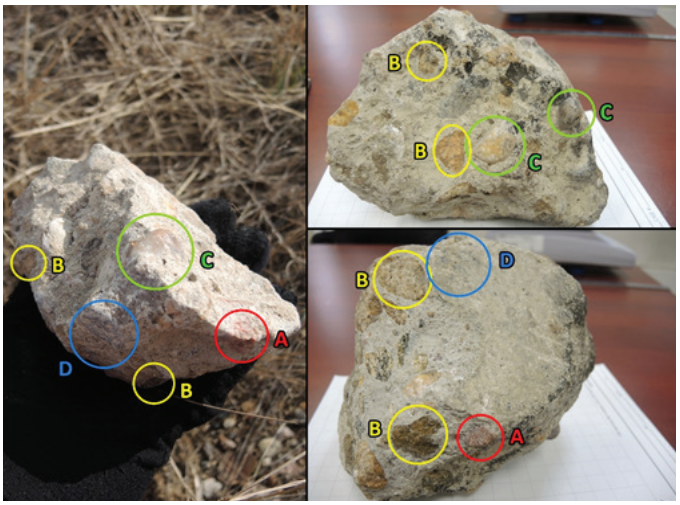

Figure 14
Visual similarities between sample recycled concrete found during inspection (left) and the concrete projectile (right). Colored circles identify areas of visual similarity.

Figure 15
Concrete of similar size and shape as projectile concrete obtained from the park embedded within the defendant trailer rear left set of dual tires.

Concrete Projectile Trajectory Through Windshield

The truck's windshield was severely damaged during the incident. The damage was concentrated near the upper-left most corner of the windshield (**Figure 19**). The damage to the windshield included a hole that was consistent with a spheroid-like object striking and penetrating the windshield. The shape of the hole was generally consistent with the shape of the piece of concrete projectile that fell out of the cab when the witness opened the cab door.

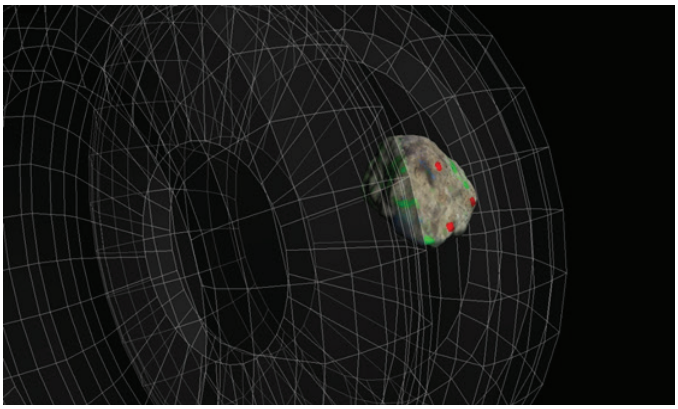

Figure 16
Graphic showing a scaled model of the concrete wedged in scaled dual tires. (Green marks = locations of black material embedded; red marks = locations of soil.)

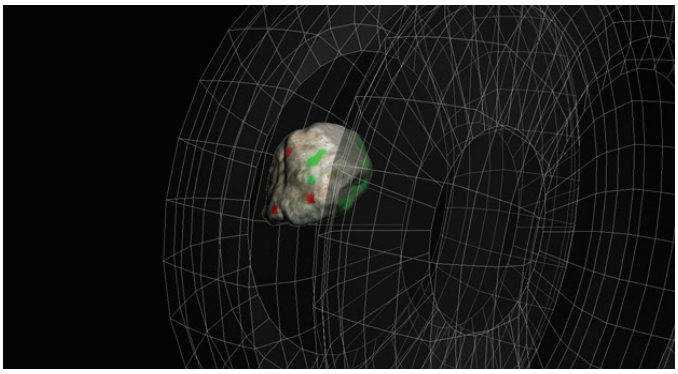

Figure 17
Graphic showing a scaled model of the concrete wedged in scaled dual tires from the other side. (Green marks = locations of black material embedded; red marks = locations of soil.)

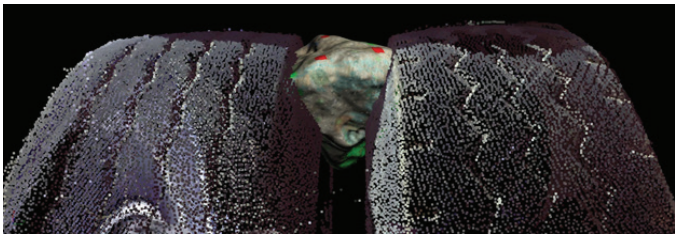

Figure 18
Visualization of the projectile concrete press-fit in HD scan of the dual tires.

There also were concrete fragments found on the rear cab wall (**Figure 20**), and the rear cab wall was dented, consistent with the concrete striking the rear cab wall after striking the windshield and the plaintiff.

The plaintiff's truck was documented approximately two years after the damage had been repaired. During the inspection, the truck was documented using photography and HD scanning. **Figure 21** is the point cloud of the truck.

The HD scans and the process of photogrammetry were used to determine where the concrete entered the windshield, the approximate location of the plaintiff's head, and the location that the concrete hit the rear wall of the cab. As an example, **Figure 22** shows the point cloud of the truck overlaid on the scene image as a result of the photogrammetry process.

After identifying the location of the hole in the windshield, approximate seating location of the plaintiff, and the location of the dent in the rear of the cab, the trajectory of the concrete projectile through the windshield was determined (**Figure 23**). The projectile entered the windshield at a height of approximately 96.6 in. The trajectory shows that the projectile entered from the left (driver's)

Figure 19
Damage to windshield consistent with projectile concrete impact (scene photograph).

Figure 20
Concrete fragments along panel behind driver's seat.

Figure 21
Point cloud of the truck.

Figure 22
Application of photogrammetry to scene photographs using HD scans to determine windshield damage location.

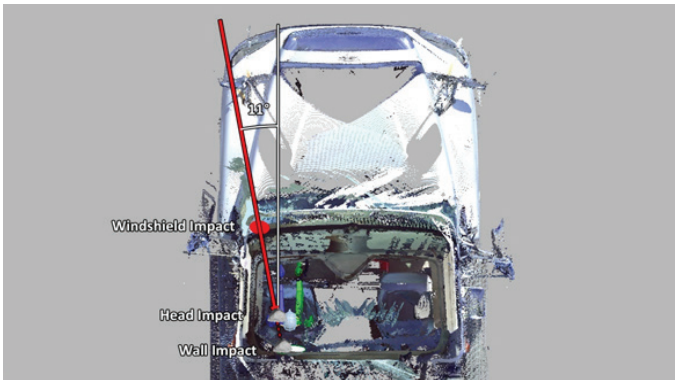

Figure 23
Trajectory of the projectile concrete through the cab top view.

side and traveled both rearward and right relative to the truck. This lateral (left-to-right) trajectory is consistent with the projectile originating in the northbound lane of the county line road, in contrast to coming from the southbound lane of the county line road from a leading vehicle.

As further validation that the concrete had originated in the northbound lane, physical evidence was identified that supported the concrete lateral trajectory angle through the windshield.

The windshield damage pattern and entry hole form a diagonal oval that extends from the left, upward to the right. The oval has a length to width ratio of 1.78 to 1 (**Figure 24**), which is a higher ratio than concrete projectile's length to width ratio. Therefore, the oval in the windshield is elongated compared to the shape of the concrete projectile. The angle, size, and shape of the oval provide insight to the direction that the projectile entered the windshield.

For example, in a shooting reconstruction[8,9,10,11], the lateral component of a bullet projectile's trajectory through a laminated windshield is given by the orientation of an elongated oval formed by the cylindrical bullet in the windshield (**Figure 24**)[12, 13]. The angle of the oval's long axis relative to the windshield's vertical axis is consistent with the lateral component of the projectile bullet's entry velocity. An example of measuring this angle is shown in **Figure 25**.

The example in **Figure 24** shows a windshield from the interior of the vehicle. The bullet hole forms an elongated oval shape. The protractor is aligned with the base parallel to the plane of the front of the vehicle. The angle of the long axis of the elongated oval is approximately 17 degrees to the right, which is consistent with the projectile bullet traveling at a lateral angle of 17 degrees from left to right (**Figure 27**).

This shooting reconstruction method was applied to the physical evidence in the subject incident. The entry oval in the windshield is substantially longer than the longest dimension of the concrete projectile (similar to a cylindrical bullet forming an elongated oval when shot at an angle), and the elongated oval distinctly forms an angle from the left upward to the right (**Figure 24**). Like the example shown in **Figure 26**, this elongated oval shape and angle is consistent with the concrete projectile entering the cab with a lateral velocity component from the left to right side of the cab.

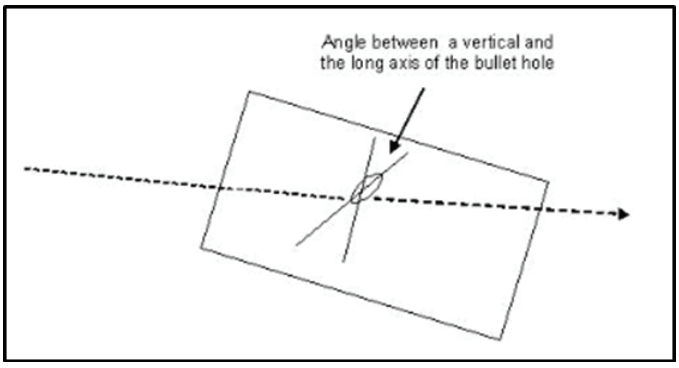

Figure 25
Projectile bullet hole produced in a windshield.
The angle of the oval indicates direction bullet is shot.
Graphic courtesy of Consolidated Consultant Co.

Figure 24
Elongated oval-shaped opening in windshield from
left to upper right. Oval length to width ratio is 1.78 to 1.

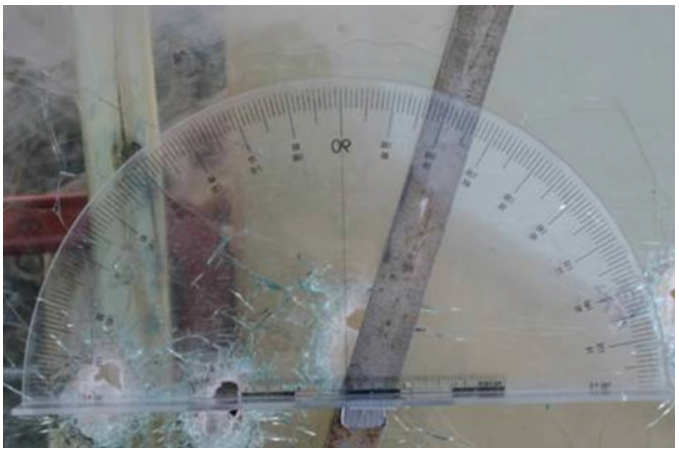

Figure 26
Example of measurement to determine lateral angle.
Graphic courtesy of Consolidated Consultant Co.

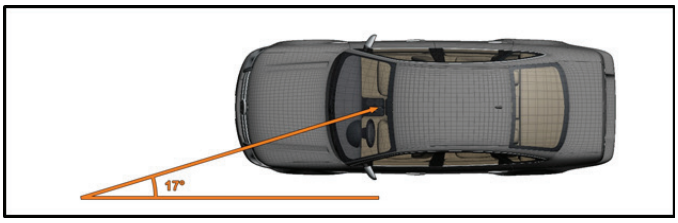

Figure 27
Example of bullet lateral angle through windshield of 17 degrees. Demonstrative graphic created by the authors.

Defendant Driver Timeline Inconsistencies

According to the defendant driver's deposition testimony, he saw the truck in the field as he was driving northbound on the county line road to the park delivering his first load of compost. Therefore, the defendant driver claimed that the accident occurred prior to his arrival at the park. After dumping his first load of compost, he then drove back southbound on the county line road past the accident site a second time. For the defendant driver's observations to be true, he would have had to have made both observations after 8:45 a.m., when the accident occurred, but before 8:58 a.m., when the county line road was shut down near the accident site as observed by the responding trooper and as recorded in dispatch records. Therefore, the defendant driver had only 13 minutes to do the following:

- Drive southbound approximately 1 minute from the incident scene to the park.
- Wait for the other side-dump truck driver, who, according to the testimony, was finishing dumping a load of compost, to finish dumping the load and drive away from the compost pile.
- Back up to the compost pile, and then dump the load of compost.
- Get out of his truck and check to be sure the load was fully dumped.
- Make a left turn onto northbound county line road and drive approximately 1 minute past the accident scene again.

According to both drivers and the defendant landscaping company's manager, the process of both drivers dumping their loads would have taken substantially longer than 13 minutes. Therefore, the county line road would have likely been closed by the time the defendant driver had approached the scene traveling northbound from the park. From the simple timeline analysis, it is highly improbable that the defendant driver saw the truck in the field as he was driving southbound on the county line road to deliver his first load of compost for the day.

Concrete Drop Testing

Investigating officers first attributed the concrete from falling off the load of a dump truck. Both static and dynamic testing were conducted to test the hypothesis that the concrete could have fallen off the load of the dump truck from a height of approximately 8 ft and rebounded vertically upward back up to 8 ft into the windshield of the truck. Static testing of concrete dropped from a height of 8 ft showed very minimal rebound. Defense experts conducted dynamic testing in which 22 exemplar pieces of concrete were dropped from a height of 8 ft from a moving vehicle traveling approximately 40 mph. The dynamic testing clearly showed that the concrete would only rebound approximately 2 to 3 ft — far lower than the rebounding to the height of 8 ft. Therefore, the static and dynamic testing were evidence that the concrete had not fallen off the load of a dump truck as initially suspected by investigating officers.

Methodology — How the Concrete Projectile Was Thrown into Plaintiff's Windshield

Several hypothetical scenarios were identified to explain how the concrete projectile was thrown into the plaintiff's windshield. The scientific method of deductive reasoning and the process of elimination (inferential reasoning) to eliminate hypotheses that were unreasonable or impossible was used. After eliminating hypothetical scenarios, there was only one scenario that was possible. Based on the process of elimination, the probable scenario was determined.

1. First, the hypothetical of a projectile thrown by a pedestrian was explored. There were no overpasses of which the concrete could be thrown from into moving traffic. Further, there was no suspicious activity of someone throwing rocks into traffic, despite typical busy traffic on the county line road.

The projectile concrete had material similar to tire rubber, which is more consistent with interaction with a tire than with a pedestrian, and fibrous material consistent with compost delivered to the park on the day of the incident. There wasn't any compost observed in scene photographs to suggest the concrete had originated near the incident scene. The lack of reported suspicious activity in the area despite heavy traffic, lack of overhead pedestrian

bridges, and presence of material consistent with rubber and compost on the concrete did not support a pedestrian throwing the projectile concrete at the plaintiff's vehicle. Therefore, the hypothesis that a pedestrian threw the concrete projectile toward the plaintiff's vehicle was eliminated.

2. The hypothesis that the concrete was thrown from a phantom southbound vehicle leading the truck was next. This hypothetical was rejected as the source of the concrete projectile due to the following:

- The horizontal trajectory of the concrete from the windshield to the plaintiff and to the rear of the truck's cab. This lateral (left-to-right) trajectory was consistent with the concrete projectile originating in the northbound lane (**Figure 23**). Therefore, the horizontal trajectory of the projectile concrete through the windshield showed the projectile did not come from the southbound lane, but rather the northbound land.

- The size, shape, and orientation of the hole in the plaintiff's windshield is further evidence that provides validation of the horizontal trajectory analysis. Consistent with the trajectory analysis, the size, shape, and orientation of the hole in the windshield showed that the concrete originated in the northbound lane of travel and was thrown west into the plaintiff's southbound lane of travel.

Therefore, the horizontal trajectory analysis, which was validated by analysis of the size, shape, and orientation of the hole in the plaintiff's windshield was consistent with the projectile thrown from a northbound vehicle.

3. The engineers analyzed whether the concrete was imbedded between dual tires of the defendant's semi prior to ejection toward the plaintiff's head. While the space between non-deflected dual tires is smaller than the general dimensions of the concrete, the flexibility of the tires allows tire to deflect and wrap around the concrete. Evidence of this deflection, in the form of black residue, surrounded opposing wedged faces of the projectile. Lab testing confirmed the black material contained a typical elastomer used in the manufacture of tires. Therefore, the concrete had physical evidence imbedded on its surface consistent with tire rubber. Further, the black material consistent with tire rubber on two opposing wedged faces was geometrically consistent with the concrete wedged between a set of dual tires.

4. The scenario in which the projectile fell off the load of a northbound truck was evaluated. There were multiple reasons that this scenario was improbable:

a. Visual testing of the concrete showed black material consistent with tire rubber (and inconsistent with asphalt) on two opposing wedged faces of the concrete. The presence of the black material was evidence that the concrete projectile had been wedged between a set of dual tires rather than being loaded on a northbound truck.

b. The static and dynamic exemplar concrete drop testing demonstrated that the concrete could not have fallen off the load of a dump truck and rebounded 8 ft into the southbound truck's windshield.

Methodology — Determining the Source of the Concrete Projectile

After determining the path in which the concrete projectile was thrown into the plaintiff's windshield, the probable source of the projectile concrete was determined. There was substantial scientific evidence linking the projectile to the park:

1. In the days preceding the incident as well as the day of the incident, compost had been delivered and dumped at the park by the defendant's dump truck drivers. Independent of any witness testimony, a fibrous material with similar physical and chemical characteristics as the compost was found embedded within the sample of material collected from the projectile concrete.

2. Independent of any witness testimony, the projectile was of similar size and shape as recycled concrete identified in photographs at the park on or near the VTC, as determined through the scientifically validated photogrammetry process.

3. Independent of any witness testimony, aggregate within a piece of concrete found at the park was visually similar to the aggregate in the projectile concrete.

Based on the above evidence, it was concluded that the projectile concrete had come from the VTC at the park.

Methodology for Determining How the Projectile Concrete was Transported

There were two defendant dump trucks traveling to and from the park on the day of the incident: a white rear-dump truck and a white side-dump truck. There were no other dump trucks reported at the park on the day of the incident.

The witness described a white rear-dump truck traveling northbound on the county line road making a thumping noise immediately prior to the incident. There was only one white rear-dump truck operating on the day of the incident. Therefore, through simple deduction, the projectile had likely been transported from the park via the white rear-dump truck.

Photographs taken of the VTC show relatively larger-sized pieces of recycled concrete (similar in size and shape as the projectile) on the VTC's left side closest to the SSA. Therefore, it is likely that the concrete projectile was embedded within a left set of the defendant's white rear-dump truck.

The driver of the white rear-dump truck alleged during his deposition that as he was initially traveling southbound on the county line road toward the park to drop his load, he saw the southbound truck in the field. After this point in time, he testified that he had driven to the park, waited for another dump truck to dump a load, dumped his load, and traveled northbound back past the accident scene a second time. The driver's testimony was considered. However, there was the significant time discrepancy in his testimony that contradicted officer testimony and dispatch records, which showed the road had been closed only 13 minutes after the incident. In comparison, it would have taken an estimated 30 to 45 minutes for the driver of the dump truck to pass the scene again traveling northbound. Therefore, the dump truck driver's testimony was inconsistent with the road closure timing.

Simulations, Visualizations, and Event Timing

Scientific visualizations were created showing the motion of the white rear-dump truck leaving the park and traveling northbound on the county line road, the concrete ejecting from the dual tires into the southbound truck's windshield, and the truck going off road.

The vertical launch angle of the concrete projectile was not known. For visualization purposes, it was assumed that the projectile was ejected rearward from the rear dual tires at approximately 45 degrees and at the tangential velocity of the tire (40 mph). Shortly after launching, the concrete projectile struck the mud flap, causing rapid forward acceleration of the projectile. During the inspection of the truck, the geometry of the mud flaps relative to the rear dual tires and mud flap weights were documented.

A conservation of rotational momentum analysis was conducted to calculate the speed loss of the projectile after interacting with the mud flap. To simplify the conservation of momentum analysis, the mud flap was assumed to be a solid rectangular prism connected with a frictionless pin connection. After impact, the delta-v of the projectile in the longitudinal direction was calculated as approximately 20 mph. An assumption was made that the mud flap decreased the vertical angle by approximately one-half.

The analysis of the concrete projectile being released due to centrifugal force, then impacting the mud flap, losing some energy, continuing rearward and finally striking the windshield of southbound semi, was performed. In other words the concrete hits the flap, loses energy, and continues in the same southbound (rearward) direction.

The analysis was done using conservation of momentum and considered the following: weight of the mud flap, geometry of the mud flap, mud flap moment of inertia (rectangular thin plate), the semi's velocity (wheel rotational angle), ejection angle and position of the mud flap in reference to the rolling wheel, and the resultant ejection height and velocity.

These calculations were not intended to be part of this paper, the author's focus was rather on other innovating technologies, such as high-definition 3D scanning, 3D modeling, simulation, and animation.

A velocity vector diagram was created. The concrete projectile had a rearward velocity component resulting from the initial tangential rearward launch and interaction with the mud flap. The concrete projectile also had an initial forward translational movement, consistent with the speed of the truck (40 mph). Combined, the exit speed of the projectile was approximately 34 mph forward (northbound direction). Based on the lateral trajectory of the concrete projectile, as determined from the physical evidence, the longitudinal and lateral velocities were determined (**Figure 28**).

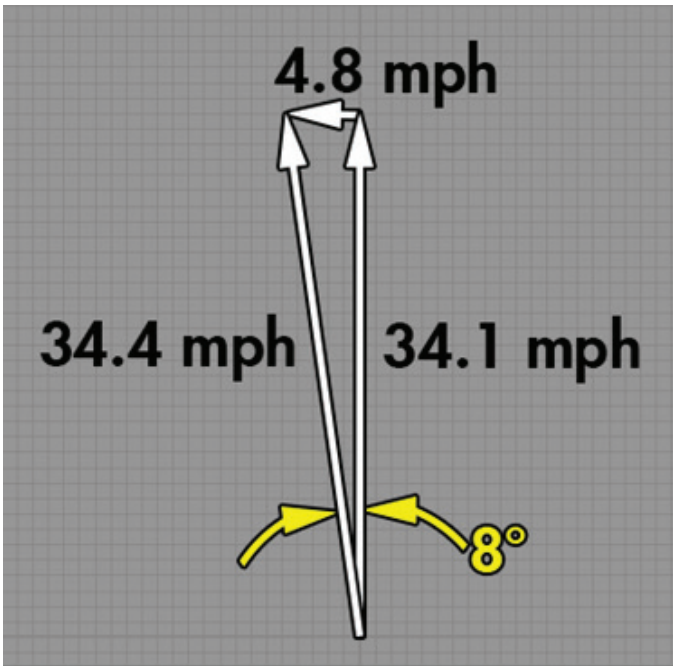

Figure 28
Forward trajectory of the concrete projectile after interaction with the mud flap.

The closing speed of the projectile and the southbound truck, assumed traveling the posted speed limit of 45 mph, was calculated as approximately 79 mph (**Figure 29**). After determining the concrete projectile's trajectory and motion, the motion of the both trucks were simulated in PC-Crash[14].

After calculating the trajectory of the concrete projectile and simulating the motions of both vehicles, scientific visualizations were created. One of the scientific visualizations included showing the trajectory of concrete projectile ejecting from the northbound dump truck and striking the windshield of the southbound truck (**Figure 30**).

A photorealistic scientific visualization showing the northbound dump truck picking up the concrete projectile, driving northbound, the ejection of the concrete projectile into the windshield of the southbound truck, and the southbound truck traveling off the roadway into the field to the west of the roadway was also created using aerial imagery and scene photographs (**Figure 31**).

A scientific visualization was created, showing the field of view of the witness (**Figure 32**). The scientific visualization showed that approximately 11 seconds after the witness first observed the northbound white rear-dump truck making a thumping sound, the southbound

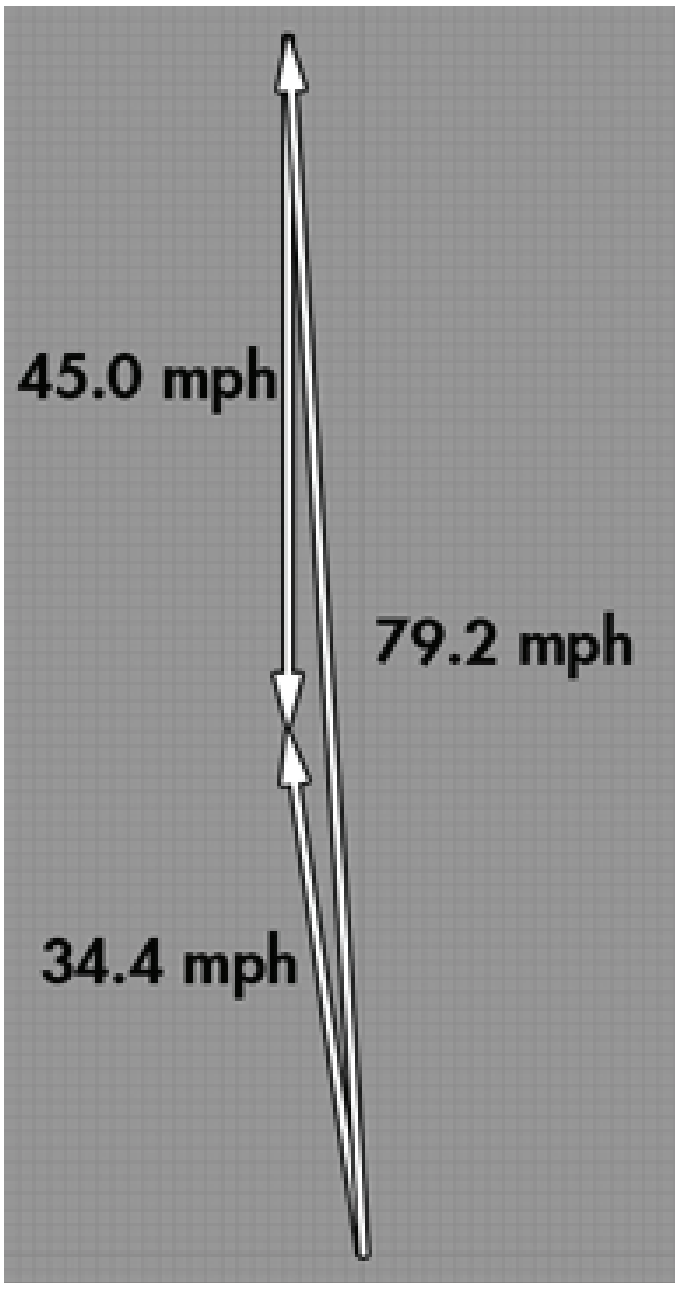

Figure 29
Concrete projectile's closing speed relative to the truck.

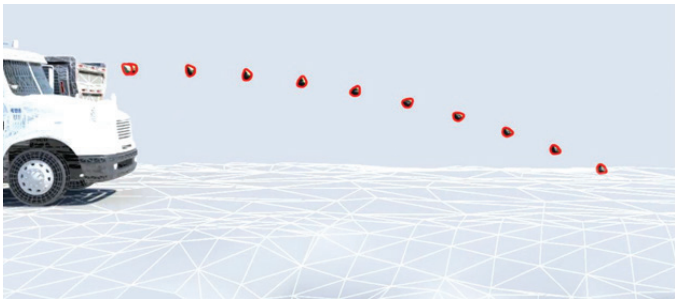

Figure 30
Still frame from scientific visualization showing trajectory of the concrete projectile.

Figure 31
Still frame from photorealistic scientific visualization of accident.

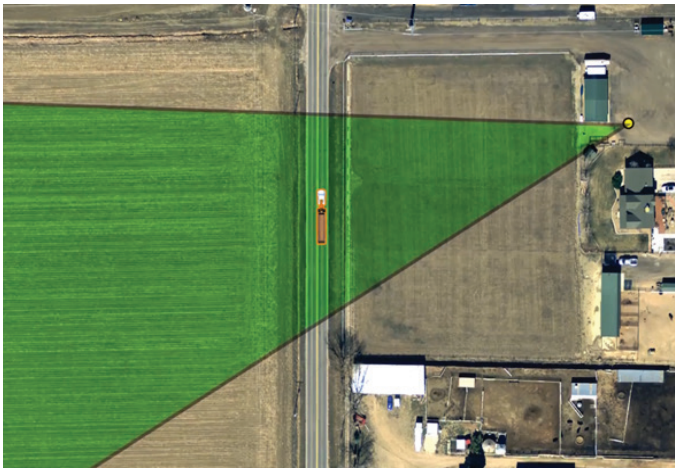

Figure 32
Scientific visualization showing the field of view of the witness.

truck struck the utility pole and knocked out the power to the witness' residence. The reconstructed timing is generally in-line with the witness' estimated time of seven to 10 seconds between him first observing the northbound white rear-dump truck and his power going out. Therefore, the witness's timing of the events is consistent with the projectile ejected from a set of the northbound white rear-dump truck's dual tires.

Conclusion

Based on the forensic engineering analysis presented in this paper, it was concluded that the concrete projectile had originated from the vehicle tracking pad at the park. The white-rear dump truck observed by the witness was confirmed to be a white-rear dump truck that had delivered a load to the park prior to the accident. While the white-rear dump truck was at the park, the concrete projectile became imbedded within the truck's left rearmost dual tires. After the white-rear dump truck left the park, it drove north on the county road. As it was driving, the concrete imbedded within the dual tires made a thumping sound heard by the witness. The concrete ejected from the dual tires of the northbound white-rear dump truck and struck the southbound truck and plaintiff. As a result of the collision, the plaintiff last control of the truck, and the truck drifted west into the ditch, striking a utility pole and knocking out the power to the witness' residence. The truck traveled approximately 470 ft, coming to rest in the field to the west of the roadway.

References

4. L. Wasser, "The Basics of LiDAR – Light Detection and Ranging – Remote Sensing," National Science Foundation [Online]. Available: https://www.neonscience.org/lidar-basics [Accessed: October 28, 2020].

5. Omnexus: The material selection platform, "Styrene-Butadiene Rubber: Complete Technical Guide on SBR and its Features" [Online]. Available: https://omnexus.specialchem.com/selection-guide/styrene-butadiene-rubber-sbr-guide# [Accessed: October 15, 2020].

6. K. Breen and C. Anderson, "The Application of Photogrammetry to Accident Reconstruction," SAE Technical Paper Series, 1986, Paper No. 861422.

7. M. Callahan, B. LeBlanc, R. Vreeland, and G. Bretting, "Close-Range Photogrammetry with Laser Scan Point Clouds," SAE Technical Paper Series, 2012, Paper No. 2012-01-0607.

8. C. Coleman, D. Tandy, J. Colborn, and N. Ault, "Applying Camera Matching Methods to Laser Scanned Three Dimensional Scene Data with Comparisons to Other Methods." SAE Technical Paper Series, 2015, Paper No. 2015-01-1416.

9. S. Fenton and R. Kerr, "Accident Scene Diagramming Using New Photogrammetric Technique," SAE Technical Paper Series, 1997, Paper No. 970944.

10. R. Ziernicki and D. Danaher, "Forensic Engineering Use of Computer Animations and Graphics." Journal of the National Academy of Forensic Engineers, Vol. 23, No. 2, pp. 1-9. Dec. 2006.

11. R. Ziernicki and A. Leloglou, "Newest Technologies Utilized in the Reconstruction of an Officer

Involved Shooting Incident." Journal of the National Academy of Forensic Engineers. (In Print).

12. R. Ziernicki, W. Pierce, and A. Leiloglou, "Forensic Engineering Usage of Surveillance Video in Accident Reconstruction." Journal of the National Academy of Forensic Engineers, Vol. 31, No. 2, Dec., pp. 9-19, 2014.

13. F. Devernay and O. Faugeras, "Straight Lines Have to be Straight: Automatic Calibration and Removal of Distortion from Scenes of Structured Environments," Machine Vision and Applications. Vol. 13. No. 1, 2001.

14. D. Danaher and R. Ziernicki. "Forensic Engineering Evaluation of Physical Evidence in Accident Reconstruction," Journal of the National Academy of Forensic Engineers, Vol. 24, No. 2, Dec., pp. 1-10, 2007.

15. E. Hueske, Practical Analysis and Reconstruction of Shooting Incidents. Florida: CRC Press, 2006.

16. Consolidated Forensic Experts, "Lateral Angle Determination for Bullet Holes in Windshields," 2016 [Online]. Available:http://www.expertwitnessnews.com/lateral-angle-determination-bullet-holes-windshields/ [Accessed 2017 July 5].

17. "PC-Crash (Version 11)," MacInnis Engineering Associates Ltd. [Online] Available: http://www.pc-crash.com/.

Misapplication of Pressure Vessel Codes in Forensic Applications

By Bart Kemper, PE (NAFE 965S)

Abstract

Engineering codes are a key method to guide designs to safe and reliable outcomes. Many such codes have prescribed calculations where the user provides specific inputs in a series of calculations, often using charts or tables, to get specific outputs. The design margins, units, and underlying theory are not always apparent. Engineering codes may not be suitable for reverse engineering an incident or providing a failure prediction. This article examines a criminal negligence case in which an initial forensic analysis incorrectly applied the ASME Pressure Vessel Code to use Finite Element Analysis (FEA) of a failed pressure vessel section. The flaws in the original analysis were revealed by applying reverse engineering using conventional stress calculations and understanding basic material science. This emphasizes the need to understand the underlying theories with both engineering codes and numerical modeling. Subsequent FEA provided an accurate analysis report that was successfully used in court. These same methods can be applied to many other engineering codes and standards.

Keywords

Finite element, computer model, numerical modeling, pressure vessel, piping, design margin, nonlinear, stress-strain, engineering codes and standards, code compliance, forensic engineering

"Although most people do not realize it, standards and the methods used to assess conformity to standards are absolutely critical. They are essential components of our nation's technology infrastructure — vital to industry and commerce, crucial to the health and safety of Americans, and basic to the nation's economic performance [1]."

A manager of a petrochemical facility in a non-U.S. jurisdiction was on trial for criminal negligence. Under that jurisdiction, there is not a "presumption of innocence" as there is in U.S. jurisprudence. The pressure vessel section failed due to erosion thinning, releasing pressurized heated hydrocarbons that killed a worker.

The crux of the prosecutorial theory was the manager eliminated hydrotesting systems to 130% of the maximum operating pressure during maintenance turnarounds. Maximum operating pressure was 362 MPa (52.4 psig). Hydrotest was 470 MPa (68.2 psig). The nominal wall thickness was 7 mm (0.276 in.) and was locally eroded by the refining process to 0.15 mm (0.006 in.). It was reasoned that hydrotesting would have revealed bulges of the thinned sections, which, in turn, would allow the equipment operators to note the discrepancy and report it prior to being put back into service. This detection would have prevented the death; therefore, the manager's decision to discontinue hydrotesting was the key event that caused the death.

Based on the rules in the jurisdiction, the experts do not testify in person. Technical reports are submitted to a "Master's Panel" with appropriate expertise and are reviewed for accuracy in terms of procedure and citation. Reports that accurately cite facts and figures, have properly executed mathematics and numerical models, and otherwise are internally technically correct are allowed to go forward to the judges. The panel of judges then assesses the reports and weighs their contributions to the legal arguments before them. Reports that are found to have significant internal errors are not entered into the record, and the legal team may not refer to them during their arguments — even if portions of the report were accepted by the review panel.

While there were multiple technical issues being addressed by defense counsel for this case, a key question was what would be the largest "bubble" or "blister" of 0.15-mm thickness that could withstand hydrotesting

Bart Kemper, PE, 4520 Jamestown Ave., #3 Baton Rouge, LA 70808, 225-923-2945, bkemper@kempereng.com

without failure. If this bubble could be noticed underneath the 25 to 50 mm (1 to 2 in.) of insulation, then the prosecution's theory would be supported. If the blister was not noticeable under the insulation, then the prosecution's theory would be moot.

Another aspect of concern was the legal team understood the original report predicted "failure." Specifically, the legal team planned to argue the combination of geometry and pressure described the physical limit of the failed section. While this was not in the report, this was the basis of specific arguments shared with their client (the defendant). The defendant, who was also an engineer, questioned the report and the underpinnings of the arguments, which, in turn, raised concerns regarding whether the report would pass the Master's Panel review. This led counsel to seek a third-party review (the author was part of this review).

The third-party review was constrained to the information already provided by the translated official forensic report, which included material testing results, measurements, and a few photographs. There was no tensile testing. Hardness testing was taken, but experience shows hardness testing is suspect after a fire or explosion due to changes in material properties at the surface. The lack of reliable mechanical testing constrained the examination to be for minimum material specifications and not the in-situ material. The review of the original engineering report indicated an error because the original team had improperly applied an engineering design and safety code. Coupled with failing to apply engineering theory to check results, this resulted in an inaccurate FEA with resultant errors.

Codes Provide Due Diligence for Design

Items like pressure vessels must be safe and reliable. Engineering codes and standards are rooted in the history of civilization. They are developed by design professionals (as a group and over time) as part of their special moral obligation to safeguard the public. They represent an ethical baseline for design due diligence. These methodologies are based on engineering fundamentals while incorporating other considerations such as acceptable design margins, construction tolerances, material variations, and other practice-based factors[2].

The American Society of Mechanical Engineers (ASME) Boiler and Pressure Vessel Code (BPVC) is an internationally used code for pressure vessels. Many U.S. states, such as Illinois, legally require this code as the standard for design and construction[3]. The pressure vessel code's general intent in its conventional Division 1 "design by rules"[4] is to establish a design margin of at least 3.5 with respect to material tensile failure at the design pressure and temperature[5,6]. If more testing and quality control is applied, Division 2 allows for a design margin of 2.4 with respect to steady-state tension. It is important to note these design margins are not constant for all combinations of tension and bending, but are for overall design guidance, since providing the means to calculate a uniform safety factor for all combinations of loading and response, as well as all geometries and materials, would be needlessly complicated[6].

Traditionally, this is accomplished with prescribed calculation procedures. These are a long series of conventional calculations that could be accomplished using a calculator or spreadsheet to develop a sufficiently safe and reliable design. This approach is highly structured with the required design factors built into the process. The engineer does not exercise independent judgement in selecting the design factors nor the methods for determining various features, such as minimum thicknesses, allowable curvatures, and other dimensions.

The fundamental issue at hand is applying a design code to a failure analysis. Like other engineering or construction codes, the ASME BPVC establishes design margins to address permissible tolerances in fabrication, variations in materials, uncertainties in loads and conditions, and other considerations. These margins are carried over into other ASME codes related to BPVC, such as B31.3 Process Piping[7] for design and the in-service guidance of FFS-1 Fitness-For-Service[8]. In some portions of a code, the design margin is explicitly shown, such as Table B1.4 in FFS-1. More often, the design margin is implicit and incorporated into the overall process. Directly analyzing a structure with respect to a code assesses "code compliance." Given the aforementioned design margins, being "out of code compliance" does not necessarily indicate failure nor predict the failure mode. It is critical designers or engineers understand the failure modes and their significance[9].

Predicting physical results, such as deflections, strains, and failure modes, requires a more detailed understanding of materials, material mechanics, and other factors compared to typical design code work. Failures typically exceed yield strength or are "nonlinear." Nonlinear mechanics are outside the scope of typical design codes, including ASME BPVC Section VIII, Division 1. Nonlinear mechanics are addressed in Division 2, Part 5, "Design

by Analysis," but are still intended to be used within the code's design envelope.

Figure 1 illustrates the ASME pressure vessel design envelope with respect to failure. The key aspect is the ASME pressure vessel code, like other design codes, is meant to be used within a given envelope. The failure line is based on ideal design assumptions, such as all materials and joints meet minimum specifications, all geometries are as designed, and all loads are within design parameters. Deviations from these minimums will change the failure curve, and experience teaches us that new materials generally exceed the minimum mechanical specifications. In-service conditions, damage, repairs, and unanticipated loads are classic contributions to failure. The failure line in **Figure 1** cannot be reliably used to "reverse engineer" a failure. This was a key concept explained to the legal team in order to assist in refining their legal arguments within the bounds of the physics of the event.

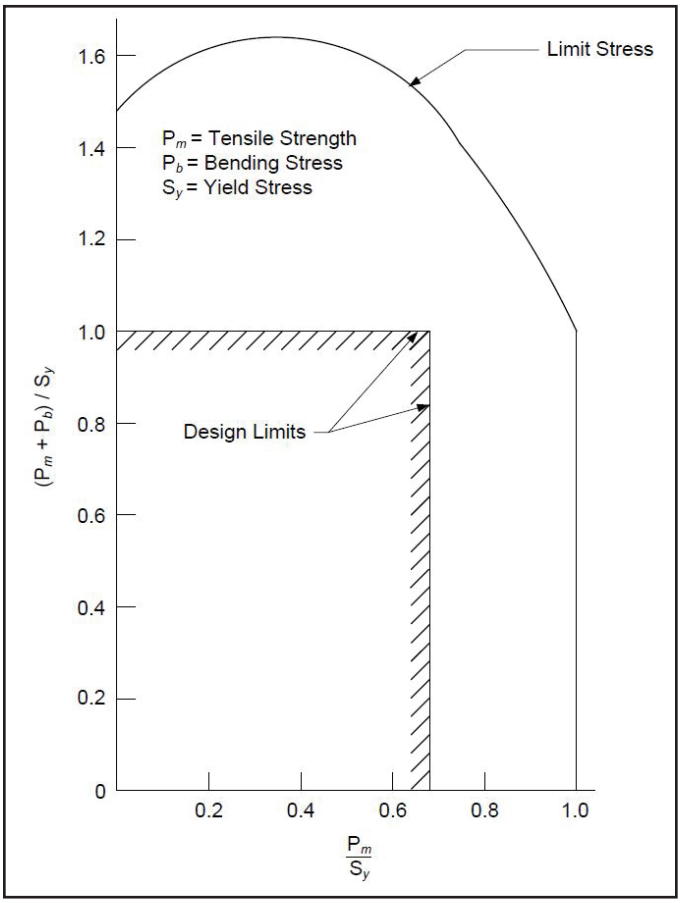

Figure 1
An illustration of the ASME pressure vessel code design envelope with respect to theoretical failure using stress intensity[6] (© ASME 2014). The ASME code is designed to prevent failure. The code does not provide a method to predict failure, since failure is outside the code's envelope.

Without the requisite understanding of failure mechanics, as well as the applicable codes, the investigator is likely to misuse a design code such as ASME BPVC by failing to account for implicit and explicit design margins. It is incumbent on the engineer to do more than carry out the rote execution of a design code. The formal education typical of modern engineers gives them the foundation for the specific design theory, but applying these building blocks requires additional study, such as sources from the code proponent like ASME[6,10,11] or independent engineering texts[12].

Finite Element Analysis As an Established Engineering Method

For expert testimony, the engineer must not only have the education and training, but also use an accepted method in a reliable manner[13]. Using an established, proven method is a key element in fulfilling the legal requirements of "the testimony is the product of reliable principles and methods[14]." Numerical modeling such as FEA has been in use since the early 1970s. It leverages the power of electronic computing to perform a vast array of matrix calculations to resolve 2D and 3D calculations for stress, strain, displacement, heat transfer, and other structural issues[15]. Section VIII, Division 2, Section 5 of BPVC provides a codified method for applying linear and implicit nonlinear FEA in lieu of the prescribed code calculations.

FEA can also be used to assess in-service equipment for useful remaining life after modifications or repairs[8]. Implicit nonlinear FEA has been used to determine whether pressure vessels and piping designed and built to other codes can be considered equivalent to ASME BPVC and under what conditions[16].This technique has been used in pressure equipment failures[17]. Use of the FEA is not only well established in the practice of engineering, but it has also been accepted by the courts[18,19]. The original team was valid in selecting implicit nonlinear FEA as a method in assessing the failure.

Examining the Failed Section and Initial Work

The failure in question was in a pipe with chemistry conforming to ASTM A106B carbon steel pipe (**Figure 2**). The inner diameter was 426 mm (16.8 in.) with a 10-mm (0.394-in.) thickness when new. The general thickness was 7 mm (0.276 in.) at the time of failure. Forensic measurement and analysis of the failed pipe showed the pipe wall at the point of failure was thinned to 0.15 mm (0.006 in.) before the failure and fire. This is more than a 65:1 aspect ratio — about the thickness of a sheet of paper. The equipment was designed and fabricated overseas and not to

Figure 2
Photo of the failed carbon steel facility piping.
Coupons had been cut out for testing.

ASME code. The original team chose ASME codes in part because it provides an accepted method for reliably using FEA for design and in-service evaluation. The equipment's original design code was not used by any party in this evaluation.

The prosecution hypothesized hydrotesting would have revealed the thinned region by bulging out, alerting workers to excessive thinning and thereby avoiding the fatal incident. Hydrotesting is a process of filling equipment with water and pressurizing it to a set amount, typically 1.3 times the maximum allowable working pressure (MAWP). Based solely on the material and geometry, or what the equipment could withstand at the time of construction with allowances for planned thinning (such as a corrosion allowance), MAWP is equal to or higher than the design pressure.

Hydrotesting is typically only conducted after initial fabrication. It is a method of using water to overpressure a containment system to proof the structure for flaw. Process equipment generally has thicknesses greater than what the pressure requires due to corrosion allowance, sizing up wall thicknesses to standard sizes, and the design margins. Since it is an overpressure, it is typically done only once. Hydrotesting in-service equipment to 1.3 MAWP could cause damage and unscheduled downtime as the forecasted wear and tear reduces the margins. This had occurred frequently in this plant when periodic hydrotesting was part of maintenance procedures. It had been discontinued in favor of modern maintenance methods, which included pressure testing to MAWP but not beyond.

As previously stated, the prosecution's case argued the use of hydrotesting would have revealed the thinning by creating bulges that would be detected, despite the insulation. The defense argued that hydrotesting damages the equipment even if it was serviceable. Further, it was argued that 25- to 50-mm insulation would hide any bulges that would have corresponded to the thinning associated with the fatal event.

Two of the forensic engineering questions posed by the defense team were how large could an area of the thinned-out pipe (0.15 mm) become and remain intact during a hydrotest, and what would be the resultant radial displacement (or size) of "bulge"? Given the bulges are permanent deformations and are beyond the elastic limit, traditional calculations would not be appropriate. FEA would be required. The original team determined a hydrotest pressure of 470kPA (68 psig) at 20°C (68°F), based on ASME code requirements for the as-designed, or uncorroded, equipment. The specified pressure for the theoretical hydrotest was accepted by the prosecution. The previous hydrotest requirements using the original design code were not presented.

Original Engineering Team's Report

The original team's report indicated the thinned region approximately 180 mm (7.0 in.) in diameter with a 3:1 transition between 7 mm and 0.15 mm could support the pressure. The reported resultant bulge was 13.8 mm (0.54 in.). The conclusion was this 13.8-mm bulge distributed over a 180-mm diameter on a 426-mm diameter pipe would not be noticeable under the insulation. This conclusion supported the defense's theory.

The client, however, questioned these results. Based on engineering experience, it did not seem likely a region that thin could be as large of an area as reported by the original team. This resulted in additional forensic analysis of the pipe, which reportedly could not substantiate sections of thinned pipe greater than a few square millimeters. This conflicted with the conclusions of the original report. Given the potential consequences of a forensic engineering report having significant discrepancies, a third-

party engineering team was tasked to review the methods and results.

The material properties are based on chemical and mechanical tests. The yield strength was 240 MPa (35,000 psi) with an ultimate strength of 413 MPa (60,000 psi) and elongation to rupture of 30% (ASTM 2002). The maximum allowable stress at 20°F to 200°F, or ambient temperature for hydrotest, is 20,000 psi per process piping code ASME 31.3.

The conventional linear calculation for circumferential (hoop) stress is:

Stress = Pressure × Radius ÷ Thickness

This has no design margin or other considerations, unlike the code calculations. It is suitable for comparison to FEA results in the linear range, or below yield. Using conventional linear hoop stress calculations, stresses for the thinned (0.15-mm) and non-thinned (7.0-mm) sections are:

Stress (thinned) = 68 psig × 8.4 in. ÷ 0.0059 in.
= 96,814 psi stress (667.5 MPa)

Stress (non-thinned) = 68 psig × 8.4 in. ÷ 0.276 in.
= 2,070 psi stress (14.3 MPa)

The calculated thin section stress is well above the yield strength of 35,000 psi. Linear methods are insufficient. The stress for the non-thinned section is 2,070 psi, which is well below the ASME allowable stress of 20,000 psi. While this only shows code compliance to the ASME code and not the original design code, it does indicate the design is generally sufficient with respect to hydrotesting.

Figure 3 is a code calculation from BPVC for wall thickness. Note when compared to theory, it has an additional variable ("E") for joint efficiency per specified criteria, as well as an additional pressure-based consideration

(1) Circumferential Stress (Longitudinal Joints). When the thickness does not exceed one-half of the inside radius, or P does not exceed $0.385SE$, the following formulas shall apply:

$$t = \frac{PR}{SE - 0.6P}$$

Figure 3
ASME code calculation for thickness of a shell under internal pressure, BPVC, Section VIII, Div. 1, UG27[4].

in the denominator ("0.6P") — or 60% of the design pressure. These are explicit design margins in the code calculations when compared to the classic "t = P×r ÷ stress". The value for S, or "allowable stress," comes from Section II of BPVC, as opposed to being selected by the user from material data. This is an example of an implicit design factor, as it limits the allowable stress to a conservative, reliable value, instead of being selected by the engineer. These three elements deviate from pure theory and demonstrate implicit and explicit design margins within the code for just the wall thickness. Similar implicit and explicit design margins are throughout the code calculations referenced codes to include the method for generating stress-stain curves.

The original team used nonlinear FEA, which was appropriate. However, the original team applied ASME FFS-1 to develop the FEA models in a manner similar to their past work in assessing process equipment fitness for service. This was an inappropriate decision because assessing whether modified or damaged equipment is "fit for service" for a given period of time (working within the code's envelope) is not the same as determining failure conditions (working outside the code's envelope).

Use Conventional Calculations to Confirm Numerical Models

The original team correctly realized linear methods are insufficient. While this problem requires nonlinear material response to address question regarding how much deflection could occur, it is important to ensure the models have correct boundary conditions, mesh density, and are otherwise appropriate before applying nonlinear conditions. Recommended practice is to use conventional calculations, then linear FEA, then nonlinear FEA[15].

In this case, the equation for circumferential stress (stress = P×r÷t) calculates the stress in a uniform pipe wall. This analysis centers upon discontinuities. A thinned section of piping is a rounded discontinuity with variable thicknesses. This does not lend itself to a linear solution. However, a simplified geometry can be used to estimate a linear response using conventional methods. A flat, elliptical disc can provide an approximation to use to evaluate linear FEA. In this case, the linear FEA displacement can be bracketed with "fixed disc edge" and "simply supported disc edge[20]."

A rounded section is stiffer than a flat plate; therefore, the calculations from Roark's[20] should have more deflection than the linear FEA. These calculations are more complex than typical code calculations but can still be done

using traditional means. The calculations were solved using MATHCAD, an equation modeling program (see **Figure 4a, Figure 4b**, and **Figure 4c)**.

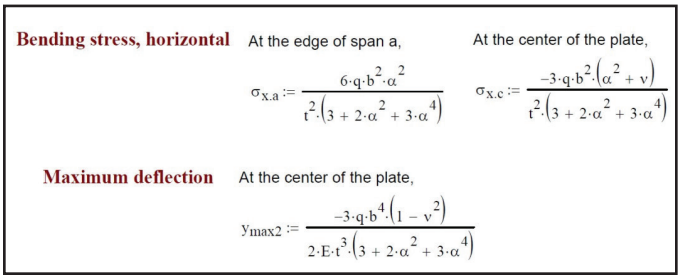

Figure 4a
Equations for a flat elliptical disc, fixed edges. Table 24, Eqns 32a[20]. The full set of variables and units is listed in Table 24 of the reference.

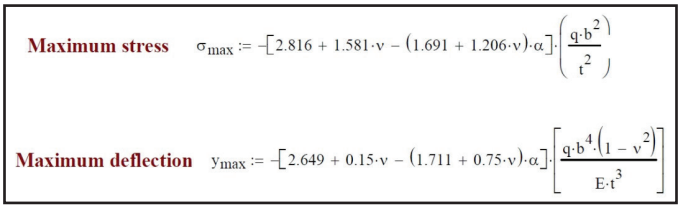

Figure 4b
Equations for a flat elliptical disc, free edges. Table 24, Eqns 32b[20]. The full set of variables and units is listed in Table 24 of the reference.

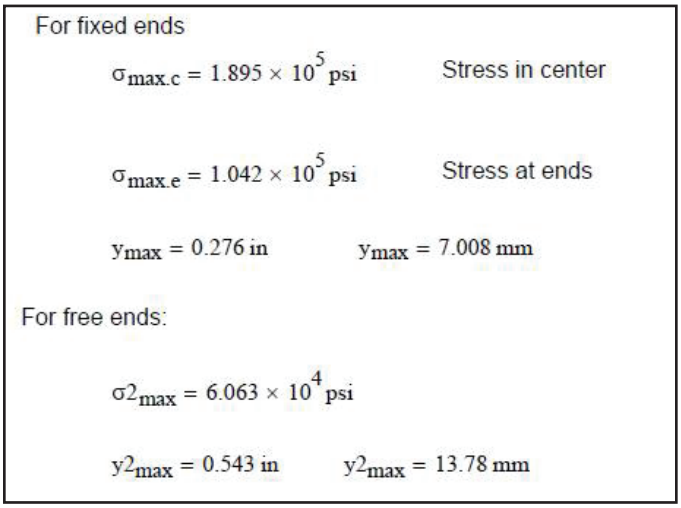

Figure 4c
Results for linear equations for a 180×215 mm (7.08×8.46 in.) long flat elliptical disc. The results for the "fixed ends" assumption was 7.0 mm (0.276 in.) and a stress of 1,306 MPa (189,500 psi). The results for "free ends," or the edges form a perfect plastic hinge with no contribution from the pipe wall, is 13.8 mm (0.543 in.) and a stress of 413 MPa (60,000 psi.) The stresses are well over the 241 MPa (35,000 psi) yield strength, indicating nonlinear analysis is needed even without considering the curvature of the pipe. The most significant result is the value of 13.78 mm of outward deflection, which is almost the same as the original team's nonlinear FEA deflection of 13.4 mm.

The fixed edge assumption keeps the thinned section in tension with no edge rotation. This is similar to a rigidly cantilevered beam. The simply supported edge assumes the edges are free to rotate. Normally this would be associated with a "simply supported" end condition, but in this instance, it also approximates a plastic hinge located in the 3:1 transition section. Based on given geometry and loads, the edge of the thinned section will form a plastic hinge, which is closer to a "free" than "fixed" condition[21]. A plastic hinge is a highly localized permanent (plastic) bending on a loaded structure creating a pivot[22]. This cannot be directly modeled in linear FEA. While the thinned section is part of a pipe and not "flat" (the stated assumption in the calculations), the values from flat disc calculations should provide the investigator an approximate solution to compare to the linear FEA.

In this case, the calculations of the 180×215 mm diameter thinned region showed deflections of 7 mm with fixed edge and 13.6 mm for the simply supported edge. The linear FEA of the geometry should have returned deflections below the "flat disc, fixed edge" solution because a plastic hinge cannot form in a linear analysis, and the rounded wall is stiffer than the flat disc. There was no report of linear calculations, nor a linear FEA to check the boundary conditions and assumptions or a report of using conventional code calculations. The original team apparently went directly to nonlinear FEA.

The reported nonlinear FEA deflection of 13.8 mm is almost the same as the linear "simply supported, flat disc" deflection of 13.6 mm (**Figure 4c**). This is highly significant with respect to material science. The linear assumption is typically valid to a 0.3 to 0.4% strain with steel — the "elastic region" below yield. A linear FEA solver returns increasingly unrealistically high stresses and unrealistically low strains above yield, whereas an implicit nonlinear solver will accurately model results above and below yield until the structure becomes mathematically unstable, such as fracturing.

The ASTM standard for A106 Grade B specifies a minimum of 30% elongation at failure[23]. The nonlinear FEA deflection should be significantly greater than the linear models, due to having about 100 times more strain allowed than the linear model using only the modulus of elasticity. If the linear calculations are within an order of magnitude of the nonlinear FEA, despite stresses being significantly above yield, it should cause the engineer to question the material models, boundary conditions, and calculations.

Materials and Failure Theory

Linear FEA uses the modulus of elasticity to calculate stress and strain. Implicit nonlinear FEA uses the true stress-strain curve, which includes the linear (or "elastic") and nonlinear material response. The original team used the code-specified method to create a curve up to 10% strain, instead of the full 30% in the material specification. It appears the original team used the method shown in Appendix B of FFS-1 to create a stress-strain curve[8]. This is the same method used in Section VIII, Div. 2, Annex 3D to create a stress-strain curve[4]. In both cases, the code intent is to work within the code's envelope and is not intended to correspond to a given failure event. It uses a series of tables applied to an equation to provide a working approximation of the true stress-strain curve as opposed to developing a curve validated by material testing.

A significant error occurred with the original team did not include the required step 3-D.13, which would have provided the plastic region from 10% strain to failure. The original team simply extended the top of the curve in a flat line to ASTM-specified minimum strain at ultimate strength. This not only resulted in a stress-strain curve atypical of any steel, but it also resulted in a mathematical discontinuity.

The third-party engineer team could not reverse engineer the provided information to replicate the original results using the original teams' stress-strain curve and loads, despite using multiple FEA packages. Since the results were not reproducible, the third-party team was subsequently directed to develop an independent analysis. Literature information for A106 Grade B[23,24] was used for the material specifications. The engineering stress/strain was converted to true stress strain[25] in lieu of the ASME pressure vessel code algorithm.

A comparison of the ASME "original curve" and the third-party team's "engineering" and "true" stress-strain curves is shown in **Figure 5**.

Detecting thinning and other defects is a long-standing industry concern. Methods for using Castilgiano's elastic strain energy theory to detect pipe thinning have been correlated to linear FEA results[26]. This method can be extended through the full elastic-plastic stress-strain curve. Integrating the stress-strain curve provides the total strain energy per unit volume, per Maximum Distortion Energy theory, also called von Mises failure theory.

Variations in the curve change the predicted failure point. One example of applying this failure theory is using annealed stainless-steel wire rope in vehicle arresting barriers. While minor difference in stress strain curves are not significant when the design intent is to operate primarily within the elastic range, minor changes in the full stress-strain proved to be catastrophically inaccurate in predicting failure points for life-safety equipment[27], which correlates to predicting the failure using minimum material specifications.

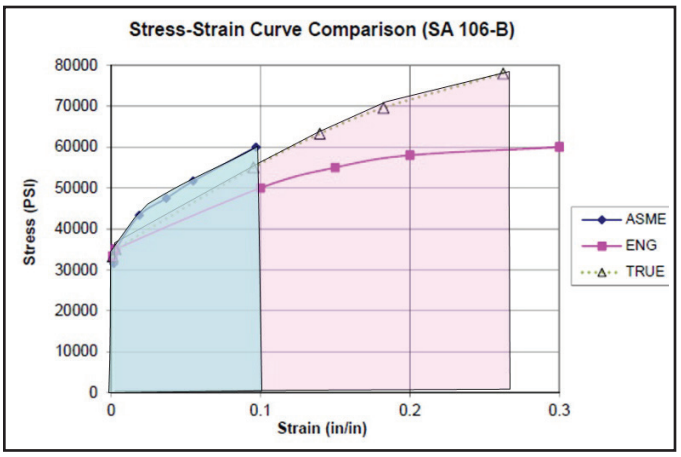

Figure 5

A106 Grade B carbon steel stress-strain curves. The red dashed line represents the original team's stress-strain curve. The "ASME" curve by the original team was only calculated to about 10% strain, then the original team extended the curve horizontally to the ASTM-specified minimum strain of 30%. This creates a discontinuity where 60,000 psi is valid from 10% to 30% strain, instead of having a unique strain value. The third-party team used material-specific data[23] to develop the engineer stress-strain, then calculated the true stress-strain curve[25].

The area under the "original curve" (blue area plus portion under the horizontal dashed line) is 5% more than the area under the "true" stress-strain (pink) due to extending out to the engineering strain maximum, instead of the true strain limit. The method to determine the true strain limit is the prescribed method per ASME BPVC Section VIII, Div. 2., 3-D.13[4] or understanding the Ramberg-Osgood method[25] as part of material theory.

In discussion with the original team, the justification for their decisions was focused on the "use of the code." They had conducted no calculations by other means to check their work nor to predict the FEA response prior to developing the models. Instead, Section 5.2.4.4. was cited. This section states if the elastic-plastic analysis converged, it meets the criteria for "plastic collapse[4]."

As discussed earlier, the original team neglected the underlying assumptions and theory regarding the code-

generated material curve. They also neglected to consider the method using the code-generated curve includes explicit load multipliers, shown in **Figure 6**, where each load combination has some form of multiplier intended to keep the end result within the design envelope shown in **Figure 1**. A code-generated stress-strain curve does not need to be precise because it was only intended to be a tool for keeping the design within the design envelope. It is not intended for mapping accurate displacement for a load or predicting failure. Applying fundamental pressure vessel theory and understanding the von Mises strain energy failure theory would have likely guided the original team to a more accurate (and defensible) report.

Revised Finite Element Analysis

A nonlinear solver accounts for the nonlinear material mechanics. Explicit nonlinear FEA is capable of modeling failure directly to include structures fragmenting or breaking. Implicit nonlinear FEA is more readily available and is the method specified by ASME. "Large strain option" was used in conjunction with "von Mises plasticity" analysis, using the true stress-strain curve in **Figure 5**. This allowed the elements to displace in a manner more consistent with steel with stresses above yield.

The third-party engineer team conducted its own iterative analysis regarding the maximum span of a paper-thin 0.15-mm thinned section. A solid model section was developed with a 3:1 transition to an initial 5.0-mm diameter thinned section. It assumes a perfectly smooth and uniform surface without defect or other stress concentrator, plus an equally smooth transition section.

A series of analyses iteratively increased the dimensions of the thinned section in order to determine the largest thinned regions, which would withstand the hydrotest pressure in order to develop the largest possible deformation to test the prosecution's theory. The largest stable region was an oblong shape about 8 mm (0.315 in.) in radius, slightly longer along the pipe run direction than the circumferential direction. Under pressure the thinned section bulged about 3.5 mm (0.137 in.) outwards. Note: Earlier iterations, all smaller than this last one, had deflections that were bracketed by the "fixed" and "free" calculations from Roark's[20].

This outwards bulge depends on the previously stated idealized assumptions. It is unlikely to occur outside of theory due to roughness or imperfections acting as stress concentrators. This represents the outside theoretical bound of the structural response of the geometry and material's minimum specifications[22].

The next iteration increased the diameter by 0.5 mm and did not converge. It was concluded this idealized geometry was the largest "thinned patch." It was more likely

Table 5.5 – Load Case Combinations and Load Factors for an Elastic-Plastic Analysis

Design Conditions	
Criteria	Required Factored Load Combinations
Global Criteria	1) $2.4(P+P_s+D)$ 2) $2.1(P+P_s+D+T)+2.7L+0.86S_s$ 3) $2.1(P+P_s+D)+2.7S_s+(1.7L \text{ or } 1.4W)$ 4) $2.1(P+P_s+D)+2.7W+1.7L+0.86S_s$ 5) $2.1(P+P_s+D)+1.7E+1.7L+0.34S_s$
Local Criteria	$1.7(P+P_s+D)$
Serviceability Criteria	Per User's Design Specification, if applicable, see paragraph 5.2.4.3.b.

Figure 6

Table from ASME BPVC, Section VIII, Div. 2 with explicit multipliers for the various variables[4] (© 2010). It is noted the value of 2.4 associated with the Division 2 design margin is only in the first load combination. The multipliers cannot be assumed to be the explicit design margins. This table changed in the 2017 code.

than not the actual thinned section regions were smaller than the approximately 16-mm diameter region due to roughness and stress concentrators. Assessing the displacement with this geometry would be defensible, based on plastic theory indicating this was optimistically large.

These results (**Figure 7, Figure 8, Figure 9,** and **Figure 10**) were consistent with the physical evidence as well as the established science. The recovered sections of thinned material were only millimeters in length and did not appear to be consistent with the original team's report. The third-party report concluded the resulting 3.5-mm (0.137-in.) "bubbles" would not be apparent under the reported 25 to 50 mm (1 to 2 in.) of insulation that covered the failed section.

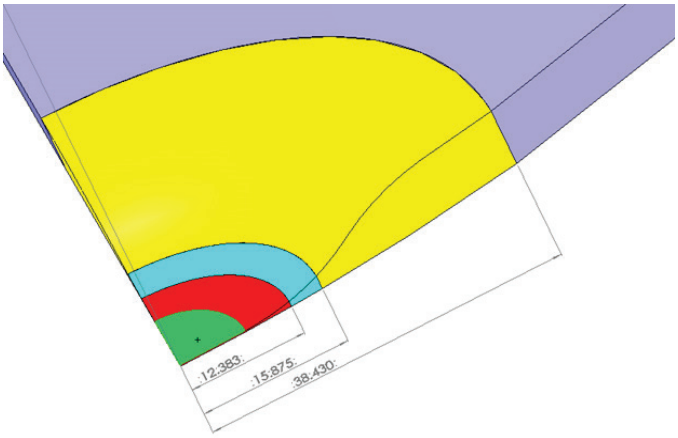

Figure 7
The third-party team determined the above geometry met the stated criteria of 0.15 mm thickness (green). The nominal thickness is 7 mm. The ellipse is 16.8 mm by 14.6 mm. The geometry is a one-quarter model using symmetry to reduce the computational size of the FEA. The thinned region's approximately 16-mm diameter is less than 1/10th of the 180-mm diameter reported by the original team.

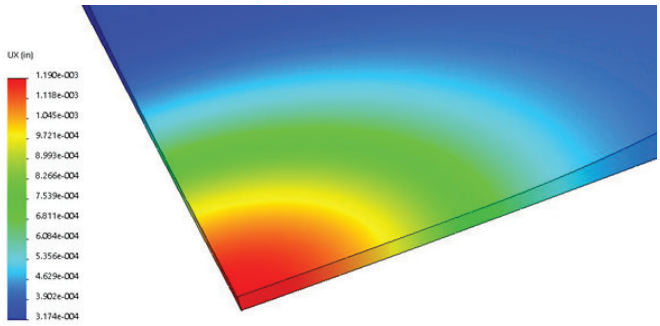

Figure 8
Linear deflection results (inches, undeformed plot) of an interim model (6.0 mm × 6.4 mm). The linear deflections calculations for the elliptical disc with fixed edges is 0.025 mm (0.0010 in.) It is with simply supported edges is 0.058 mm (0.0023 in.). These linear calculations bracket the linear FEA results of 0.030 mm (0.0012 in.).

The third-party report was accepted by the Master's Panel and was part of an overall defense against the prosecution's case regarding the facility's published maintenance procedures. The report provided hard numbers to counter the prosecution's assumptions. Arguments were made regarding "accepted engineering practice using minimum material standards" as opposed to the blister's dimensions being part of a definitive finding of a failure threshold. The significance is while the original team and the third-party team had the same conclusion that the deformations would not be visible under the insulation, it is more likely than not that the anomalies in the original report would have eliminated the direct engineering rebuttal of the prosecution's theory. It was also offered that the original legal arguments were vulnerable due to an imprecise understanding of the original report. It is the assessment of the defendant's legal team that the accepted third-party engineering report and associated work was indispensable in refining and presenting their case.

Conclusion

Engineering codes and standards are vital tools for engineers to master. They explicitly evaluate compliance and implicitly provide the reliability associated with the codes and standards when all of the elements of the code

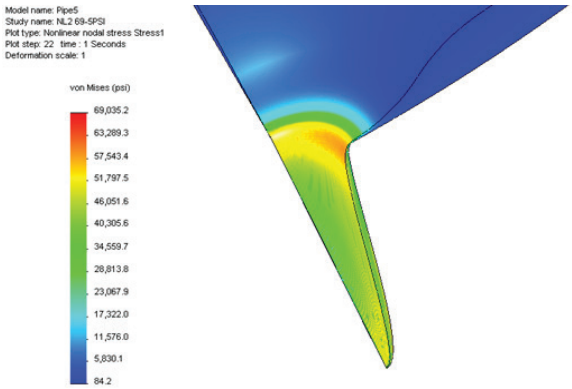

Figure 9
Nonlinear von Mises stress results (psi) of the final iteration. This plot shows the deflection to scale. This is significantly different that the original team's prediction. The high stress regions are localized to the formation of the plastic hinge and show far greater stress and strain than the rest of the thinned section. The stress in the non-thinned section is around 2,000 psi, which is consistent with linear calculations. The paper-thin section of the one-quarter model "blisters" outwards in tension while the thicker 3:1 transitional area forms a plastic hinge, pivoting radially outwards in response to the load. Increasing the size of the thinned section another millimeter resulted in the model failing to converge. Note the magnification and angle of this view of a one-quarter model gives a distorted view of the shape. The view was chosen for the clarity of the stress distribution.

methods are met. These standards are part of an overall system to provide the reliable, consistent, and safe application of engineering within the design envelope. This case illustrates how an investigator must look beyond the traditional engineer role of "design to the code." The investigator must understand the underlying theory and assumptions of codes as well as tools such as the Finite Element Method in order to understand the differences between analyzing a failure versus analyzing for code compliance. Failing to understand applicable theories and properly apply them could result in failing to meet court guidance for expert testimony, such as Federal Rule of Evidence 702, and potentially disqualify the testimony. While this case study focuses on ASME pressure vessel codes, the same principles can be applied to other engineering codes and standards.

Acknowledgment

I would like to thank Professor A.J. McPhate, PE, for his review of this paper and continued guidance regarding computer modeling and failure analysis.

References

1. R. G. Kammer. "The Role of Standards in Today's Society and in the Future." https://www.nist.gov/speech-testimony/role-standards-todays-society-and-future (accessed 02 January 2018).

2. B. Kemper, "Evil intent and design responsibility," Science and Engineering Ethics, vol. 10, no. 2, pp. 303-309, jun 2004, doi: 10.1007/s11948-004-0026-4.

3. Boiler and Pressure Vessel Safety Act, S. o. Illinois § 430 ILCS 75, 2017.

4. Boiler and Pressure Vessel Code, ISBN 0517-5321, ASME, New York, 2010.

5. W. J. Sperko, "Reduction of Design Margin ("Safety Factor") in the ASME Boiler and Pressure Vessel Code in the 1999 Addenda," Sperko Engineering, June 1, 2000 2000. [Online]. Available: http://sperkoengineering.com/html/articles/Margin.pdf.

6. D. A. Osage and J. C. Sowinski, "ASME Section VIII—Division 2 Criteria and Commentary,"ASME PTB-1, 2007.

7. Process Piping (B31.3-2008), Engineering Code 0791831507, ASME, New York, NY, 2008.

8. Fitness-for-service (API 579/ASME FFS-1), ISBN 0791831027, API and ASME, Washington, D.C., 2007.

9. T. Seipp and M. Stonehouse, "Writing and Reviewing FEA Reports Supporting ASME Section VIII, Division 1 and 2 Designs: Practical Considerations and Recommended Good Practice," in ASME 2014 Pressure Vessels and Piping Conference, 2014, vol. Volume 3: Design and Analysis, V003T03A076, doi: 10.1115/pvp2014-28958.

10. J. R. Farr and M. H. Jawad, Guidebook for the design of ASME section VIII pressure vessels. New York: ASME (in English), 2010.

11. K. R. Rao, Companion guide to the ASME boiler & pressure vessel code : criteria and commentary on select aspects of the boiler & pressure vessel and piping codes, 2nd ed. New York: ASME Press (in English), 2006.

12. D. R. Moss, Pressure vessel design manual : illustrated procedures for solving major pressure vessel design problems. Amsterdam; Boston; Heidelberg: Elsevier/Gulf Professional (in English), 2004.

13. D. Renfroe, "Forensic Engineers Preparing to Meet the Challenges To Credibility in a Court of Law," Journal of the National Academy of Forensic Engineers, vol. XXIV, no. 1, p. 8, June 2007 2007.

14. Federal Rules of Evidence, § 702 Testimony by Expert Witnesses, 2014.

15. O. C. Zienkiewicz and R. L. Taylor, Finite Element Method: Vol. 2: Solid and Structural Mechanics. Vol. 2. (in English.), 2000.

16. B. Kemper, "Jurisdictional Acceptance of Non-ASME Pressure Vessels for Human Occupancy," in Joint ASME/USCG Workshop on Marine Technology & Standards, Arlington, Virginia USA, July 2013 2013: ASME, doi: 10.13140/2.1.1144.9927.

17. K. Karpanan and W. Thomas, "Local Failure

Analysis of HPHT Subsea Tree Components due to Triaxial Stress," in ASME 2014 Pressure Vessels and Piping Conference, 2014, vol. Volume 5: High-Pressure Technology; ASME NDE Division; 22nd Scavuzzo Student Paper Symposium and Competition, V005T05A009, doi: 10.1115/pvp2014-28722.

18. W. T. Yaxley and W. Bracken, "Forensic Engineering Structural Failure Review By Finite Element Analysis," Journal of the National Academy of Forensic Engineers, vol. XIX, no. 1, p. 5, June 2002 2002.

19. J. W. Ozog and R. M. Frierott. (2017) The Eroding Distinction Between Strict Liability and Negligence in Illinois Product Liability Cases. IDC Quarterly. 3.

20. W. C. Young and R. J. Roark, Roark's formulas for stress and strain, 6th ed. New York: McGraw Hill (in English), 1989.

21. M. Jirásek and Z. P. Bazant, Inelastic analysis of structures. Chichester, West Sussex, England; New York, NY: Wiley (in English), 2002.

22. J. Lubliner, Plasticity theory. Mineola: Dover Publications (in English), 2008.

23. A106 / A106M-19a. Standard Specification for Seamless Carbon Steel Pipe for High-Temperature Service, ASTM, West Conshohocken, PA, 2010.

24. X. Duan, M. J. Kozluk, T. Gendron, and J. Slade, "Alternative methodology for assessing part-through-wall cracks in carbon steel bends removed from Point Lepreau Generating Station," Nuclear Engineering and Design, vol. 241, no. 3, pp. 630-637, 2011/03/01/ 2011, doi: https://doi.org/10.1016/j.nucengdes.2010.07.035.

25. ASM, Atlas of Stress-Strain Curves, 2nd ed. Materials Park, OH: ASM International, 2002.

26. V. Nascimento and L. Nunes, "Analysis of asymmetric radial deformation in pipe with local wall thinning under internal pressure using strain energy method," in Technical Committee on Solid Mechanics, Brazilian Society of Mechanical Sciences and Engineering (ABCM), 2009, p. 399.

27. B. Kemper, "Application of Annealed Cable for Vehicle Arresting Barriers," in Safety Engineering and Risk Analysis, 2002 2002: ASME, doi: 10.1115/imece2002-32464.

Forensic Engineering Analysis of Residential Underdrain Design Methodologies, Performance, and Failures

By Edward L. Fronapfel, PE (NAFE 675F)

Abstract

In 2014, the basement of a single-family home in a residential subdivision flooded. The homeowner's insurance company engaged an engineer to conduct forensic investigations, which ultimately determined that the resultant flooding was caused by blockage of an underdrain system to which the home was connected. This system included a main line in the street and a lateral that connected the underdrain to the home's foundation drain. Subsequent to this event, other homes in the subdivision reported flooding in the basements and crawlspaces. The author was engaged by the subdivision homeowners association (Common Interest Ownership Community or CIOC). The CIOC's declarations and recorded documents contained no information regarding the existence of the underdrain system. In addition, there was no clear information about the ownership or maintenance responsibility. The author's field investigations determined the underdrain was not constructed to the applicable minimum standards, and the developer did not provide adequate flow capacity for the number of homes served by the underdrain. The CIOC entered into litigation against the developer, and the author evaluated issues associated with the design, construction, transition, and maintenance of the underdrain system.

Keywords

Underdrain, foundations, cleanouts, common interest ownership community, homeowners association, video inspection, sump, sump pump, calcite, pipe blockages, forensic engineering

Background

In 2014, approximately 12 years after construction began on a development that included common areas, public roadways, parks, a clubhouse, school, and more than 1,350 residential homes located in the Front Range of Colorado, flooding occurred in the basement of a home. That home's foundation system consisted of poured-in-place concrete walls on drilled piers.

The basement foundation was constructed with a structural steel/concrete composite floor bearing on interior piers, and a crawlspace was created below the structural floor to mitigate the issues of expansive soils that were identified in the feasibility studies and the site-specific geotechnical evaluations. The foundation system, perimeter drain, common lot underdrain, and site grading were designed to reduce the potential for water migration into the soils and the subsequent damages that can occur with construction of residential lots on expansive soils. Proper control of the subsurface water was necessary to permit the home's basement to be habitable space.

In response to the flooding event, the homeowner's insurance company hired a forensic engineer, who determined that the efflorescence and water staining were representative of long-term flooding present in the structural crawlspace located below the suspended basement floor. The cause of the resultant flooding was ultimately determined to be blockage of an underdrain system. This was discovered by excavating the property from the back of the walkway to expose the lateral that was constructed from the home's perimeter drain and connected to the underdrain. This connection between the home's lateral and the underdrain was found to have been made with duct tape rather than the proper pipe fittings. The forensic evaluation of this home resulted in a further need to

Edward Fronapfel, PE, 5926 McIntyre Street, Golden, CO 80403, (303) 425-7272, efronapfel@callsbsa.com

understand the ramifications of the construction of the underdrain, its use in the subdivision, its records, and ultimately its legal (contractual) ownership because it was within the public roadway and under the public sewerage system.

Installation of underdrain systems can reduce water migration from the more porous backfill materials in utility trenches that lead to a structure. Underdrains can reduce perched water conditions that occur when water is trapped in lenses of more pervious materials. They also mitigate the negative impact of water from developed landscaping and can positively impact overall drainage conditions within a development. In addition, when combined with dendritic systems, underdrains can aid in lowering the ground water table. In order to evaluate the need for and properly design an underdrain system, the site's geology must be reviewed in combination with the effects of the development on the original materials. An example of one jurisdiction's underdrain criteria is shown below.

City of Colorado Springs, "Colorado Springs Utilities Groundwater Underdrain Voluntary Criteria – 2015," Section 13.01 "General," states the following:

"The purpose of the underdrain system is to provide a method for conveying subterranean groundwater from around a structure/building foundation via gravity to an acceptable discharge point in a drainage channel or storm drain. All new residential developments within the City of Colorado Springs shall install a gravity underdrain system, unless a variance is given by the City of Colorado Springs, Engineering Division. Foundation perimeter drains, whether inside or outside the foundation walls, shall be connected by gravity to the underdrain main line via an underdrain service line."

Feasibility studies provided by geotechnical engineers generally specify the conditions that warrant the use of an underdrain. The incorporation of that underdrain into the subdivision design properly begins with the Official Development Plan and is continued throughout the preparation of land development plans, including utility layouts, home layouts, overlot grading plans, and independent lot drainage plans.

The design of underdrain systems is conceptually similar to the design of sewers and water lines, and underdrain lines must be sized in accordance with the number of homes, floor plan areas, and number of linear feet associated with the foundation types that the systems will serve. The diameter and slope of underdrain lines must be adequate for the expected flow rates that are developed from the ground water conditions that will occur post-development.

The underdrain system collects, directs, and conveys these flows within the pipes. In order to reduce maintenance, the pipe size and slope are designed to provide self-cleansing velocities that will minimize deposition and sediment buildup. The underdrain system can be supplemented at each home with a back-up sump pump. The pump should not activate in normal usage. However, if the system has an overcharge of water beyond its capacity — or if the system is clogged and backs up — the sump provides short-term protection to the foundation while the system can be examined. This is similar in concept to the use of a primary and secondary roof drain system; when the observable secondary drain activates, maintenance personnel can respond to the issues.

Following this first reported instance of flooding, subsequent water intrusion issues, such as flooded basements/crawlspaces and excessive sump pump operation (passive systems should not require the use of pumps), were reported to have occurred at more than 60 residences within the subdivision. The owners of the original home where the flooding was reported ultimately sought legal recourse from the CIOC and the city regarding the underdrain lines. The homeowners were not able to repair the underdrain portion that was in the roadway and the connection to the lateral without involvement of the CIOC or the city. During this process, it was determined that the failed portion of the underdrain responsible for the flooding of the home was located entirely within the right-of-way owned by the jurisdiction. No portion of either the private perimeter drains around the foundation or the 4-in. lateral line to the street was found to have contributed to the flooding.

In order to evaluate the system, the CIOC engaged a geotechnical engineering firm to provide a preliminary report of the system and engaged legal firms to review their governing documents. Based on those initial reviews, it was determined that the original construction of the underdrain and the laterals was improper. In addition, the rights of the common interest community were not clearly assigned. Upon discovery that the underdrain was to be controlled by the community — and that the city would not partake in the repairs to the system — the CIOC entered into a legal dispute with the subdivision's developer to determine the ownership, transference, responsibilities, and jurisdictional issues.

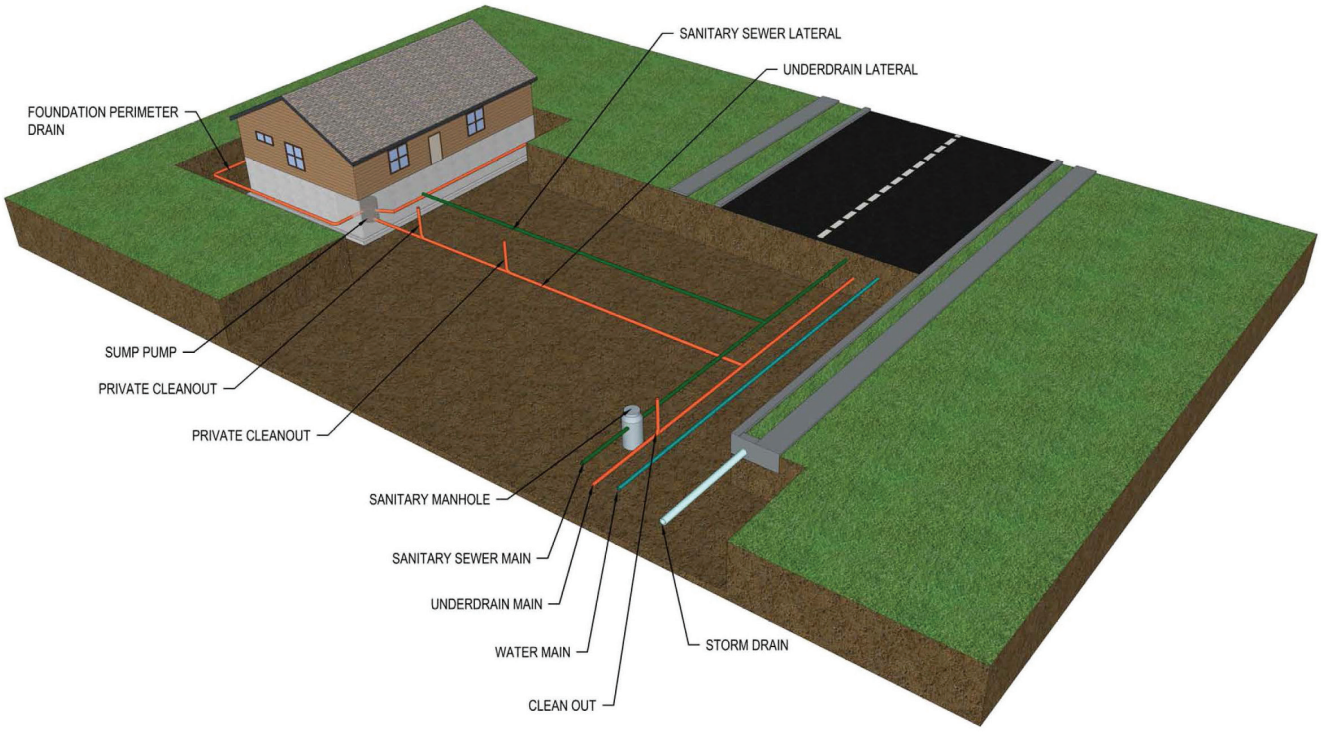

Figure 1
Schematic layout showing typical building perimeter drain, lateral and underdrain located within the right-of-way under the street.

The finding of the forensic engineering work necessary in the litigated matter determined that of the 1,350 homes in the subdivision, 1,180 (87%) were connected to the common underdrain. The complete as-constructed collection system generally consisted of 4-in. perforated drains installed around the perimeter of each home, main underdrain lines in the streets and laterals connecting the two systems. The 4-in. perforated foundation drains terminated at a sump pit in the basement of each home or at tee connections along the perimeter of the foundations, and 4-in. non-perforated laterals connected these to the main underdrain lines in the streets. The underdrains were installed alongside and slightly below the city-owned sanitary sewer lines, and generally followed the sanitary sewer laterals from the homes for discharge into the subdivision-wide underdrain located under the underdrain in the street (**Figure 1**).

The subdivision was divided into four separate areas (**Figure 2**), each served by a separate, dedicated underdrain system. These four separate systems served 12, 201, 678, and 289 residential structures.

Since the individual homes were constructed by multiple builders, varying construction techniques were used for the residential buildings in each area. The municipality required that a site-specific geotechnical report be provided for each individual lot; however, the builder of each home may or may not have relied on the findings and recommendations contained in those specific geotechnical reports.

The underdrain systems were generally co-located (installed below and adjacent to) with the sanitary sewer mains. To provide access to the underdrain, cleanouts were generally constructed near the sanitary sewer manholes. The underdrain systems were intended to discharge to the surface at specific locations within drainage easements via non-pressurized gravity flow. At least one builder provided sump pumps in the passive pits as a redundant backup in the event of a failure or overwhelming of the underdrain or perimeter drain systems.

A number of builders and homeowners also installed sump pumps in response to high water levels in the pits or actual flooding of the basements. The methods of warranty request documents, CIOC reports, disclosure of previously unreported incidents, and other potentially forensically important documents were reviewed. These reviews resulted in an imperfect record resource that was used in determining the underdrain's performance.

The forensic evaluations also included review of many

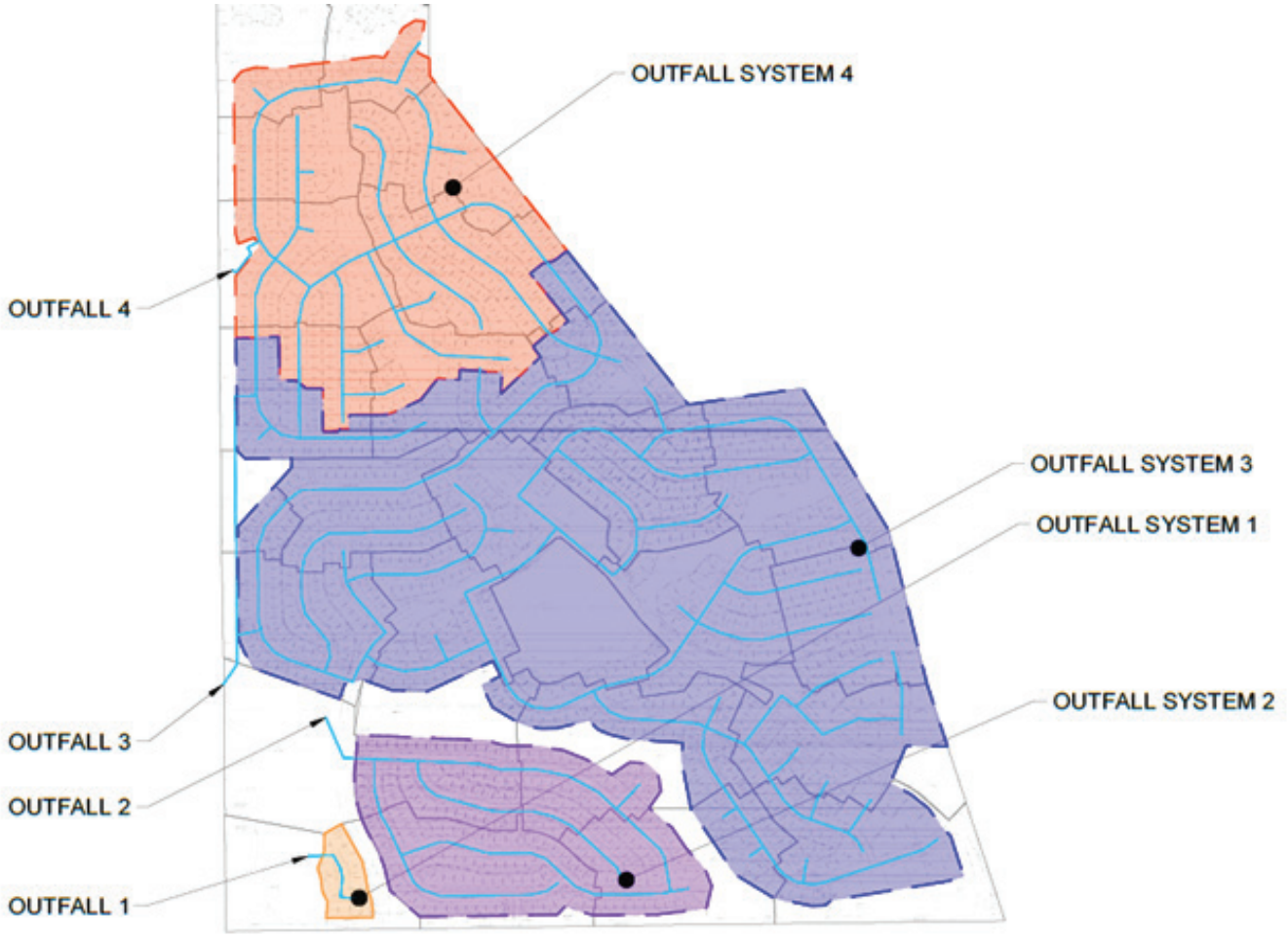

Figure 2
Identification of separate underdrain systems. Each system is labeled by an outfall number, and outfall systems 1, 2, 3, and 4 served 12, 201, 678, and 289 lots, respectively.

potential sources of information from multiple builders, developers' records, and reported flooding events. In some cases, where structural basement floor systems were constructed, flooding of the crawlspaces below the visible floor areas was not previously reported because the owners were unable to see below the floors without directly accessing them.

Determining the ownership of the systems was also critical to the forensic analysis of the subdivision and the underdrain systems. Detailed review of the CIOC's declarations, plat maps, and other recorded documents revealed no information indicating the presence of the underdrain systems or the CIOC's responsibility to own and maintain these systems. However, the underdrains were shown on the Civil Sanitary Sewer Construction Plans, and review of aerial mapping during construction indicated that they were being placed in the street system.

Approach

To provide a comprehensive review of the system, the forensic evaluation began with an analysis of publicly available documents. Once the project entered the judicial system, further information could be obtained (in part). Several aspects of the project (involving its design, construction, and documentation) were identified for forensic investigation, including:

1. Review of applicable design codes, standards, criteria, and other reports.
2. Review of the design of the underdrain system.
3. Review of documentation from the developer to the CIOC at turnover.
4. Inspection of locations where problems were reported.

5. Inspection of the as-constructed underdrain system.
6. Documentation of the findings.
7. Repairs.
8. Design flows.
9. Applicable codes.
10. Hydraulic analysis.

Applicable Codes

Review of the Jurisdiction with Authority's "Standards and Specifications, Water, Sanitary Sewer and Storm Drainage Infrastructure," applicable at the time of design and construction, determined that underdrains were never (and will never be) maintained by the jurisdiction — and that these systems remain private in perpetuity. The developer's obligation was therefore to provide the CIOC with a properly designed, constructed, and maintainable underdrain system.

The developer's obligation was also to clearly inform the CIOC that the private underdrain system would become its property, and that it would be responsible for the system's maintenance and all costs associated with damages due to potential failures of the system. The underdrains should have been transferred patently to the CIOC in the Declaration of Covenants, Conditions and Restrictions, wherein the designation of lots, common elements, and limited common elements are transferred to the CIOC.

Proper transfer of ownership allows the receiving entity, the CIOC, to set budget guidelines and develop a complete understanding of the system's needs. These include legal access to the lines as well as performing maintenance duties and budgeting for regular observations, repairs, and replacement of the lines on the municipally owned lots and within those areas where the underdrain laterals transition from the right-of-way to the individual properties. Proper transfer of ownership also allows for the legal discharge of the underdrain flows into the storm drainage infrastructure owned by other districts or municipalities. The forensic investigations established that the CIOC was never informed of the existence of the underdrains or the fact that it was the owner of the system and required to maintain it.

Design of the Underdrains

Several geotechnical investigations and reports were provided prior to design and construction of the subdivision. The earliest, dated August 1999, found that the soil and groundwater conditions on the site required the construction of foundation drains around the buildings' foundations and an underdrain system in the streets. The report went on to state that the underdrains should be smooth, perforated, or slotted polyvinyl chloride (PVC) pipe and should be installed below the sanitary sewers at a minimum slope of 0.5%. The report also noted that a single 4-in. PVC line would be adequate for the flows expected from up to 100 homes and that the system should be provided with cleanouts. This geotechnical report also noted that the underdrains were to be maintained by the CIOC or another entity. This report was not provided to the forensic investigator in a timely manner but served to confirm research.

The forensic evaluation included contact with the original geotechnical engineer, which resulted in the discovery that the engineer was providing expert consulting to the developing entity as a non-disclosed expert. The legal ramification of the original designer working on the case would likely have prejudiced those opinions, making it difficult to obtain any information that was lacking in the public or produced files. The engineer provided a statement noting that the standards used around the state could not be relied on in this case. Without telling the forensic evaluator of their present involvement in this matter, that information would ultimately be used in the discovery and depositions.

The Jurisdiction with Authority's "Standards and Specifications, Water, Sanitary Sewer and Storm Drainage Infrastructure" stated that the underdrains were required to be designed by a registered professional engineer. In addition, the standard drawings contained in that document required a minimum underdrain size of 6-in. PVC.

The forensic investigations determined that the civil engineer's Sanitary Sewer Construction Plans correctly referenced the municipality's standard underdrain cleanout detail, which clearly showed that the underdrains and cleanouts were required to be constructed of 6-in. PVC pipe. However, within the same note, the civil engineer specified that the underdrains were required to be constructed of solid 4-in. PVC pipe. This discrepancy shows a lack of understanding on the part of the designer regarding underdrain systems. In addition, no engineering calculations were provided for review by the municipality or in the files provided to the developer regarding determination of the flows into the underdrain system from the perimeter drains in each lot or the combined flows into each branch

of the underdrain system and ultimately into the outfall of each underdrain system.

During discovery, it was found that the underdrains were, in fact, never designed for any standard rates of flow. In lieu of performing detailed geohydraulic and hydraulic calculations, a prescriptive approach similar to water system or sanitary sewer design could have been used to size the underdrain pipes. Typically, a geotechnical engineer would recommend a 4-in. diameter underdrain line for the first 100 lots in a region when ground water is not a consideration. Reference is made to reports prepared by geotechnical engineering firms in Colorado for various communities in the Front Range area of Colorado. However, because of the litigation of this project, the names of those firms cannot be disclosed. These geotechnical reports contain preliminary underdrain sizing tables that provide minimum required pipe sizes based on the number of residences connected at varying longitudinal slopes.

The jurisdiction did not have prescriptive requirements for the sizing and layout of the underdrains and instead relied on engineering to develop this system. Therefore, the geotechnical report had to provide sufficient information and forecasting of the developed effects on the lots and subdivision to determine the flow that would occur from each home's foundation drain system.

Using Manning's equation, the steady state hydraulic capacity of a 4-in. PVC line at 2% slope is 0.32 cfs (144 gpm). Per **Figure 3**, a 4-in. line would have the capacity to serve 100 lots; therefore, each lot would generate approximately 0.0032 cfs or 1.4 gpm over 24 hours. Performing these reverse calculations for non-pressurized flow would have allowed for design of the underdrain system as the number of homes served increased. The largest system constructed on the site, which serves 678 lots, would have been constructed with lines starting with 4-in. pipe for the first hundred homes and increasing the size of the lines for each subsequent 100 homes.

PRELIMINARY UNDERDRAIN SIZING

SLOPE = 0.05 (0.5 PERCENT)				
Pipe Size (in)	4	6	8	10
Maximum Number of Residences	50	100	200	400
SLOPE = 0.01 (1.0 PERCENT)				
Pipe Size (in)	4	6	8	10
Maximum Number of Residences	75	150	300	600
SLOPE=0.02 (2 PERCENT)				
Pipe Size (in)	4	6	8	10
Maximum Number of Residences	100	300	600	1200

If this underdrain system is planned to connect to up-gradient systems, larger

Figure 3
Preliminary underdrain sizing guidelines from a geotechnical report for a middle school in Colorado Springs, Colorado. These preliminary sizing guidelines show that a 4-in. underdrain at 2% slope is required for 100 residences.

This 678-lot system would have therefore required a collection system that would convey the full flows and would have required pipes increasing in size from 4-, 6-, 8-, 10-, and 12-in. lines. Similar to the way the sanitary sewer system was designed for the subdivision with the pipe sizes expectedly ranging in size from 4 to 18 in., the underdrain sizing methodology requires determination of the number of units served, the per capita flows from each lot and an estimation of the quantity of water infiltration from the ground surrounding each home. An example of a codified underdrain sizing requirement can be found in the City of Longmont Municipal Code, Section 15.05.070 "Underdrains," which states:

"C. Area underdrains and underdrain collection systems.

1. Design and plan approval.

a. The area underdrain or underdrain collection system must comply with all applicable city, state, and federal regulations in place at the time of construction.

b. A professional engineer registered in the State of Colorado must design, and stamp the area underdrain plans, underdrain collection system plans, and underdrain report. The system shall be designed in consideration of seasonal high groundwater levels anticipated at the project site.

c. All area underdrains and underdrain collection systems shall have a positive gravity outlet piped to an approved underdrain collection system, to a storm sewer, or to a drainage channel. The use of any conveyance system other than a gravity system, such as a lift station, must be approved in writing prior to installation by the public works and natural resources director or designee.

d. Area underdrains and underdrain collection systems, six inches in diameter or smaller, placed adjacent to and in the same trench as sanitary sewer mains shall be rigid walled nonperforated pipe and shall have a minimum clearance of one foot from the side of the underdrain pipe to the side of the sanitary sewer main pipe. Access points on underdrain systems are not allowed to connect to or surface into sanitary sewer manholes."

Determining the quantity of water infiltrating into the soils around the buildings must take into account the contribution of water from the loose backfills around the homes in addition to the native materials. The flow of water on the excavated cuts for each foundation can

impact downstream lots, and even the bedrock geology can change the flow rates to each individual lot. The flow rate and volume from each lot entering the underdrain are thus dependent on a number of factors that include soil permeability, building size, the duration of the rainfall events causing the infiltration, the moisture content of the soils, bedrock profiles, ground water, and even the lot's grading characteristics.

There are a number of published sources that can provide the expected flow rates to a perimeter drain. Using these published sources as a guideline, the infiltration can be estimated to range from 0 gallons per lot per day to more than 20,000 gallons per lot per day for a representative 1,000-sq-ft building footprint. In addition to the individual lot, the design of the underdrain collection system must anticipate each lot's cumulative contribution to the flow in the overall system. The cumulative flow rate would, at peak design, have to estimate the potential number of lots contributing to the system at the same time and determine what that potential number of contributing lots would be at any single event.

Duane Friend and Doug Peterson, University of Illinois Extension, College of Agricultural, Consumer and Environmental Sciences, "Land & Water," August 2005, Number 8, "Sizing Up a Sump Pump," states:

"If you're building on sandy soil, plan for a system capacity of 14 gallons per minute for every 1,000 square feet of home. If you're building on clay soil, plan for a system capacity of 8 gallons per minute for every 1,000 square feet of home."

City of Ann Arbor - Developer Offset-Mitigation Program, Guidelines for Completion of Footing Drain Disconnections, Updated November 30, 2005, states:

"A typical single-family residence in Ann Arbor contains 1,200 square feet of footprint area, most often with a standard basement depth of 5' to 8'. These structures have been found to generate an average of 4 gallons per minute (gpm) from monitoring data within the City during peak wet weather conditions."

Those same features should have been considered in the analysis by the civil engineer providing the underdrain design at the subject site. Based on this author's experience, the incorporation of infiltration from water sources pre- and post-development must be considered, and a factor of safety to ensure the longevity of the system used must also be accounted for in the design. An underdrain system would not be designed to operate at full flow conditions, and the peak capacity of the system should also be considered in the design to allow for the acceptance of risk of the system's capacity during its useful life. The system can also be diminished in capacity by long-term scale buildup. Thus, similar to the sewer system, the developed system must include a means to allow maintenance.

Upon forensic evaluation of the property, substantial sediment and hardness buildup were identified in the pipes. Laboratory testing confirmed the calcite materials within the drain line. Ultimately, the defense concluded the most likely source was the decalcification of the soils in the subdivision. The findings in this forensic analysis indicated that no original engineering work for the development was ever provided in the actual sizing of the system. In addition to the lack of engineering analysis, the construction failed to comply with both the provided engineering details or the city's requirements. There are, as mentioned, a number of prescriptive requirements, such as one Colorado geotechnical engineering firm's "Geotechnical Subsurface Exploration Program," which states:

"Geotechnical Parameters for Underdrain Design. The underdrain system(s) for the project should be designed in accordance with the parameters below. The actual underdrain layout, outlets, and locations should be developed by a civil engineer...

8) The underdrain system should be designed to discharge at least 25 gallons per minute of collected water.

9) The high point(s) for the collection pipe flow lines should be below the grade beam or shallow foundation bearing elevation as shown on the detail. Multiple high points can be beneficial to reducing the depths to which the system would be installed. The collection and discharge pipe for the underdrain system should be laid on a slope sufficient for effective drainage, but a minimum of 1 percent. (Flatter gradients may be used but will convey water less efficiently and entail an increased risk of local post-construction movements.) Pipe gradients also should be designed to accommodate at least 1 inch of differential movement after installation along a 50-ft run.

10) Underdrain 'clean-outs' should be provided at intervals of no more than 100 feet to facilitate maintenance of the underdrains. Clean-outs also should be provided at collection and discharge pipe elbows of 60 degrees or more.

11) The underdrain discharge pipes should be connected to one or more sumps from which water can be removed by pumping, or to outlet(s) for gravity discharge.

We suggest that collected waters be discharged directly into the storm sewer system, if possible.

12) Underdrain systems should be periodically inspected and flushed/cleaned as necessary. Maintenance/repairs should be performed to ensure proper performance."

Documentation Review

The forensic evaluation included a review of the CIOC's Declaration of Covenants, Conditions and Restrictions and other developer-provided documentation. These documents are required for proper identification, transition, and turnover of common elements and limited common elements from the control of the developer to the CIOC. The Municipality's Standards and Specifications, the overall and site-specific geotechnical report, and the Sanitary Sewer Construction Plans all stated that the underdrains are private and are required to be owned and maintained by the CIOC.

A review of the file found that the developer/builder provided a letter to the management company indicating that the underdrain was transferred to the CIOC. It included an engineering evaluation using a dye test to determine that the underdrain was functional. This letter and engineering evaluation were prepared near the front end of the construction of the project. Specifically, the tested portion of the underdrain was within an upstream location on the site and the letter, as written, did not inform that other underdrains had been constructed in the subdivision or that the CIOC was the owner of that system.

In the documents reviewed, two reserve studies were also discovered, both of which were prepared by the developer/builder and the management company. One reserve study pre-dated the other, and that included a fixed fee cost in a 20-year reserve projection for an underdrain. The second reserve study did not include that line item. In fact, it was provided through the management company as the official reserve study.

Based on the author's experience with common interest communities, in most controlled associations, the best interest of the community is served by the creation of a clear and comprehensive framework, which should include financial stability and budget setting guidelines. The inspection, maintenance, repair, and replacement of the underdrain system should have been fully considered similar to if the work involved a municipality providing capital expenditure planning for sanitary sewer or water lines.

Site Inspections

Field observations and mapping of the as-constructed underdrain systems were necessary components of this forensic evaluation. Due to the lack of available information in the public record, such as as-built drawings or daily construction logs, the system had to be video-scoped and specific portions excavated for analysis. The underdrains constructed in the street right-of-way could only be accessed by removal of the asphalt pavement and roadway subbase to expose the cleanouts or, in some cases, the underdrain itself. Secondly, inspections were also required at specific homes, and, where necessary, these could only be accomplished through separate access.

Determining which homes would be reviewed would be reached after review of lengthy owner questionnaires and/or maintenance records were discovered from the multiple builders, insurance reports, or management reports. These reports would have to be evaluated based on flow rate issues, flooding, failures, or as other systematic issues related to perimeter and underdrain problems became known. The locations of the reported flooding or sump pump incidents were then overlaid on each underdrain system's map to allow the forensic team to develop potential correlations between incident locations and types, and the knowledge of the underdrain construction based on the plan reviews and/or physical findings.

In a best-case scenario, the entire underdrain would have been physically inspected. However, because of many constraints, the first phase of the forensic work involved locating approximately 40 cleanouts on one segment of one of the underdrain systems. The first phase of work found that no cleanouts meeting the municipality's standards were provided, and the non-compliance included location, type, depth, and accessibility.

The municipality's standard detail for underdrain cleanouts (capped vertical risers) required that an underdrain cleanout be provided at each sanitary sewer manhole. The vertical riser sections of the cleanouts were required to be constructed along the outside of the vertical portion of the manhole barrel, and each was required to be connected to the manhole wall with stainless steel straps for stability. The riser sections were also required to be capped and terminated directly below the street pavement. Per the standard detail, access to the underdrain cleanouts would require removal of a small section of asphalt immediately adjacent to the manhole covers to expose the caps at the tops of the riser sections. After removal of the asphalt on

the appropriate side of the manholes, it was found that the cleanouts were not located at the manholes, as required. The asphalt removal was then extended all the way around the manhole, yet no caps or risers were found.

The next step was the vertical excavation of the roadway around each manhole, which required street closures and safety measures at the areas being examined. Those excavations revealed varying non-commonality of construction of the cleanouts at each manhole. This included improper placement of the vertical risers, lack of structural attachment to the manhole barrels, damage of the risers, de-attachment of the pipes, and, in some cases, cleanouts that were never extended or installed.

This non-compliant construction made the entire system inaccessible and unmaintainable, and considerable effort was required to provide excavations at each manhole in order to expose and raise each cleanout to allow access to the subsurface lines. It should also be noted that per the municipal standard, cleanouts were required to be 6-in. lines; however, all cleanouts were discovered to be 4-in. lines. The transfer of the underdrain system to the common interest community without the ability to access, maintain, and thus inspect, clean, or repair the system was evaluated as part of the forensic work on this project.

The capital plan that would have provided reserve funding should have included the operational and capital expenses necessary to provide for access, inspections, maintenance, and repair of the system. This capital plan should also have provided for the replacement of the system at the end of its expected useful life (EUL), which with equivalency to the city sewer located above it would be 50 to 100 years. In comparison, a home's foundation would require an EUL of up to 200 years based on FHA criteria, and there would be little expectation that an owner would excavate a basement to replace the drain system.

Following the exposure of the cleanouts, camera inspections were attempted on the underdrains. Due to the presence of calcites, construction debris, sediment, and damaged lines, this proved to be difficult. The camera inspections found that the majority of the randomly selected underdrain segments contained blockages and were either partially or completely filled with water. At many locations, blockages were also found within the riser sections of the cleanouts, and underdrains were completely inaccessible. During the litigation process, segments of the underdrains were excavated and physically examined, including the repairs that were necessitated by the flooding of another residence, where the excavation of the lateral, the street lines, and significant length of the underdrain had to be undertaken to reduce the damages occurring to the properties upstream from the determined location of blockage.

The discovered conditions of the excavated line segments were correlated with the reported flooding and excessive sump pump operation locations, revealing that the lines were completely blocked with construction debris, gravel and/or calcite buildup — and that the systems were neither operational nor maintainable. Where complete blockages occurred, all underdrain flows backed up into the closest upstream basements, and the sump pumps installed at these homes had been operating continuously for several months. In some cases, the affected homeowners directed the sump pump flows to the curbs and gutters in the streets, which was in violation of the municipality's ordinances that prohibit the flow of the water across the walkways and into the roads.

Documentation

Since the CIOC was found to be responsible for ownership and maintenance of the underdrain system, a comprehensive map of the system was prepared for ongoing use. This map showed the known locations of cleanouts and blockages in the lines, and also identified non-flowing line segments discovered up to the time of the creation of this work. However, it was based on limited access to the underdrain, and it is likely that not all problems had been discovered. Based on this information, to the extent possible, a comprehensive repair plan was also developed for the existing underdrains. The intent of the repairs was to provide access to repair, restore or upgrade the entire underdrain based on the potential flow rates to create a functional system, and to allow for the necessary access, inspection, maintenance, and repair of the system over its EUL.

Repairs

Following successful litigation, repair plans were developed for the CIOC based on the following:

1. Determination of expected flows in the underdrain systems.

2. Review of applicable design codes, standards and criteria in the design and construction of the system.

3. Hydraulic analysis of the system to determine the

critical velocities, potential surcharge areas, and impacts of the flows on the private residences.

4. Coordination with the districts and municipalities for permitting, design, inspection and transfer of maintenance or acceptance of easement agreements.

Design Flows

The current state-of-the-art of underdrain design and construction was researched by the forensic engineer, and the findings were used in part to determine the expected design flows in the underdrains. Some examples of the industry knowledge are shown below:

Duane Friend and Doug Peterson, University of Illinois Extension, College of Agricultural, Consumer and Environmental Sciences, "Land & Water," August 2005, Number 8, "Sizing Up a Sump Pump," states:

"If you're building on sandy soil, plan for a system capacity of 14 gallons per minute for every 1,000 square feet of home. If you're building on clay soil, plan for a system capacity of 8 gallons per minute for every 1,000 square feet of home."

The City of Ann Arbor - Developer Offset-Mitigation Program, Guidelines for Completion of Footing Drain Disconnections, Updated November 30, 2005, states:

"A typical single-family residence in Ann Arbor contains 1,200 square feet of footprint area, most often with a standard basement depth of 5' to 8'. These structures have been found to generate an average of 4 gallons per minute (gpm) from monitoring data within the City during peak wet weather conditions."

ASCELIBRARY.org, Narender Kumar, PE, M.ASCE, FACEC, Kumar & Associates, Inc., Denver, Colorado, "Effective Use of Underdrain System in Construction on Expansive Subsoils," states:

"Measurements in the underdrain systems indicate continuous flow of groundwater throughout the year and that the amount of flow far exceeds the surface drainage and water use in the area. The author has measured continuous ground water flow between 0.23×10^{-2} m^3/h (0.01 gpm) and 0.45 m^3/h (2 gpm). This flow is sufficient to cause additional expansion of subgrade and distress."

The variables analyzed included the site surface and bedrock topography, soil permeabilities, groundwater expectations post-development, land use and climatic data. In addition to reviewing available design guidelines, the existing flows in the system were measured and correlated with the analysis to arrive at design flows that were consistent with the actual conditions observed on the properties.

Additional geotechnical investigations were also performed to evaluate the soil conditions, aid in determining the potential permeability of the backfill soils next to the buildings' foundations, and, in some cases, to evaluate the general geohydrology of the developed site. The evaluation was based on average soil conditions and resulted in the evaluation of non-saturated versus saturated conditions of the native and re-mixed or re-used soil. These evaluations determined that hydraulic conductivity of the onsite soils ranged from 10^{1} to 10^{-5} centimeters per second for backfill material or native clays, respectively.

It was determined that proper selection of hydraulic conductivity values is critical to proper design of underdrains, and it was possible that this parameter was incorrectly determined in the provided conditions of design. This underestimation of the permeability would have resulted in difficulty in determination of the flows to be used in the design of the system. As stated, there are a number of peer-reviewed publications that could serve the designer in sizing the system. One such publication is the American Society of Civil Engineers Manuals and Reports on Engineering Practice, No. 95, Urban Subsurface Drainage, which indicates that the following parameters should be considered: topography, geography, climate, water table, geology, water sources, soils information, environmental factors, physical constraints, and legal or political constraints.

American Society of Civil Engineers, "Standard Guidelines for the Design of Urban Subsurface Drainage ANSI/ASCE 12-92 ANSI Approved March 15,1993 Standard Guidelines for Installation of Urban Subsurface Drainage ASCE 13-93 Standard Guidelines for Operation and Maintenance of Urban Subsurface Drainage ASCE 14-93," 1994, states:

"5.0 Site Inspection

5.2 Surface Features

The surface features of the site should be located through a topographic survey and shown on the plans. The plans should be compared with existing field conditions to determine whether there are any differences between the topographic survey and present conditions. Discrepancies are to be brought to the attention of the engineer or project

manager.

5.3 Subsurface Features

Subsurface features principally consist of utilities and geological conditions. All subsurface conditions are subject to field verification by the contractor prior to construction.

5.3.2 Geologic Conditions. All appropriate and available geological conditions should be shown on the plans. An assessment should be made with respect to rock and groundwater conditions.

7.2 Water Sources

7.2.1 Subsurface Water Sources.

In this document, subsurface water is considered to be all water beneath the ground or pavement surface and will be sometimes referred to as groundwater. Soil water is generally of three types: drainable water, plant-available water, and unavailable water. Plant-available water is often referred to as "capillary water," since it is retained by the soil in small soil pores where capillary forces prevent gravity influenced drainage and is available for plant root absorption.

Drainable water may be considered to be water that readily drains from soil under the influence of gravity. Drainable water moves through soils in direct proportion to the soil's permeability and hydraulic gradient, thus low permeabilities result in slow natural drainage of saturated soils.

Unavailable water is held tightly in thin films surrounding individual soil particles. The strong film bond makes this water nondrainable and unavailable to the vegetation. The amount of this hygroscopic water varies with the surface area of the soil particles and, therefore, is highest in clay and organic soils.

Most subsurface water results from surface infiltration, although water can enter the subsoil from adjacent areas. Another potential contributor to excess soil wetness is a perched water table that generally forms above an impermeable soil layer.

Water infiltration in soils is governed by soil type, season of the year, degree of soil moisture content at time of rainfall or irrigation, type and extent of vegetative cover, surface "crusting" tendency from rainfall impact, and characteristics of the particular rainfall event.

7.2.2 Surface Water Sources.

Water from a rainfall or irrigation event that does not infiltrate the soil appears as surface water. An exception to this generalization is a condition of interflow, wherein infiltrated water moves along an impermeable strata and exits the soil mass at a hillside or cut. Surface water becomes a consideration in subsurface drainage analysis when it becomes runoff or interflow to the drainage area under study and contributes to the anticipated water removal requirements of the subsurface drainage system. Surface water runoff is a major concern in urbanized areas, where development results in a high percentage of impervious surfaces such as roofs, driveways, and streets. In evaluating the subsurface water removal requirements of a specific area, adjacent areas that represent potential watersheds must be considered. Urban watersheds usually have greatly reduced water absorption and interception capacity, resulting in significant surface water discharge quantities. Surface water may be free to flow to adjacent areas (runoff) and contribute to soil saturation in another zone and/or streamflow. Some surface water is retained on the ground surface in depressions which, if soil permeability is extremely low, will evaporate or pond.

7.3 Establishing the Need

7.3.2 Removal Criteria for Different Environments and Climates.

Climatic conditions must be considered. Soils in humid regions often require more extensive drainage systems than soils in arid regions. Temperature and humidity conditions interact with soil characteristics to influence moisture control requirements."

Another publication that provides such guidance is the "Standard Guidelines for Operation and Maintenance of Urban Subsurface Drainage ASCE 14-93," 1994, which states the following:

"5.0 Water Quality

5.2 Environmental Indicators

A review of the area should be performed to determine any changes since the construction of the subsurface system. These changes will then have to be evaluated as to possible effects on the subsurface flow. Water sampling of aquifers and watershed sources representing existing and potential sources of subsurface water supply may be required. Certain parameters and their background levels can be expected to occur naturally in the water due to the existing environment. By visual inspection or through personal observation, a determination can be made for the necessity and extent of a field sampling program. If test results show unusual concentrations or unexpected constituents in the water, further investigations could be necessary. A treatment program may need to be implemented, or modifications may need to be proposed that would mitigate or eliminate adverse impacts caused by the problem constituents".

The forensic evaluation included the review and analysis of each of these parameters in the ultimate design of the

system. Only the common interest portion of the underdrain, located within the street right-of-way, was evaluated. The traverse systems (laterals) that provided connections to the homes were neglected in the evaluation of construction, unless repairs to that residence were necessitated by the failure of the main underdrain.

The ownership and legal responsibility of the lateral was assumed for the purpose of this author's work to begin and end at the right-of-way. The portion on the private lot would not be maintained as common elements and, therefore, would be required to be maintained by the individual lot owners. Based on the failures occurring in the system, the portions of the underdrain systems constructed on the individual lots will likely also have similar damages that are not discoverable until excavation of the systems is performed, primarily in regard to scale buildup from the leaching of the materials in the native and backfill soils into the poorly sloped sections of the underdrain's system.

The determination or averaging of hydraulic conductivity values used in the design of an underdrain system encompassing more than 490 acres was critical to the sizing determination to be used. Averaging of soil types is one method that could be used. This method is based on the properties and extents of the near surface soils from the United States Department of Agriculture, Natural Resources Conservation Service mapping for non-saturated or saturated permeability conditions. For example, if the site was overlain with 50% Nunn loam and 50% Renohill-Buick loam with a saturated hydraulic conductivity (Ksat) of 6-micrometers per second (0.85 in. per hour) and 4-micrometers per second (0.6 in. per hour), it would produce an average of 5 micrometers per second on average.

According to the USDA Web Soil Survey, Arapahoe County, Colorado (CO005):

"Renohill-Buick loam
Properties and qualities
Slope: 3 to 9 percent
Depth to restrictive feature: 20 to 40 inches to paralithic bedrock
Natural drainage class: Well drained
Runoff class: Medium
Capacity of the most limiting layer to transmit water (Ksat): Moderately low to moderately high (0.06 to 0.20 in/hr)"

Weld County, Colorado, Southern Part:

"39 — Nunn loam
Properties and qualities
Slope: 0 to 1 percent
Depth to restrictive feature: More than 80 inches
Natural drainage class: Well drained
Runoff class: Medium
Capacity of the most limiting layer to transmit water (Ksat): Moderately low to moderately high (0.06 to 0.20 in/hr)"

However, if one soil type, such as the terrace escarpments, was more conductive by a factor of 40 times, (14-micrometers per second or 2.0 in. per hour), that condition could result in a surcharging effect not accounted for in averaging.

Arapahoe County, Colorado (CO005):

"Tc — Terrace escarpments
Properties and qualities
Slope: 10 to 60 percent
Depth to restrictive feature: 10 to 30 inches to paralithic bedrock
Natural drainage class: Well drained
Runoff class: High
Capacity of the most limiting layer to transmit water (Ksat): Moderately low to high (0.06 to 2.00 in/hr)"

The hydraulic conductivity (Ksat) of the on-site soils, therefore, significantly affects the quantity of water entering the underdrain system. **Figure 4** is excerpted from the 2007 edition of the publication "Hydraulics of Groundwater" by Jacob Bear. This figure shows the variance in hydraulic conductivity and permeability for various soil

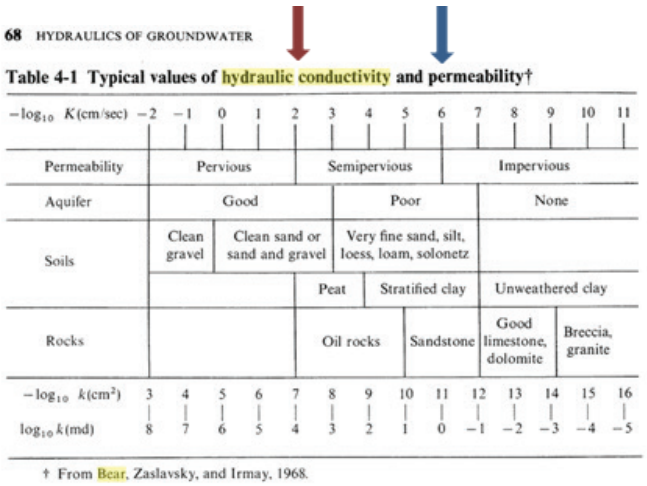
68 HYDRAULICS OF GROUNDWATER

Table 4-1 Typical values of hydraulic conductivity and permeability†

$-\log_{10} K$(cm/sec)	−2	−1	0	1	2	3	4	5	6	7	8	9	10	11
Permeability	Pervious					Semipervious				Impervious				
Aquifer	Good						Poor			None				
Soils	Clean gravel		Clean sand or sand and gravel				Very fine sand, silt, loess, loam, solonetz							
						Peat		Stratified clay		Unweathered clay				
Rocks						Oil rocks			Sandstone	Good limestone, dolomite		Breccia, granite		

$-\log_{10} k$(cm²)	3	4	5	6	7	8	9	10	11	12	13	14	15	16
$\log_{10} k$(md)	8	7	6	5	4	3	2	1	0	−1	−2	−3	−4	−5

† From Bear, Zaslavsky, and Irmay, 1968.

Figure 4
Typical values of hydraulic conductivity and permeability. "Hydraulics of Groundwater," 1979, by Jacob Bear, p. 68, 2007 Edition.

types. The hydraulic conductivity of typical backfill soils around a building's foundation can range from clean sand, Ksat = 102 (red arrow), to stratified clay, Ksat = 105 (blue arrow).

The soil permeability between the trench gravels and the fine silts varies by a factor of more than 1,000. Based on multiple sensitivity analyses performed by this author, the variation in hydraulic conductivity of the backfill soils can significantly impact the sizing of underdrain systems. The design of these systems must take into account the presence of water in the backfill and other site conditions, including ground or perched water and water conveyed in the gravel bedding used in utility and other trenches within the site.

In addition to the sensitivity analyses regarding the impact of placing low permeability backfill around the buildings, this author's work also determined that sequential grading (upslope lots discharge onto downslope lots) of multiple residential lots can also significantly affect the quantity of water introduced into the soils directly adjacent to the buildings' foundations where this water is directly intercepted by the perimeter drains and conveyed to the underdrain system.

By contrast, a generic site analysis would assume that construction of the residences and roads could result in impervious features covering up to 70% of the original site, concentrating the rooftop flows from precipitation into gutters and downspouts or delivering that flow directly into the backfill or rework zones. It is difficult to fully evaluate the effects of water migration into the foundation backfill soils for the conditions described above in determining the required sizes of the underdrains. The impact of multiple storms, time between storms, and rainfall intensities also contribute to variations in the rates of infiltration since the hydraulic conductivity of the backfill soils is directly dependent on whether the soils are saturated or unsaturated when water is collected in the backfill areas.

The material characteristics of the backfill soils as well as the presence and condition of utility trenches, basement excavations and the in situ native soils all play a role in the amount of water that ultimately reaches the underdrain system, both at the house locations as well via the trenches themselves. An attempt could be made to determine the infiltration characteristics of the site by averaging the hydraulic conductivities of the various soil types; however, even such an analysis could not, on its own, account for the multitude of poor construction practices that cause additional quantities of water to pond next to foundations and within sites and infiltrate into the soils after construction. Other engineering considerations such as the seasonal variations in precipitation, irrigation, evapotranspiration, and localized drainage conditions at the backfill boundaries create conditions where the use of engineering judgment must be relied upon in determining the contributory flows from each residence and the cumulative flows to the common underdrain.

Therefore, in this author's opinion, in light of the engineering difficulties in accurately ascertaining what the actual quantity of infiltrated water would be as a factor of a site's post-developed soil conditions, a reasonable factor of safety should be considered in the ultimate design of these systems. Similar to geotechnical studies, the range of assumptions made should be provided with a reasonable factor of safety. Put in this author's words: "The less you know, the safer your design should be. The more you know, the more economical and precise you can be."

Reverse hydraulic calculations based on the previous preliminary pipe sizing guidelines used in the design industry that allowed 50 to 150 homes per 4-in. diameter lines (depending on pipe slope) provide some method of determining the contributions of individual lots to the underdrains. Secondly, the impact of other sources of water must also be considered in this evaluation. This author's analysis involved solving Manning's equation for open channel flow for each of the conditions, and the forensic engineering calculations performed determined that at full pipe flow conditions, the design flows in the pipes ranged from 1.16-gallons per minute per house to 2.27-gallons per minute per house.

It should also be noted that the design should not allow pipes to operate at more than 80% full flow capacity under gravity flow conditions so that pressurized flow conditions do not develop. In addition to evaluating the hydraulic capacities of the underdrain lines, consideration should also be given to the designed pipe slopes, since the selected slope of the pipe is critical to the achievement of self-cleansing velocities at the given flow rates, typically 1.5 ft per second or greater.

A number of other resources from across the United States were reviewed, and flow rates varying from 0.5 gallons to 8 gallons per minute were found to be typical expected flow rates for residential properties.

Duane Friend and Doug Peterson, University of

Illinois Extension, College of Agricultural, Consumer and Environmental Sciences, "Land & Water," August 2005, Number 8, "Sizing Up a Sump Pump," states:

"If you're building on sandy soil, plan for a system capacity of 14 gallons per minute for every 1,000 square feet of home. If you're building on clay soil, plan for a system capacity of 8 gallons per minute for every 1,000 square feet of home."

The City of Ann Arbor - Developer Offset-Mitigation Program, Guidelines for Completion of Footing Drain Disconnections, Updated November 30, 2005, states:

"A typical single-family residence in Ann Arbor contains 1,200 square feet of footprint area, most often with a standard basement depth of 5' to 8'. These structures have been found to generate an average of 4 gallons per minute (gpm) from monitoring data within the City during peak wet weather conditions."

The loss of a pipe's smoothness over its lifespan should be considered as well as the impact of loss of slope due to the expansive nature of the local soils. All of these parameters underscore the need for higher factors of safety being used in the original designs. Some municipalities now require that underdrain lines be sized for no more than 50 percent of full flow, allowing some factor of safety and reduced potential for surcharging the laterals from the residence to the underdrain.

During the litigation, the original geotechnical site report was provided, and that report indicated that a 4-in. pipe should be used to serve 100 residential homes. Reverse calculating the pipe hydraulics at minimum slope and 80% full flow conditions for PVC pipe would equate to a flow rate of 0.85 gallons per minute per residential lot. To put that into context, a standard residential sump pump, typically rated at 25 gallons per minute flow rate operating with 10 ft of head pressure and operating for 10 minutes every four hours, would have a similar rate of flow.

Based on the review of the as-functioning systems and multiple hydraulic scenarios, updated soils data and field measurements, the design flows in the underdrains were ultimately determined to be based on each lot contributing 0.85 gallons per minute as a reasonable design rate of flow, which falls within standard design rates for the industry. The system could then be analyzed and properly sized for each of the four sections of underdrains.

Applicable Codes and Design Criteria

In this author's opinion, based on the research performed, in many jurisdictions, the design criteria and guiding documents related to underdrain design are unclear and not definitive. The Jurisdiction with Authority for this project has recently proposed updates to the relevant sections of their Standards and Specifications Manual for underdrain design and construction. Although not yet adopted, these updates were incorporated into the design of repairs to the existing underdrain systems.

Hydraulic Analysis

Since the original underdrain system was never hydraulically designed — and given the constraints of the as-constructed conditions — accurate hydraulic modeling of the system was necessary to determine the repairs required to make the system functional and to provide the required level of protection to the individual homes. Using the information contained in the Sanitary Sewer Construction Plans and the results of this author's field observations, a hydraulic model of each underdrain system was developed. The software application "Autodesk Storm and Sanitary Analysis, 2015" produced by Autodesk, Inc. of San Rafael, California, was utilized for the hydraulic modeling of the underdrains because of its easy integration with the previously prepared drawings and other data.

The hydraulic design was optimized through multiple iterations to develop repairs that minimized the percentage of the system that needed to be replaced to provide a hydraulically functional and maintainable underdrain system.

Conclusions and Professional Opinions

Significant research was performed to complete the extensive forensic investigations related to this project. Because of the particular geographic and climatic conditions, the research was predominantly restricted to Colorado and included the following findings:

1. The responsibility for ownership and maintenance of underdrain systems varies across municipalities and jurisdictions. In a few cases, the authority having jurisdiction (city, county, metro district, etc.) will own and maintain the underdrains. More often, these systems are private and are the property of the Common Interest Ownership Community in perpetuity. As such, the private owner is required to provide all maintenance and repairs as needed, thus requiring proper legal

conveyance, easement agreements, access, and funding.

2. There is no standard or consistent industry guidance and design information available to enable civil engineers to determine flows in underdrains to properly size these systems. Forensic engineering research (as per the references below) has found literature stating that underdrains should be designed for flows varying from 1 gallon per minute per lot to more than 20 gallons per minute per lot depending upon the building footprint sizes and local conditions.

Duane Friend and Doug Peterson, University of Illinois Extension, College of Agricultural, Consumer and Environmental Sciences, "Land & Water," August 2005, Number 8, "Sizing Up a Sump Pump," states:

"If you're building on sandy soil, plan for a system capacity of 14 gallons per minute for every 1,000 square feet of home. If you're building on clay soil, plan for a system capacity of 8 gallons per minute for every 1,000 square feet of home."

The City of Ann Arbor - Developer Offset-Mitigation Program, Guidelines for Completion of Footing Drain Disconnections, Updated November 30, 2005, states:

"A typical single-family residence in Ann Arbor contains 1,200 square feet of footprint area, most often with a standard basement depth of 5' to 8'. These structures have been found to generate an average of 4 gallons per minute (gpm) from monitoring data within the City during peak wet weather conditions."

3. In many cases, geotechnical engineers state that a certain number of homes can be serviced by underdrains of a particular size. These guidelines vary widely, however, and in many cases are not incorporated by the design professionals. As noted above, geotechnical reports provide preliminary sizing tables that state that no more than 50 lots can be served by a 4-in. PVC line while others allow up to 200 lots can be on a 4-in. PVC line. However, in this author's opinion and based on the observed field condition and analyses performed under this project, these preliminary sizing guidelines appear not to be substantiated by sound engineering principles.

4. Specific underdrain design procedures need to be developed, and the design of underdrains should be required by municipalities or other approving jurisdictions. Designers should understand the relationship between the permeability of the backfill soil used next to the foundations of the buildings on a site. Failure of portions of underdrains can have significant negative impact to homes or other buildings served by those systems.

5. The CIOC must understand that it owns the underdrains and is required to maintain these systems in perpetuity, even though the underdrains may not be located in common tracts. In many cases, the existence of the underdrains is not communicated to the owners — only when problems develop are these discovered.

6. Similar to other utilities, the responsibility for ownership and maintenance of underdrain systems needs to be clearly established. The foundation perimeter drains and the laterals from the buildings to the underdrains in the streets are the responsibility of the homeowners, and the underdrains within the streets or common elements or tracts are the responsibility of the CIOC or other authority. However, a clear line of demarcation needs to be established for the laterals. This may be at the property lines, the backs of curbs or sidewalks, or other easily identifiable elements.

7. Underdrain systems need to be maintained on a regular basis and developers need to communicate this to the CIOC at the transition of ownership. This should also be contained in operation and maintenance manuals and programmed into reserve or capital studies.

The author appreciates the assistance of Dane M. Dasent, PE, CFM, LEED-AP, in the preparation of this paper and the underlying work.

Machine Safeguarding: Theory, Practice, and Case Studies

By Nicholas A. Petrucci, PE, CSP (NAFE 650M)

Abstract

A machine is a device that uses energy to perform some type of useful mechanical work. Therefore, it must have at least one (and more often many) moving parts. A safeguard is a measure taken to protect someone from physical harm. The sources of harm from a machine typically stem from moving parts and/or electric current. Effective machine safeguards substantially reduce personnel exposure to these hazards and/or the resulting harm, and, as a result, optimize machine productivity. A common image that comes to mind in regard to a machine safeguard is a physical barrier that prevents a worker from inadvertently placing a body part into a hazardous space of a large industrial machine. While this is one important aspect of machine safeguarding, it is a much broader topic that requires a more in-depth analysis to achieve the goal of ensuring personnel safety without unduly compromising machine productivity. Different types of machine safeguards will be discussed in this paper. The safeguarding hierarchy will be presented, which is a guide to determine what safeguarding method(s) should be employed. Case studies of injuries that were caused, at least in part, by various machine safeguarding deficiencies will be presented. Relevant matters that arose during an OSHA National Emphasis Program on Amputations audit at a manufacturing facility will also be discussed. These topics will provide insight on how to better develop and employ more effective machine safeguards.

Keywords

Machine, safeguard, hierarchy, lockout, tagout, OSHA, pinch point, guarding

History

Safeguards are by no means unique to machinery. One of the earliest safeguards was likely a sheath for a knife or a sword, which helps protect its user from being cut when the blade is not in use.

Moskowitz provided a chronology of machine safeguarding[1]. Patents for machine guards were issued in the 1890s. "The Prevention of Factory Accidents" by John Calder, published in 1899, defines hazards and describes methods for elimination or mitigation. The National Safety Council (NSC) was established in 1913, which advanced machine guarding and many other aspects of safety. The NSC published the "Accident Prevention" manual from 1946 through 1974, which was widely accepted by machine operators and designers.

The American Standards Association (ASA) was founded in the 1920s, which became the present-day American National Standards Institute (ANSI). The first ASA standard on power transmission guarding was published in 1927.

Although many ASA/ANSI standards applied to specific machinery and were generally accepted, the standards were largely legally unenforceable until incorporated into or adopted by the Occupational Safety and Health Administration (OSHA), which was established in 1970. OSHA's first standard related to machine safeguarding was adopted in 1989[2].

Current Requirements

OSHA's Machinery and Machine Guarding standard states:

> **1910.212(a)(1)**
>
> *Types of safeguarding*. One or more methods of machine safeguarding* shall be provided to protect the operator and other employees in the machine area from hazards such as those created by point of operation, ingoing nip points, rotating*

Nicholas A. Petrucci, PE, CSP, 2366 Golden Mile Hwy. #452, Pittsburgh, PA 15239, forensic@petrucciengineering.com

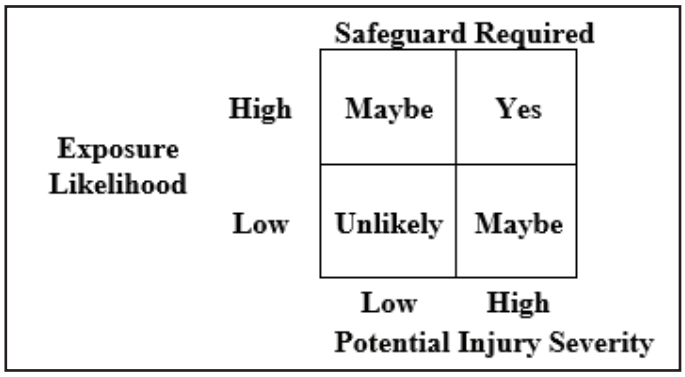

Figure 1
Machine safeguard requirement chart.

parts, flying chips and sparks. Examples of guarding methods are barrier guards, two-hand tripping devices, electronic safety devices, etc.

The author added the word "safe" to the original language above to update it to current usage, as indicated by the asterisks.

This is a broad requirement. Some machine hazards are obvious. Other not-so-obvious hazards are too often not discovered until they cause, or contribute to, an injury. Many incidents involve personnel performing unsafe acts, negligently, recklessly, or even intentionally. Whether such acts were reasonably foreseeable and should have been safeguarded against is often a central matter, if not the central matter, in machine safeguarding litigation.

Machine Safeguarding — What and How?

The following are two key questions that must be answered to properly safeguard a machine, along with general guidance on how to respond to them:

1) What machine hazards should be safeguarded?

To best answer this question, the following two factors should be evaluated:

- Likelihood of exposure to the hazard. This would generally be considered "high" if it is reasonably foreseeable that someone would be exposed to the hazard.

- Severity of potential injury from the hazard. This would generally be considered "high" if a reasonably foreseeable injury from exposure to the hazard will require the attention of a medical professional.

Figure 1, a basic risk assessment matrix developed by the author, illustrates how to determine if a safeguard is required based on the above factors:

2) How should the machine hazard be safeguarded?

Quite simply, a machine hazard should be safeguarded with an effective machine safeguard, which has the following characteristics:

- Reduces the likelihood of exposure to the hazard to an acceptable level (i.e., one where the exposure is not reasonably foreseeable).

  and/or

- Reduces the harm from being exposed to the hazard to an acceptable level.

  and

- Does not unduly compromise machine productivity.

There are various ways to reduce the likelihood of exposure to a machine hazard, several of which will be discussed in the next section. Reducing harm from exposure to a machine hazard is most often accomplished with personal protective equipment (PPE).

Note that reducing the likelihood of exposure to a hazard and reducing harm from exposure to a hazard are two separate concerns. Hazard elimination, guarding, engineering controls, etc., reduce the likelihood of exposure to the hazard. PPE reduces the harm from an exposure that one has already been exposed to. The author has personally had the benefit of safety glasses, safety shoes, work gloves, welding jackets, auto-dimming welding helmets, etc., as protection from harm from many hazards that could not have been reasonably avoided.

If a safeguard unduly compromises the productivity of a machine, there is a good chance that it will be removed or otherwise disabled, thereby rendering it ineffective.

Machine Safeguarding Hierarchy

The purpose of the machine safeguarding hierarchy is to categorize safeguarding methods based on their effectiveness, which will hopefully result in the most effective safeguard being employed. The safeguarding hierarchy has been established by various technical

Safeguard Methods	Examples
Hazard Elimination	New design without the hazard. Eliminate/reduce human interaction (automation).
Hazard Substitution/Mitigation	Energy reduction (speed, force, voltage, etc.).
Physical Guard	Belt/chain/gear drive cover. Retractable circular saw blade guard. Switch guards (foot pedal guard). Relocate hazard to less accessible location (a.k.a. guarding by location).
Engineering Controls	Presence sensing devices (light curtain, safety mat). Interlocks. Two-hand switch. Control logic (manual reset required if the emergency stop button is pressed).
Awareness	Visual/audible alarms. Danger/warning labels.
Administrative Controls	Safety training. Procedures (lockout/tagout).
Personal Protective Equipment	Safety glasses. Safety shoes. Ear plugs. Work gloves.

Figure 2
Machine safeguarding hierarchy from most effective at the top to least effective at the bottom.

organizations, such as the American National Standards Institute[3]. There are some variations to the hierarchy among these organizations, which, for the most part, are relatively subtle. **Figure 2** shows examples of the most common safeguarding methods in the safeguarding hierarchy.

There are exceptions; that is, a safeguarding method lower on the hierarchy can be more effective than a higher one. For example, utilizing well-trained, safety-conscious personnel is often one of the most effective ways to prevent machine-related injuries. Although highly desirable, a well-trained and safety-conscious workforce is by no means justification for not having other effective safeguards in place.

Another example that the author has witnessed on numerous occasions is that a physical guard of some type unduly interferes with the operation of the machine, and as a result, is removed. Although lower on the machine safeguarding hierarchy, a presence-sensing device is often more effective in many of these cases.

Safety and Productivity/Economics

Although it is typically bad practice to sacrifice safety for economic considerations, it is done every day. If, for example, automobile manufacturers truly put safety above all other concerns, cars would look like tanks and be cost prohibitive to just about everyone. The impact on the overall quality of life would be detrimental. Similarly, if every machine had to be redesigned and/or completely safeguarded against any and all possible hazards, they would be prohibitively expensive, difficult to operate, nonproductive, etc. This approach would substantially increase the cost of nearly all manufactured products, which would be detrimental to society. Nonetheless, the safety of personnel working on or otherwise exposed to machine hazards must be paramount. The likelihood of personnel exposure to a machine hazard, coupled with the potential severity of the resulting injury, should be the primary factors used to determine if a machine hazard should be safeguarded, by which method, and to what degree. Economic and productivity concerns are secondary to safety, but nonetheless are also important factors that warrant consideration when selecting a method of machine safeguarding.

A safe workplace is requisite for a productive workplace. The "safety first" approach must be upheld. This requires spending the necessary time, effort, and resources to determine how to make safety and productivity complementary instead of competing interests.

Case Studies

The following are three case studies of personal injury incidents that were caused, at least in part, by machine safeguarding deficiencies. Each includes a description of the incident and an examination of what machine safeguards were in place compared to those that should have been in place to prevent the resulting injuries.

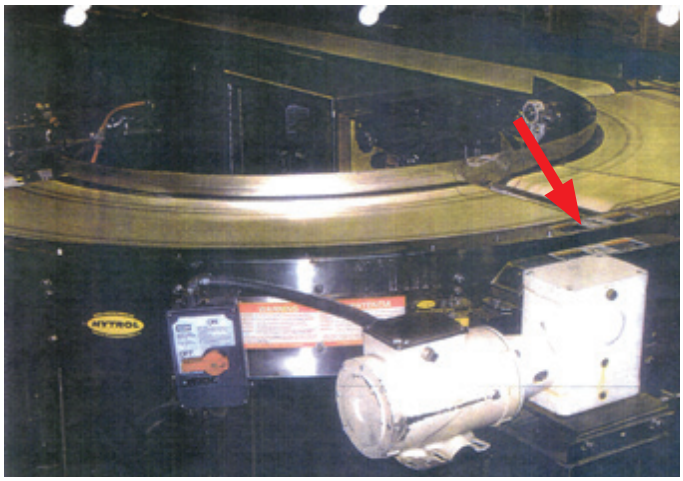

Figure 3
Arrow shows where worker was injured between two 90° conveyor sections while removing cookie nuggets from the conveyor. Product flows from left to right.

Figure 4
Incident pinch point showing how a worker severed her right thumb. Product moves from right to left.

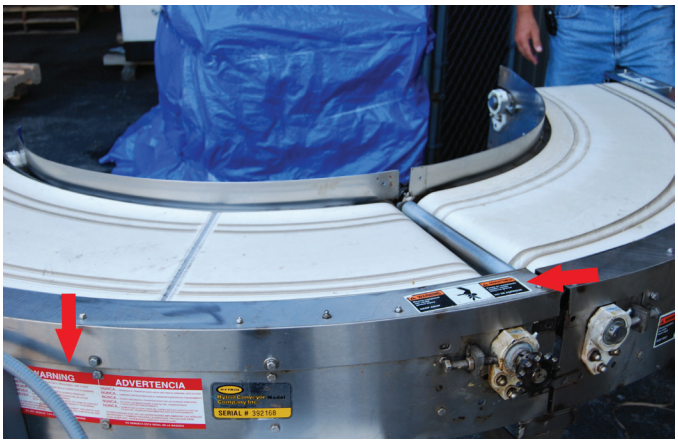

Figure 6
Warning labels in the vicinity of the incident location.

Case 1: Frozen Cookie Bags Conveyor

Bags of frozen cookie nuggets were being transported by a conveyor system. One of the bags ripped open, which resulted in frozen cookie nuggets spilling onto the conveyor. As a worker was gathering the cookie nuggets by hand near the interface of two 90° conveyor sections (**Figure 3**), she unknowingly placed her right thumb into a gap between the moving conveyor belt and the conveyor frame (**Figure 4**). This resulted in her thumb being severed from her hand.

This incident unfortunately was caused by the absence or ineffectiveness of various machine safeguards. Consider the following:

Hazard Elimination

There are inherent dangers at the interface of two conveyor sections. The incident pinch point would have been eliminated by using a single 180° conveyor section instead of two abutting 90° sections (compare **Figures 3** and **5**). However, similar hazards would still have existed at the interfaces between other abutting conveyor sections.

Figure 5
180° conveyor section.

Physical Guard

The conveyor manufacturer claimed that it sold the unit with "filler plates" that covered the gaps between the conveyor belt and the frame, thereby guarding the incident pinch point. Why these guards were not in place at the time of the incident is unknown. Having an interlock fitted to the four guards at each conveyor interface may have been impractical. However, a conspicuous "Danger — Install Guard Before Operating Conveyor" label that would be exposed when a guard was removed would not have been unduly burdensome.

Awareness

There was a conspicuous label in the immediate vicinity containing the text, "Warning — Moving equipment can cause severe injury. KEEP AWAY." Another less conspicuous nearby warning label contained the text: "NEVER…PUT YOUR HANDS ON THE CONVEYOR OR IN THE CONVEYOR WHEN IT IS RUNNING" (see **Figure 6**).

Administrative Controls

The worker testified that her training did not include what to do if frozen cookie nuggets were dispersed on the conveyor belt from a ripped bag — or how to stop the conveyor belts. Representatives from her employer testified that she was trained on how to stop the conveyor belts; however, they were unsure if she was specifically trained on what to do if frozen cookie nuggets spilled onto the conveyor — and it would have been appropriate for her to stop the conveyor belts if that occurred.

This incident is a good example of the greater effectiveness of methods higher on the safeguarding hierarchy (e.g., hazard removal and physical guards) than those

Figure 7
Wheelchair lift in the lowered position. Upper arrow shows the inboard roll stop in the vertical position. Lower arrow shows the outboard roll stop in the horizontal position.

lower on the safeguarding hierarchy (e.g., awareness and administrative controls).

Case 2: Wheelchair Lift

An individual in a wheelchair was being lifted from the ground to the floor level of a transport vehicle (**Figure 7**). There were vertically oriented inboard and outboard roll stops that prevented the wheelchair from rolling off of the ends of the lift platform. When the lift platform was at the ground level, the outboard roll stop was oriented horizontally to allow for loading and unloading of the wheelchair passenger. Similarly, when the lift platform was at the transport vehicle floor level, the inboard roll stop was oriented horizontally (**Figure 8**). During the initial portion of the lift, the wheelchair occupant's right foot entered the approximate 1.5-in. gap between the inboard edge of the platform and the inboard roll stop (**Figure 9**). When the lift was near its raised position, the inboard roll stop transitioned to the horizontal position, the gap between the inboard roll stop and the platform closed, and the occupant's right foot was crushed (**Figures 10** and **11**).

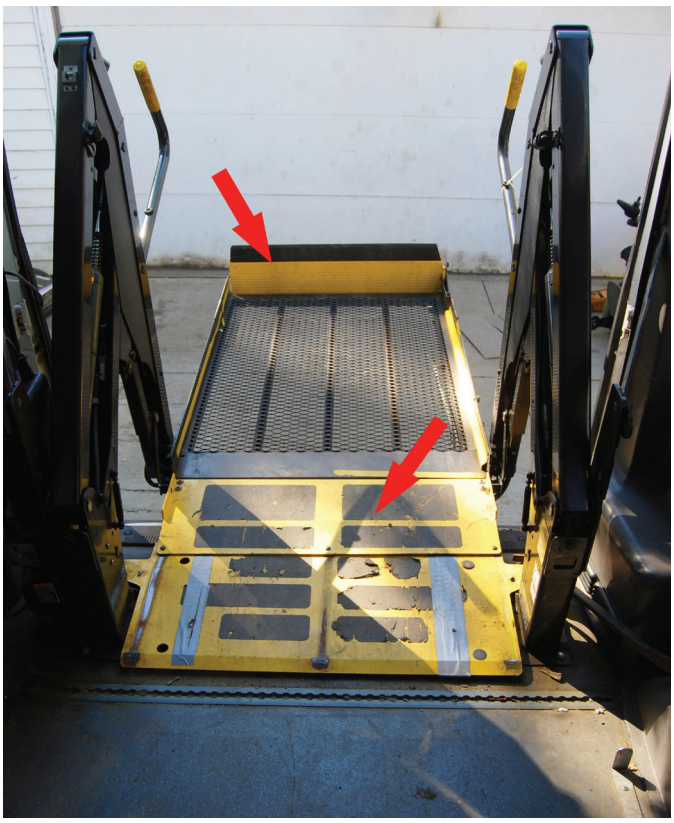

Figure 8
Wheelchair lift in the raised position. Upper arrow shows the outboard roll stop in the vertical position. Lower arrow shows the inboard roll stop in the horizontal position.

Figure 9
Inboard roll stop in the vertical position. Arrow shows an approximate 1.5-in. gap between the inboard roll stop and the platform.

This incident unfortunately was caused by the absence or ineffectiveness of various machine safeguards. Consider the following:

Hazard Elimination

The incident pinch point between the inboard roll stop and the platform should not have existed. An example of

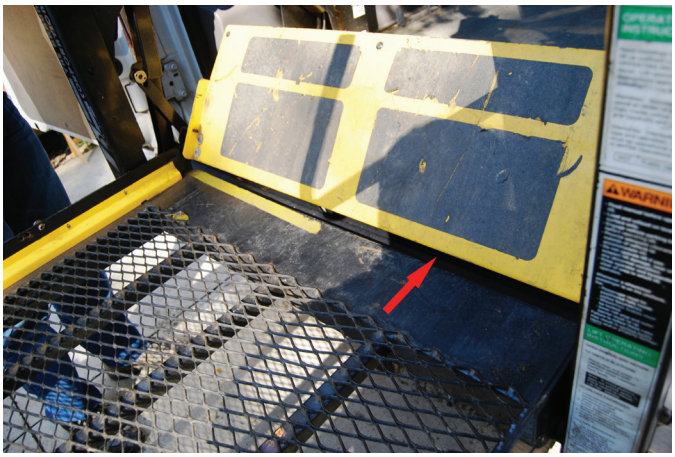

Figure 10
Inboard roll stop about halfway between its vertical and horizontal positions. Arrow shows the reduced gap between the inboard roll stop and the platform.

Figure 11
Inboard roll stop in the horizontal position. Arrow shows essentially no gap between the inboard roll stop and the platform.

an alternative design without the pinch point is an inboard roll stop that rotates about a hinge that is always coplanar with the platform (i.e., there would never be a gap between the roll stop and the platform).

A representative from the lift manufacturer testified that, "In a couple of our international lifts, we use a similar type… hinge (connecting the inboard roll stop to the lift platform) because it was requested by the customer… I've been told that the continuous hinge is less expensive." There was no mention of an operational or other benefit for the incident inboard roll stop design.

Physical Guard

A less desirable, but nonetheless likely effective, safeguard would have been the installation of a guard to prevent accessing the pinch point.

Awareness

A warning placard on the wheelchair lift frame contained the text: "Read manual before operating lift," and "Load passenger onto platform and lock wheelchair brakes." The operator's manual contained the following text: "Inboard facing of wheelchair lift passengers is **not prohibited**, but outboard facing of passengers is **recommended**". These awareness safeguards were inadequate as an explicit warning of the pinch point was not included, nor was the requirement to face the wheelchair occupant outboard during the lift.

Administrative Controls

What, if any, training the lift operator received is unknown. Such training should have included locking the wheelchair brakes during the lift and facing the occupant outboard or at least well away from the inboard roll stop during the lift.

The most effective safeguard, eliminating the hazard with a hinge connecting the inboard roll stop to the lift platform, was reportedly the least costly. It is the author's opinion that this is an example of spending too much time and effort on awareness safeguards — warning labels in particular. Many of these could be considered self-preserving, and unfortunately appeared to have stifled the manufacturer's ability to identify and relatively easily eliminate a clear hazard. Further, although a manufacturing company's legal counsel may advise otherwise, awareness safeguards should contain few words and include some type of relevant pictorial. Wordy awareness safeguards may reduce legal exposure, but are frequently not read, which compromises safety.

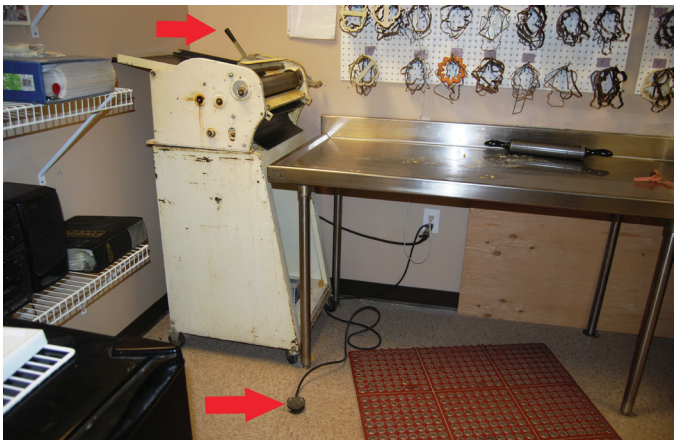

Figure 12
Dough rolling machine. Upper arrow shows its handle control. Lower arrow shows its foot pedal control.

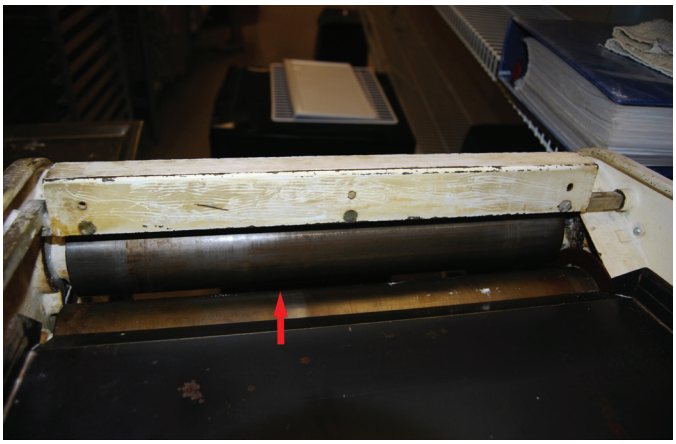

Figure 13
Pinch point between the rollers where the worker injured her hand.

Case 3: Dough Rolling Machine

As a worker was cleaning the rolls of a dough rolling machine, she inadvertently stepped on the foot pedal that controlled the operation of the rollers. This resulted in her hand being injured as it was pulled through the ½-in. gap between the rollers (**Figures 12** and **13**).

Before examining how the safeguarding hierarchy applies to this incident, a few noteworthy complicating factors that contributed to this incident will be presented.

1. The dough roller was manufactured in 1965. OSHA was established in 1971. OSHA's first standard related to machine safeguarding was adopted in 1989. Applying the requirements of a standard to a machine that was manufactured 24 years before the standard came into existence can be a challenge.

2. Although who did what and when could not be established, the dough roller was likely modified after it was manufactured. A representative from the dough roller manufacturer testified that the dough roller was controlled by the movement of a black handle (**Figure 12**). This handle could be pressed downward about $^{3}/_{8}$ in. with little effort, and subsequently returned to its original position upon release. It was not confirmed, but the intended operation of the dough roller was likely for its rollers to rotate when the handle was pressed downward, and for the rollers to stop when the handle was released. This would keep one of the operator's hands away from the rotating rollers. However, when the dough rolling machine's electrical plug was inserted directly into a 120V outlet, the rollers rotated when the handle was pressed downward and continued to rotate when the handle was released.

3. Nonetheless, the electrical plug of the dough roller was inserted into the plug connected to a foot pedal that was in turn inserted into a 120V wall outlet. This configuration allowed the operation of the rollers to be controlled by the foot pedal, which likely required a modification of the dough roller controls as noted in Item 2 above.

Based on the information above, and other factors, the author concluded that the foot pedal was not supplied by the dough roller manufacturer and was added sometime after the machine was put into service. Whether using a foot pedal to control the operation of the rollers was acceptable is a reasonable question. However, the incident foot pedal was unguarded; therefore, it was not suitable to control the operation of a machine such as a dough roller. There was a label affixed to the side of the foot pedal containing the text: "WARNING TO AVOID PERSONAL INJURY, DO NOT USE THIS CONTROL ON MACHINERY WITH AN UNGUARDED POINT OF OPERATION." This warning is consistent with OSHA's foot pedal guarding requirement noted in the following section.

The modification of the dough roller control system rendered it unsafe specifically because its rollers were controlled by an unguarded foot pedal. The following machine safeguards would/may have prevented the incident:

Hazard Elimination/Mitigation

The small gap between the rollers is a point of operation pinch point and necessary for the dough roller to function. However, this hazard could have been mitigated when cleaning the rollers by increasing the gap between them.

Physical Guard

The dough roller could have been fitted with a point of operation guard, such as a hopper, that would have prevented contact with the rollers during its normal operation. However, the incident occurred during a cleaning operation, and any such guard would likely have been removed to clean the rollers. In addition to preventing personnel from putting a body part into a hazardous area of a machine, physical guards can also prevent the inadvertent energization or activation of a machine. In these cases, hinged or limited access guards are placed over machine switches (see **Figure 14**).

Figure 14
Toggle switch guard (left). Foot pedal guard (right).

The following is an excerpt from OSHA's Machinery and Machine Guarding Standard:

> **1910.217(b)(4)(i)**
> *The (foot) pedal mechanism shall be protected to prevent unintended operation from falling or moving objects or by accidental stepping onto the pedal.*

The incident foot pedal did not meet this requirement. If it had, the incident likely would not have occurred.

Engineering Controls

At the time of the incident, the dough roller did not have an operational engineering control safeguard. To the contrary, the likely modification of its control logic, coupled with the addition of an unguarded foot pedal had a detrimental effect to its operational safety and was causal to the incident.

Awareness

It would be difficult to argue that a reasonable person would not have been aware of the danger associated with the pinch point between the two rollers. Nonetheless, an associated warning label may have prevented the incident. It is not known if such a label was installed on the dough roller when it was manufactured.

Administrative Controls

The owner of the dough roller and the establishment where it was located demonstrated how the rollers were cleaned, which was done daily for many years. The rollers were sprayed with a cleaning solution and wiped by hand with a rag. Hands were then removed from the rollers, the rollers were rotated slightly by tapping the foot pedal, and the process was repeated several times. This was how the injured worker was trained to clean the rollers. Although this method of cleaning was performed without incident for many years, it was unsafe to do so with an unguarded foot pedal.

Although more time consuming, the rollers could have been removed from the machine to clean them.

Personal Protective Equipment (PPE)

Apart from the rollers being removed for cleaning, it was necessary to jog the rollers to clean them and thereby not to de-energize the machine. Cleaning the rollers is a minor, routine, and repetitive operation that takes place during normal production operations. It should have been performed with a sponge on a utensil, or a similar wipe-down device, that does not require one's hand to be at the point of operation. Such a device would have been an acceptable safeguard during the cleaning of the rollers. This safeguard not only would have kept the operator's hands out of harms way, but may also have allowed the rollers to be rotated continuously during the cleaning operation, thereby shortening the process.

OSHA National Emphasis Program on Amputations

The author performs various engineering and safety consulting services at a medium-size manufacturing facility. One day an OSHA inspector made an unannounced visit and informed company executives that the facility had been randomly selected for an audit as part of OSHA's National Emphasis Program on Amputations. Shortly thereafter, the author was summoned to a meeting with company management and the OSHA inspector, and was assigned to be the required main contact person for the inspector.

Although not always enjoyable, the ensuing multiple-visit and several month-long audit process was a valuable experience that has served the author well. Many machine safeguarding issues were raised, addressed, debated, etc., during the audit. While a discussion of these issues may be valuable to safety professionals, many are beyond the scope of this paper. Nonetheless, the following are three selected issues raised during the audit that a forensic engineer who investigates machine safeguarding matters may find to be of value.

Engineering Controls vs. Physical Guards

When a physical guard unduly interferes with the operation of the machine, an engineering control can be used as a safeguard, provided that its effectiveness can be proven. One example is that a presence-sensing device must be far enough away from the hazard it is safeguarding, such

Figure 15
Sheet metal press safeguarded by a light curtain (see arrow).

that the hazard must be eliminated (e.g., stroke of a power press stopped) before someone can contact it.

Figure 15 shows a sheet metal power press with a presence-sensing light curtain. A stopping time of 0.360 seconds was measured from when the light curtain was tripped until the downward stroke of the press ram was stopped. This time coupled with OSHA's stipulated 63 in./second hand speed yielded a minimum safety distance of 22.68 in.[4]. The actual shortest distance from the light curtain to the press was approximately 25 in., which was acceptable (**Figure 16**). It should be noted that if the presence-sensing device is too far from the hazard, other safeguards may be necessary between these two items.

Figure 16
Distance of approximately 25 in.
from the light curtain to the closest hazard of the press.

Lockout/Tagout Procedures

To help prevent the uncontrolled discharge or release of energy while a machine is being repaired, serviced, modified, etc., it is important that all forms of energy (e.g., electrical, hydraulic, pneumatic, potential, kinetic, etc.) first be secured or otherwise eliminated. Properly written and followed lockout/tagout procedures ensure that this occurs and serves as a means of hazard elimination.

If an injury occurred while someone was working on a machine that was not operational, and related to the uncontrolled release of energy, the investigating forensic engineer should request the lockout/tagout procedure of that machine. The procedure, which should have been audited during the past year, should be reviewed for effectiveness and proper implementation. All switches, valves, gauges, etc., noted in the lockout/tagout procedures should be clearly labeled. Whether or not relevant personnel received proper lockout/tagout training should be determined.

Lockout/tagout procedures for machines with only one form of energy, typically electrical, are generally not required as long as other related criteria are met per OSHA 1910.147(c)(4)(i). However, that form of energy should still be locked out while the machine is being worked on.

OSHA Lockout/Tagout Minor Servicing Exemption

There are many instances when machinery must be serviced, adjusted, or otherwise modified, and performing a full lockout/tagout procedure between each iteration of these activities would be unduly burdensome. Recognizing this dilemma, OSHA developed a lockout/tagout exemption that applies when ALL of the following conditions are met:

First, the activity must be conducted during normal production operations (i.e., while the machine or equipment is actually performing its intended production function).

Second, the activity must be:

- *Routine*: The activity must be a regular course of operation and be in accordance with established practices.
- *Repetitive*: The activity must be regularly repeated as part of the production process.
- *Integral*: The activity must be essential to the production process.

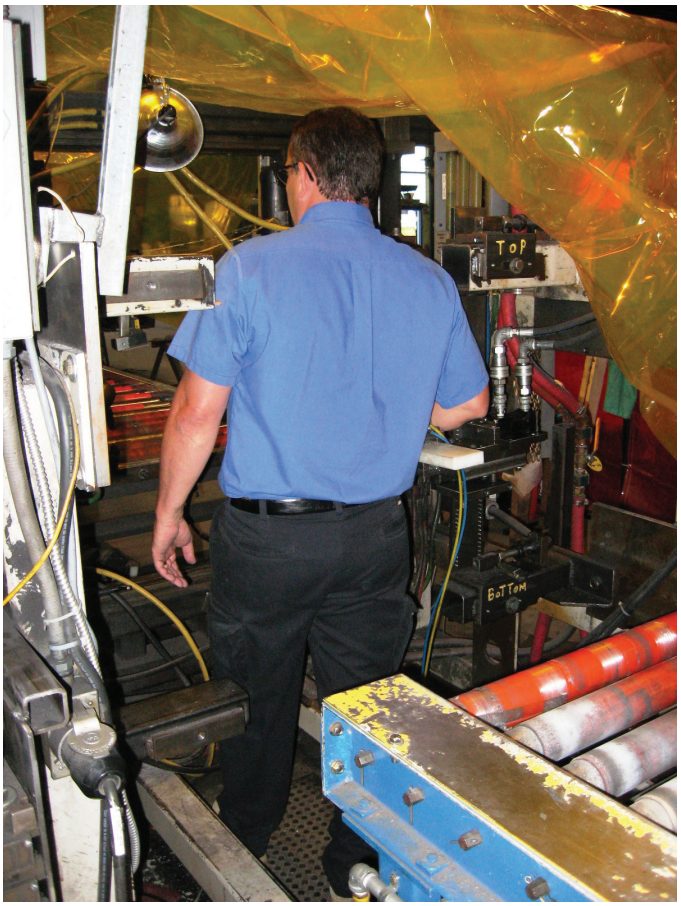

Figure 17
Worker cleaning weld tips on a resistance welder
while standing on a safety mat that secures power to the machine.

Third, if all of these apply, the employer must use alternative measures to provide effective protection from the hazardous energy. Acceptable alternative measures include specially designed tools, remote control devices giving the operator exclusive control of the machine, interlocked barrier guards, local disconnects, and control switches under the exclusive control of the employee performing the minor servicing[5].

Figure 17 shows a worker cleaning tips of a resistance welding machine, which meets all of the above criteria. The alternative safeguard in this case is the safety mat that prevents the welder from being energized while the worker is standing on the safety mat.

Conclusion

Machine safeguarding is a vital component of safety in many industries and consumer products. A good criterion is that if it is reasonably foreseeable that someone could be exposed to part of a machine that could cause them bodily harm requiring the attention of a medical professional, a safeguard should be employed to eliminate, ideally, or substantially mitigate the associated exposure likelihood and/or the severity of harm.

An effective machine safeguard is one that prevents machine hazards from harming personnel by substantially reducing the risk of exposure to the hazard and/or the severity of the associated harm. The safeguard also must not unduly interfere with the productivity of the machine; otherwise, the safeguard is more susceptible to being removed or otherwise disabled by its operator/user.

The safeguarding hierarchy is a valuable tool for selecting the appropriate method(s) for safeguarding a machine hazard, and it should always be given due consideration. However, a solid understanding of the machine hazards, operation, and maintenance, along with human factors, must also be considered to develop an effective machine safeguard.

A closing thought for consideration: It is easy and wrong to make safety and productivity competing interests. It is difficult and right to make safety and productivity complementary interests. Do the right thing!

References

1. Moskowitz L. History and practices of machine guarding. Journal of the National Academy of Engineers. 1991; 8(1); 53-58.

2. Occupational Safety and Health Administration. Washington (DC): United States Department of Labor [accessed 2018 July]. https:www.osha.gov. https://www.osha.gov/osha40/OSHATimeline.pdf.

3. ANSI B11.0-2015. Safety of Machinery. Washington, D.C; American National Standards Institute.

4. Occupational Safety and Health Administration. Washington (DC): United States Department of Labor [accessed 2018 July]. https:www.osha.gov. https://www.osha.gov/SLTC/etools/machineguarding/presses/safetydistance.html.

5. Occupational Safety and Health Administration. Washington (DC): United States Department of Labor [accessed 2018 July]. https:www.osha.gov. https://www.osha.gov/dts/osta/lototraining/hottopics/ht-relche-1-2.html.

Forensic Engineering Analyses of Right-Turning Trucks Impacting Bicyclists

By Richard M. Ziernicki, PhD, PE (NAFE 308F) and William H. Pierce, PE (NAFE 846C)

Abstract

Right-turning trucks present a serious hazard to bicyclists. When a collision between a right-turning truck and a bicyclist occurs, the truck driver often does not realize an impact occurred, and the bicyclist is pushed down and dragged by the truck. Such collisions result in serious injury or death. Forensic engineers are retained to investigate and reconstruct such complex collisions. Oftentimes, there are disputes between forensic engineers as to the impact location, visibility, and reaction processes of both the driver and bicyclist. For example, physical evidence related to impact is usually faint and is a subject of debate between forensic engineers. Forensic engineers also disagree on the direct line-of-sight or line-of-sight through mirrors. Further, reactions (or lack thereof) are typically subject to debate. This paper presents the application of various techniques and methodologies to effectively reconstruct collisions between right-turning trucks and bicyclists. Such techniques and methodologies include the identification and verification of faint physical evidence regarding impact location using computer simulation and/or testing, the use of high-definition laser scans and virtual scenes to replicate mirror line-of-sight or obstruction line-of-sight, evaluation of driver and bicyclist reaction processes, and the use of scientific visualizations to effectively communicate complex issues of a case.

Keywords

Semi, truck, bicycle, pedestrian, accident reconstruction, high-definition laser scanning, mirror, side mirror, line-of-sight, perception, reaction, physical evidence, right-turning truck, multibody simulation, scientific visualization, PC-Crash, forensic engineering

Introduction

Forensic engineers are often retained to investigate and reconstruct complex incidents involving a right-turning truck impacting a bicyclist. This paper is a compilation of advanced scientific methodologies available to forensic engineers for evaluating such complex collisions. The methodologies are presented in the form of two case studies.

Case Study 1: Pillar Line-of-Sight Obstruction

A bicyclist was riding on the sidewalk under a newly constructed overpass on the sidewalk (**Figure 1**). The bicyclist approached the crosswalk shown in **Figure 1** with a pedestrian signal illuminated with a "walk" designation. As the bicyclist approached the crosswalk, a truck was turning right on a green light into the path of the bicyclist. However, the bicyclist testified he did not see the truck due to an overpass pillar obstructing his view until moments before impact. The bicyclist steered sharply to the left but was unable to avoid the collision. Similarly, the truck driver claimed he did not see the cyclist, but rather felt a minor bump at impact. As a result of the collision, the bicyclist was thrown onto the ground and dragged under the truck's front axle for 65 ft, sustaining serious injury.

The plaintiff was the seriously injured bicyclist, and

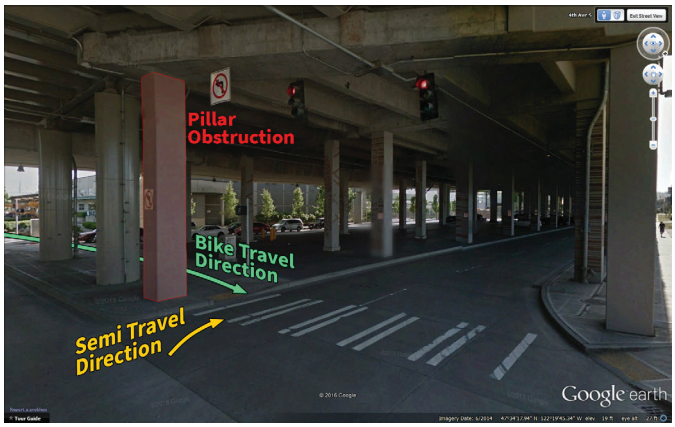

Figure 1
Path of bicyclist and semi pre-impact.

Richard M. Ziernicki, PhD, PE, 7185 S. Tucson Way, Centennial, CO 80112, 303-925-1900, rziernicki@knottlab.com

the primary defendant was the city for improperly designing the placement of the crosswalk such that there was a line-of-sight issue between pedestrians and right-turning vehicles due to the pillar obstruction. The purpose of the forensic investigation was to determine whether or not the pillar created a visual obstruction to both the bicyclist and right-turning truck driver and whether or not the bicyclist's reaction was reasonable for the conditions. Methodologies used for this forensic engineering analysis included:

1. Enhancement of photographs to identify faint physical evidence.
2. Determining the impact configuration based on physical evidence.
3. Simulating the accident.
4. Conducting a line-of-sight study to determine whether or not the pillar caused a visual obstruction.
5. Evaluating the bicyclist's reaction to determine whether or not the bicyclist reacted reasonably.

Enhancement of Photographs to Identify Faint Physical Evidence

The first step to reconstructing right-turning truck vs. pedestrian accidents is to study the police report, scene surveys, witness statements, and photographs. Witness statements and scene surveys can be used to generally identify the impact location. However, witnesses are often inconsistent in reporting the impact location, and police surveys often miss faint physical evidence that establishes the area of impact. Therefore, the investigating forensic engineer must carefully examine scene photographs for evidence that may have been overlooked during the initial scene investigation.

Bicycle tires will often leave some sort of scrubbing evidence on the roadway during impact. However, such evidence is often very faint and overlooked. Failure to identify such faint evidence may result in improper positioning of the area of impact, which may adversely affect the entire investigation. Therefore, digital scene photographs must be thoroughly analyzed before reaching the conclusion that there was no evidence related to impact or mistaking more pronounced evidence after the collision, such as the bicycles dragged along the roadway, as the area-of-impact.

Figure 2
Scene photograph with brightness and contrast adjusted to identify faint physical evidence related to impact.

A useful technique for identifying potential physical evidence related to impact is through the adjustment of brightness and contrast of digital scene photographs. **Figures 2** and **3** show scene photographs taken by police with the brightness and contrast adjusted to identify potential evidence related to the area-of-impact in the first case study.

The locations of the marks were established using the principles of photogrammetry[1,2,3,4,5,6,7,8]. The photogrammetry process first involved correcting the photograph for lens distortion. Next, real-world 3D coordinates were established for 2D objects seen in the photograph using the point cloud generated from high-definition laser scanning. Commercially available dedicated photogrammetry software (PhotoModeler) then solved for virtual camera positioning, orientation, and properties matching that of the real-world camera that took the photograph.

Figure 3
Scene photograph with brightness and contrast adjusted to identify faint physical evidence related to impact.

Figure 4
Viewing the high-definition point cloud through a virtual camera that matched the properties and orientation of the real-world camera that took the photograph. Faint tire marks "painted" onto the point cloud, thereby establishing the locations of the tire marks.

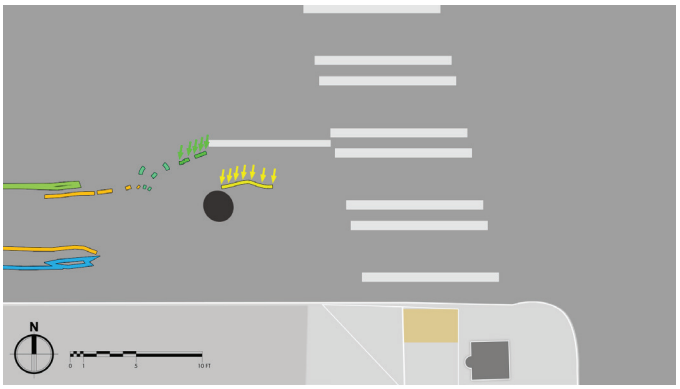

Figure 5
Locations of the faint tire marks from top view (shown with arrows).

The virtual camera was then put into the virtual point cloud scene. By viewing the point cloud through the virtual camera, the marks were "painted" onto the point cloud, thereby establishing the positions of the marks (**Figures 4** and **5**).

Impact Configuration Based on Physical Evidence

The impact configuration between the right-turning truck and bicycle was established using physical evidence on the truck's front bumper and bicycle. Scratches were observed on the truck's front bumper consistent with an impact with a bicycle (**Figure 6**).

The locations of the bumper scrapes were added to a virtual truck model to-scale. A scaled virtual bicycle was aligned with the truck's bumper so that the bicycle was properly aligned with the bumper scrapes. The bicycle's rear bike rack aligned with the contact marks on the bumper (**Figure 7**).

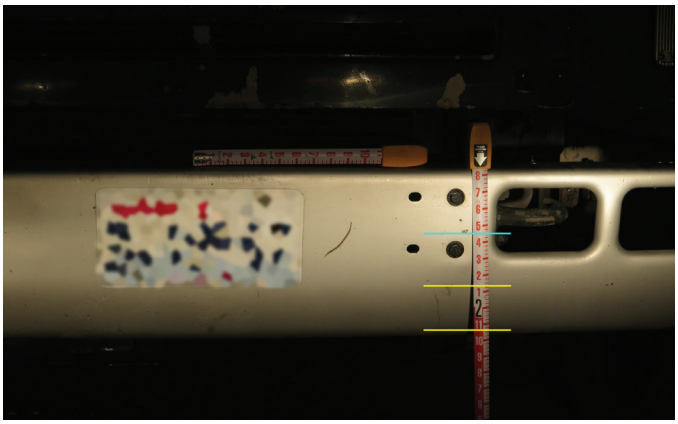

Figure 6
Evidence on truck bumper. Horizontal lines added to show scrape heights.

The bicycle's rear rack was deformed, consistent with impact between the semi's front bumper and the right side of the bicycle's rear rack. **Figure 8** shows the rack damage and approximate principal direction of force (PDOF), a term defined to simplify collision analysis. The PDOF is the direction of the summation of all collision forces required to deform the vehicle. The PDOF was consistent with an angled impact between the truck bumper and bicycle (**Figure 9**).

PC-Crash Simulation Turning Dynamics

PC-Crash was used to simulate the dynamics of the truck's turn[9,10,11]. First, the PC-Crash scene and tractor-trailer were developed. The point cloud from the high-definition laser scan of the accident site was used to generate a terrain mesh of the accident site. The terrain mesh and physical evidence locations were imported into the PC-Crash scene. A scaled truck model was also imported into the scene.

Figure 7
Virtual model of bicycle aligned with bumper scrapes. The bicycle's rear rack aligned with the bumper scrapes.

Timing of similar-sized exemplar right-turning trucks at the intersection were provided. The timing values were used to establish acceleration and velocity profile for the truck that were input into the PC-Crash simulation. The path of the model truck was adjusted until the simulation of the truck's path matched the physical evidence and rest position of the truck (**Figure 10**).

PC-Crash Multibody Impact Simulation

After the truck's turning dynamics and path were established in PC-Crash. A multibody impact simulation was used to simulate the collision between the truck and the bicycle. The purpose of the multibody impact simulation was to:

1. Verify impact speed estimate based on exemplar turning truck dynamics.
2. Validate whether or not faint physical evidence was related to the incident.
3. Refine area of impact.
4. Provide scientific imagery of the impact phase of the collision.

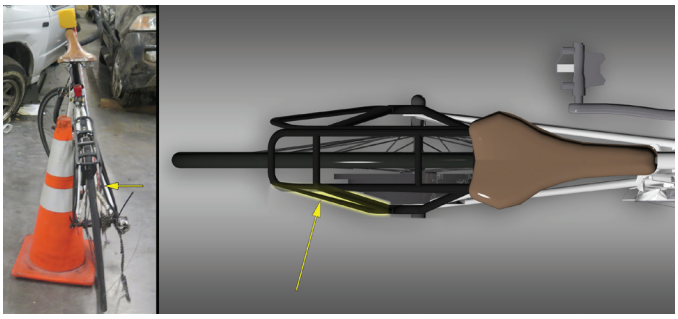

Figure 8
Inspection photograph of subject bicycle. Yellow arrow showing deformation to the right side of the bicycle's rear rack.

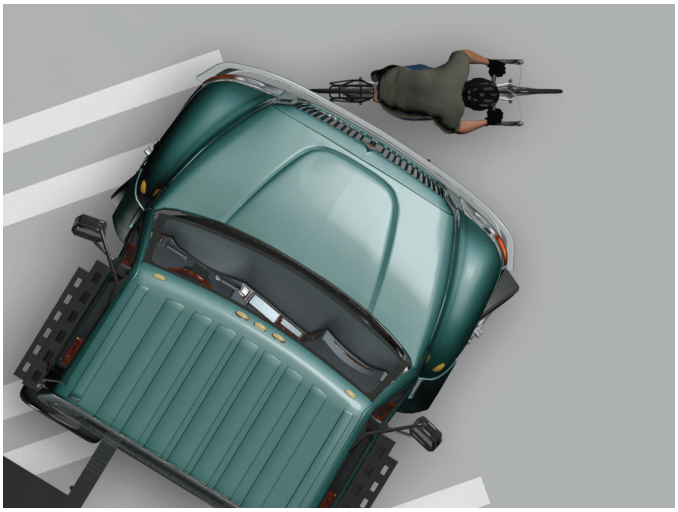

Figure 9
Bicycle rear-rack damage consistent with angle between truck bumper and bicycle at impact. The bicyclist is shown diagrammatically. In actuality, the front wheel of the bicyclist was leaning in a turn in response to the pending impact.

The bicycle multibody simulation involved first modeling the bicycle multibody and rider. A pre-packaged bicycle and rider multibody model was used as a template. The bicycle and rider multibody geometry, size, and weight were adjusted to closely match those of the subject bicycle and rider (**Figure 11**).

Further, using the PC-Crash simulation software's multibody model of bicycle and rider, the joint properties of the bicycle were adjusted by the authors to allow articulation of the front wheel and handlebars that were not included in the template multibody model. The articulation of the front wheel and handlebars allows from more realistic post impact movement of the bicycle.

The multibody bicycle was placed in the established

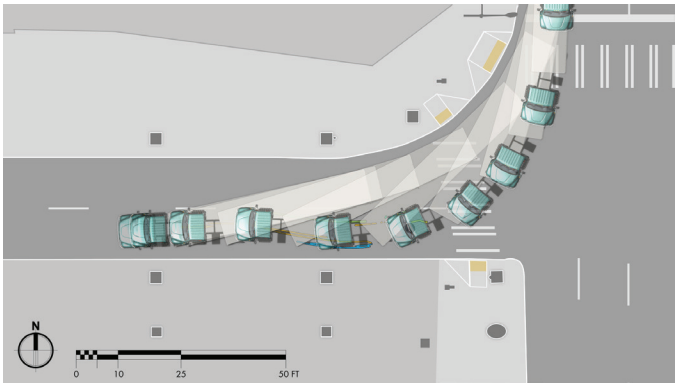

Figure 10
Turning dynamics of the truck based on the physical evidence and rest position of truck simulated using PC-Crash. The location of physical evidence is depicted in Figures 2, 3, 4, and 5.

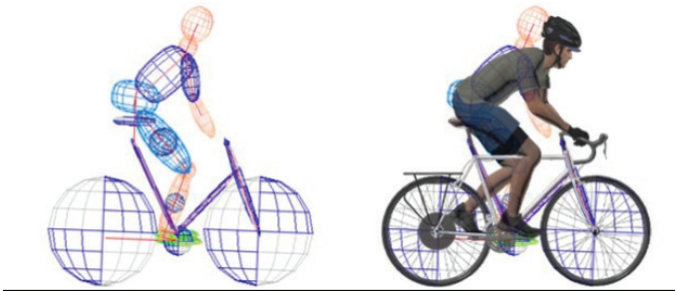

Figure 11
Bicycle and rider multibody model (left) closely matching the geometry, size, and weight of the subject bicycle and rider (right).

Figure 12
Impact progression of bicycle and rider based on PC-Crash simulation.

impact configuration relative to the truck based on analysis of the physical evidence. Simulations were conducted at various impact locations along the turn path of the truck until the impact dynamics of the bicycle best matched the physical evidence. **Figure 12** shows the progression of impact matching the physical evidence based on the PC-Crash simulation.

The bicycle movement after impact shown in **Figure 12** shows the that faint physical evidence identified in scene photographs is consistent with the bicycle's tires scrubbing against the ground as the bicycle was pushed down. After the bicycle was pushed down, the semi-tractor's right front wheel ran over the bicycle's front wheel creating an imprint in the pavement.

Bicycle Pre-Impact Motion

After the and impact configuration were established based on physical evidence and multibody simulation, pre-impact motion of the bicycle was simulated using PC-Crash using a kinematic simulation model. The pre-impact trajectory of the bicycle was based on the deposition testimony of the bicyclist. The bicyclist testified that he was riding on the right side of the sidewalk and swerved when he first observed the truck beyond the pillar. **Figure 13** shows the trajectory of the bicycle leading to impact and the throw distance of the bicycle.

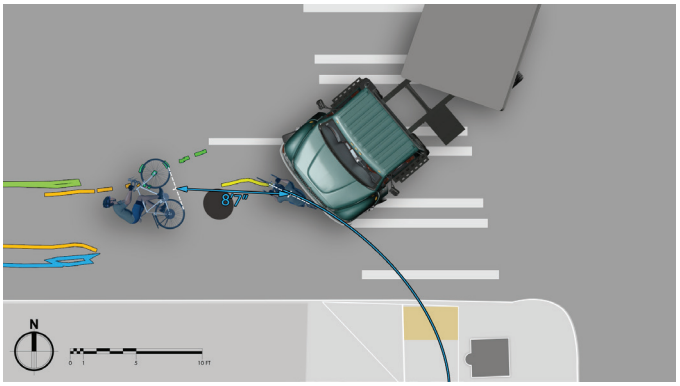

Figure 13
Simulated trajectory of bicycle pre-impact and throw distance of bicycle.

Line-of-Sight Evaluation (Obstruction)

After simulating the motion of the truck and bicycle pre-impact, line-of-sights can be evaluated if needed. The process of evaluating line-of-sight can be done in either 2-D and 3-D space. PC-Crash's "sight-lines" feature was used to draw a sight line between the bicyclist and the corner of the truck. **Figure 14** shows the sight-line in 2D and the sight-line in 3D within PC-Crash.

Case Study 1: Conclusions

The sight-line analysis showed the bicyclist first saw the truck turning approximately 2.25 seconds before

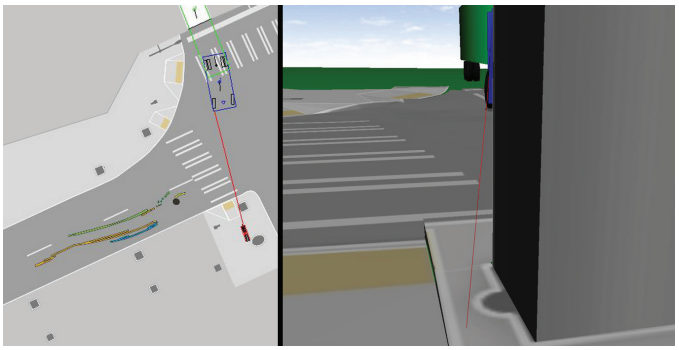

Figure 14
2D line-of-sight (left) and 3D line-of-sight in PC-Crash.

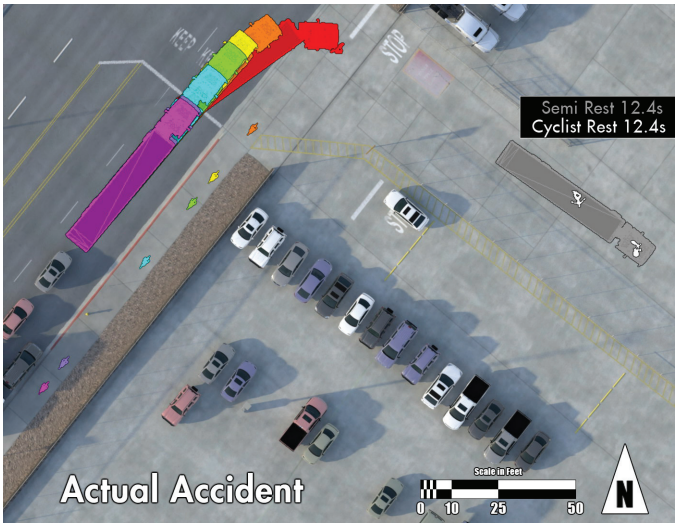

Figure 15
Bicyclist was riding on sidewalk and was struck by right-turning semi. Bicyclist was dragged 95 ft after impact.

impact. Pre-impact simulation showed that the bicyclist reacted for approximately 1 second and then made a swerve maneuver to the left to avoid the semi. However, the bicyclist was unable to avoid impact and was struck by the semi. Therefore, the line-of-sight obstruction contributed to the bicyclist's inability to react in time to avoid being impacted by the semi.

Case Study 2: Truck Turning into Warehouse Driveway

A bicyclist was riding on the sidewalk during rush hour traffic. The bicyclist approached the driveway to a warehouse facility. According to witnesses, a semi-tractor was stopped and was preparing to make a right turn into the driveway. As the bicyclist approached the driveway, the semi-truck driver turned in front of the bicyclist The bicyclist was struck by the semi and dragged under the semi-tractor approximately 95 ft before the truck stopped. As a result of the collision, the bicyclist sustained serious injuries. A general graphic showing the movement of the truck and bicycle is shown in **Figure 15**.

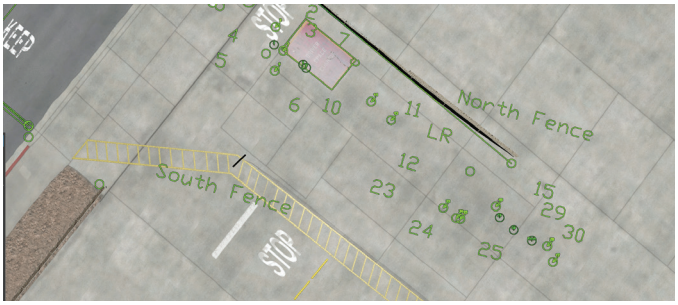

Figure 16
Plotted scene survey data.

The purpose of the investigation was to determine whether or not the bicyclist reacted reasonably to the truck and to determine whether or not the truck driver could have seen the bicyclist had the driver used his side-mirrors. Methodologies used for this forensic engineering analysis included:

1. Identification of faint physical evidence related to the area-of-impact.
2. Determining the impact configuration based on physical evidence.
3. Using video footage and videogrammetry to test exemplar truck motion.
4. Simulating the accident and evaluation of the bicyclist's reaction.
5. Testing to validate faint physical evidence related to the area-of-impact.

Figure 17
Cropped scene photograph analyzed for faint physical evidence related to impact.

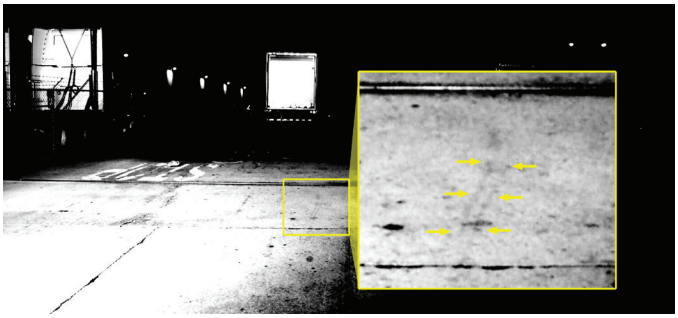

Figure 18
Scene photograph in black-and-white with adjusted brightness and contrast. Arrows pointing to suspected tire scrub marks related to impact.

6. Using high-definition scans to create virtual mirror models to test mirror line-of-sight.

Identifying Area of Impact

The police photographed and surveyed the accident scene. **Figure 16** shows a scene diagram depicting physical evidence surveyed by scene investigators. While the survey was very thorough, there was no evidence identified in the survey that was clearly related to impact.

Figure 19
Subject bicycle (left) and exemplar bicycle (right). Subject bicycle and exemplar bicycle had the same brand and model tires.

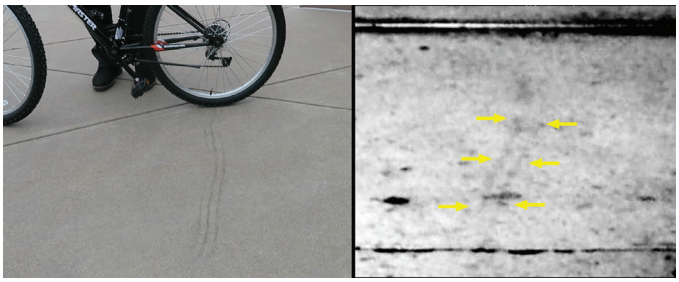

Figure 20
Tire scrub marks generated through testing (left) consistent with scrub marks identified in scene photograph (right).

Figure 21
Scrapes on right corner of truck's front bumper consistent with the bumper impacting the bicycle's frame.

Therefore, the scene photographs were evaluated to identify faint physical evidence consistent with impact, such as bicycle tire scrubbing against the pavement.

Similar to the first case study, the contrast and brightness of scene photographs in the second case study were adjusted to identify potential evidence related to the area-of-impact. **Figure 17** shows an original scene photograph, and **Figure 18** shows the same scene photograph in black-and-white with contrast and brightness adjusted. **Figure 18** also shows faint physical evidence suspected as a bicycle tire scrubbing mark during impact.

Testing to Confirm Tire Mark Pattern

After identifying suspected scrub marks related to impact, testing was conducted to establish whether or not the marks were consistent with tire scrub marks during impact. An exemplar bicycle with the same make of tires as the subject bicycle was tested (**Figure 19**).

The exemplar's bicycle tires were inflated to the manufacturer's recommended operating pressure. The bicycle was then pushed down and dragged, closely replicating the motion of the bicycle pushed down by a semi's bumper. **Figure 20** shows the bicycle tire formed parallel scrub marks similar to the faint marks identified in the scene photographs. Therefore, the parallel scrub marks identified in the scene photograph is consistent with scrub marks left by the subject bicycle's rear tire as it is pushed down by the truck.

Impact Configuration Based on Physical Evidence

The truck was inspected for physical evidence related to impact. There were scrape marks surrounding the corner of the right front bumper consistent with the bumper impacting the bicycle's frame (**Figure 2**1). There were also scrub marks on the front bumper consistent with the front bumper impacting the front tire of the bicycle (**Figure 22**).

Truck Turning Dynamics and Simulation

Several exemplar trucks were video recorded making right turns into the facility. One of the trucks had very similar geometry as the subject truck and made a wide turn into the driveway very similar to the turn made by the driver during the incident.

The video footage of the truck was processed using the principles of videogrammetry (or the application of photogrammetry to multiple frames of a video) to identify the acceleration profile of the exemplar truck. The

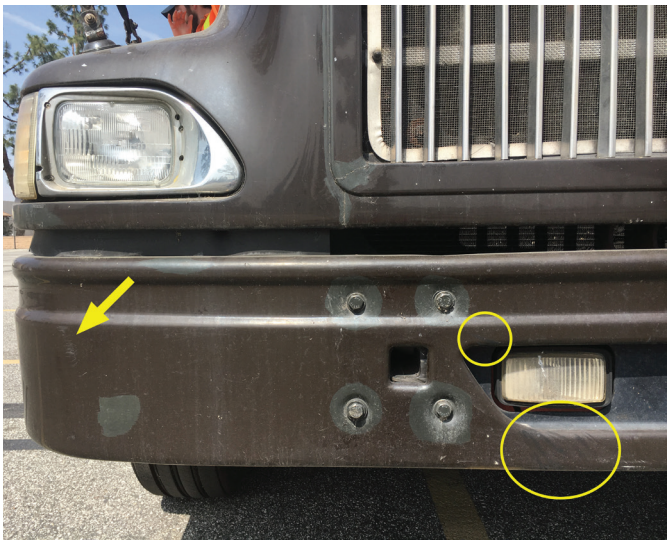

Figure 22
Scrapes on front corner (arrow) and front bicycle tire scrub marks (circles) on truck's front bumper.

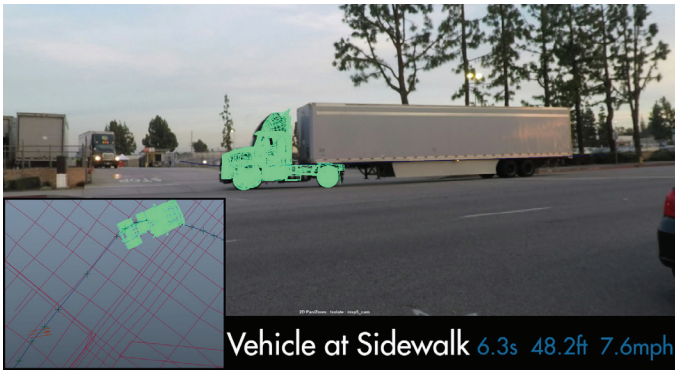

Figure 23
Example of camera matched virtual truck model position overlaid on video footage.

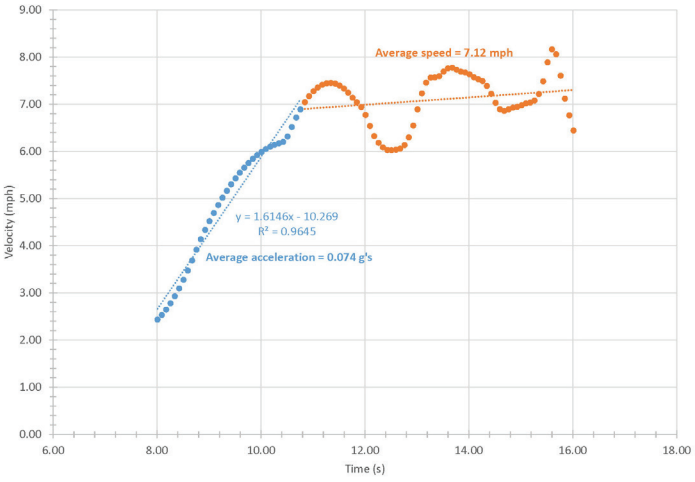

Figure 24
Velocity and acceleration of exemplar making wide right turn.

videogrammetry process involved first calibrating the camera used to capture the video to correct for lens distortion.

High-definition laser scan data was then used to identify real-world coordinates of fixed objects seen in the video footage. The real-world coordinates were then input into the photogrammetry software to solve for the video-camera's properties, position, and orientation. After solving for the video-camera's properties, position, and orientation, a virtual camera was placed into a virtual scene with the point cloud generated from the high definition scanning. Captured video frames were placed in the virtual scene. The 3D model of the truck was placed into the scene to match the position and orientation of the truck seen in the video footage over multiple frames (**Figure 23**).

After matching the position and orientation of the truck over multiple frames, the velocity and acceleration of the truck were determined throughout the video sequence. **Figure 24** shows the velocity profile of the exemplar truck making a right turn. The exemplar truck accelerated at approximately 0.074 g's and reached a peak speed of approximately 7 mph during the turn.

After establishing the acceleration rate and peak speed of an exemplar truck turning into the facility, PC-Crash was used to simulate the dynamics of the truck's turn. The acceleration and peak speed values were input into the PC-Crash simulation. The path of the model truck was adjusted until the simulation of the truck's path matched the physical evidence and rest position of the truck (**Figure 25**).

The truck driver testified that he did not make a buttonhook turn, but rather proceeded to go forward and then made a 90 degree turn. The turning path in **Figure 25** and **Figure 15** is consistent with the driver's deposition testimony/physical evidence and shows that the truck turned

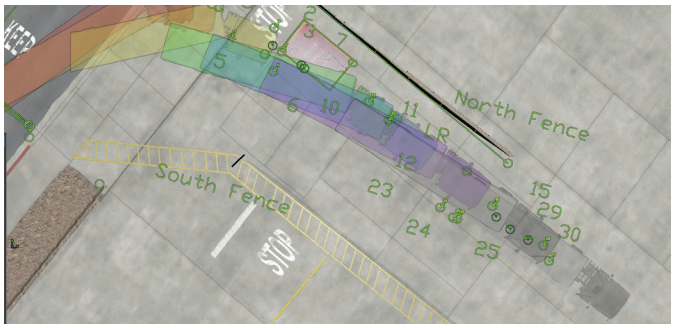

Figure 25
Turning dynamics of the truck simulated using PC-Crash.

into the driveway's opposing lane of travel. Therefore, when the truck reached the driveway, the truck would have appeared to have been going straight rather than turning into the driveway from the perspective of the bicyclist. However, when the truck reached the middle of the driveway, it made a sharp right turn in front of the bicyclist, creating an emergency situation.

Impact Simulation

After establishing the area of impact, impact orientation, and the dynamics and path of the truck turn, the impact with the bicycle was simulated using the multibody simulation model in PC-Crash. Similar to case study 1, the purpose of the multibody impact simulation was to:

1. Verify impact speed estimate based on exemplar turning truck dynamics.

2. Validate whether or not faint physical evidence was related to the incident.

3. Refine area of impact.

4. Provide scientific imagery of the impact phase of the collision.

The geometries, sizes and weights of the bicycle and rider multibody models were adjusted to closely match those of the subject bicycle and rider. Further, the joint properties of the bicycle were adjusted to allow articulation of the front wheel and handlebars that were not included in the template multibody model.

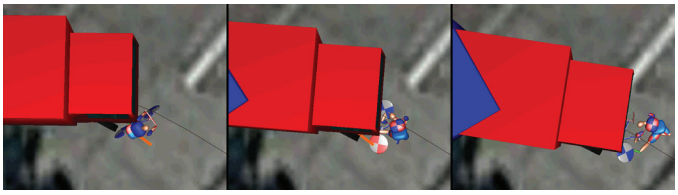

Figure 26
Impact progression of bicycle and rider based on PC-Crash simulation. Orange line shows location of tire scrub mark identified in scene photograph.

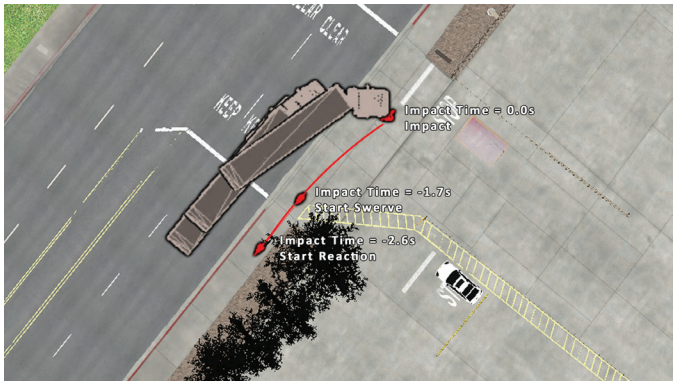

Figure 27
Bicyclist pre-impact motion start of reaction to impact.

The multibody bicycle was placed in the established impact configuration relative to the truck based on analysis of the physical evidence. For the analysis purposes, the speed of the bicycle was set at 15 mph consistent with multiple witness statement and the speed of the truck was estimated at 7 mph, based on turning dynamics of the exemplar truck. Simulations were conducted at various impact locations along the turn path of the truck until the impact dynamics of the bicycle best matched the physical evidence. **Figure 26** shows the progression of impact matching the physical evidence based on the PC-Crash simulation.

The bicycle movement after impact shown in **Figure 26** shows the that faint physical evidence identified in scene photographs is consistent with the bicycle's tires scrubbing against the ground as the bicycle was pushed down. Further, the bicycle and rider ended up under the center of the truck and dragged consistent with the physical evidence. Therefore, the multibody simulation provided additional basis for impact speeds, identification of physical evidence related to impact, and area of impact. In addition, the multibody simulation was used as basis for the motion of the bicycle and rider after impact in scientific visualizations.

Bicycle Pre-Impact Motion

Pre-impact motion of the bicycle was simulated using PC-Crash's kinematic simulation model. The pre-impact motion of the bicycle was based on:

1. Area of impact.

2. Impact configuration.

3. Impact speed.

4. Deposition testimony that the bicyclist was initially riding on sidewalk and swerved immediately prior to impact.

5. Assumption that the bicycle made an emergency swerve maneuver at 0.3 g's lateral acceleration prior to impact.

Figure 27 shows the bicyclist started reacting at approximately the same time that the truck began turning

near the middle of the driveway, 2.6 seconds before impact. After a reaction time of approximately one second, the bicyclist began swerving, but was unable to avoid striking the semi.

Mirror Analysis

Truck driver line-of-sight through truck mirrors was also conducted in virtual space[12]. The geometry of the truck's interior, exterior and side-mirrors was documented using high-definition laser scanning. These scans don't register points on highly reflective materials, such as mirrors. Therefore, blue painter's tape was applied to the mirrors to mask the reflective material.

Detailed virtual models of the bicycle and truck were created from the point cloud generated from the high definition laser scans. Meshes of the mirrors were created from the high-definition laser scans, detailing the curvature of the mirrors. (**Figure 28**).

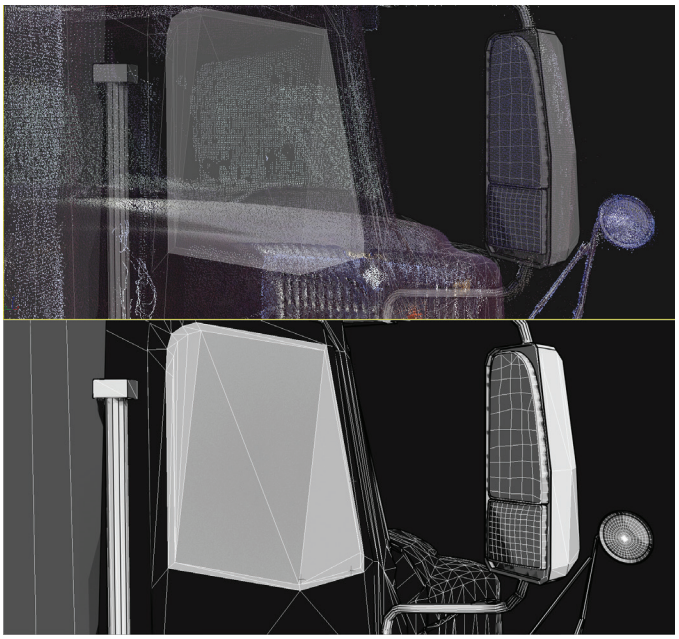

Figure 28
Mesh of mirror created from point cloud (top) and resulting mesh (bottom).

Motion of the bicycle and truck were exported from PC-Crash to the virtual bicycle and truck objects in visualization software. Within the visualization software, reflective material properties were assigned to the mirror meshes. The lighting within the scene was adjusted to account for the sun position and brightness at the time of the incident. A virtual camera was added to replicate the driver's perspective looking at the mirrors while making the turn.

Once simulation motion, material properties, lighting, and virtual cameras were added to the scene, the visualization was rendered. **Figure 29** shows an example of a still frame showing the driver's view out of each of the mirrors eight seconds before impact. The figure clearly shows that the bicyclist was visible in two mirrors eight seconds before impact. Further, the bicyclists speed, 8 seconds before impact, is approximately 7 mph. It is consistent with witnesses statements and time-space of semi and bicyclist approaching the point of impact. After traveling at the speed of 7 mph, the bicyclist sped up to 15 mph, attempting to avoid right turning semi.

Figure 29
View out of each of the right hand side mirrors 8 seconds before impact from the driver's perspective.

Further, mirror visibility cones were created using the rendered visualization of the mirrors. The visibility cone for each mirror was calibrated by plotting the extent of the visibility in a 2D top view. **Figure 30** shows an example of the visibility cones 8 seconds before impact.

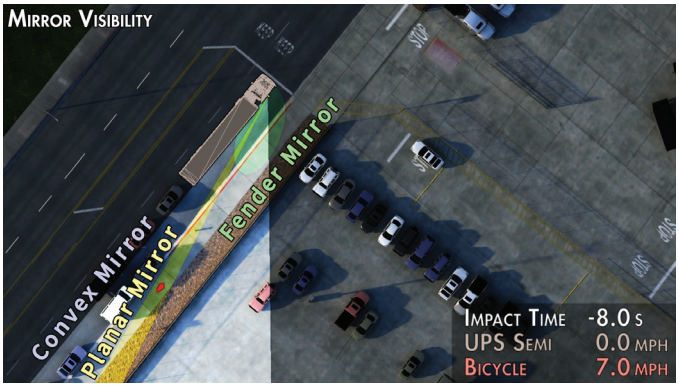

Figure 30
Visibility cones created for the three mirrors 8 seconds before impact.

Case Study 2: Conclusions

There were some major conclusions made in the second case study:

1. The analysis showed the bicyclist first saw the truck turning approximately 2.6 seconds before impact.

2. Pre-impact simulation showed that the bicyclist, for a 1 second reaction time, made a swerve maneuver to the right to avoid the semi at 1.7 second prior to impact; however, the bicyclist was unable to avoid impact

3. The truck driver could have seen the bicyclist in one or more of the mirrors for more than 12 seconds before impact.

Conclusion

Two case studies were presented regarding right-turning trucks impacting bicyclists. They show that faint physical evidence related to impact is often overlooked by investigators. However, adjusting the brightness and contrast of scene photographs is helpful to locate overlooked physical evidence. Photogrammetry can be used to identify the locations of identified physical evidence. Testing and PC-Crash multibody simulations can be used to validate whether or not suspected physical evidence is consistent with impact.

Truck impact speeds can be estimated by video recording exemplar trucks making similar right turns and evaluating speeds and accelerations by timing or videogrammetry techniques. The truck turning path can be established through PC-Crash simulation by following the trail of physical evidence and matching the truck's rest position.

Once the impact speeds are established, PC-Crash multibody simulations can be used to validate estimated impact speeds, impact location, and/or identified impact scuffing. The multibody simulations are also useful in providing a visualization of the severity of the accident.

In both case studies, major debate revolved around the visibility that the bicyclists and the trucks had of one another. The line-of-sight tool in PC-Crash is useful in establishing whether or not an obstruction limited driver and rider visibility leading up impact. Further, truck mirror visibility cones can be created by capturing high-definition scans of the truck's mirrors, creating virtual mirror geometry, applying reflective material properties to the virtual mirrors, and rendering the truck driver's view looking at the virtual mirrors.

References

1. K. Breen and C. Anderson, "The Application of Photogrammetry to Accident Reconstruction," SAE Technical Paper Series, 1986, Paper no. 861422.

2. M. Callahan, B. LeBlanc, R. Vreeland, and G. Bretting, "Close-Range Photogrammetry with Laser Scan Point Clouds," SAE Technical Paper Series, 2012, Paper no. 2012-01-0607.

3. C. Coleman, D. Tandy, J. Colborn, and N. Ault, "Applying Camera Matching Methods to Laser Scanned Three Dimensional Scene Data with Comparisons to Other Methods." SAE Technical Paper Series, 2015, Paper No. 2015-01-1416.

4. S. Fenton and R. Kerr, "Accident Scene Diagramming Using New Photogrammetric Technique," SAE Technical Paper Series, 1997, Paper no. 970944.

5. W. Neale, S. Fenton, S. McFadden, and N. Rose, "A Video Tracking Photogrammetry Technique to Survey Roadways for Accident Reconstruction," SAE Technical Paper Series, 2004, Paper no. 2004-01-1221.

6. R. Ziernicki and D. Danaher, "Forensic Engineering Use of Computer Animations and Graphics." Journal of the National Academy of Forensic Engineers, vol. 23, no. 2, pp. 1-9. Dec. 2006.

7. D. Danaher and R. Ziernicki. "Forensic Engineering Evaluation of Physical Evidence in Accident Reconstruction," Journal of the National Academy of Forensic Engineers, Vol. 24, no. 2, Dec., pp. 1-10, 2007.

8. R. Ziernicki, W. Pierce, and A. Leiloglou, "Forensic Engineering Usage of Surveillance Video in Accident Reconstruction." Journal of the National Academy of Forensic Engineers, Vol. 31, no. 2, Dec., pp. 9-19, 2014.

9. "PC-Crash (Version 11)," MacInnis Engineering Associates Ltd. [Online]. Available: http://www.pc-crash.com/

10. W. Cliff and D. Montgomery, "Validation of PC-Crash – A Momentum-Based Accident

Reconstruction Program," SAE Technical Paper Series, 1996, Paper no. 960885.

11. A. Moser, F. Hoschopf, H. Steffan, and G. Kasanicky, "Validation of the PC-Crash Pedestrian Model," SAE Technical Paper Series, 2004, Paper no. 2000-01-087. J. Ball,

12. D. Danaher, and R. Ziernicki, "A Method for Determining and Presenting Driver Visibility in Commercial Vehicles," SAE Technical Paper Series, 2007, Paper no. 2007-01-4232.

Forensic Engineering Analysis of a Failed ROPS

By Daniel J. Cowley, PE (NAFE 909M)

Abstract

Agricultural, commercial, and some lawn and garden tractors (tractors) have been known to tip and roll over. Roll-over protective structures (ROPS) are designed and tested to assure seat-belted occupants can survive in a zone of clearance within the structure, during and following a roll-over event. Within the laboratory testing parameters established in the current standards, energy absorption is based on tractor mass alone, apart from any other forces that may be acting on the tractor. Current standards allow tractor manufacturers to determine the "reference mass" used for ROPS testing. Most manufacturers fail to include the mass of any attached implements. Serious consideration should be given to upgrade the current standards to include the mass of large implements and spreaders in the "reference mass" used for testing. When implements remain attached to the tractor throughout the roll-over event, ROPS should still be designed to protect operators. In the past, tractors were mainly employed in soil-engaging or surface-grooming exercises. The center of gravity (CG) of these attached implements was relatively low. Today, however, tractors may tow larger, taller, and heavier implements with high CG on multiple axles, such as large liquid manure tank spreaders. The purpose of this paper is to investigate the physical issues associated with tractors towing high CG implements, such as geometrically tall, articulated steerable axle spreaders operating in sloped terrain that cause an ROPS to fail.

Keywords

Slopes, stability, tractors, ROPS, liquid manure spreader with steerable axles, articulated steering device of semi-mounted trailers, tire wear, forensic engineering, OECD-Code 4, ISO 11783, ISO 26402, ISO 3463, ISO 5700, ISO 6489-3, SAE J 1194, SAE J 2194

Introduction

Only 50 years ago, cattle grazed in the open range. Much of the pasture land across the United States was sloped. Things have changed with time, however. Unlike the past practices of cattle grazing in pasture lands, cows are increasingly confined to buildings and modern feeding methods. The pasture lands have since been converted to fields growing hay for feeding cattle, but the slopes still exist. Modern tractors and spreaders now travel the highways of the country heading from farmstead to field filled with liquid manure in nurse tanks behind semi-tractors or multi-axle spreaders to disperse on the nearby fields.

Roll-Over Protective Structures (ROPS)

Occupants operate the tractors that travel on highways and into fields. To better safeguard the operator, the industry encourages self-propelled machines to include protective structures called:

- Roll-over protective structures (ROPS)
- Tip-over protective structures (TOPS)
- Falling-object protective structures (FOPS)
- Operator protective guards (OPG)
- Overhead guards (OHG)

The ROPS is intended to protect the occupants in the tractor enclosure in the case of vehicle overturn[1] (**Figure 1**).

History of the ROPS in the United States

John Deere patented the ROPS in 1966, and turned it over to the industry shortly after that. Between 1967 and

Daniel Cowley, PE, 42671 W Anne Ln, Maricopa, AZ 85138, 520-840-1246, dan.cowley@facet-ics.com

1976, the ROPS was optional on tractors.

Survivability was the goal for ROPS (**Figure 2**). Although the industry tries to encourage farmers to install ROPS on these vintage tractors, many are still not equipped with an ROPS. Significant efforts are being made by the industry to retrofit tractors originally sold without ROPS. Kits are provided at minimal cost to these tractor owners to retrofit their tractors with ROPS[2].

The ROPS is tested before sale, and the manufacturer certifies the testing is compliant with industry standards. The standard meant to assure the occupant of vehicle protection within a defined zone is known as the "crush clearance zone" or simply the "clearance zone." This level of protection is determined by the energy level specified in the standard for the specific vehicle.

Current standards vary only slightly on matters of testing temperature and seat belt anchor requirements, but all represent an equivalent energy level tied specifically to the mass of the tractor[3]. If the tractor were to overturn under conditions of its mass alone, this energy level should provide a safety factor to protect the operator in a roll-over event. However, this current standard allows tractor manufacturers to determine the "reference mass" based solely on tractor mass rounded to the next 500 kg, not taking into account any of the mass from an implement that may remain attached and roll-over with the tractor.

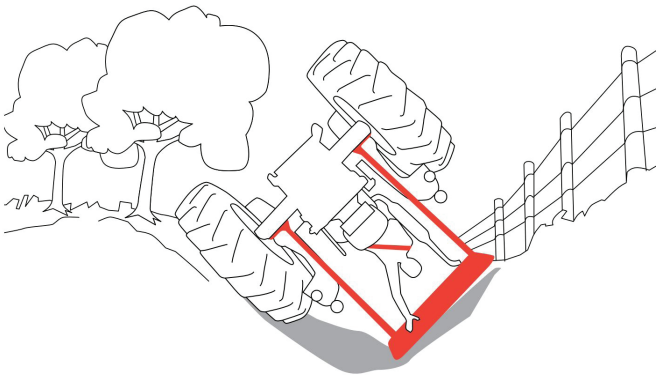

Figure 1
ROPS – operator zone of protection from OSHA and NIOSH.

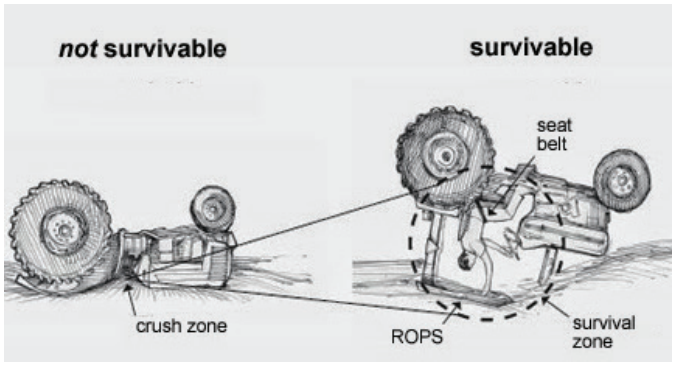

Figure 2
Crush zone and survivability[4] from an unknown source.

How an ROPS Is Tested

The ROPS is designed to absorb sufficient energy to keep the enclosure's structural members from encroaching into the "clearance zone" while still providing for sufficient visibility to the work environment. The clearance zone is defined in the standards as a safe area in the ROPS for a seat-belted operator (**Figure 3**).

Load-carrying members of the ROPS are placed in strategic locations to deflect (strain) under applied forces (stress). The absorbed energy is observed from reviewing the area measured beneath a stress-strain curve before any encroachment occurs into the clearance zone by any portion of the ROPS.

Between tests, the ROPS is examined to make sure the welds for structural member do not fracture. Cracks or tears in parent material of structural member are permissible as long as the operator's clearance zone is intact at the end of the testing cycles.

Crush loads are applied to the ROPS from the rear, top and sides in a specific sequence that are identified in the standards.

From a general understanding of the stress-strain relationship, there is an elastic (then a plastic) deformation that can take place with the ROPS. The more stress and strain added, the more the structure fails to return to the initial shape when the load is removed. Once crushed, very large and permanent deformations that intrude the clearance zone of the ROPS provide evidence of the energy absorption of the structure. If energy absorption is insufficient for the loads applied, the crushed members encroach the operator's clearance zone, and the ROPS fails the test.

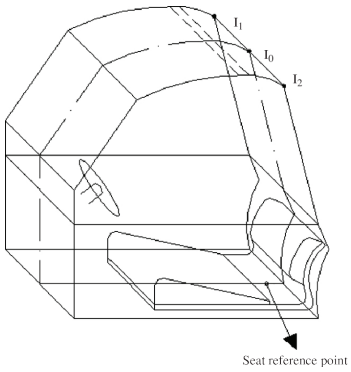

Figure 3
Clearance zone from the standard.

The current standards clearly define the

energy levels proportional to a "reference mass" cited in the standards. The tractor manufacturer determines the "reference mass" used for testing based on the mass of the specific tractor to be certified. The ROPS must demonstrate that it can withstand the specific crush loads without encroaching into the "clearance zone" to be certified for a particular make and model of tractor.

Up to this point, the selection of "reference mass" is left to the tractor manufacturer and must be within the guidelines provided in the standards. In most cases, the mass is rounded to the next 500 kg above the mass of the unladen tractor. This assumes that the tractor mass is the only consideration in the roll-over event.

Why the Current Standards Are Deficient

Currently, industry standards do not generally test the combination of tractor and spreader for a roll-over event. Industry standards only consider the tractor mass and assume the decoupling of the implement during the roll-over event. For example, the standards infer chain connections between tractor and implement, as in the case of stump pulling or prior drawbar pin failure like a fuse. The inertial contribution of a spreader (or any other heavy implement that rolls with the tractor) is generally ignored in the industry standard's energy absorption and crush force thresholds for ROPS.

Based on the author's experience during the development process, there may be numerous design iterations that change the stress flow path in order to address cracked welds or to eliminate encroachment into the zone of clearance.

As a matter or conformance, manufacturers of ROPS use highly controlled processes to maintain traceability of materials for the quality of the ROPS. Continuous sampling of ROPS materials and keeping records are part of the process of manufacturing ROPS. Corrosion protection, material selection, and quality are strictly observed in the production of ROPS.

The industry has developed numerous voluntary standards that address various aspects of material utilization, manufacturing, energy dissipation necessary for worldwide use on machinery. Although standards are developed by the industry, ROPS testing is also regulated by government authorities. Since 1976, OSHA has used the ROPS standards as legal requirements for industrial uses, including agriculture and construction. Unfortunately, the standards have not remained current with industry's changing practices.

If the ROPS industry is so highly standardized and regulated, why do ROPS still fail? One would have to conclude that for an ROPS to fail, something drastically out of the ordinary must have occurred. Ruling out issues of defective material, corrosion, defective manufacturing processes, negligent misuse of the equipment, one can only conclude the equipment is misappropriated for the intended purpose; that being pulling stumps with a chain and the tractor being independent of implement when rolling into a ditch.

Tractor manufacturers simply fail to take into consideration the additional energy that an implement (such as an articulated steer axle spreader that remains attached to the tractor) contributes during a roll-over event. They simply hope or assume the implement breaks free in the roll-over. As we know now from failed ROPS, the standards must be updated to account for the inertia increases of added implement mass when the tractor and implement remain coupled through the roll-over.

Current Requirements in Standards

Numerous industry standards apply to the design of tractors and spreaders individually. ROPS testing standards all contain diagrams of the test apparatus and application of loads used for testing. The documents that impact this analysis most directly include:

A. ROPS - Applicable Standards

- Code 4 - OECD Standard Code for the Official Testing of Protective Structures on Agricultural and Forestry Tractors (Static Test - Like ISO 5700).

- ISO 3463 - Tractors for agriculture and forestry - Roll-over protective structures (ROPS) - Dynamic test method and acceptance conditions.

Figure 4 demonstrates the dynamic testing apparatus. Tests incorporate a large pendulum weight dropped on a chain onto the ROPS structure while the tractor is lashed to the ground. The energy the structure must absorb from the side impact is described in the following equation appearing in the standard, where E is the energy in kilojoules absorbed from the side impact loads, m_t is the "reference mass" of the vehicle in kilograms, and H is the raised height of the pendulum specified in the standard.

$$E = 19.6\ H, \text{ where } H = 0.125 + 0.15m_t \quad [1]$$

$$\text{therefore, } E = 2.45 + 2.94m_t \quad [2]$$

This equation takes into account the energy absorbed by the tires, so it is significantly larger than the energy described in the static test method of ISO 5700.

- ISO 5700 - Tractors for agriculture and forestry - Roll-over protective structures -Static test method and acceptance conditions.

The ROPS is mounted to the vehicle fixed components, which may include the rear axle housing, the transmission case, the tractor frame or the clutch housing, throughout the test. The tires are removed and the components are mounted solid to keep them from moving.

An actuator, generally a large hydraulic cylinder is used to apply the loading to the ROPS. The energy the ROPS must absorb from the side impact is described in the following equation appearing in the standard, where E_{si} is the energy in kilojoules absorbed from the side impact loads and m_t is the "reference mass" of the vehicle in kilograms.

$$E_{si} = 1.75\ m_t \qquad [3]$$

E is larger than E_{si} because it takes into account the energy absorbed by the tires, so E_{si} is significantly less than the energy described in the dynamic test method of ISO 3463.

Both ISO 3463 and ISO 5700 subject the ROPS to a vertical crush after the side impact testing. The magnitude of the force used for crush is described in the following equation appearing in the standard.

$$F = 20\ m_t \qquad [4]$$

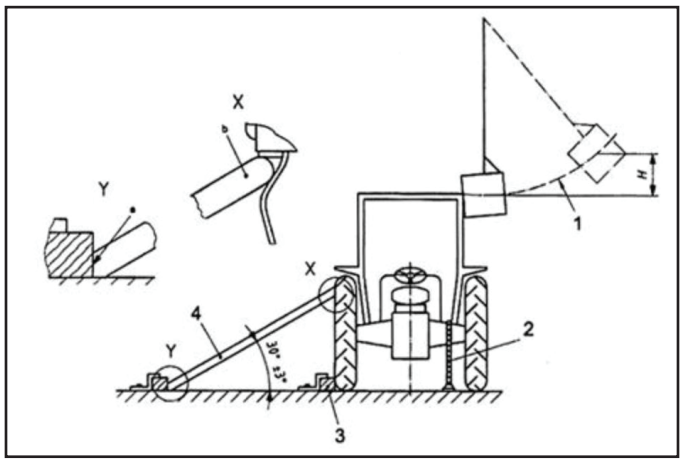

Figure 4
Tractor side impact tests from the ISO 3463 standard.

- SAE J 1194 - Roll-over Protective Structures (ROPS) for Wheeled Agricultural Tractors

The standard states, "Fulfillment of the intended purpose requires testing as follows:

A laboratory test, under repeatable and controlled loading, to permit analysis of the ROPS for compliance with the performance requirements of this SAE Standard.

- Either the static test (6.1) or the dynamic test (6.2) shall be conducted.

- A crush test to verify the effectiveness of the deformed ROPS in supporting the tractor in an upset attitude

- An upset field test under reasonably controlled conditions, both to the rear and side, to verify the effectiveness of the protective system under actual dynamic conditions (See 6.4.1.1 for requirements for the omission of this test).

In addition to the laboratory and field loading requirements, there is a temperature-material requirement."

- SAE J 2194 - Roll-Over Protective Structures (ROPS) for Wheeled Agricultural Tractors

The standard states: "Any ROPS meeting the performance requirement of ISO 5700 (Static ROPS Test Standard) or ISO 3463 (Dynamic ROPS Test Standard) meets the performance requirements of this SAE Standard if the ROPS temperature/material and seat belt requirements of this document are also met."

The energy absorption and crush force thresholds, as defined in these standards, depend strictly on the "reference mass" of the tractor, without consideration for attached implements.

In addition to the direct ROPS issues, if the vehicle fixed components fail during the roll-over event, the ROPS itself becomes more vulnerable to failure since it loses its anchoring base. For instance, an overloaded drawbar can cause a transmission case to break. The transmission case breakage may cause the cab mounts to leave their anchored positions and affect the stress flow through the ROPS, ultimately causing complete ROPS failure.

There are standards for vertical drawbar loads that do

not take into account the roll-over event. For example, as long as most of the implement's weight is supported on a series of axles, the tongue load may meet the vertical loads on the drawbar of the tractor. However, in a roll-over event, the tractor may be suspended from its drawbar and exceed the maximum vertical loads of the standard. Tractor manufacturers may not have considered dangling the tractor from its drawbar as a prerequisite to ROPS testing, as may be the case with the spreaders. The tall structure of the spreader fails to collapse in the roll-over event and can suspend the tractor from its drawbar.

Currently, the integrity of the ROPS mounting points is considered a given by tractor manufacturers. There appears to be little awareness or interaction between technical committees for connecting ROPS and tractor/implement interface standards. Each committee works in its own silos on projects within a limited scope. Therefore, ROPS testing standards do not currently consider drawbar vertical overload conditions in the testing process, which may compromise the ROPS mounting points in actual practice. The drawbar vertical load is only one example, but there are others; ISOBUS is another area of interest.

In the past when approached on these issues, both ROPS and tractor/implement interface standards committee members have pointed to external trade organizations for this coordination. The trade organizations, they say, provide educational resources, safety, and otherwise, for the industry as a whole, since every tractor manufacturer is not always aware of the equipment that may be used with their product.

Trade organizations do play an important role. Educating the users of equipment may provide some assistance; however, more technical solutions, such as new ISOBUS standards, may ultimately need to be called upon to control the tractor implement compatibility issues. Safeguards should be put in place that specify if the implement has not yet been approved by the tractor manufacturer, it simply will not operate with that tractor.

B. Equipment Applicable Standards

- ISO 26402 - Agricultural vehicles - Steering systems for agricultural trailers - Interface for articulated steering device of semi-mounted trailers

- ANSI/ASABE AD6489-3, Agricultural vehicles – Mechanical connections between towed and towing vehicles – Part 3: Tractor drawbar

Current OSHA regulations in Agriculture (29 CFR 1928) Subpart C – Roll-Over Protective Structures were derived from the standards listed above.

C. OSHA Regulations

- 29 CFR 1928.52 - Protective frames for wheel-type agricultural tractors - test procedures and performance requirements.

- 29 CFR 1928.53 - Protective enclosures for wheel-type agricultural tractors - test procedures and performance requirements.

- 29 CFR 1926.1001 - Minimum performance criteria for roll-over protective structures for designated scrapers, loaders, dozers, graders, and crawler tractors.

- 29 CFR 1926.1002 - Protective frames (roll-over protective structures, known as ROPS) for wheel-type agricultural and industrial tractors used in construction.

Examples of Equipment and ROPS Failure Risk

One of the by-products of raising cattle in confined space is the concentrated nitrogen-rich supply of manure that is produced from cattle production.

Getting the most value from the manure on the farm, as well as minimizing the potential for water pollution requires careful management of the manure resource. Manure management equipment has grown in dimensions and capacity to meet these challenges. Tractors and spreaders[5] now make up the bulk of the equipment used to dispense liquid manure on the nearby fields (see **Figure 5** for a typical tractor with spreader).

The more common method to spread liquid manure is to use an agricultural tractor to pull a spreader (equipment). Today, the spreader can weigh 72,000 lb or more. Usually, when the terrain is sloping, the tractor is ballasted according to the tractor manufacturer's recommendation and equipped with dual liquid-ballasted tires. The fully ballasted tractor with enough power to pull the load is generally less than half the mass of the full spreader[6] (**Figure 5**).

Articulated steering spreader axles reduce tire scrub in the field that disrupts turf and increases axle loading. Although implement articulated steering appears to work properly on level operations, where tire sideslip is not a factor, catastrophic events can quickly develop when

equipment operates on steeper slopes. Sideslip on sloping terrain occurs more readily when the implements, having low stability characteristics, are combined with conventional implement articulated steering functions.

On flat land, the force of gravity on the tires is normal to the ground. Unless the equipment is performing an unusual maneuver at higher speeds, the equipment remains relatively stable since the CG remains within the footprint of the tires, even in reasonable speed transport modes. On occasion, however, a spreader overturns along a roadway as a result of slippery weather, shoulder conditions, and a high CG[7].

Articulated steering, a slight berm along the side of the road and high CG contributed to the overturn of the spreader shown in **Figure 6**. Clearly, the spreader has a high propensity to roll-over due primarily to its high CG, but there are other contributing factors as well.

Equipment Stability

The static stability angle testing is conducted by the vehicle manufacturer on a tilt table under controlled conditions. The vehicle is blocked and chained to the tilt table with sensors placed under the up-slope tires to determine when lift-off occurs. The tilt table is slowly raised, and the angle of the table is measured along the way. At lift off of the up-slope tires, the angle of the tilt table is recorded.

Since some vehicle are used in various configurations (e.g., decks up or decks down in the case of commercial mowers), the angle is measured and recorded for each. The worst configuration is recorded, and then published in tractor certifying test results. However, the static stability angle limit information is generally not provided to the equipment user in the operator's manual. There are currently no known requirements for the implement manufacturers to conduct static stability angle testing of their equipment.

How the Equipment Rolls Over

The geometry of the multi-axle tires in turning maneuvers tends to increase axle stresses and cause tire scrub that forms ruts or disturbs the sod. Steering the spreader allows it to follow the path of the tractor more closely. Numerous methods are employed to articulate the spreader's axles. One such standardized method senses the differential angle between the tractor's drawbar and the longitudinal plane of the trailing spreader and adjusts the lead and trailing axles' tire steering angles accordingly.

By design, due to the mass of the full spreader in the field, the spreader's tires are generally articulated to follow more closely in the tracks of the tractor[8] (**Figure 7**). Steering the spreader tires reduces axle stresses in the field and reduces turf damage from tire scrub.

The dual, tridem, and quad-axle spreader steering systems vary by manufacturer. Some are now providing more elaborate electronic-sensing steering systems that allow the spreader to crab or offset the spreader's tire tracks from those of the tractor[8]. However, consistent with ISO 26402 but slightly different in design, the U.S.- and Canadian-made spreaders are steered with proprietary designed mechanical linkage that senses the differential angle between the tractor's drawbar and the longitudinal plane of the trailing spreader and adjusts the lead and trailing axles' tire steering angles accordingly (**Figure 8**).

Although most implement manufacturers utilize

Figure 5
Tractor with a spreader in the field
From Valmetal (2018). Reprinted with permission.

Figure 6
Overturned spreader along the roadway due to icy road conditions
from The Sentinel (2013). Reprinted with permission.

hydraulic pressure assist, they apply the same general principles of ISO 26402. This means the mechanical linkage senses the differential angle between the tractor's drawbar and the longitudinal plane of the trailing spreader to determine the proper tire steer angles for the spreader. Mechanical sensing may be accomplished in different ways than the one described in the standard, but still has the same result.

There are numerous spreader designs on the market that include articulated steering utilizing some method for mechanical sensing of the differential angle to affect "… the movement of the steered trailer wheels… [are] firmly linked to the relative angle between the longitudinal axis of the towing vehicle and that of the trailer" as outlined in the ISO 26402 standard.

The following not-to-scale graphic shows the events that transpire during an equipment roll-over event that occurs while traversing a slope. On sloping terrain, the gravitational pull on both the tractor and implement provide lateral forces that cause the equipment to ease its way down-slope (**Figure 9**). The spreader tracking follows the tractor on flat ground; the spreader tires follow the steering lead of the tractor front tires (**Figure 10**). The operator must generally steer the tractor slightly up-slope to compensate for this tendency. The tractor is forced to retain or maintain the implement's position on the slope. The tractor's steering tires are directed up-slope to compensate for the gravitational pull of both the tractor and implement.

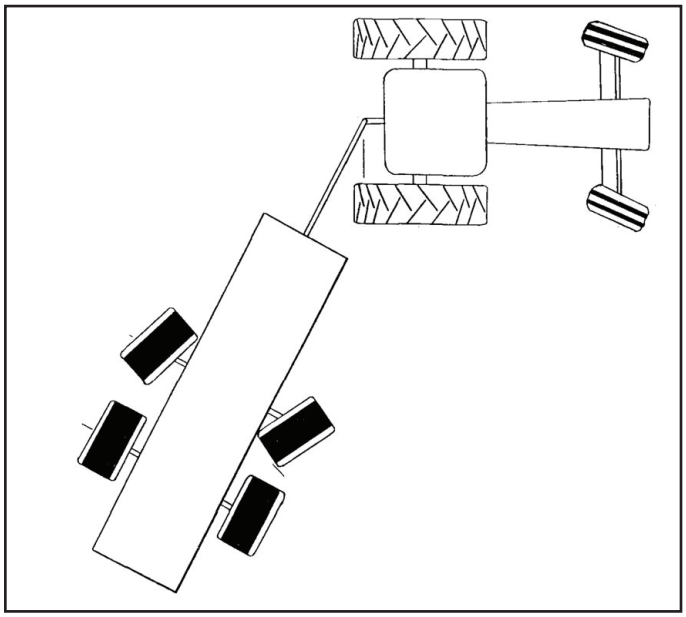

Figure 7
Trailer articulated steering (dual-axle is shown) from Laguë (1991). Reprinted with permission.

But the equipment follows a more direct path across the slope, so long as the tractor has enough power to compensate for the force of gravity on the equipment.

Furthermore, as the angle steepness of the side-slope increases, the CG for the equipment moves toward (and often over) the down-slope tires, increasing the weight they must carry. Operating in this fashion over long periods causes more rapid wear of the tread on the down-slope tires, even more than when compared to the up-slope side. Tread-worn tires provide less resistance to side forces and slide down-slope more readily than tires with full tread. In

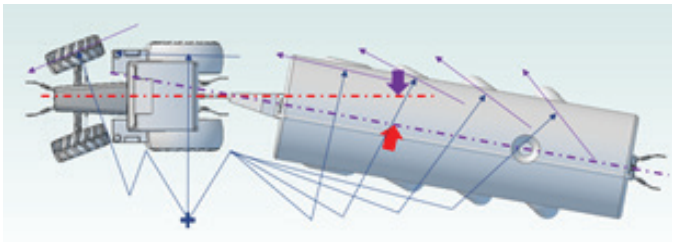

Figure 8
Spreader tires steer depending on the tractor front tires on the flat ground, but independent of tractor front tires on a slope.

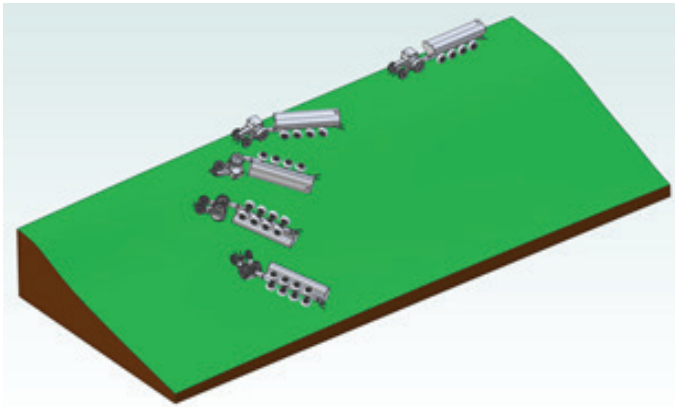

Figure 9
Sequence of the roll-over event.

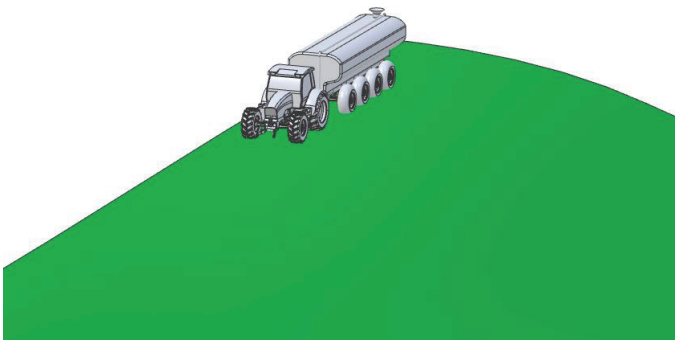

Figure 10
Equipment traverses the slope.

addition, as the side-slope angle increases, both the tractor and the implement may approach their static stability angle.

Role of Inertia in ROPS Failure

When a spreader filled with liquid manure tips over, the results are different than when an open wagon filled with silage tips over, for example. When an open wagon tips over, the mass the wagon is carrying dumps out, and is no longer part of the inertial mass that is revolving around the longitudinal axis of the vehicle.

In the case of a spreader or nurse tank, the mass of the content is contained and acts in a manner that contributes to the roll-over inertial loading. Unless the spreader or nurse tank breaks free (and is jettisoned from the drawbar pin during the roll-over event), some of the implement's inertial energy, which can be significant, will more likely than not be dissipated into the ROPS.

Role of the Articulated Steering System in ROPS Failure

By far the largest issue causing the roll-over event is with the conventional articulated steering system on the implement (**Figure 11**). When the implement slides down the slope, the conventional articulated steering function does what it is designed to do: It senses the differential angle between the tractor's drawbar and the longitudinal plane of the trailing implement and adjusts the lead and trailing axles' tire steering angles accordingly. Unfortunately, the implement's articulated steering tires are turned in the wrong direction to assist the operator with maintaining position of the equipment on the slope. The force vectors are reversed as the implement attempts to turn down-slope quickly because of its mass, increasing the lateral force on the equipment's articulated tires due to the force of gravity (**Figure 12**).

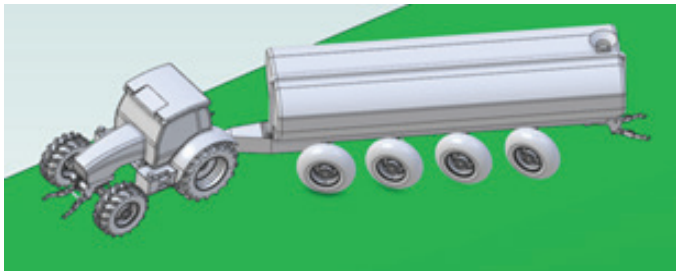

Figure 11
Spreader accelerating down slope as a result of articulated axle steer of the spreader.

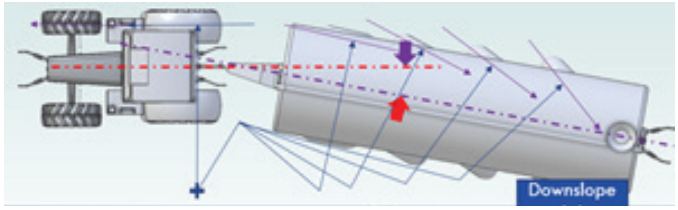

Figure 12
On a slope, the spreader mass pulls the spreader downslope in the direction of the articulated tires, loading the tractor drawbar.

A free-body diagram of the spreader would demonstrate an increasing longitudinal force on the tractor at the height of the drawbar as a result of the lateral forces on the articulating tires of the spreader. The largely resistive forces of the articulated tires would eventually initiate a counter-clockwise roll of the implement. The up-slope tires of the tractor are raised off the ground when the spreader starts to tip over as shown in **Figure 13**.

The tractor operator may react by increasing the up-slope angle of the tractor's steering tires to compensate for the error, and in moments, due to the accelerating slide of the implement, the tractor quickly loses enough power to overcome the additional force, as a result of misdirection of the implement's steered tires.

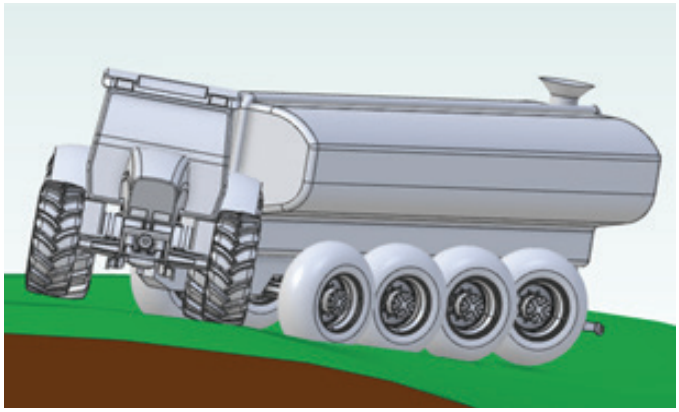

Figure 13
Spreader accelerating down slope as a result of articulated axle steer of the spreader.

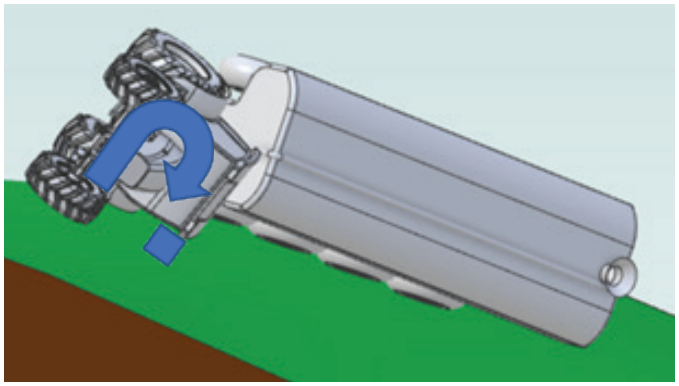

Figure 14
Spreader tips and drives the tractor roll, which applies the enormous side impact to the ROPS.

Once the implement slides far enough down-slope from the tractor, the moment generated by the draft force applied by the drawbar to the spreader's tongue, tips the spreader over (**Figure 14** and **15**). When the hitch pin connection remains intact and the implement is a spreader, the rotational inertia properties contribute greatly to the energy the ROPS must absorb in the roll-over event. The spreader tongue lifts and rolls the tractor's drawbar. This additional rotational inertia contributed by the spreader is extremely significant, adding much more energy that the cab must absorb. This will be discussed further in the analysis section of the paper.

The incident demonstrated in **Figure 16** and **17** shows a liquid manure spreader overturned on a roadway in Landcaster, Pennsylvania in September of 2017.

Even though the terrain is only slightly sloped, the rear of the tractor is clearly elevated from the ground. The tractor would have continued to roll if it had not been obstructed by a tree. Clearly, the liquid manure tank is of sufficient mass to raise the rear of the tractor by its drawbar (**Figure 18** and **19**).

In the worst scenario, the ROPS is crushed to the height of the hood and rear wheels in the overturn (**Figure 20** and **21**). There is no room left in the crush zone for operators, especially if they are properly wearing their seat belt. The roll-over event under these circumstances is catastrophic, and survivability is low (**Figure 2**). The resulting crush is unreasonably dangerous to the operator and

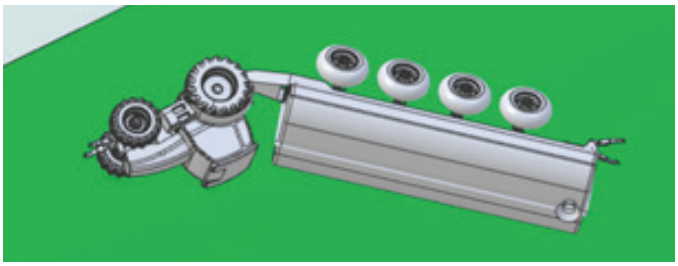

Figure 15
Spreader tips and drives the tractor roll,
which applies the enormous side impact to the ROPS.

Figure 16
Overturned spreader along the roadway.
LNP – Lancaster Online (2017)[9]; reprinted with permission.

Figure 17
Overturned spreader along the roadway.
LNP – Lancaster Online (2017)[10]; reprinted with permission.

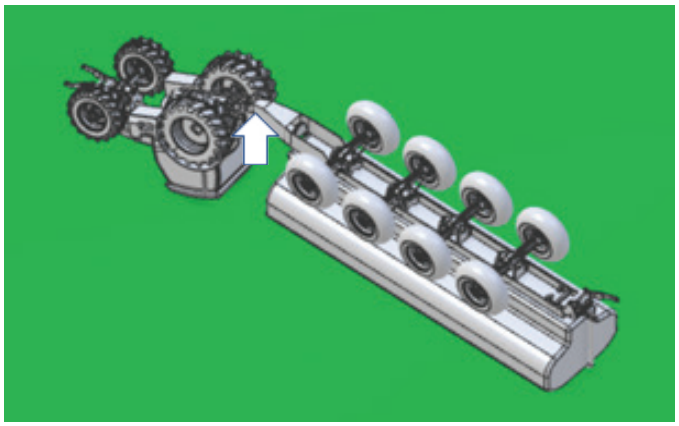

Figure 18
Spreader lifts the tractor up by the drawbar,
causing tractor frame damage.

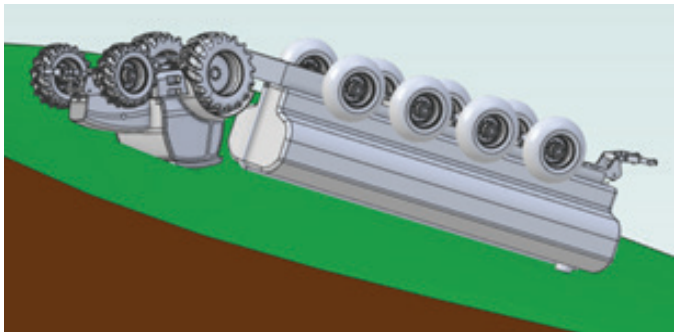

Figure 19
Spreader lifts the tractor up by the drawbar,
causing tractor frame damage.

the occupants of the ROPS. When the tractor and spreader remain coupled (**Figure 22**), high vertical forces (**Figure 23**) are introduced to the tractor by the spreader.

ROPS That Have Been Known to Fail

In addition to the case the author investigated, authorities from Workplace Health and Safety Queensland, Australia, recognize the limitations of ROPS under the special circumstances and issued a bulletin in 2010 titled, "Tractor roll-over protective structure (ROPS) limitations," which stated that use of large spreaders are not permissible with the ROPS standards in place today. They showed a tractor whose ROPS had failed as a result of a roll-over event with an articulated spreader (**Figure 24**).

They state that:

"Calculations have shown that the energy of ***the combined masses of the tractor and trailer*** *... would be*

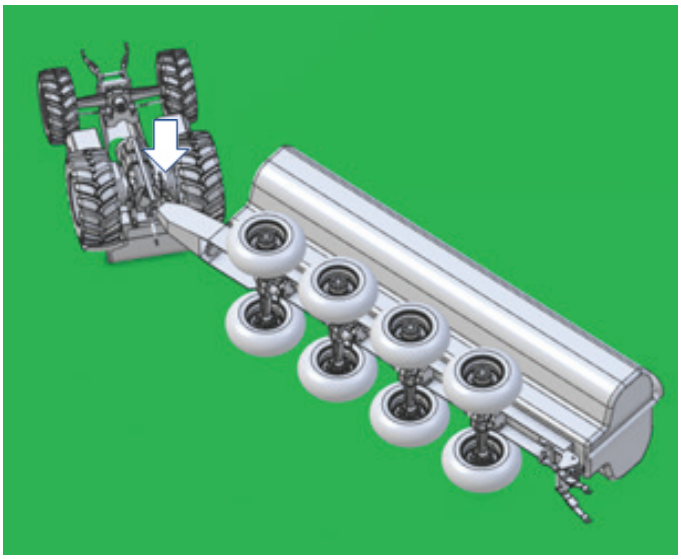

Figure 20
Spreader tongue crushes the tractor down
by the drawbar causing further damage to the ROPS.

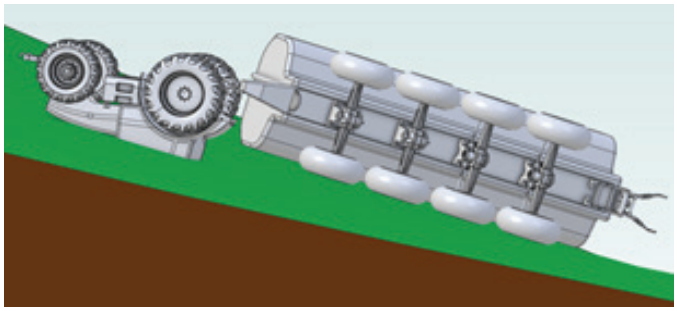

Figure 21
Spreader tongue crushes the tractor down by the
drawbar causing further damage to the ROPS.

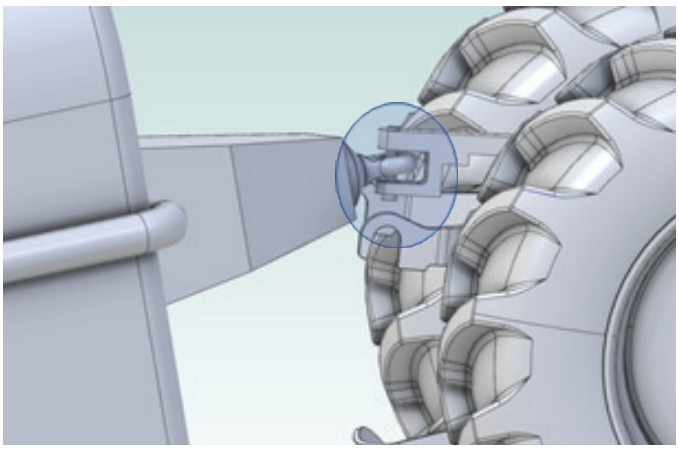

Figure 22
Hitch pin connection remained intact after the roll-over event.

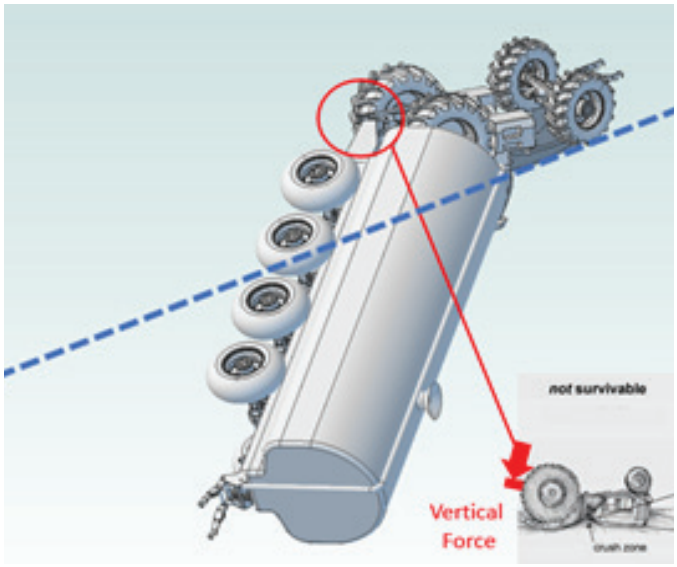

Figure 23
Final position tractor and spreader after the roll-over event.

Figure 24
Exemplar photograph of failed ROPS From
WorkCover Queensland (2010). Used with permission.

Figure 25
Exemplar photograph of failed ROPS.
From WorkCover Queensland (2010); reprinted with permission

more than that required by the code and could not be dissipated by the ROPS.

Significant contributing factors to this incident were the speed and mass of the tractor and trailer combination, as well as the use of [articulated steering] on the front axle of the trailer (emphasis added)[9]*."*

Manufacturers set the "reference mass" for testing. Industry standards do not directly specify "the energy of the combined masses of the tractor and trailer," as the Australian authorities would suggest. The manufacturer of the tractor determines the "reference mass" for ROPS certification (**Figure 25**). The only criteria in the standards, the "reference mass" needs to be greater than the tractor mass.

All other energy sources, except for the mass of the tractor, are largely ignored by most tractor manufacturers, but probably should not be. Manufacturers often set the "reference mass" by rounding up to the nearest 500 kg above the tractor mass of the largest tractor in the tractor line up that is named on the test certificate.

Summary of Causes for ROPS Failure

ROPS are tested according to industry standards. However, simply meeting the requirements of a standards does not absolve a manufacturer from producing a safe product. Furthermore, some standards are more stringent than others. In a study of 300 tractors overturn tests, C. Jarén, et al. concluded that "[SAE J2194] is less aggressive than SAE J1194 in side-load comparisons[10]."

Energy levels differ as a result of the tire interaction in the dynamic testing. There are known cases when the tractor's ROPS failed due to excessive side and crush loads applied during an overturn with a spreader. The operators of the equipment were seriously injured or killed.

Weight of Responsibility for ROPS Failure

The tractor and spreader manufacturers knew (or should have known) that a spreader can weigh almost double or more than the weight of the tractor. Furthermore, spreaders are becoming larger than standards have accounted for in the past. A review of the operator's manuals (OMs), however, shows that none of the manufacturers appears to provide proper warning or instructions precluding the operator from simultaneously operating the equipment across slopes — and if a warning for not traversing slopes is stated, the nature of the slopes are not defined.

The tractor and spreader manufacturers knew (or should have known) that the mass and the geometry of the spreader, including its liquid cargo, can contribute significantly to the forces imposed on the tractor's ROPS during the overturn. While the hitch components stay together, forces imposed by the tipping and rolling of the spreader are directed to the tractor drawbar — then into the ROPS.

Spreader Characteristics Causes for ROPS Failure

Considering the mass of a spreader, the tall shape of the tank and the low attachment point of the hitch, the tongue on the spreader acts like a crane when the spreader starts to tip, lifting the rear of the tractor (**Figure 26**). As the spreader rolls, the swiveling clevis and tongue of the spreader follow the contour of the upper tank (since the tank is full of liquid, little apparent deformation of

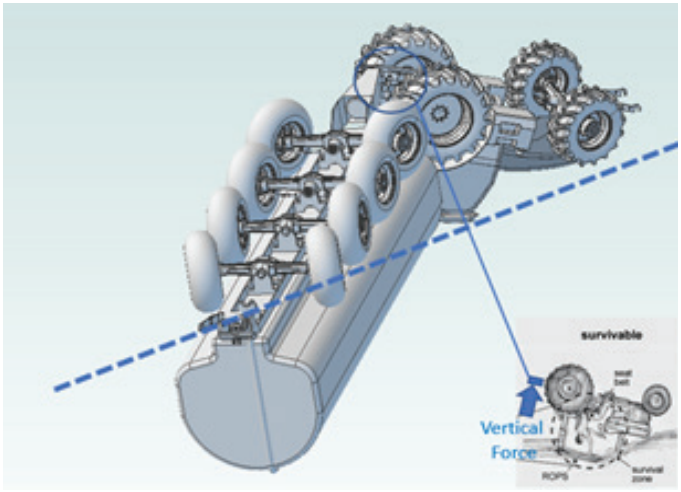

Figure 26
Spreader tongue acting like a crane raises the rear of the tractor.

the tank shape occurs).

The spreader's tongue first lifts the rear of the tractor by the drawbar, yielding a rotational acceleration of the tractor into the side impact with the ground that is greater than anticipated by the standard. The drawbar and spreader tongue then acts like a cam follower, applying downward forces again to the tractor drawbar. This adds crushing forces larger than the forces anticipated in the standards to the ROPS structure with the tractor turned completely upside down.

During the lift described above, the spreader's tongue also introduces a very large vertical load on the drawbar that jeopardizes the integrity of the ROPS mounting points. The vertical load physically lifts the tractor off the ground by the drawbar and can cause tractor chassis components that provide ROPS mounts to fail. ROPS standards should be revised to introduce spreader induced drawbar vertical loading consist with a roll-over event in future testing procedures. Additionally, the logic used to steer the spreader on relatively flat ground works well (**Figure 27**). However, when on slopes, this logic is flawed — making the problem of controlling the position of the spreader on a slope worse, if not impossible, for the tractor operator to maintain control.

Crab Steer to Compensate for Slopes

With limited effectiveness, some manufacturers in the spreader industry recognize the safety implication of drawbar differential angle sensing and are beginning to design sensors that detect slope angles as the vehicle crosses a slope. Some of these systems use electronically controlled steering systems to compensate for slope by steering the tires of the spreader up-hill (**Figure 28**) especially in sloped conditions (referred to as "crab steer mode")[11].

One such manufacturer states in its brochure that, "Optional Crab Steer Mode [is] available which steers the front and rear axle the same direction to steer up the slope [emphasis added][11]." In this mode, the steering of the spreader is set to systematically and continuously climb the hill at the appropriate speed and thus maintain its position on the slope.

Although the spreader can still slide downslope with crab steering, the tire angle remains fixed and does not accelerate the spreader into a sharper turn, as does articulated steering. This gives the operator a little more time to respond. Unfortunately, this option has not yet become standard equipment for all spreaders. Furthermore, along with crab steering, it is foreseeable that ISOBUS has the potential to assist with vehicle-to-vehicle controls necessary to properly trail vehicles in slope conditions.

The spreader's conventional power-steering logic flaw with mechanical drawbar angular sensing causes the spreader to accelerate the down-slope slide, making it difficult or impossible for the operator to control or recover the position of the spreader on the slope by maneuvering the tractor alone.

Operator Attentiveness and Skills

Caught up in the moment and from the awkward position of the tractor holding the jack-knifed spreader on the hillside, the operator runs out of obvious options, so he decides to continue moving the tractor forward. The operator's decision to proceed only causes the side load and increasing tipping moment on the implement tongue that rolls the spreader followed quickly by the tractor.

Probably the safest, yet least obvious maneuver is to slowly stop the tractor, shut off the spreader's discharge pump, put the tractor into reverse, and slowly ease the

Figure 27
Comparison of regular and crab steer modes on flat ground.
From Nuhn (2017); reprinted with permission.

Figure 28
Comparison of regular and crab steer modes on flat ground.
From Nuhn (2017); reprinted with permission.

spreader down the slope onto flat ground. Such a maneuver allows the heavier vehicle (the spreader) to take the lead down the hill. With proper maneuvering, the tractor would follow right behind the spreader to safer ground. Such a maneuver, however, would necessarily require a great deal of user training to help develop the skills to recognize the onset of the implement slide.

Equipment manufacturer associations develop information and training to assist the industry with safety and compliance. Thus far, there has been no training materials published by these associations on proper use or misuse of articulated steering spreaders.

Analysis

There are several reasons ROPS fail. They include:

- Vertical loading of the drawbar hitch pin exceeds the industrial standard vertical drawbar design load for the tractor, causing chassis component failure eliminating the solid connection between the tractor chassis and the ROPS.

When the ROPS mounting points fail, the ROPS no longer performs as designed.

- When the drawbar hitch pin remains intact throughout the roll-over event, the energy from the inertia induced by the spreader is unaccounted for and must be considered in the ROPS design to prevent failure from occurring, especially during crush loading conditions.

Spreaders are designed to be transported on highways as well as operate in soft field conditions. The spreader is therefore designed with large flotation tires. The bulk of the tank is raised to clear the tires, which increases the height of the CG.

Although most of the USA/Canadian spreaders do not use control linkage connection described in the ISO 26402 standard directly, the principle for the control link between tractor and implement is very similar. The connection between the drawbar and the trailer generally includes a proprietary articulated sensor device connecting some part of the tractor drawbar to some part on the spreader. Hydraulic assist on the mechanical sensor is used to steer the spreader tires. The logic used to turn the multi-axle steer wheels is conventionally based on the angular difference between the drawbar of the tractor and the tongue of the spreader. Furthermore, the equipment is often used in old grazing land to spread liquid manure on a field as it traverses across slopes on hill farms; some of the terrains being significantly steep.

Since the tread on the spreader tires is designed for flotation and not necessarily for traction, the tires are more prone to sliding. Specific surface coverage from manure dispensed from the tank can cause an even further reduction of coefficient of friction between the tires and grass surface from subsequent passes across the field. If the tires have excessively worn tread, this may also increase the likelihood of slide on a slope in steeper terrain conditions.

The CG of the spreader is high; therefore, the spreader rolls first, followed shortly after that by the tractor through its direct coupling with the drawbar. The dimensions of the spreader tank and the location of the spreader tongue produce a cam action that transfers the inertia of the spreader to the tractor from the onset of the overturn. The spreader coupler, working as a crank, accelerates the tractor's roll. The mass of the tractor and the spreader are virtually combined and exceed the "reference mass" (m_t) determined by the tractor manufacturer. The tractor and spreader do not necessarily separate during the roll-over event with the spreader tongue hook is design to swivel 360 degrees.

Furthermore, the roll event abruptly suspends the tractor from the spreader tongue, imposing loads greater than half the mass of the tractor. Industry standard ISO6489-3 limits the vertical drawbars loads for various categories of tractor based on horsepower, but in all cases they are well under half the mass of a fully ballasted tractor.

The suspension of the tractor from its drawbar hitch pin produces an unreasonably dangerous condition that causes the failure of chassis components that support the ROPS attachment. When the spreader tongue is at its apex in the roll-over event, it imposes large forces on the drawbar hitch pin (**Figure 19**) that exceeds the tractor's industrial standard vertical drawbar design load[12].

Spreaders can range from 1.5 to 4.5 times the mass of the tractor, depending on whether the spreader is equipped with brakes[13]. There are studies to identify ways to determine the moment of inertia of mass for tractors[14]. The same methodologies could also be extended to equipment.

When the tractor and spreader remain connected, the inertial loads of the spreader must be accounted for and included in the ROPS testing. The connection between the tractor and the spreader are coupled together by the

spreader's tongue connected to the tractor's drawbar. During the roll process the axis of rotation is generally aligned through the tractor and spreader with the coupling offset to the height of the hitch, much like a piston throw on an engine crankshaft.

In broad concept, however, the energy to stop a rotating equipment is dependent on moment of inertia of mass and the angular velocity of the body. We know from basic course work in kinematics and dynamics of machines that energy (E),

$$E = \tfrac{1}{2} J_M \omega^2 \quad [5]$$

where "J_M" is the moment of inertia of masses and is generally dependent on the geometry and the mass of the rotational object and "ω" is the angular velocity of the body.

The moment of inertia, J_M, for a cylinder with reference to the longitudinal axis of that cylinder is:

$$J_{M \text{ for a cylinder}} = \tfrac{1}{2} m_{\text{cylinder}} r^2 \quad [6]$$

The tractor could be approximated by a cylinder as shown in **Figure 29**. The cylinder for the combination tractor and spreader is only longer to include the spreader (**Figure 30**). Since the tractor and spreader do not separate at the drawbar, the equipment rolls together, and the spreader has much the same shape as the tractor.

Assuming the tractor and the spreader are about the same diameter. Radius r, is roughly half the height of the tractor (**Figure 30**) and the same for the spreader. If the distribution of mass is homogeneous within the approximated cylinder, then the value of JM equipment is proportional to the total mass of the equipment as compared to the tractor for JM tractor to the "reference mass."

Adding the "reference mass" of the tractor (m_t) to the mass of a full spreader (1.5 mt to 4.5 m_t) can yield the mass of the equipment as much as 5.5 m_t (1 m_t + 4.5 m_t) times the "reference mass" of the tractor alone.

Rewriting the energy equations [2] and [3] from the current standards, but substituting 5.5m_t to account for the equipment in place of m_t for the tractor alone, the maximum energy requirements for side impact when the spreader inertia is accounted for could be roughly 5.5 times larger and expressed as follows:

$$E = 2450 + 16.17\, m_t \quad [7]$$

$$E_{is} = 9.625\, m_t \quad [8]$$

The crush force should also reflect the additional load imposed by the spreader.

$$F = 55\, m_t \quad [9]$$

When the hitch pin stays intact during the roll-over event, adding the spreader's mass increases the testing "reference mass" by 2.5 to 5.5 times. Failing to include the spreader in the calculation of test "reference mass" produces an unreasonably dangerous condition. Rearranging terms and solving for ω from equation [5],

$$\omega = (2 * E_{is} / J_{M \text{ equipment}})^{0.5} \quad [10]$$

Substituting $J_{M \text{ equipment}}$ from equation [6] and E_{is} from equation [8] in equation [10] yields the following:

$$\omega = 2.65 * r \text{ (rad/s)} \quad [11]$$

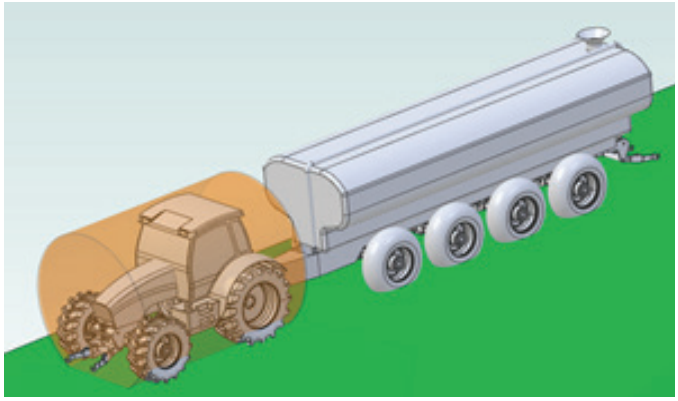

Figure 29
Tractor approximated by a cylinder of vehicle length.

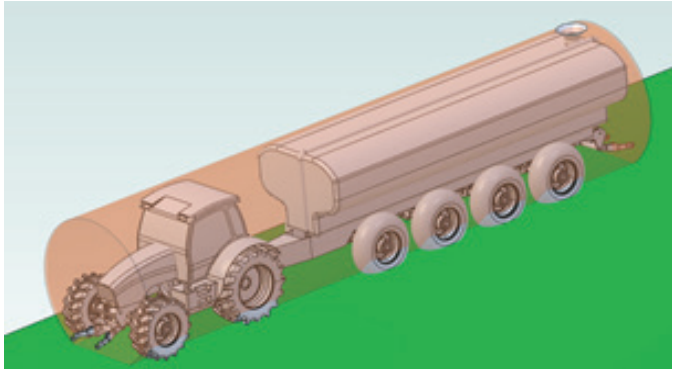

Figure 30
Equipment approximated by a cylinder is longer but as the same radius.

Stated another way, instead of lashing the tractor to the ground, one could visualize testing the tractor at the current "reference mass" by rotating it about its longitudinal axis at a constant speed ω, into the pendulum drop of the current dynamic test (see **Figure 31**). The timing of rotation would necessarily be such that the impact occurs when the tractor is vertical. This would be much like what actually occurs in practices as demonstrated in **Figure 14**. The ROPS' initial impact with the ground includes the inertial loads of the spreader in addition to the tractor.

Currently, tractor manufacturers grossly understate required energy absorption levels by only selecting "reference mass" representative of the tractor mass, ignoring the contribution of inertia induced by attached implements. They generally do not account for the combined mass of the tractor and spreader, assuming (hoping) the tractor and implement break free from each other during a roll-over event. Standards should be updated to reflect significant larger inertial loads on the ROPS structure when a roll-over event occurs with a spreader attached or a spreader should be prohibited from use on slopes that could result in a tractor roll-over.

Foreseeable Use and Misuse of the Equipment

Some of the significant questions the analyst must address are as follows:

- Was the tractor maintained and operating properly?
- Was the spreader maintained and operating properly?
- Did the information in the owner's manuals (OMs) address the circumstances and situation?
- Were there any errors or omissions from the instructions by the manufacturer?
- Were all the instructions and warnings in the OMs followed?
- Was the operator using the equipment properly?

Safety Engineering/Risk Management

As a means of mitigating this risk, vehicle manufacturers' compatibility study groups and industrial standards committees with oversight of tractor/implement interfaces should employ standardized risk assessment techniques such as the one proposed by ANSI/AIHA Z10-2012 section 5.1.2, i.e., "Hierarchy of Controls" and explained by Fred Manuele in his book "Advanced Safety Management[15]." The preferred order of control is as follows:

- Risk avoidance
- Elimination
- Substitution
- Engineering controls
- Warning systems
- Administrative controls
- Personal protective gear

As pointed out by Manuele in chapters 14 "Hierarchy of Controls: Section 5.1.2 of Z10" and 16 "Prevention through Design: Section 5.1.1 to 5.1.4 of Z10," this order of application is important and leads to the most effective way to minimize risk.

Many perceptive vehicle manufacturers conduct equipment compatibility studies to understand the interfaces and interactions of their vehicle with other vehicles in the same power class to determine vehicles that are free

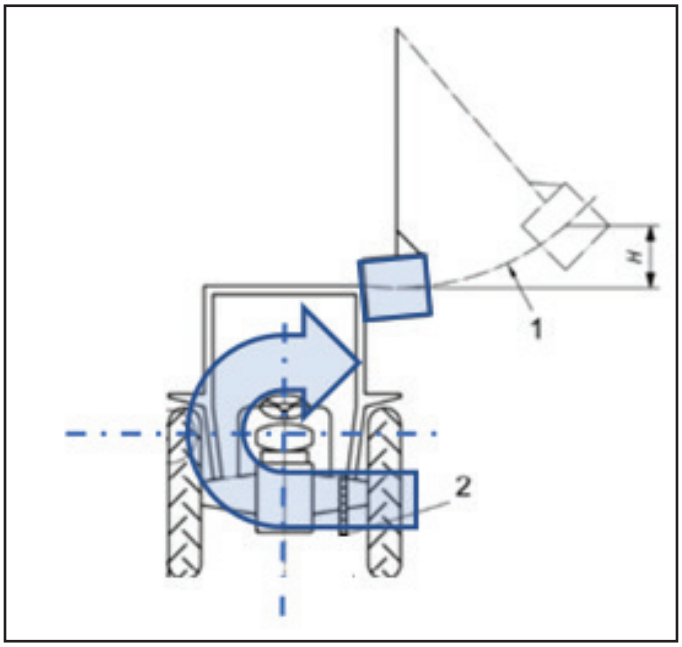

Figure 31
The additional inertia contributed by the spreader must be included, much like rotating the vehicle into the pendulum drop.

of interferences and can work safely together. The ISOBUS, described in the ISO 11783 standard, for instance, requires the combined efforts between vehicle manufacturers that incorporate significant testing before a specific farm implement is permitted to control the tractor's functions, such as ground speed, steering, and braking.

Risk avoidance is the most effective approach and must be undertaken by the manufacturers in cooperation. The interface between tractor and implement requires a group effort, so the occupants of the tractor are safe while operating this equipment. Standards for tractors and implements were generally appropriate for individual use, but ROPS may still fail when tractor and spreader are used together on steeper slopes due to the inertial contribution of the attached spreader during the roll-over event.

Safer Alternatives Exist for Spreading Liquid Manure

There are several known methods for applying nitrogen-rich slurry to the land[16,17]. A couple of methods require the liquid manure to be pumped from a lagoon into transport vehicles. These vehicles could be spreaders with tanks in the size of 1,000 to 12,000 gallons or truck-mounted tanks in the size of 3,000 to 6,000 gallons or more. They use the public road systems to carry the manure in its liquid-slurry form to the field. Over time, the size of tank trailers has increased to reduce the number of trips from the lagoon to the field.

One method to spread liquid manure includes a tractor-mounted implement that pulls a length of hose across the field (**Figure 32**)[18]. A nurse tank and pump provide the source and power to move the slurry across the field, but the nurse tank and pump are static and located at one end of the field. In such cases, the CG of the implement remains low and is not a significant factor in the tractor/implement interface for slurry distribution.

Rather than spray, some choose to knife the liquid manure in to the ground (**Figure 33**). This practice of direct injection keeps the turf from becoming slippery on subsequent passes.

More Attention to the Tractor/Implement Interface

Standards committees should also continuously examine the broader scope and implications of standards they approve to be sure all the known issues have been addressed and mitigated to the greatest extent possible; meaningful oversight of standards at the equipment level

Figure 32
Drag-line application of liquid manure from the Livestock and Poultry Environmental Learning Center (2019); used with permission.

is imperative. It is the author's belief that ROPS and tractor/implement interface standards committees must interact with each other more than they do today to make sure the combination of vehicles and implements is also safe and appropriate for public use.

Compared to the tractor industry, the spreader industry has fewer industry standards and regulations, such as hitch pin sizing and type, tow chains, performance brakes, and road lighting. One such voluntary standard is the ISO 26402, which regulates the size and location of a ball used to steer semi-mounted trailers[19]. This standard presumes the semi-mounted trailer uses an attachment to the drawbar frame itself or on the rear of the tractor to mechanically steer the trailer[20].

Figure 33
Direct injection of liquid manure from the Livestock and Poultry Environmental Learning Center (2019); used with permission.

The industry makes use of steering axles on multi-axle spreaders because of the high stresses that would otherwise be induced into the axle components when the laden spreader turns in the field. The spreader steering system is sold to customers as a means of preventing rutting, smearing, and tearing up the sod in their grasslands. The operator turns the trailer steering on when working in the field. The trailer steering is generally locked out in road transport.

ISOBUS is also being used to interface implements with tractors logically and electronically. This technology is important going forward to determine what functions are possible, given a specific tractor/implement context. More use will be made of this interface on new products reaching the market.

Symbols, Warnings, Displays, and Manuals

Warnings are placed on vehicles to identify known hazards and how to avoid them. Manuals provide the operator with the proper way to select and use the equipment he is using. It is incumbent on the manufacturers to describe limitations and the dangers of using the equipment. The warnings are further explained throughout the manuals to assist the operator with background and knowledge for the directive.

Numerous standards have been written and provide direction for manufacturers to follow[21]. The Association of Equipment Manufacturers (Agricultural) has compiled a list of those standards which may affect the vehicles used by their constituents. Proper instructions must be documented, and warning alerts must be placed in such a manner that the operators are aware of the limitation of the vehicles they are operating. The operator's manual states how to use the vehicles from a manufacturer's independent perspective but fails to identify the issues with the combined vehicle and implement or at the equipment level of use.

Summary and Recommendations

To prevent ROPS tragedies from occurring, it is recommended that authorities having jurisdiction and industry standards committees include requirements that more closely represent the loads spreaders induce into the tractor in a roll-over event. A vertical load, based on gross vehicle weight (GVW) should be applied to the drawbar to determine if the chassis is capable of being lifted off the ground by the spreaders tongue, attached to the tractor's drawbar, while the spreader remains connected to the tractor. ROPS standards should reflect this added step in the standard ROPS testing process.

Industry, in general, encourages operators to depend upon the protection of ROPS during roll-over events and wear their seat belts. Although the frequency of accidents resulting from ROPS failure may seem low, exposure is rising with market growth of the subject equipment. Sales of liquid manure spreaders have increased year by year; liquid manure is being applied by spreaders onto sloped hill farms across the country. Most importantly, the severity of ROPS failure is high under these conditions, resulting in a level of certainty for serious injury and fatality if the spreader rolls over.

With market growth trends toward larger equipment, OSHA should reconsider minimum energy thresholds incorporated in 29 CFR 1928.52, 1928.53, 1926.1001 and 1926.1002 and increase the energy absorption levels for ROPS to accommodate implements like spreaders.

Trade and standards organizations responsible for tractors, ROPS, spreaders, tractor implement interface (including drawbar and hitch pins), PTO and ISOBUS should be encouraged to find ways to work across committee boundaries to identify tractor/implement characteristics. The topics may include such items as implement stability and directionality (including steering or side slip); methodologies to mitigate vehicle incompatibilities in growing market segments; and finally considering automation where necessary to prevent high-risk exposure to unsuspecting operators. Other topics may require review and increasing the energy absorption levels in existing ROPS standards based on what implements the tractor is pulling, adding appropriate warnings for operations on slopes, and removing conflicting standards that contribute greatly to energy levels ROPS must absorb to protect the occupants in a roll-over event.

Manufacturers of both tractors and larger, heavier, and higher CG implements, including spreaders, should be encouraged to work together through tractor/implement compatibility issues along with the appropriate voluntary industrial standards committees. They should be encouraged to take oversight of this unreasonably dangerous use of the subject type of equipment on slopes. It may even require that manufacturers agree to withdraw dangerous products from the market place. This includes for example, tractor and spreader with steerable axles sensing the differential angle between the tractor's drawbar and the longitudinal plane of the trailing spreader that steer the trailer and increase the propensity to roll the equipment. Higher energy absorption levels for ROPS should be considered when designing for contributing implement inertia

when it is significant in the roll-over event.

A risk avoidance approach would encourage industry manufacturers to work together to sense side slip of the spreader in slope conditions and use this information in steering logic for both vehicles. Manufacturers of vehicles should be encouraged to use electronic steering systems with crab-steer and tractor tire steer angles sensing to maintain spreader position on feasible slopes. Using ISOBUS technology, the same electronic steering systems should prevent the use of the spreader on non-feasible slopes where side slip is too extreme to operate the equipment (shut the spreader discharge pump off and warn the operator to seek more level ground).

At a minimum, a slope indicator should be mounted in the cab of the tractor, and slope limitation should be spelled out clearly in all the operator's manuals. Wherever possible, proper warnings[22] should be displayed, alerting operators of the danger of operating high CG and stee able implements on steeper slopes. All forms of educational information should be provided to operators, including the OMs of both combinations of tractor and spreader. Finally, the minimum tire tread height should be monitored more closely by the operator when this type of equipment is used on slopes. Manufacturers' recommendations should be properly documented, and maintenance should be performed to provide adequate traction on reasonably steep slopes where hill farms exist.

References

1. OSHA Agricultural Safety Fact Sheet, "Protecting Agricultural Workers from Tractor Hazards, Overturns." Internet: https://www.osha.gov/Publications/OSHA3835.pdf [12/29/2020].

2. Northeast Center for Occupational Health and Safety in Agriculture, Forestry, and Fishing (NEC). "National ROPS Rebate Program." Internet: https://www.ropsr4u.com/ [12/01/2020].

3. OECD. "CODE 4 - OECD Standard Code for the Official Testing of Protective Structures on Agricultural and Forestry Tractors (Static Test)." Internet: http://www.oecd.org/agriculture/tractors/codes/04-oecd-tractor-codes-code-04.pdf [12/01/2020]. (See paragraph 3.5.3.1).

4. Ipinaskil. "Toolbox 14- Rollover Protective Structures (ROPS)." Internet: http://desertknightfm.blogspot.com/2014/04/toolbox-14-rollover-protective.html [12/01/2020].

5. Manure Management. "GEA delivers 10,000th liquid manure spreader" Internet: https://www.manuremanager.com/gea-delivers-10000th-liquid-manure-spreader-30698/ [12/29/2020].

6. Jamesway. "Maxx-Trac Dura-Tech." Internet: https://jamesway.valmetal.com/wpcontent/uploads/2018/11/Michigan-10200-1.jpg [12/01/2020].

7. The Sentinel. "Road reopens after manure spill in South Middleton Township Friday." Internet: https://cumberlink.com/news/local/road-reopens-after-manure-spill-in-south-middleton-township-friday/article_5dd1f6ea-7d33-11e2-956f-0019bb2963f4.html [12/01/2020].

8. Lague, C. "A Steering System for Trailers with Multiple Axles" 1991 American Society of Agricultural Engineers 0883-8542/ 91 / 0706-0649].

9. WorkSafe, The State of Queensland. "Tractor roll over protective structure limitations." Internet: https://www.worksafe.qld.gov.au/injury-prevention safety/alerts/whsq/2010/tractor-roll-overprotective-structure-limitations#lr [12/01/2020] .

10. Jarén, C., Alfaro, J. R., Arazuri, S., Ponce de León, J. L., Arana, J. I., Assessing Rollover Safety Provided by ROPS Tests Following SAE Standard J1194 versus OECD Code 4; Transactions of the ASABE Vol. 52(5): 1453-1459; American Society of Agricultural and Biological Engineers; 2009.

11. Nuhn. "Electra-Steer Vacuum." Internet: http://nuhn.ca/products/manure-tanks/electra-steervacuum/[12/01/2020].

12. ANSI/ASABE AD6489-3:2004 JUL2017, Agricultural vehicles — Mechanical connections between towed and towing vehicles — Part 3: Tractor drawbar (See paragraph 5).

13. ANSI/ASAE S365.9 NOV2011 (R2017), Braking System Test Procedures and Braking Performance Criteria for Agricultural Field Equipment (See paragraph 10.1 and 10.3).

14. Mishra. "TTS 2.6 : TRACTOR CENTER OF GRAVITY & MOMENT OF INERTIA" Internet: https://youtu.be/H2s-Zu53hVw [12/29/2020].

15. Manuele, F. Advanced Safety Management – Focusing on Z10 and Serious Injury Prevention, Hohoken, NJ: John Wiley & Sons, Inc.; 2014, Chapter 14 &16.

16. eXtension. “Liquid Manure Application Equipment.“ Internet: https://articles.extension.org/pages/8904/liquidmanure-application-and-irrigation-equipment [02/07/2019].

17. Livestock and Poultry Environmental Learning Community (LPELC). “Liquid Manure Application and Irrigation Equipment.“ Internet: https://lpelc.org/liquid-manure-application-and-irrigation-equipment/ [12/01/2020].

18. NC State Extension Publications. “Hose Drag Systems for Land Application of Liquid Manure and Wastewater.“ Internet: https://content. ces.ncsu.edu/hose-drag-systems-for-landapplication-of-liquid-manure-and-wastewater [12/01/2020].

19. ISO 26402 - Agricultural vehicles - Steering systems for agricultural trailers - Interface for articulated steering device of semi-mounted trailers; International Standards Organization.

20. Waltersheid, “Waltersheid Forced Steering Devices ZWL 50 and ZWL 30 Brochure, GKN Land Systems, ATASC1303.1400013“ Internet: https://www.walterscheidcoupler.de /out/pictures/media/ba_6.01+6.02+6.03.6.04_zwl50_zwl30.pdf [02/07/2019].

21. Association of Equipment Manufacturers (AEM). “Standards for Safety Signs and Symbols.“ Internet: https://www.aem.org/safety-and-technical/safety/standards-for-safety-signs-and-symbols [12/01/2020].

22. Association of Equipment Manufacturers (AEM). “Standards for Safety Signs and Symbols.“ Internet: https://www.aem.org/safety-and-technical/safety/standards-for-safety-signs-and-symbols [12/01/2020].

Bibliography

ANSI/AIHA/ASSP Z10 - Occupational Health and Safety Management Systems; American National Standards Institute, American Industrial Hygiene Association and American Society of Safety Professionals .

ANSI/ASABE AD6489-3:2004 JUL2017, Agricultural vehicles — Mechanical connections between towed and towing vehicles — Part 3: Tractor drawbar.

ANSI/ASAE S365.9 NOV2011 (R2017), Braking System Test Procedures and Braking Performance Criteria for Agricultural Field Equipment.

ANSI/ASSP Z590.3 - Prevention through Design Guidelines for Addressing Occupational Hazards and Risks in Design and Redesign Processes; American National Standards Institute and American Society of Safety Professionals.

ANSI/NEMA Z535 SET - Safety color code - environmental facility safety signs - criteria for safety symbols - product safety sign & labels and accident prevention tags; American National Standards Institute and the National Electrical Manufacturers Association.

OECD. “CODE 4 - OECD Standard Code for the Official Testing of Protective Structures on Agricultural and Forestry Tractors (Static Test).“ Internet: http ://www.oecd.org/agriculture/tractors/codes/04-oecd-tractor-codes-code-04.pdf [12/01/2020].

CSA B352.1 - Rollover Protective Structures (ROPS) for Agricultural, Construction, Earthmoving, Forestry, Industrial and Mining Machines - Part 2: Testing Requirements for ROPS on Agricultural Tractors (Inactive); Canadian Standards Association.

OSHA - Agriculture (29 CFR 1928) Subpart C – Roll-Over Protective Structures; U.S. Department of Labor

ISO 3463 - Tractors for agriculture and forestry — Roll-over protective structures (ROPS) — Dynamic test method and acceptance conditions; International Standards Organization.

ISO 5700 - Tractors for agriculture and forestry — Roll-over protective structures — Static test method

and acceptance conditions; International Standards Organization.

ISO 11783 – Tractors and machinery for agriculture and forestry -- Serial control and communications data network; International Standards Organization.

ISO 26402 - Agricultural vehicles - Steering systems for agricultural trailers - Interface for articulated steering device of semi-mounted trailers; International Standards Organization.

SAE J 1194 – Roll-Over Protective Structures (ROPS) for Wheeled Agricultural Tractors; Society of Automotive Engineers, International.

SAE J 2194 - Roll-Over Protective Structures (ROPS) for Wheeled Agricultural Tractors; Society of Automotive Engineers, International.

Forensic Engineering Investigation of the Catastrophic Breakdown of a Diesel Engine in an Emergency Generator Set

By Daniel P. Couture, PEng (NAFE 951M)

Abstract

A large-displacement 16-cylinder diesel engine was coupled with a 1750 kW-rated generator set to provide emergency power to an international airport parking facility. It had been in service for seven years, and had accumulated only 242 operating hours from a regular monthly test procedure. On the day of the incident, less than three minutes after starting up, the engine began smoking, running roughly, and then failed catastrophically. A forensic engineering investigation was undertaken to determine the cause. Two cylinders in opposite banks had been damaged. The proverbial "smoking gun" was found — an obstruction comprising a rubber gasket within the main oil gallery leading to these cylinders. The investigation explored the probable method and means that this gasket was entrained into the gallery. The results of the analysis attempted to provide for an assessment of relative liability of the parties.

Keywords

Generator set, diesel engine failure, oil gallery obstructions, filter gasket, forensic engineering

Overview

An Airport Authority operates a 9,000-stall, eight-story parking garage at an international airport in Ontario, Canada. The mechanical room of the garage contains a 1,750ekW-rated emergency generator powered by an 1,879kW diesel engine. During the annual maintenance and load capability testing held on Nov. 3, 2010, smoke was reportedly observed emanating from the engine, and a catastrophic shutdown ensued. The author's forensic engineering firm was engaged to determine the cause of the engine failure.

Investigations and Observations

In this paper, the following actors were involved to various degrees:

- Company A, the local maintenance and monthly test firm;
- Company B, the local specialized electrical systems and load test contractor;
- Company C, the engine manufacturer;
- Company D, the aftermarket oil filter manufacturer; and
- Company E, a prior maintenance and monthly test firm.

The forensic engineering team attended the site three times to document the engine damage. The dismantlement of the diesel engine was witnessed at a local remanufacturing facility in early January 2011. The involved engine had been manufactured by Company C and was a simple mechanical engine without any electronic controls or engine control module (ECM), as shown in **Figure 1**. The lack of logged information obstructed the investigation of the engine breakdown. The generator set had been installed for emergency operation to support the power supply to the parking garage. The set had been commissioned for service approximately seven years prior, and the engine's hour meter showed around 254 hours of operation, 242 of which were known to be after installation.

Reported Circumstances

Under the supervision of the airport authority,

Daniel P. Couture, PEng, 352 Consumers Road, Toronto, ON M2J 1P8, daniel.couture@arconforensics.com

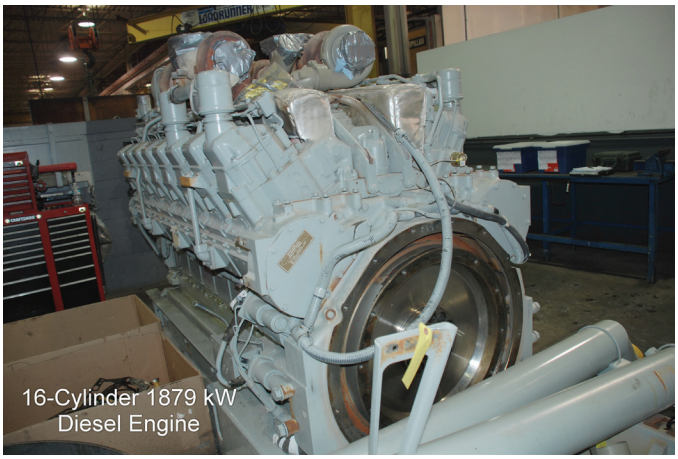

Figure 1
Diesel engine for parking garage generator set.

Company A started the engine every month. It was also serviced once yearly by Company B, which changed the oil filters and organized performance checks with a load bank.

The check sheets from the local maintenance company for Sept. 27 and Oct. 26, 2010 were reviewed and found to be uneventful. The engine oil levels were described as "good." The annual service procedures, including an oil change and replacement of oil filters, had been undertaken on the date of failure (**Figure 2**). Documents submitted for the maintenance history confirmed this narrative.

For example, the work orders by Company B for Sept. 7, 2007 and for June 10, 2008, indicated that four Company D filters had been changed, and 400 liters of 15W-40 engine oil had been added. The next oil change occurred on Oct. 20, 2009, at which time the filters were also changed. Paperwork for the annual inspection of November 2010 was incomplete because of the engine failure. It was assumed that the oil filters and oil were changed on that date as well. No performance anomalies were listed for the engine and generator on any of these records.

There had not been any power outages at the terminal requiring the operation of the generator prior to the 2010 service work. The specifications sheet noted that the average power output would be 70% of the standby power rating — and that typical operation would be 200 hours per year, with a maximum expected usage of 500 hours per year. The two-year warranty from Company C expired in 2004, according to correspondence.

The technician from Company B reported that engine began smoking heavily about three minutes after it was started while it was warming up to operating temperatures, prior to the application of the load bank to the generator.

Component Examination Findings

Company C, which had a large engine remanufacturing facility nearby, sent a crew who reported that the bolts on rods of cylinder #8 were loose, and its bearing was spun. The bearing shell had seized on to the crankshaft, and the shell had been spinning inside the big end of the connecting rod. The technicians opened the cylinder bank at this shop (**Figure 3**).

The spun bearing could have been the result of a lack of torque on the bolts, per the Company C's technician. Since Company B stated that it did not intervene at those cylinders, a suggestion was put forth that the bolts may not have been correctly torqued during the manufacturing process. One objective of the investigation was to determine whether this could have been the root cause.

Figure 2
Post-incident view of oil filter housing.

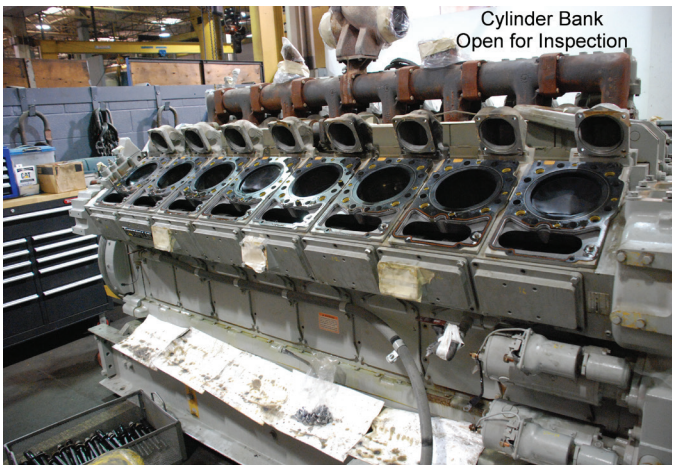

Figure 3
Cylinder bank open for inspection at the Company C shop.

Critical components located high up in the engine, such as the turbocharger shafts and bearings, indicated exposure to fine metal particles. The engine's sump contained metal fines, and the suction screen had metal particles embedded within it. The presence of fines within the sump (immediately after an oil change) suggested that fines were not being picked up by the oil filtration system.

The four new and four old oil filter canisters that were on the engine were identified as crucial to the investigation. The four new oil filter canister exteriors were examined visually at the site, and maintenance staff were requested to keep them with the engine for opening and inspection of the filter elements. However, they were misplaced somewhere between the garage and the remanufacturing facility, which prevented additional evaluation of the quantity and distribution of metal particles in the engine, under a few minutes of exposure to a new supply of oil and new filters.

In the lower engine, each of the bearing shells for the main and rod journals had notable contamination, again from metal particles, with some concentrated damage on big end and rod cap inserts for #7 and #8 cylinders (see **Figures 4** through **8**). Light wear was reported on the shanks of some cap bolts, showing movement and contact with the rod cap had occurred, such as bolt thread impressions (**Figure 9**). The crankpin journals for cylinders #7 and #8 were examined, and these showed (**Figure 10** through **13**) symptoms of frictional overheating and premature wear.

Figures 14 and **15** depict the crank throw shell sets, with the significant difference in appearance for cylinders #7 and #8 sets, while the heat discoloration damage can be seen in the shell on the fourth support block.

Figure 4
Shell damage on rod cap for cylinder #7.

Figure 5
Destroyed big end shell for cylinder #7.

Figure 6
Shell damage on rod cap of cylinder #7.

Figure 7
Shell damage on big end for cylinder #8.

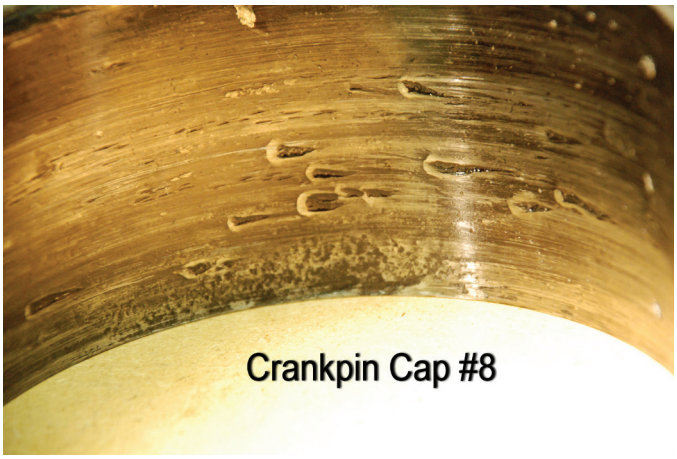

Figure 8
Shell contamination and damage on rod cap, cylinder #8.

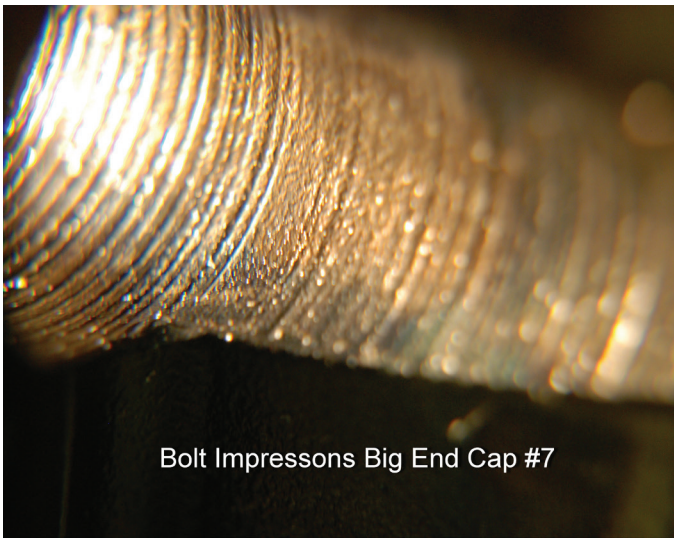

Figure 9
Bolt thread impressions on the rod cap, cylinder #7.

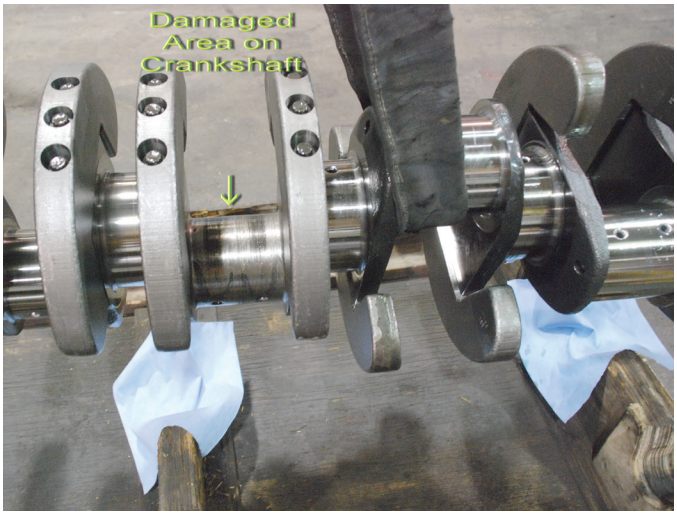

Figure 10
Damaged area on crankshaft rod journal for cylinders #7 and #8.

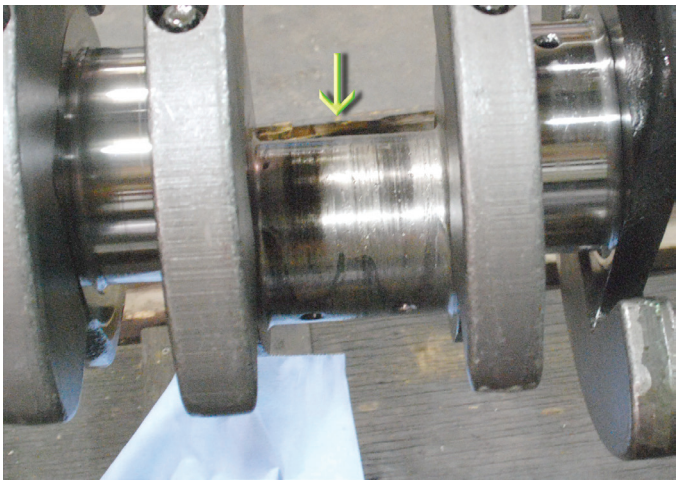

Figure 11
Damaged rod journal for cylinders #7 and #8.

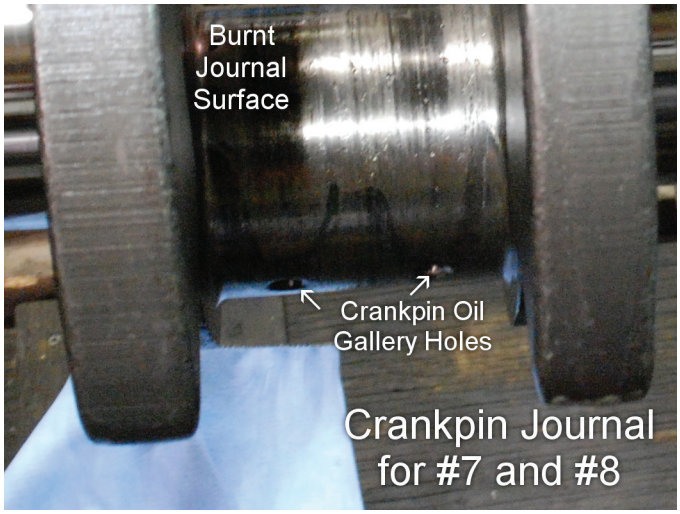

Figure 12
Zoom in on damaged rod journal, cylinders #7 and #8.

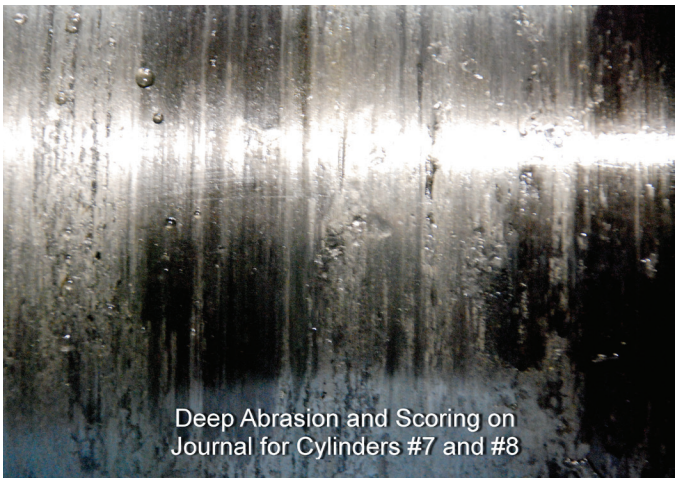

Figure 13
Deep abrasion and scoring at
the rod journal for cylinders #7 and #8.

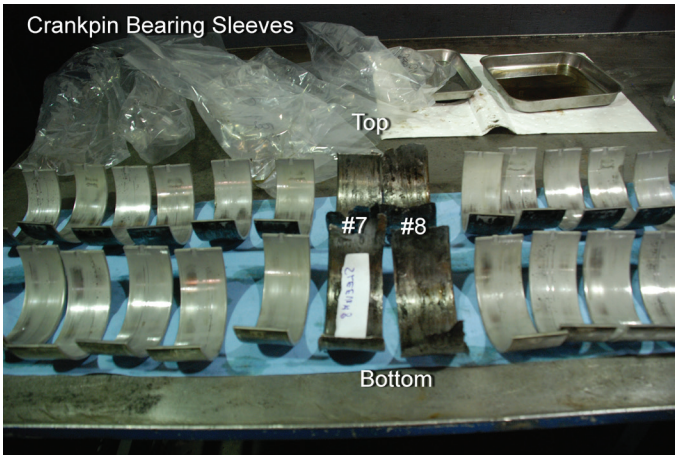

Figure 14
Crank throw shell sets — big end (top) and rod cap (bottom).

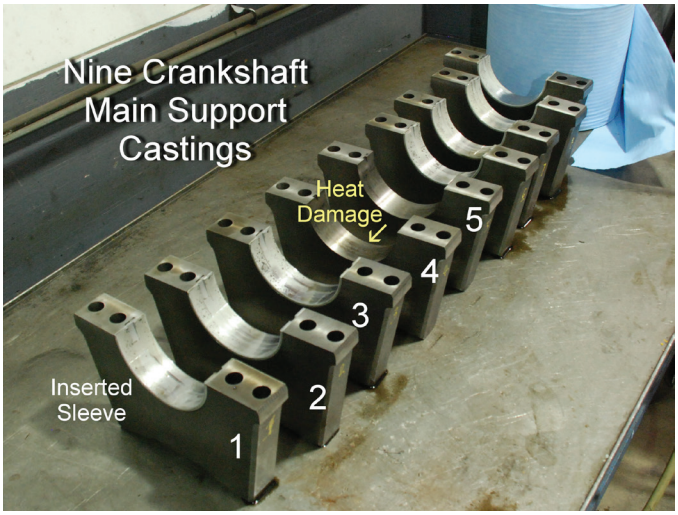

Figure 15
Crankshaft support castings with inserted shells for the main journals.

The engine oil pump gears are driven by the front gear train, and the engine oil is pulled by the oil pump from the pan through a suction bell (with a screen) and elbow. The engine oil is pumped past the engine oil cooler (**Figure 16**) and the engine oil filter housing via the pipe to the main oil gallery in the cylinder block.

The engine oil bypass valve will open if the oil cooler becomes plugged or the engine oil is too thick. According to the engine service manual, if the oil filters become blocked during operation, this regulator opens the bypass to keep oil flowing to the engine. The pressure difference for this to occur is from 26 to 29 +/- 1 p.s.i. (180 to 200 +/- 7 kPa). The oil flow regulator and the bypass assembly were found to be in normal operating condition, ruling out oil starvation because of blocked filters or bypass malfunctions at the cooler or the filter housing. Given that most

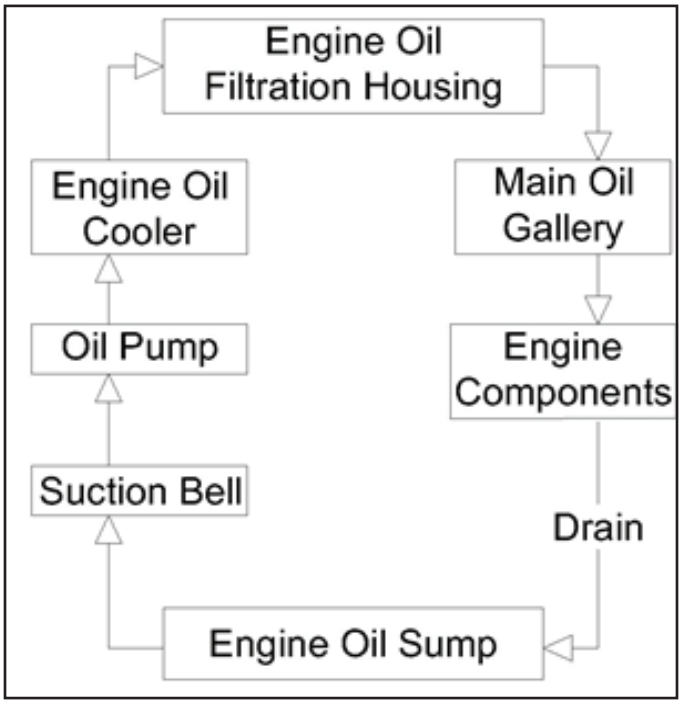

Figure 16
Approximate oil path configuration in the engine.

other bearings were found in good condition, the author concluded that they were being supplied with lubricant. This is consistent with the run to destruction philosophy, as the engine will run longer with dirty oil than with a limited supply.

After passing through the oil filters at the front of the engine, the filtered engine oil goes through an adapter into the cylinder block, circulating into the main oil gallery, with part of the flow going to the left camshaft oil gallery.

An oil analysis was completed after the incident on the new oil supplied on Nov. 10, 2011, and the findings compared to previous yearly oil test results. These were found to be in the normal range for wear elements such as copper and zinc (**Figures 17** and **18**). Given the normal range of results from the prior year, when extra elemental content would arise from premature wear, it followed that the degradation of the sleeves was a recent event, rather than one that occurred years earlier.

The symptoms of localized overheating and major oil supply failure to just two of the bearings on a common crank pin required that careful attention be paid to the side passages supplying oil to those areas. A boroscope with digital viewing screen was used to probe the side passages (**Figure 19**). The length for the probe to reach within to the other side of the main gallery in the block was 8.75 in.

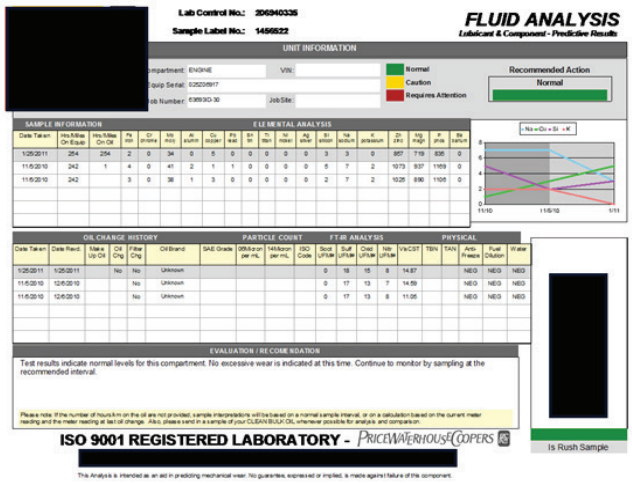

Figure 17
Oil analysis history for the engine.

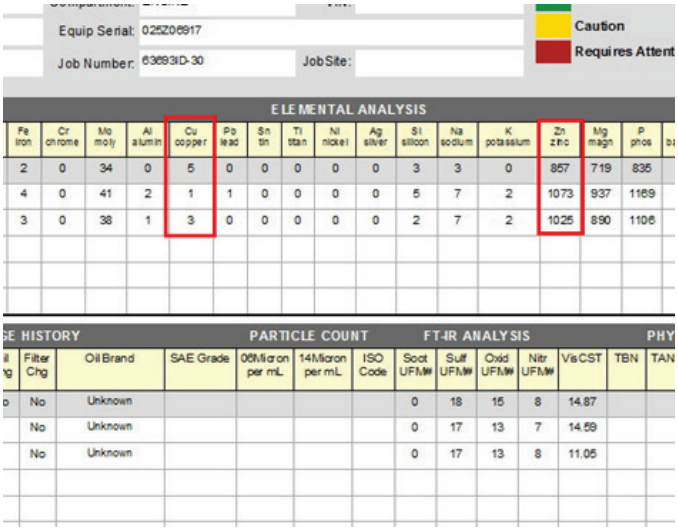

Figure 18
Zoom in on oil element analysis.

Figure 19
Probe of side passage from main
oil gallery to cylinders #5 and #6 — all clear.

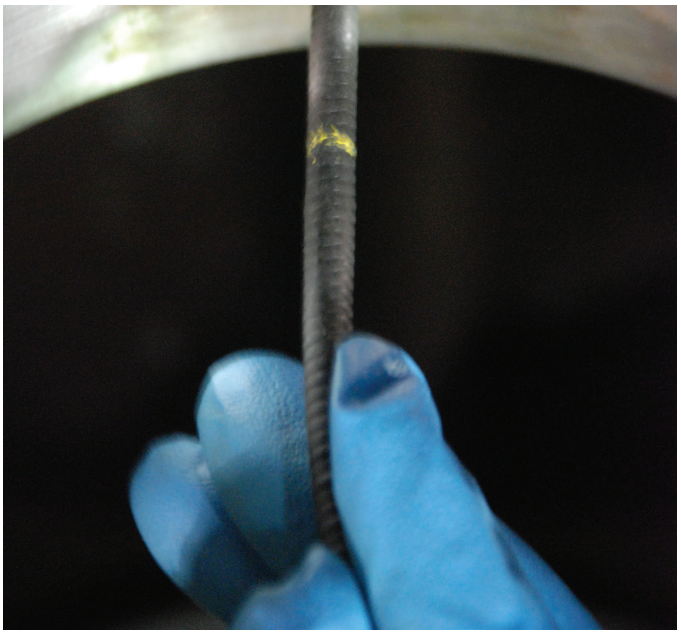

Figure 20
Recreation of the detection of obstruction
within the port for main #4 and cylinders #7 and #8.

(222 mm). However, during the inspection of the lateral port leading to cylinders #7 and #8, the probe met an obstruction at 7.5 in. (190 mm) depth, as shown in **Figure 20**.

The dark foreign object was visible in the boroscope device screen (**Figure 21**). Continued inspection along the length of the main gallery within the block found this dark object at 35 in. (890 mm) from the front end of the engine (**Figure 22** and **Figure 23**). The object was carefully removed by the mechanics with a pincer attachment on a telescopic rod. The object was 3-in. OD, 1½-in. ID, black rubber polymer gasket, with the letters NX 1 visible on one side (**Figure 24**).

Figure 21
Boroscope screen image with foreign object.

Figure 22
A longitudinal view toward the foreign object in the main oil gallery.

Figure 23
Removal of the object with a telescopic tool.

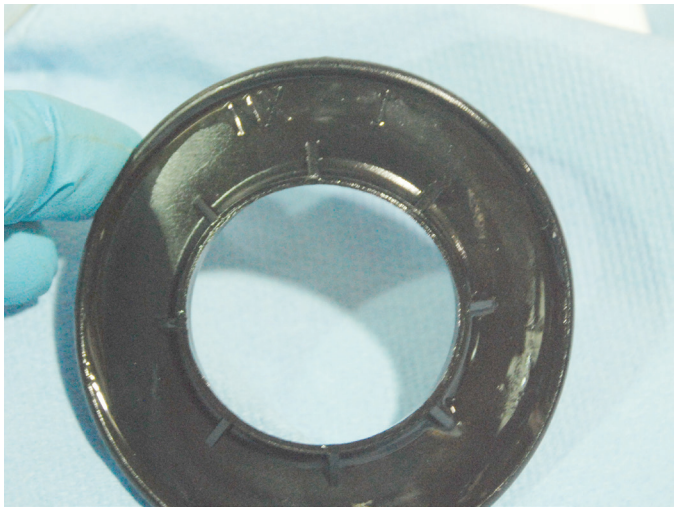

Figure 24
Foreign object extracted from the engine.

Figure 25
Comparison of Company D gaskets and the foreign object.

Continued disassembly of the engine did not reveal any alternate means of causing oil starvation to the crankshaft bearings of cylinders #7 and #8. The obstruction did not affect oil flow downstream from the main gallery to the other six cylinders, suggesting that only the port jointly serving these two was partially or fully blocked.

Analysis

When compared to the components of a Company D brand oil filter taken from the site, it was immediately apparent (**Figure 25**) that the foreign object was an inner end gasket from such a filter. The found object was still flexible, soft to the touch, and did not appear to have physically degraded by heat, when compared to the one just removed from the Company D filter. It wanted to retain its curved shape, matching the diameter of the main oil gallery, suggesting that some permanent set had been acquired. The width of the ring was wide enough to fully block the oil port. The lines seen in **Figure 24** were a portion of the letters identifying the gasket. The original equipment manufacturer's (Company C) canister was a different configuration with similar overall length (**Figure 26**). The Company D model had an outer and inner gasket, while the original equipment model had only the outer gasket ring, as seen in **Figure 27**.

The evidence showed that the rubber gasket escaped from the end of a canister and entered into the oil delivery system manifold and piping — and that it became lodged at the main oil gallery port for cylinders #7 and #8. This reduced and restricted oil flow to the journal, and initiated the overheating and wear issues.

The current set of filters were witnessed being put in place during the oil change operation, and each had

gaskets in the expected place. It was inferred from this fact that the gasket had to have come from a prior annual oil change, rather from the current one.

Since the canisters were not OEM style, it was deduced that the replacement with Company D style canisters had to have happened after the first year of operation, but before the current date. This gave a range of five to six years; however, the scope of damage was restricted to one area and did not correspond to several hundred hours of running time without lubrication.

Figure 26
Company D and Company C OEM canisters were compared.

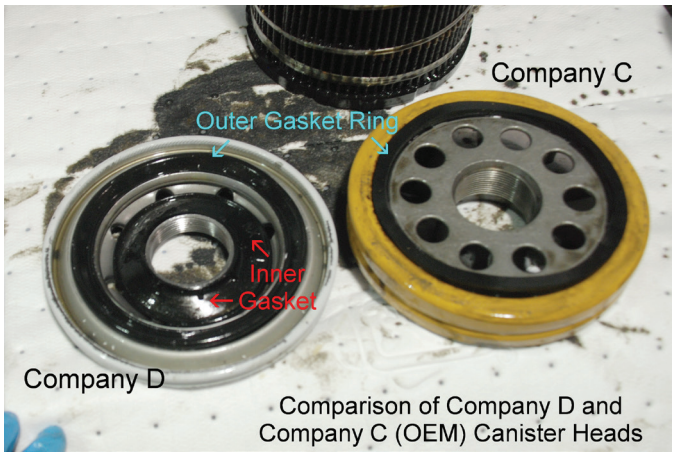

Figure 27
Comparison of different model canister heads.

The theoretical gasket path based on engine schematics was reviewed to determine how the gasket had travelled almost three feet into the engine. **Figure 28** shows the probable path in red from the entry point in the engine oil filtration housing to the blockage at the port in the main oil gallery. The gasket would be pushed along the path by oil pressure in the system.

The gasket had to pass from the top of the Company D model canister, into the port in the oil filter housing, shown in **Figures 29** and **30**. Each of the four housing positions contains one port, but there were no means of determining which port the gasket had entered. In **Figure 29**, the cut-away end of the Company D model canister is shown. Note: This is put on from below, such that if a gasket "stayed behind" as seen in **Figure 30**, it might not be visible from above (**Figure 2**).

The potential path of the folded gasket was traced through the port (**Figure 31**) and up into the housing (**Figure 32**). From here, the gasket must cross into the supply pipe to the engine (**Figure 33**) and past the end of this pipe at the engine end (**Figure 34**). The gasket must pass by the adapter and then into the main oil gallery (**Figures 35** and **36**).

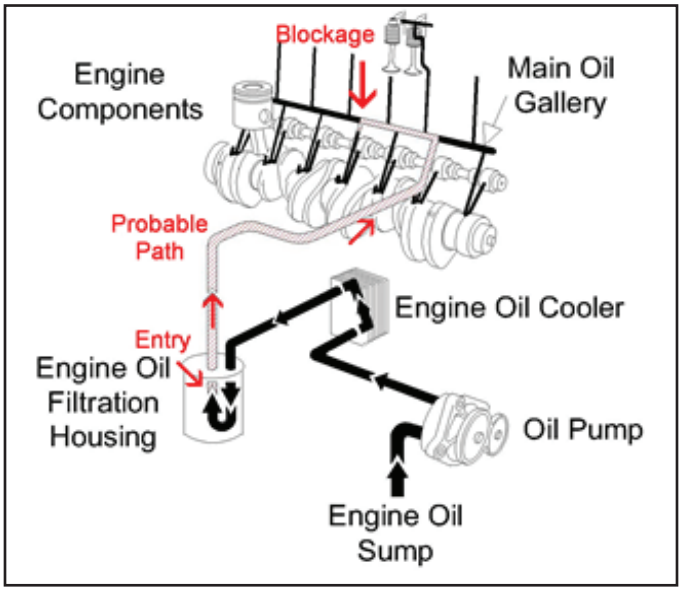

Figure 28
Probable path of the gasket from
the oil filtration housing to the blockage location.

Figure 29
Underside view of housing with port,
with underside tope of a Company D filter.

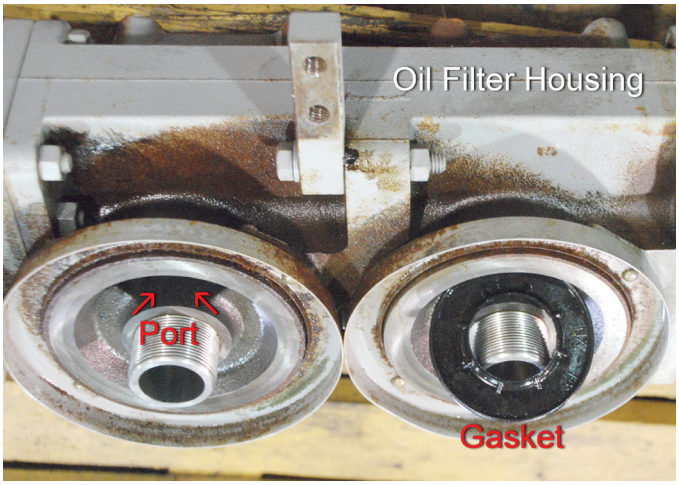

Figure 30
Underside of housing with port and gasket in loss position.

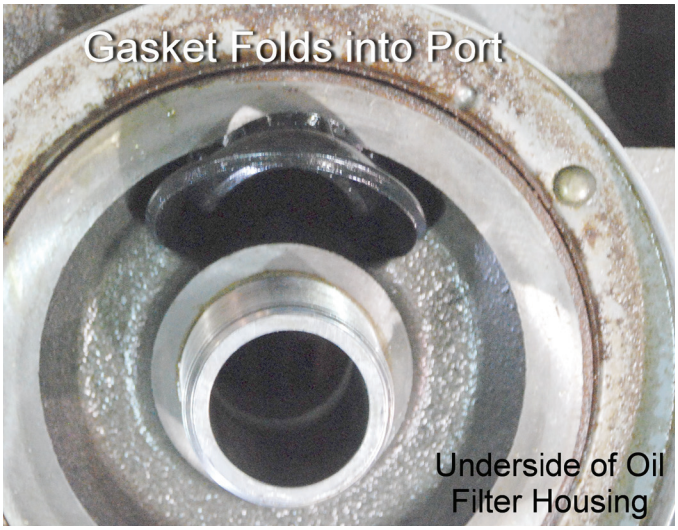

Figure 31
Gasket folded into port demonstration.

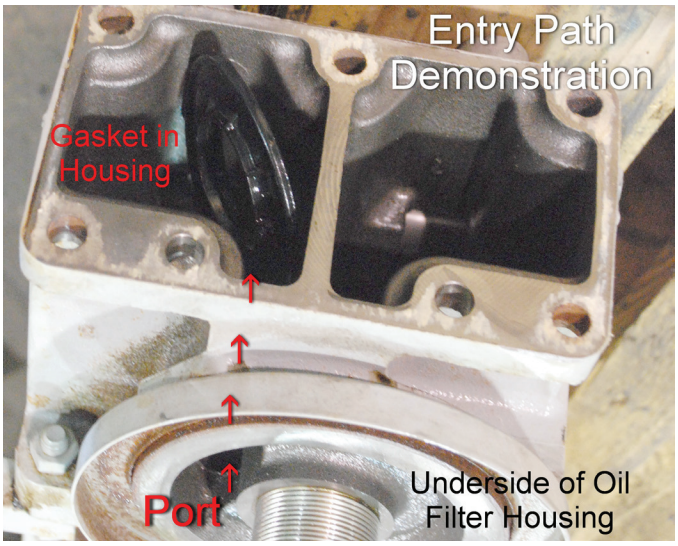

Figure 32
Entry path demonstration from port into housing.

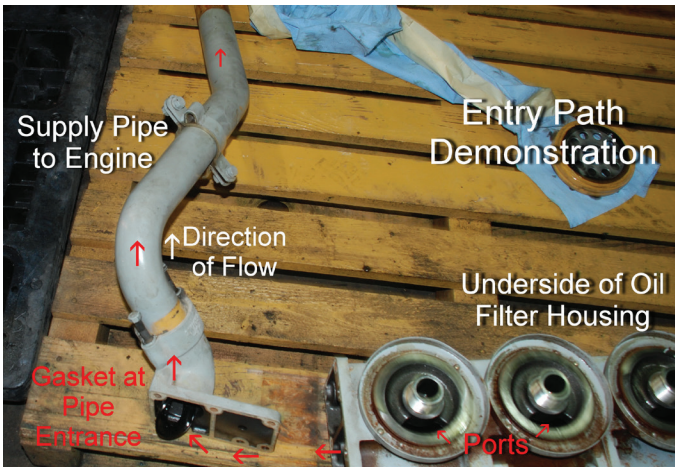

Figure 33
Entry path from housing into supply pipe.

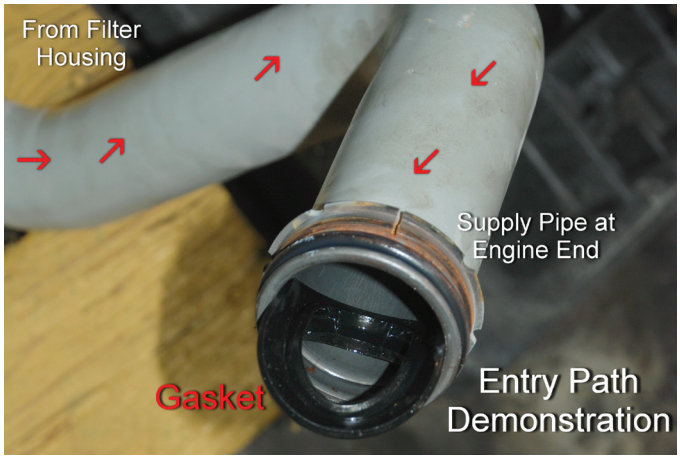

Figure 34
Continued entry path into end of supply pipe.

Gasket movement during the initial start-up on the day of the incident was considered but ruled out because the oil starvation and overheating evidence did not correspond to only three to five minutes without oil. This gasket was not degraded by heat, but it had become semi-permanently set to the curvature of the main oil gallery, which would have taken some time to induce. Had it been in place and exposed to localized heating, its properties would be expected to change.

The gasket was likely pushed along until a balance between friction with the main oil gallery wall and the flow kept it in place. The combination of the force from oil pressure and the tendency of the gasket to resist bending were enough to keep one side firmly against the port, partially or completely blocking flow to main #4 and the rod journal for #7 and #8 cylinders. The latter force kept the gasket in place — up until it was discovered during the overhaul.

Much thought was directed to the mechanism of detachment and entrapment of the gasket, the exemplar of which could be removed easily by hand from the end of a Company D filter canister. The chain of events leading to the movement of the gasket into the engine required that the gasket would have become loose when a canister was changed, sit near the bottom of the stem, and then free up from the threaded stem, before being rotated upward in place while the replacement filter was screwed in place. The gasket must come off the stem, which would otherwise hold it in place between the housing and the new filter canister. This is the key to permitting the gasket entry. Purposeful action (sabotage) was considered, but there were no obvious motives for such an act — and it was discounted as unlikely.

Company B performed independent tests to attempt to loosen a gasket on a canister under typical operating conditions, and could not duplicate or create a scenario in which the gasket would leave the end of the canister and pass into the engine. Its technicians were last in contact with the four oil filters on the engine but could not explain what had happened to these, or the four that had been on the engine before the incident. An argument of spoliation was put up against Company B by the plaintiff's counsel.

Company D also tested its aftermarket canister and compared it to Company C's OEM unit. Under low flow conditions, at between 50 to 70 p.s.i., the Company D version could not loosen the gasket on the current style.

The OEM canisters are much more expensive than the Company D version. On the other hand, there would have been absolutely no opportunity for a gasket from a Company C model to escape, since there was no inner ring gasket on that model at all.

Without an ECM to download because it was a mechanically driven diesel, there were no data showing temperature increases in the areas affected by oil starvation, until the catastrophic failure date. The presence of an ECM might have detected temperature problems at cylinders #7 and #8, inducing an auto-shutdown and preventing the engine damage.

Another firm, Company E, had provided service and oil changes at beginning of the engine's life, so there were questions about whether it was that company or Company B that would have been responsible. Whether or not Company E had used OEM canisters or Company D style canisters during that period was also a point of contention.

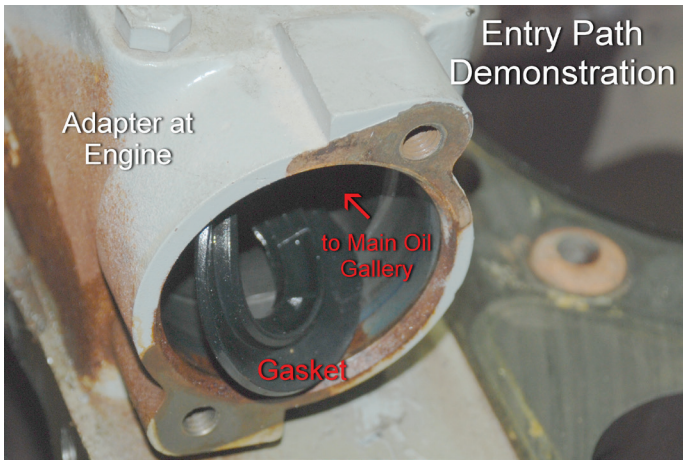

Figure 35
Entry path of gasket at the adapter on the engine.

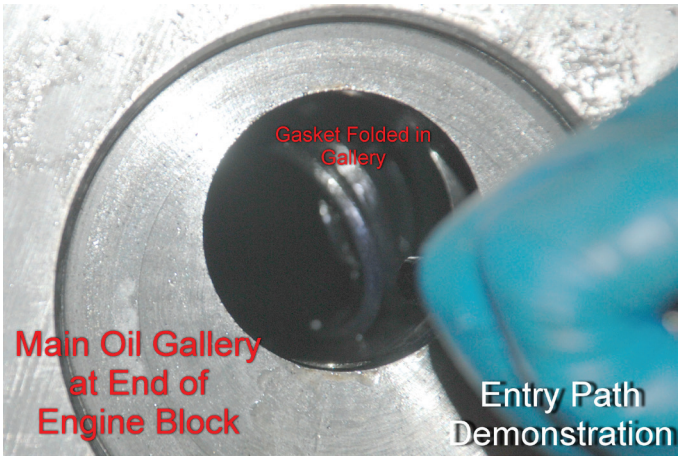

Figure 36
Entry path at the side of the engine block into the main oil gallery.

The active blockage ruled out the possibility that the big end bolts had been loose at the time of the manufacturing of the engine by Company C, and this was discounted.

To have prevented the incident, a technician would have needed to notice that the gasket of the older canister was missing, and then undo the new canisters, in turn, to discover its location prior to it entering into the housing.

Discussion

The evidence was clear that a foreign object blocked the port in the main oil gallery to a certain pair of cylinders, leading to an absence of lubrication, which, in turn, engendered frictional heating to the level at which the unlubricated bearing material could deform and detach. The debris from this failure bypassed the filter assembly and engaged the engine's bearings and turbocharger components, resulting in significant damage.

The engine was operated monthly for several hours, which (for this type of diesel engine that typically lasts thousands of hours) was at the front end of its expected service life. The engine was not expected to have any wear or overheating issues. At its typical speed of 1,800 revolutions per minute (or 108,000 revolutions per hour), it would have had only about 26 million revolutions completed at the time of the incident. The engine was barely broken in, compared to similar models in the field.

The physical properties of the gasket were not assessed with FTIR or other methods, although this may have provided insight into heat exposure. The gasket was soft and undamaged when found in the engine, with only minor semi-permanent set, which suggests a medium range rather than a short period of exposure — or possibly at high temperature for a brief period.

The gasket can be present and be pushed along and through the manifold, yet not create havoc until it blocks a gallery porthole. It must come from the front of the engine through the adapter into the main oil gallery. **Figures 29** through **36** showed the probable path that it took before it was lodged in the oil supply port for the main journal #4 and the rod journal for cylinders #7 and #8. The gasket demonstrably fitted in each part of the path, when folded over upon itself.

Even though the proverbial "smoking gun" had been revealed, there was substantial uncertainty about how long it took for the blockage to develop once the gasket was left in the oil pipe. As a result of this uncertainty and that of the involvement and the timing of the interventions, the specific negligent party remained unidentified.

Conclusions

1. The diesel engine catastrophically failed when there was an oil starvation event for cylinders #7 and #8, caused directly by a foreign object that traveled into the engine until it became lodged about halfway down the main oil gallery, partially or fully blocking the oil porthole for these cylinders and main journal #4.

2. The method of entry of the rubber gasket into the engine was postulated, but was not conclusively identified, as through the oil filter housing assembly.

3. The gasket, given its exact similarity to a gasket from Company D's filter canister, must have originated from such a filter model.

4. Since the oil circuit is closed to the outside, an external human intervention was necessary to allow entry of the gasket into the oil circuit.

5. In the absence of ECM downloads for this mechanically controlled engine, the maintenance and oil analysis records were not enough to derive a valid conclusion about when the gasket had entered into the oil distribution system, or at which of six oil changes this had occurred.

6. As a result of this uncertainty in the involvement of the companies and the timing of the interventions, the specific negligent party remained unidentified.

Epilogue

Sometimes, even with the "smoking gun" in hand, one cannot develop a definitive opinion on causation from which the trier of fact may base its assessment of relative liability. The matter settled at mediation.

Forensic Engineering Analysis of a Wheel Spindle Failure Due to Pre-Load and Fatigue

By David A. Danaher, PE (NAFE 703F)

Abstract

Typically, most vehicles equipped with non-powered wheels use a spindle that not only supports the weight of the vehicle but also allows the rotation of the tire. The rotation of the hub and wheel on the spindle is accomplished with the use of either a tapered or double row ball bearing. Bearings are mounted between the spindle and hub/wheel assembly, then secured with a castle nut set to a specified torque. Tapered bearings are chosen for this application because they are designed for applications where forces are generated radially (vertically) and axially (laterally) during use. Although tapered bearings are ideally suited for use in wheel and spindle assemblies, they must be installed properly to perform as designed. As part of that installation, the spindle nut must be properly torqued in order to apply a sufficient pre-load to the tapered bearings. Without the proper pre-load, the bearings can either generate too much friction or ride improperly on the spindle, generating forces that are not properly distributed. This paper will discuss the failure of a spindle and wheel assembly that experienced fatigue due to improper pre-load of the spindle nut.

Keywords

Tapered bearing, fatigue, failure, loading, wheel, spindle, pre-load, torque, axle, bending, stress, forensic engineering

Background

The accident involving the tapered bearing failure occurred on a two-lane highway in a rural part of eastern Colorado. The equipment was a Case IH combine that was traveling northbound on the highway when the left rear tire and wheel detached from the vehicle. Following the detachment, the combine rolled onto its roof and came to rest on the roadway near the intersection with a county road. **Figure 1** shows the rest position of the combine. The scope of the investigation was to determine if the detached wheel of the combine was a result of the accident or if it was the cause of the accident.

Accident Site

In investigating the wheel assembly failure, the dynamics of the accident were analyzed to determine if any external influences may have contributed to the wheel separation. To that end, the accident site was inspected and documented.

In the area of the crash, the northbound highway is a

Figure 1
Rest position of combine.

David Danaher, PE, 6070 Greenwood Plaza Blvd., Suite 200, Greenwood Village, CO, 80111, 303-733-1888, ddanaher@kineticorp.com

straight and level asphalt road that comes to an intersection with a county road. The highway has one northbound and one southbound lane. The road is bordered by asphalt shoulders followed by grassy terrain. The speed limit for this highway is 65 mph.

The accident site was inspected, surveyed, and scanned to document any remaining physical evidence as well as the geometry of the roadway. At the time of the inspection, numerous gouges and fluid deposits were visible on the road. The evidence at the scene was surveyed with a total station and scanned with a Faro Focus 3D Laser scanner. The Faro collected 65,525,091 data points that captured the geometry of the roadway, roadway markings, signage, physical evidence ,and other features around the area of the incident[1]. The data from the site inspection was then used to create a scaled diagram of the accident site. The site data was supplemented with photogrammetric analysis[2,3,4,5,6,7,8] of the photographs taken shortly after the accident. **Figure 2** depicts an example of the author's photogrammetry analysis. The upper image is the original photograph; the lower image depicts the results of our analysis. **Figure 3** depicts the scene diagram overlaid with an aerial photograph. The diagram is oriented with north to the right.

Figure 2
Camera matched rest position of the combine.

Figure 3
Scene diagram showing the physical evidence and the rest position of the combine.

Case Combine

The Case IH Axial-Flow 8230 involved in this crash was a 2013 model year combine. A placard on the vehicle listed the unladen weight as 18,100 kg (39,904 lb). This agricultural equipment was equipped with Firestone 28L-26 tires on the rear and Deep Tread 23° tires on the front, which have a maximum speed of 25 mph and 30 mph, respectively. The tires on the vehicle were directional and intended to be mounted in a specific orientation. The front tires were mounted in the correct orientation. The rear tires were mounted backward, such that they rotated in the incorrect direction.

Directional tires are designed for traction/performance. For a combine, the design would be for traction purposes. When the tires are rotating in the correct direction, they would provide optimal traction since the combine is driven on soft soil and muddy conditions. Therefore, the incorrect direction of the tires did not contribute to the accident; however, it could be an indication that the combine had been recently serviced.

The Case combine utilizes rear axle hydraulic steering and has an optional top speed of 18.6 mph. **Figure 4** and **Figure 5** show the vehicle at the time of the inspection. The combine was scanned using a Faro Focus 3D Laser

Figure 4
Right side of combine.

scanner, which collected more than 5 million data points that accurately captured the geometry of the combine[1]. **Figure 6** shows the 3D scan of the vehicle.

Accident Sequence

Having gathered all the evidence and geometry from the scene as well as the combine, the data was then analyzed in a scaled environment. The gouge found in the roadway matched with the left-rear axle prior to the vehicle rolling over. Furthermore, the tire marks that run parallel to the gouge also matched the right-rear tire of the combine. The gouging could only occur with the left rear tire already separated from the vehicle and therefore did not separate as a result of the rollover. Based on the above, the following sequence was determined.

Figure 5
Left rear corner of combine.

Figure 6
Scanned three-dimensional model of the combine.

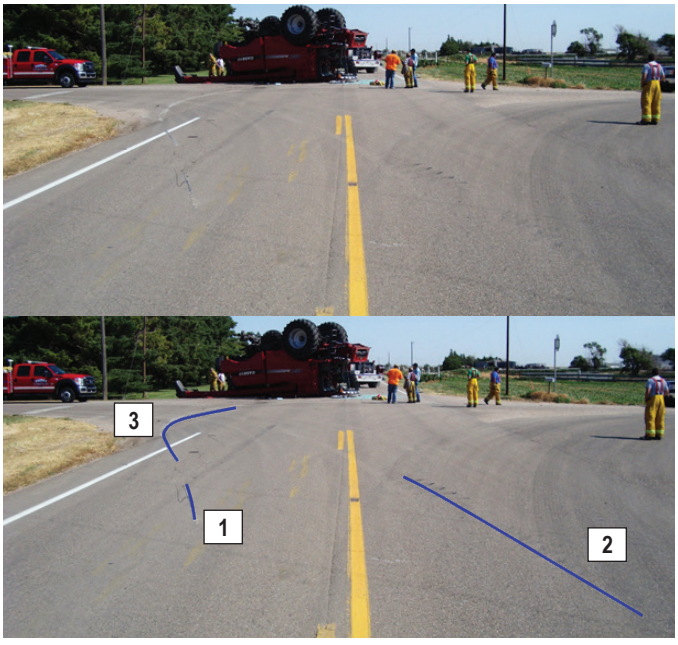

Figure 7
Top image by police; bottom image highlights the physical evidence.

The combine was initially traveling north on the highway. The 14-ft-wide vehicle was likely occupying the shoulder and the entire (or nearly the entire) 11-ft-wide northbound lane. As the left-rear tire and rim detached, the vehicle was pulled to the left when the left-rear axle began gouging the southbound lane (labeled 1 in **Figure 7**). As the vehicle was pulled to the left, the right-side tires deposited yaw marks in the northbound lane (labeled 2 in **Figure 7**). The driver then steered to the right, causing the vehicle to yaw clockwise and curve to the right (as indicated by gouge number 3 in **Figure 7**). The combine then rolled one half time before coming to rest on its roof. **Figure 8** depicts the approximate motion of the combine through the physical evidence.

The evidence at the scene and the dynamics of the accident[8,9,10,11,12,13,14,15] showed that the failure and separation of the wheel assembly was not due to any environmental factors or interaction with another vehicle — and not as a result of, but rather the cause of, the rollover. Had the wheel separated from the combine due to an external force, there would have been significant damage to the tire and rim, which showed no evidence. Also, had the wheel assembly been attached before the rollover, there would have been no gouging left in the roadway prior to the rollover. Therefore, the wheel assembly separated prior to the rollover, requiring a deeper look at the damaged components of the wheel assembly (specifically the tapered bearings and spindle).

Figure 8
Motion of the combine prior to rest along the physical evidence.

Case Combine Wheel Assembly

The failed left rear tire and wheel were attached to the combine with a spindle, tapered roller bearings, washer, and a castle nut with a cotter pin. The spindle and hub are machined as one piece, with one end of the hub being bolted to the wheel, and the other end threaded with a provision for a cotter pin through a castle nut securing the hub and spindle assembly to the tractor. When assembled within the steering knuckle housing, the spindle is held in place and allowed to rotate via two tapered roller bearings. A tapered roller bearing uses hardened steel cylindrical bearings that are held in place by a steel cage. The tapered design allows the bearings to handle radial and axial loads. A washer is then placed on the inner bearing, and a nut is used to set the axial pre-load of the bearings. Once the pre-load is set correctly, a cotter pin is inserted through the nut and spindle. **Figure 9** shows the general layout of the assembled components. The tire assembly would be to the left of the diagram.

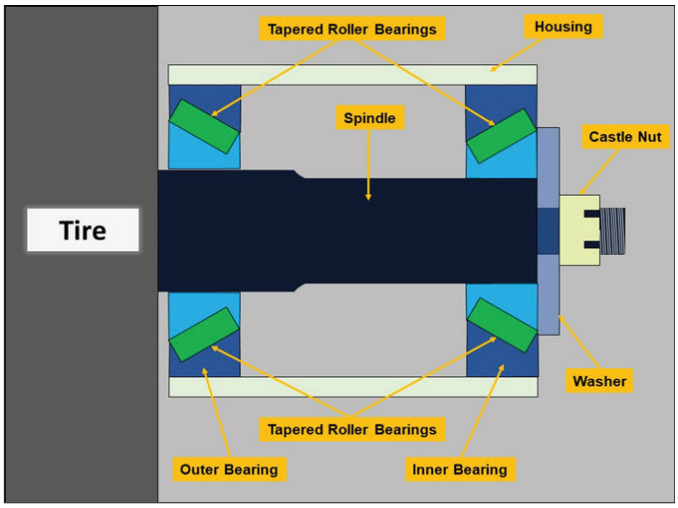

Figure 9
An example of a spindle and tapered bearing assembly.

As can be seen in **Figure 9**, the roller bearings are set at an angle relative to the spindle to allow for force along the axle. The relative angle of the bearing also generates thrust that will force the bearing off the spindle, requiring the use of a retention nut that is tightened to a specific torque, applying the proper amount of pre-load. The purpose of the pre-load is to maintain the location of the bearings relative to the spindle both radially and axially, maintaining the running position of the shaft and properly distributing the loading. The pre-load of the assembly is specified by the manufacturer.

One method for measuring the pre-load is to tighten the nut while measuring the axial displacement of the spindle with a dial indicator. The second method correlates the displacement to a specific nut torque that will set the proper pre-load. Improper pre-load can lead to excessive heat generation, increased frictional torque, and reduced bearing life due to fatigue.

To better illustrate how the spindle and bearing assembly is attached to the combine, **Figure 10** shows the right rear of the combine where the assembly is still intact. The image from **Figure 9** has now been overlaid onto the hub assembly in **Figure 11**.

At the time of the inspection, the left rear steering knuckle/housing were still attached to the rear axle. As depicted in **Figure 12**, the outer surface of the knuckle did not show signs of failure and was still attached to the combine.

Figure 10
Right rear tire and hub assembly.

Figure 11
Right rear tire and hub assembly
showing spindle and bearing diagram.

Additionally, the dust/grease cap was still attached to the inboard portion of the steering knuckle. At the time of this engineer's inspection, several components (such as the inner bearing, washer, and nut) were found inside the housing as well as an adequate amount of grease (see **Figure 13**). Within the steering knuckle housing, the tapered roller bearing, washer, castle nut, and cotter pin were removed and cleaned. **Figure 14** depicts these components cleaned as well as the dust/grease cap.

At the time of the inspection the left wheel was located next to the vehicle. The spindle, shown in **Figure 15**, was still attached to the wheel, covered in grease, and still had the outer tapered bearing seated on the spindle.

Damaged Components

Inspection of the components revealed that the spindle, spindle threads, washer, and nut were damaged and showed signs of wear prior to the failure. The following outlines the damage exhibited by each component:

Figure 12
Left and right images oriented with vehicle's front to the left and top, respectively.

Figure 13
View inside left rear steering knuckle
showing spindle components and grease.

Spindle Threads

The diameter of the threaded portion of the spindle measures approximately 0.9 in. Examination of the spindle shows that the threaded portion where the castle nut attaches was damaged (**Figure 16**). The threads were damaged in two ways: the end portion of the threads was fractured off and remained in the castle nut, and the remaining threads were flattened around the circumference of the shaft.

Castle Nut

As shown in **Figure 17**, a portion of the threaded shaft

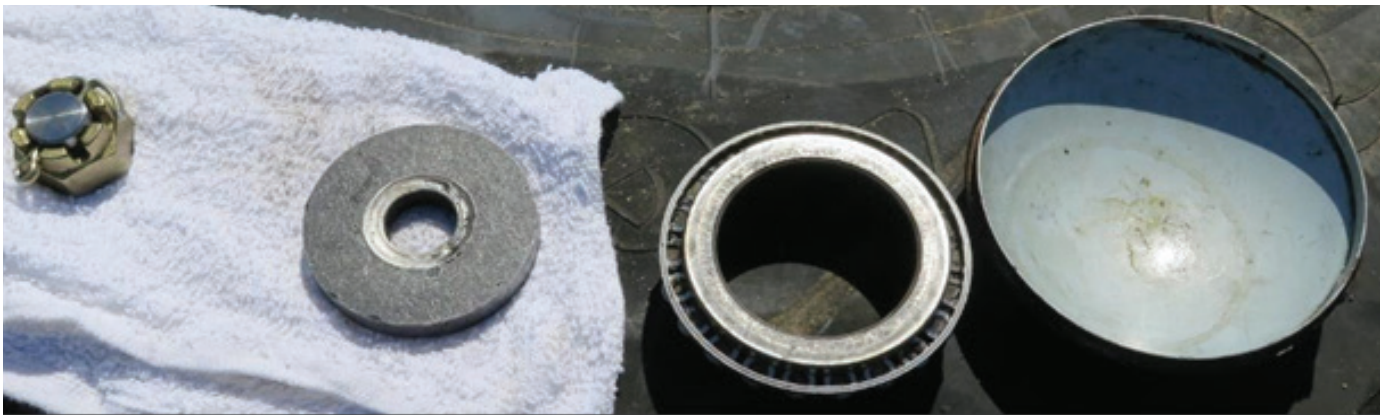

Figure 14
From left to right – castle nut, washer, inner bearing, and dust/grease cap.

Figure 15
Attached section of the spindle and outer bearing.

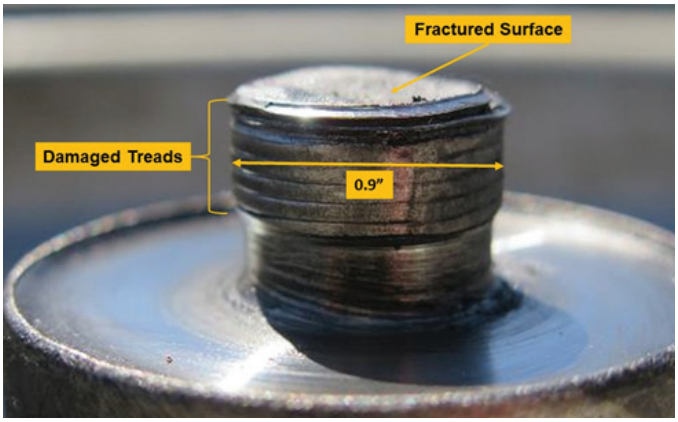

Figure 16
Spindle threads.

Figure 17
Nut, washer side.

is still attached to the nut, and there is damage to the surface of the nut that mates to the washer. The damage to the surface of the nut was due to the rotation of the nut relative to the washer and displaced/removed material from the mating surface. Furthermore, the damage and removal of the material to the nut would have increased the distance in the assembly, thereby decreasing the axial load, allowing more displacement of the bearing, and increasing misalignment in the assembly.

Washer

The washer in **Figure 18** was damaged with material displaced/removed on both sides from the contact with the inner bearing and the nut. The washer depicted in **Figure 18** shows damage from the rotation and impact damage of the washer relative to the bearing on the left and the nut on the right. The damage displaced some of the material of the washer, which is a softer

Figure 18
Washer bearing side (left), nut side (right).

material than the bearing. A depression was made on both sides of the washer, increasing the amount of axial and radial movement of the spindle and also decreasing the pre-load. All three components — the washer, the tapered bearing, and the castle nut — were assembled on site and are shown in **Figure 19**.

Spindle Shaft

The spindle measures approximately 2.50 in. in diameter and had visible signs of damage near the threaded end of the shaft. The damage was the result of the inner bearing race moving relative to the spindle. The damage to the spindle shaft as well as the described dimensions is shown in **Figure 20**. In this photograph, the area denoted by the yellow rectangle shows where the inner race of the inner bearing was rotating and impacting on the spindle. The damaged area to the spindle outlined in yellow is approximately 1.50 in. in width, approximately 0.25 in. greater than the width of the bearing. Furthermore, at the bottom of the rectangle, there is also a depression from the spinning race that dug into the spindle. This damage to the spindle was consistent with the relative movement of the bearing on the spindle. On the right in **Figure 20**, material was also displaced over the surface where the diameter changes from the bearing landing to the threaded section, giving the end of the spindle a dished shape.

Figure 19
Assembly of the tapered bearing, washer, and castle nut.

Inner Bearing

The thickness of the bearing measures approximately 1.25 in. with an inner diameter of approximately 2.50 in. The inner bearing showed markings on the edge of the inner race from contact with the washer. The bearing shown in **Figures 21** and **22** shows the scratches to the race and the condition of the cylindrical roller bearings.

In the right image of **Figure 21**, marks can be seen from the bearing moving against the washer, causing abrasion marks. This indicates that the inner race of the bearing was allowed to move relative to the washer [16,17]. **Figure 22** depicts the rollers of the bearing. The faces of the roller bearings are smooth with no gouge or pitting marks evident as well as no discoloration, which would indicate that there was proper lubrication to the bearing at the time of the spindle failure[17].

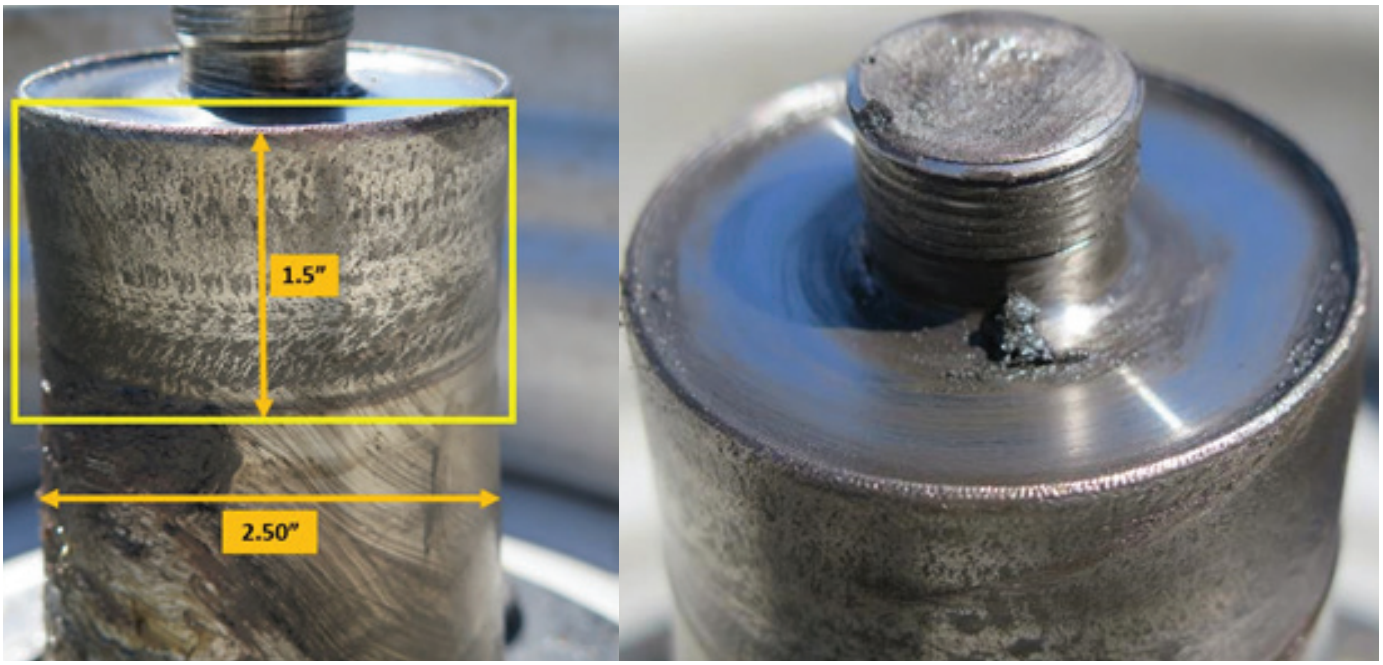

Figure 20
Spindle section attached to the separated wheel of the combine.

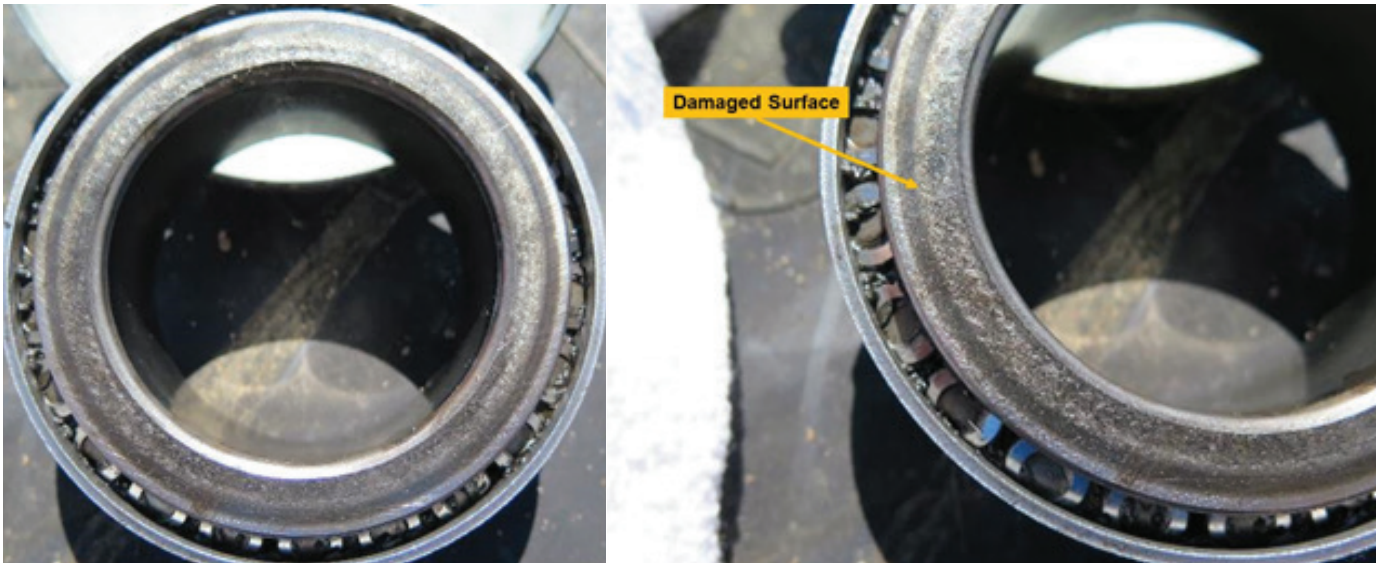

Figure 21
Scratch pattern on inner race edge.

Spindle Thread Failure

The root cause of the spindle, bearing, washer, and nut moving independently of each other was the insufficient pre-load on the bearings[18,19,20,21]. The lack of pre-load resulted in insufficient frictional force between the components and allowed relative rotation of the mating parts. The lack of pre-load also allowed the increase in axial force from the weight of the combine, which results in a thrusting force toward the castle nut that should be applied perpendicular to the axel. Once the components started to move relative to each other, the washer and spindle began

Figure 22
Outer roller bearing.

to wear, further exacerbating the problem. The increased axial and radial motion increased the stress in the spindle thread area and generated an unintended moment about the threaded portion of the spindle. In the left image of **Figure 23**, the castle nut is properly tightened, and the tapered bearings are fully seated on the spindle. In the right image of **Figure 23**, the nut is now loose, allowing the inner bearing to unseat from the outer race and the spindle.

The movement of the inner bearing toward the threaded portion of the spindle places a moment not only on the smallest cross section of the spindle, but also on the greatest location of stress concentrations, namely the threads. **Figure 24** shows the moment placed on the threaded portion of the spindle and the corresponding forces as the spindle is allowed to freely move inside the housing.

Examination of the fracture surface shows that the threaded area was subjected to repetitive overloading and fatigue. For comparison, the fracture surface of the spindle thread is shown in **Figure 25**, and an example of a fracture surface that failed due to fatigue is shown in **Figure 26**.

In **Figure 25**, a relatively smooth area with beach marks can be seen as well as a rougher area with no beach lines. This is consistent with the example of a fatigue failure in **Figure 26**, specifically the presence of an area of fatigue and an area of overload.

The pattern on the nut end and the mating spindle (shown in **Figure 27** is consistent with unidirectional bending[22] where the force is applied from one direction as seen with the fatigue area making a horse-shoe shape

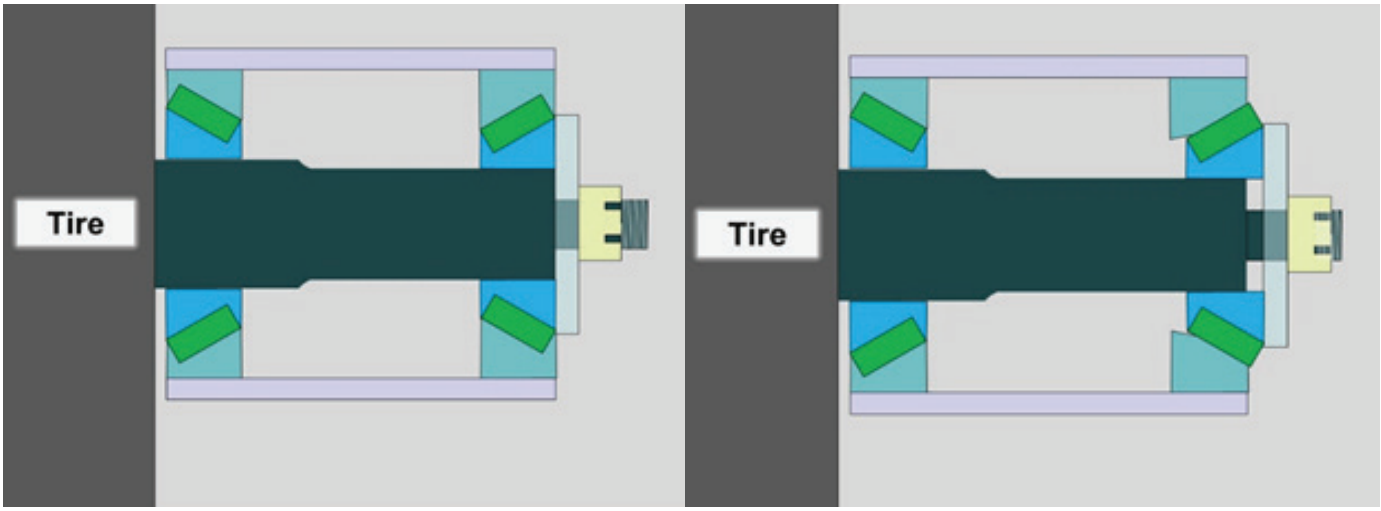

Figure 23
(Left image) properly tightened nut – (right image) improperly tightened nut.

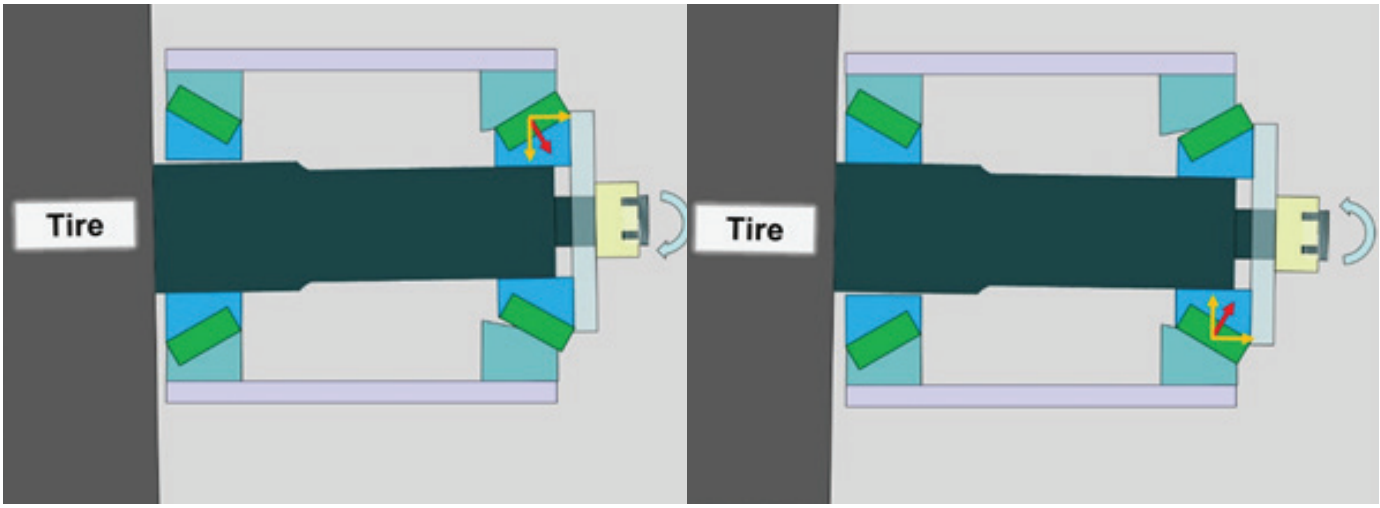

Figure 24
Moment placed on the threaded portion of the spindle.

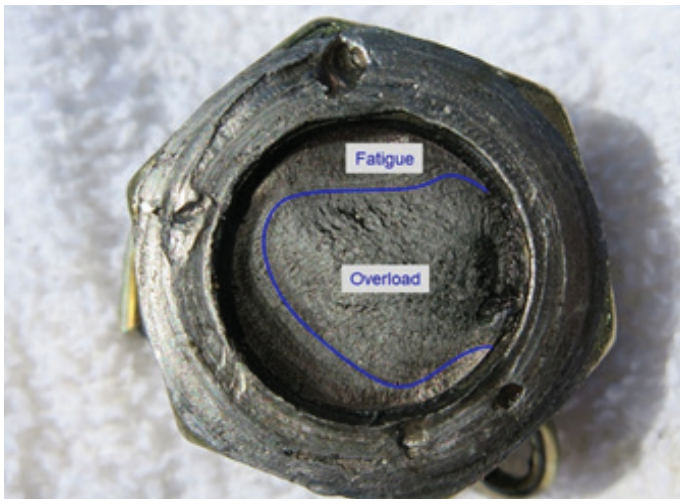

Figure 25
Fracture surface on castle nut.

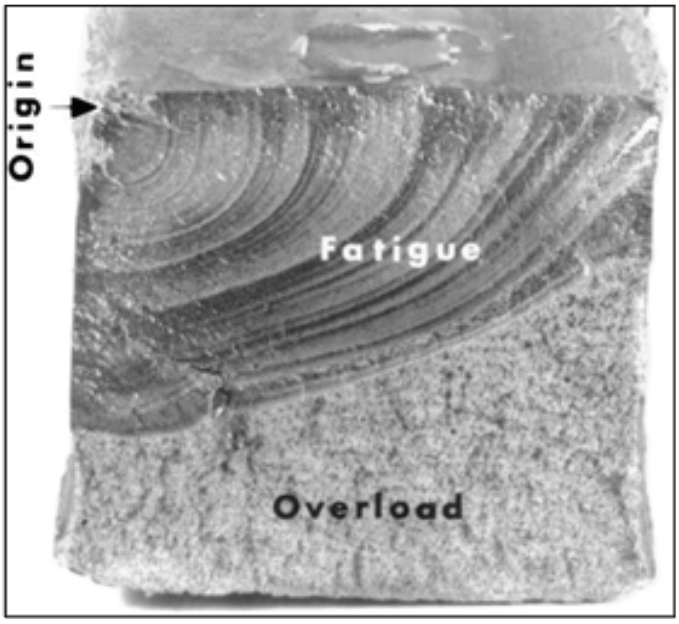

Figure 26
Example of fatigue[21].

around the overloaded area. **Figure 28** shows an example of unidirectional bending from the ASM handbook[22].

Conclusion

The insufficient pre-load allowed the inner race of the inner bearing to move on the spindle, causing damage to the spindle and allowing the spindle to move in an axial and radial direction. This further decreased the pre-load, which allowed the washer to start rotating relative to the bearing and nut. This rotation damaged the washer and further increased the amount radial and axial motion.

The increased axial and radial motion increased the stress in the spindle thread area and generated an unintended moment about the threaded portion of the spindle. The movement of the inner bearing toward the threaded portion of the spindle placed a moment not only on the smallest cross section of the spindle, but also on the greatest location of stress concentrations, namely the threads.

The insufficient pre-load allowed a portion of the load on the spindle to be distributed to the smaller cross-sectional

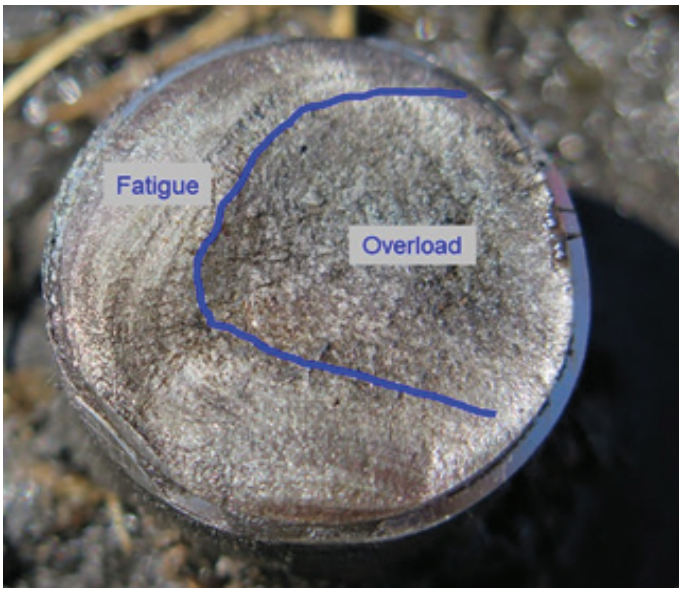

Figure 27
The fatigue horse-shoe pattern shown on spindle.

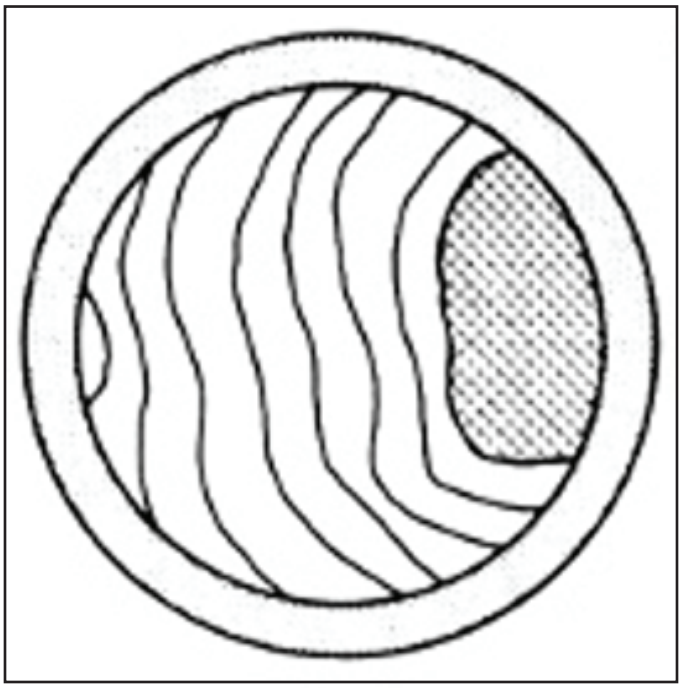

Figure 28
Unidirectional bending – ASM Handbook[22].

area of the threaded section. The correct pre-load allows for the proper positioning of the bearings on the spindle and by extension the proper distribution of the force. When the nut is not tightened to the correct position, the bearings inherently want to migrate out as far as they are allowed. In this instance, the bearing traveled toward the smaller threaded cross-sectional area, which applied an unintentional bending moment to the weakest part of the spindle. The threaded section was not designed to have a bending moment applied to it; the threaded section was simply there to keep the bearing in place. However, when the nut was not tightened sufficiently, the load from the combine on that axle created a bending moment.

A bending moment creates a stress on the threaded section that is a function of the load carried on that axle and the cross-sectional area of the spindle. The formula(s)[23] to determine stress is shown in equations 1, 2, and 3.

Eq. 1: $M=Fx$

Eq. 2: $I= (\pi r^4)/4$

Eq. 3: $\sigma=(M\ c)/I$

The cross-sectional area of the spindle is approximately 4.9 $in.^2$ compared to approximately 0.64 $in.^2$ of the threaded portion — more than seven times smaller than the spindle. When calculating the stress in the spindle compared to the stress in the threaded section, the stress is increased by 25 times.

The stress in the threaded portion of the spindle exceeded the fatigue limit of the material over time and eventually led to a sudden fracture, which allowed the wheel to separate from the combine — and the combine to subsequently rollover.

Acknowledgments: I would like to thank Gray Beauchamp, PE, for his contribution in investigating this case. Mr. Beauchamp provided much of the analysis in vehicle dynamics and accident reconstruction.

References:

1. N. Carter, Evaluation of the Accuracy of Image Based Scanning as a Basis for Photogrammetric Reconstruction of Physical Evidence, 2016-01-1467, Warrendale: Society of Automotive Engineers, 2016.

2. R. M. Brach, Vehicle Accident Analysis and Reconstruction Methods, Warrendale: Society of Automotive Engineers, 2005.

3. C. Chou, Image Analysis of Rollover Crash Tests Using Photogrammetry, 2006-01-0723, Warrendale: Society of Automotive Engineers, 2006.

4. Steve Fenton, Accident Scene Diagramming Using New Photogrammetric Technique, 970944, Warrendale: Society of Automotive Engineers, 1997.

5. Steve Fenton, Using Digital Photogrammetry to Determine Vehicle Crush and Equivalent Barrier Speed (EBS), 1999-01-0439, Warrendale: Society of Automotive Engineer, 1999.

6. James Funk, Occupant Ejection Trajectories in Rollover Crashes: Full-Scale Testing and Real World Cases, 2008-01-0166, Warrendale: Society of Automotive Engineers, 2008.

7. William Neal, Photogrammetric Measurement Error Associated with Lens Distortion, 2011-01-0286, Warrendale: Society of Automotive Engineers, 2011.

8. Nathan Rose, A Method to Quantify Vehicle Dynamics and Deformation for Vehicle Rollover Tests Using Camera-Matching Video Analysis, 2008-01-0350, Warrendale: Society of Automotive Engineers, 2008.

9. K. Baker, Traffic Collision Investigation, Evanston: Northwestern University Center for Public Safety, 2001.

10. G. Beauchamp, Determining Vehicle Steering and Braking from Yaw Mark Striations, 2009-01-0092, Warrendale: Society of Automotive Engineers, 2009.

11. R. Brach, Vehicle Accident Analysis and Reconstruction Methods, Warrendale: Society of Automotive Engineers, 2005.

12. J. Daily, Fundamentals of Traffic Crash Reconstruction, Jacksonville: Police Technology and Management, University of North Florida, 2006.

13. N. Rose, Factors Influencing Roof-to-Ground

Impact Severity: Video Analysis and Analytical Modeling, 2007-01-0726, Warrendale: Society of Automotive Engineers, 2007.

14. N. Rose, Development of a Vehicle Deceleration Rate Approach to Rollover Crash Reconstruction, 2009-01-0093, Warrendale: Society of Automotive Engineers, 2009.

15. L. Fricke, Traffic Accident Reconstruction, Warendale: Society of Automotive Engineers, 2010.

16. SKF, "Principles of Rolling Bearing Selection," SKF, 2018. [Online]. Available: 16. https://www.skf.com/group/products/bearings-units-housings/principles/bearing-selection-process/bearing-type-arrangement/arrangements-and-their-bearing-types/index.html. [Accessed 2018].

17. Timken, "Timken Bearing Damage Analysis with Lubrication Reference Guide," Timken, North Canton, 2015.

18. E. Avallone, "Mark's Standard Handbook for Mechanical Engineers 10th Edition," McGraw-Hill, 1996.

19. Morton & Control, "NSK Rolling Bearings Preload," NSK, Japan, 2018.

20. R. Norton, Machine Design an Integrated Approach, Prentice-Hall, 1996.

21. N. Dowling, Mechanical Behavior of Materials, 4th Edition, Pearson Education, 2013.

22. ASM, ASM Handbook Committee, Fractography, Vol 12, Visual Examination and Light Microscopy, pg. 118, ASM International, 1987.

23. M. Lindeburg, Mechanical Engineering Reference Manual for the PE Exam, Eleventh Edition, Belmont: Professional Publications, 2001.

Forensic Evaluation of Construction Noise and Vibrations Associated with an Urban Drainage Project

By Rune Storesund, DEng, PE, GE (NAFE 474S)

Abstract

This study performed a forensic evaluation of construction noise and ground vibration propagation to surrounding residential and commercial structures as a result of an urban drainage improvement construction project. Noise and vibration data collected during the course of the drainage project was first evaluated for conformance with the project specifications and data collection protocols. Construction equipment utilization logs were used to create a "time history" of daily maximum noise levels, which were contrasted with the maximum allowable per the project specifications. Attenuation relationships were used to delineate ground vibration extents and magnitudes propagating from the source to adjacent receptors (i.e., structures). The forensic engineer (FE) found significant deviations from the required data collection protocols and a high degree of "under-reporting." Construction-induced noise and ground vibrations were determined to be "substantial factors of harm" to the adjacent structures.

Keywords

Construction dispute, construction noise, construction vibrations, drainage culverts, historic district, loss of use, noise monitoring, structural damage, vibration monitoring, residential impacts, urban construction, forensic engineering

Overview

A lawsuit was filed by residents situated adjacent to a major urban drainage improvement construction project in a historic district against the utility owner (utility) for damages including physical distress and loss of use as a result of the construction activities. The intent of the drainage improvement project was to minimize inundation associated with a 10-year recurrence interval precipitation event. The project entailed the construction of new, below-grade, drainage culverts to temporarily store and more rapidly convey stormwater to discharge points within the larger drainage network. The new culverts were installed primarily beneath a center median of a four-lane residential roadway, which resulted in partial closure and construction activities abutting residential properties.

The FE approach applied to this engagement consisted of the following steps:

- Perform a literature review of the standard of practice for noise and vibration damage;
- Review the project-specific construction bid package (plans and specifications);
- Review the project-specific construction submittals and requests for information (RFIs);
- Review available construction documentation (daily field reports, photographs, etc.) during the course of the work; and
- Analyze impacts relative to the litigation claims.

For this engagement, the determination of specific structural damage was the responsibility of another expert team. The role of the author, for this case, was to evaluate if the construction-induced construction noise and ground vibrations were "a substantial contributing factor" to the realized damages.

Summary of the State of the Practice — Noise

A number of sources provide insights as to impacts of noise[1,2,3,4,5,6,7,8,9,10,11,12]. Construction activities, much like highways, generate noise or "unwanted sound"[12]. The Federal Transit Administration (FTA) notes that[12]:

Rune Storesund, DEng, PE, GE, 154 Lawson Road, Kensington, CA 94707, 510-526-5849; rune@storesundconsulting.com

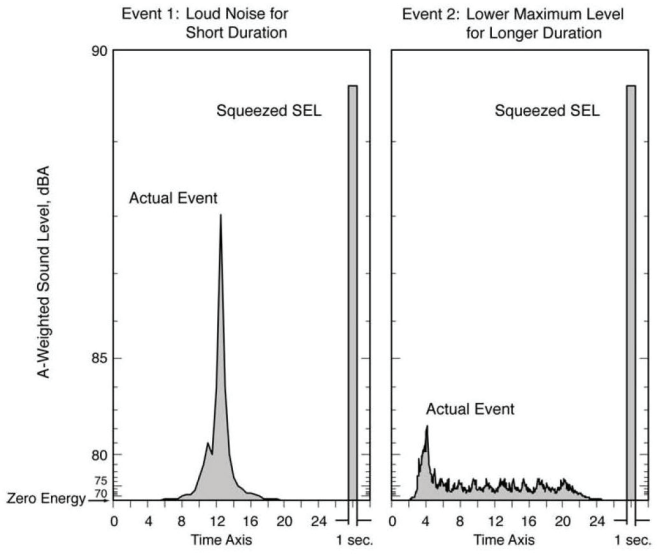

Figure 1
Sound energy is a cumulative phenomenon where short-duration loud noises can have similar sound energy as longer duration low noise[12].

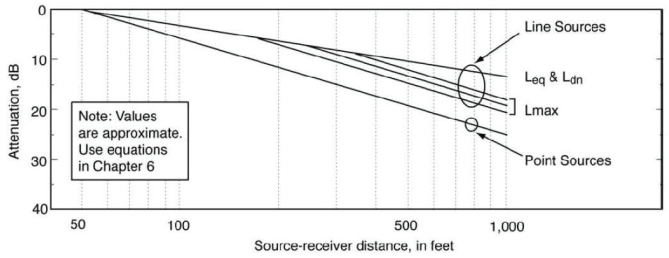

Figure 2
Example attenuation due to distance between source and receiver[12].

Noise is generally considered to be unwanted sound. Sound is what we hear when our ears are exposed to small pressure fluctuations in the air. There are many ways in which pressure fluctuations are generated, but typically they are caused by vibrating movement of a solid object. This manual uses the terms "noise" and "sound" interchangeably, since there is no physical difference between them. Noise can be described in terms of three variables: amplitude (loud or soft); frequency (pitch); and time pattern (variability).

The FTA[12] notes that the Sound Exposure Level (SEL) is a quantitative measure of the noise exposure for single noise events. The SEL is a cumulative measure (**Figure 1**), which means that louder events have a greater SEL than quieter ones, and vents that last longer in time have a greater SEL than shorter ones. FTA notes that "people react to the duration of noise events, judging longer events to be more annoying than shorter ones." When two or more combinations of sound pressure sources exist, the sound energies are added for an increase in overall sound level. For example, doubling identical sound sources (such as two jackhammers operating at once) result in a 3dB increase. Sound levels decay with distance. Typical attenuation relationships are shown in **Figure 2**.

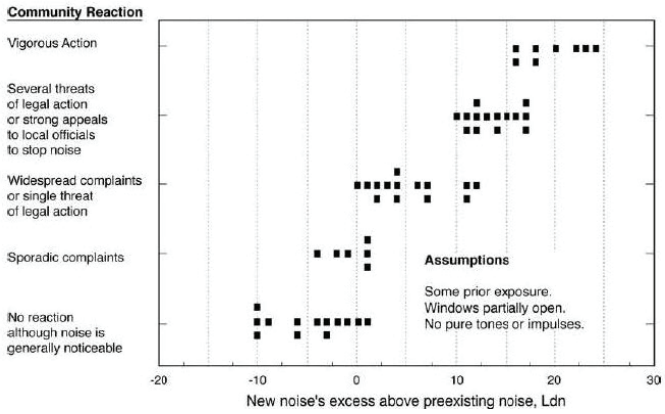

Figure 3
Community reaction to elevated noise levels[12].

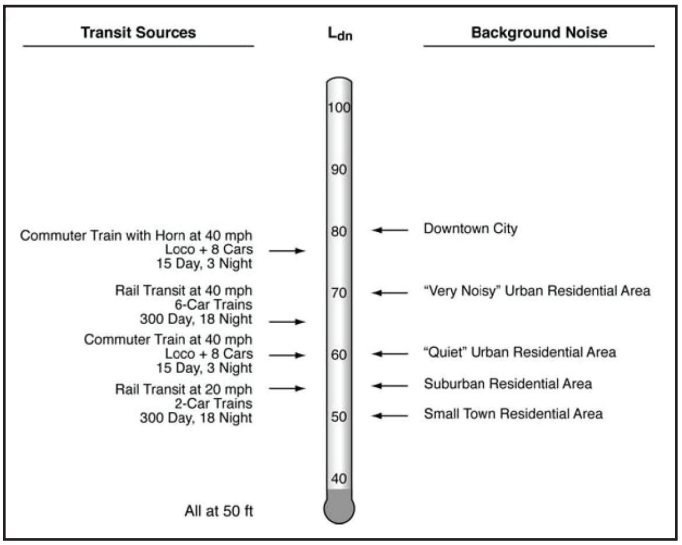

Figure 4
Typical background noise levels[12].

Increased noise level has been documented to generate response from exposed communities (**Figure 3**). Typical background noise levels for urban residential areas is on the order of 60dB (**Figure 4**). **Figure 5** shows typical background noise levels for various conditions. Typical noise ranges for various construction equipment are presented in **Figure 6** and **Figure 7**.

Summary of the State of the Practice — Vibrations

Guidance exists on impacts to structures from construction vibrations[13,14,15,16,17,18,19,20,21,22]. These reports identify the challenges associated with correlating vibration damage to structural damage. Structure response to ground vibrations depend on many factors, such as the soil

conditions, structure foundation type, structure mass, and structure stiffness[13]. For example, wood and steel are more elastic materials than brick and stone. As a result, wood and steel may be more resistant to ground vibrations[13]. NCHRP 25-25 (Task 72) notes that "[t]he condition of a building and its maintenance are important factors when assessing susceptibility to vibration damage and must be taken into account when setting vibration limits"[13]. In addition, shaking effects of construction-generated ground vibrations can cause ground settlement or shifting that significantly reduces support provided by the soil, causing damage to the structure(s)[13,23,24,25,26].

Sound	dBA
Thunderclap	120
Thunder	110
Stream, water flowing	73
Surf, pounding	70
Wind, breeze through trees	62
Birds, singing	60
Wind, gusty with rustling tree foliage	55
Rainfall, moderate	50
Rainfall, light	40
Rustling leaves	40
Olympic National Forest	40
Mountaintop	35
Wilderness ambient	35
Lake, quiet	30
Meadow, low wind conditions	30
Insects	25
Mountain slope, open	23
Rustling leaves	20
Grand Canyon, remote trail	15
Grand Canyon at night	10
Haleakala volcano crater, no wind	5

Source: Federal Highway Administration 2011.
dBA = A-weighted decibels

Figure 5
Background noise levels for various conditions[10].

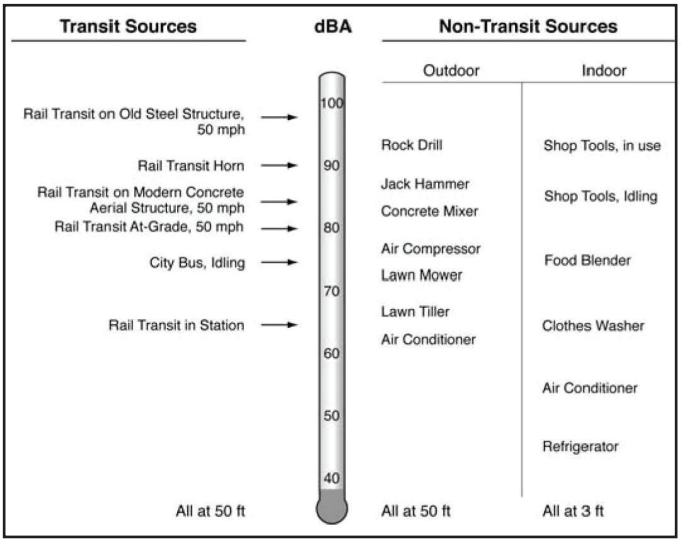

Figure 6
Typical sound levels[13].

For continuous vibrations such as vibratory compaction and vibratory pile driving, NCHRP 25-25 Task 72 suggests[13] the following thresholds for "Peak Particle Velocity" or PPV:

- PPV that exceeds 0.035 in./second is generally considered to be distinctly perceptible;
- PPV of 0.10 in./second would be strongly perceptible and begins to annoy;
- PPV of 0.2 in./second is definitely annoying;
- PPV between 0.4 and 0.6 in./second would be unpleasant.

Figure 8 shows typical peak particle velocity (PPV) ranges/responses and typical vibration sources. Impact pile driving and vibratory pile driving typically have PPVs on the order of 0.8 to 1.0 in./second at a distance of 25 ft from the source. **Figure 9** shows typical vibration source levels for construction equipment[13]. The Federal Transit Agency[13] offers a formula to estimate vibration attenuation based on distances greater than 25 ft from the source (**Figure 10**). This simplistic formula is based on distance, the reference PPV, and an adjustment factor based on "competent" soil and "hard" soil. A minimum

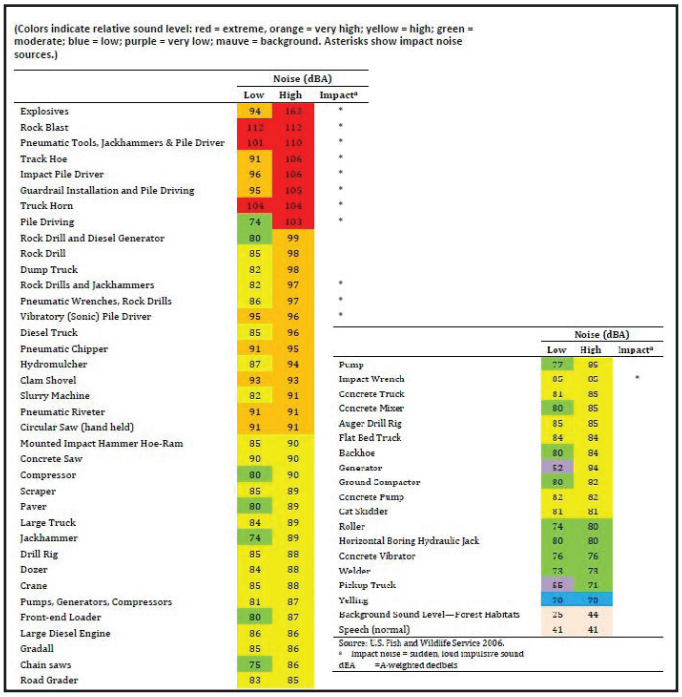
(Colors indicate relative sound level: red = extreme, orange = very high; yellow = high; green = moderate; blue = low; purple = very low; mauve = background. Asterisks show impact noise sources.)

	Noise (dBA) Low	High	Impact[a]
Explosives	94	162	*
Rock Blast	112	112	*
Pneumatic Tools, Jackhammers & Pile Driver	101	110	*
Track Hoe	91	106	*
Impact Pile Driver	96	106	*
Guardrail Installation and Pile Driving	95	105	*
Truck Horn	104	104	*
Pile Driving	74	103	*
Rock Drill and Diesel Generator	80	99	
Rock Drill	85	98	
Dump Truck	82	98	
Rock Drills and Jackhammers	82	97	*
Pneumatic Wrenches, Rock Drills	86	97	*
Vibratory (Sonic) Pile Driver	95	96	*
Diesel Truck	85	96	
Pneumatic Chipper	91	95	
Hydromulcher	87	94	
Clam Shovel	93	93	
Slurry Machine	82	91	
Pneumatic Riveter	91	91	
Circular Saw (hand held)	91	91	
Mounted Impact Hammer Hoe-Ram	85	90	
Concrete Saw	90	90	
Compressor	80	90	
Scraper	85	89	
Paver	80	89	
Large Truck	84	89	
Jackhammer	74	89	
Drill Rig	85	88	
Dozer	84	88	
Crane	85	88	
Pumps, Generators, Compressors	81	87	
Front-end Loader	80	87	
Large Diesel Engine	86	86	
Gradall	85	86	
Chain saws	75	86	
Road Grader	83	85	

	Noise (dBA) Low	High	Impact[a]
Pump	77	95	
Impact Wrench	85	05	*
Concrete Truck	81	85	
Concrete Mixer	80	85	
Auger Drill Rig	85	85	
Flat Bed Truck	84	84	
Backhoe	80	84	
Generator	52	84	
Ground Compactor	80	82	
Concrete Pump	82	82	
Cat Skidder	81	81	
Roller	74	80	
Horizontal Boring Hydraulic Jack	80	80	
Concrete Vibrator	76	76	
Welder	73	73	
Pickup Truck	55	71	
Yelling	70	70	
Background Sound Level—Forest Habitats	25	44	
Speech (normal)	41	41	

Source: U.S. Fish and Wildlife Service 2006.
* Impact noise = sudden, loud impulsive sound.
dBA =A-weighted decibels

Figure 7
Noise ranges for various construction equipment[10].

screening distance of 500 ft is recommended[13]. NCHRP 25-25 notes that "vibration measured at ground level can sometimes be lower than vibrations inside the building due to amplification of vibration caused by resonances in building floors."

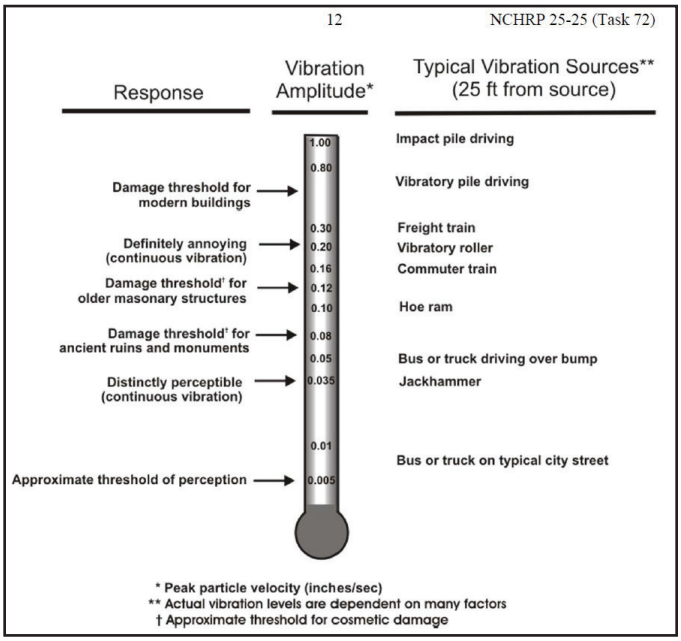

Figure 8
Vibration guidance from NCHRP 25-25 (Task 72)[13].

Vibration Source Levels for Construction Equipment

Equipment	PPV at 25 feet
Pile driver (impact)	0.644 to 1.518
Pile drive (sonic/vibratory)	0.170 to 0.734
Vibratory roller	0.210
Hoe ram	0.089
Large bulldozer	0.089
Caisson drilling	0.089
Loaded trucks	0.076
Jackhammer	0.035
Small bulldozer	0.003

Source: Federal Transit Administration 2006.

Figure 9
Table of vibration source levels for typical construction equipment[13].

$$PPV_{equip} = PPV_{ref} \times (25/D)^{n}$$

where: PPV (equip) is the peak particle velocity in in/sec of the equipment adjusted for distance

PPV (ref) is the reference vibration level in in/sec at 25 feet

D is the distance in feet from the equipment to the receiver

n is the attenuation exponent

n = 1.5 for *competent soils:* most sands, sandy clays, silty clays, gravel, silts, weathered rock (can dig with a shovel)

n = 1.1 for *hard soils:* dense compacted sand, dry consolidated clay, consolidated glacial till, some exposed rock (cannot dig with a shovel, need a pick to break up)

Figure 10
Adjustment equation for estimated vibrations at distances greater than 25 ft[13].

There is a wide range of opinion on appropriate vibration limits for structures. At one end of the spectrum is a limit of 0.10 in./second (except for ancient ruins/monuments where 0.08 in./second is thought to be appropriate) and at the other end of the spectrum, 0.5 in./second to 2.0 in./second are suggested.

Project Documentation — Noise

Documentation for the project generated during discovery was reviewed and included: the project plans and specifications; contractor submittals and RFIs; contractor daily field reports; and contractor photos. A review of the project specifications identified requirements for noise. The project specifications required the utility to contract with an independent company to monitor noise levels at the construction easement and notify the contractor of any exceedance instances. "Noise levels shall be limited to 85 decibels measured at the construction easement." Upon a review of the construction contracts, it became evident that no such independent company had been retained, and no monitoring occurred over the course of the project.

The contractor for the project maintained daily field logs noting the hour of operation of each type of equipment used on the project site each day as well as the number of hours the piece of equipment was in use (**Figure 11**). **Figure 12** presents a summary of the portfolio of equipment used during the course of the construction project.

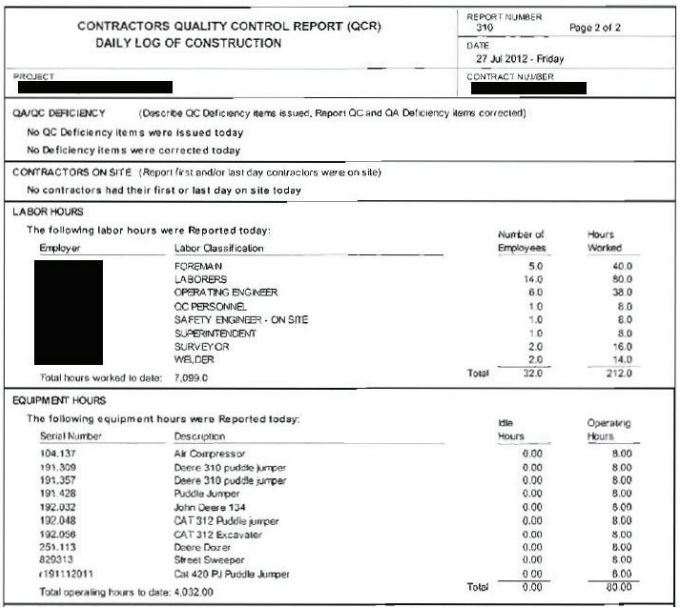
CONTRACTORS QUALITY CONTROL REPORT (QCR)
DAILY LOG OF CONSTRUCTION

REPORT NUMBER 310 Page 2 of 2
DATE 27 Jul 2012 - Friday
PROJECT [redacted]
CONTRACT NUMBER [redacted]

QA/QC DEFICIENCY (Describe QC Deficiency items issued, Report QC and QA Deficiency items corrected)
No QC Deficiency items were issued today
No Deficiency items were corrected today

CONTRACTORS ON SITE (Report first and/or last day contractors were on site)
No contractors had their first or last day on site today

LABOR HOURS
The following labor hours were Reported today:

Employer	Labor Classification	Number of Employees	Hours Worked
[redacted]	FOREMAN	5.0	40.0
	LABORERS	14.0	80.0
	OPERATING ENGINEER	6.0	38.0
	QC PERSONNEL	1.0	8.0
	SAFETY ENGINEER - ON SITE	1.0	8.0
	SUPERINTENDENT	1.0	8.0
	SURVEYOR	2.0	16.0
	WELDER	2.0	14.0
	Total	32.0	212.0

Total hours worked to date: 7,099.0

EQUIPMENT HOURS
The following equipment hours were Reported today:

Serial Number	Description	Idle Hours	Operating Hours
104.137	Air Compressor	0.00	8.00
191.309	Deere 310 puddle jumper	0.00	8.00
191.357	Deere 310 puddle jumper	0.00	8.00
191.428	Puddle Jumper	0.00	8.00
192.032	John Deere 134	0.00	8.00
192.048	CAT 312 Puddle jumper	0.00	8.00
192.056	CAT 312 Excavator	0.00	8.00
251.113	Deere Dozer	0.00	8.00
829313	Street Sweeper	0.00	8.00
r191112011	Cat 420 PJ Puddle Jumper	0.00	8.00
	Total	0.00	80.00

Total operating hours to date: 4,032.00

Figure 11
Example contractor daily field report showing equipment used and number of hours. Source: Discovery Docs.

Equipment Description	Serial No.	Noise Type
185CFM Air Compressor	104.118	1
185CFM Air Compressor	104.137	1
210G LC John Deere Trackhoe	193.148	1
Air Compressor	104.137	1
Air Compressor	104.154	1
Air Compressor	108.760	1
Air Hammer	691.056	1
American 5299A Crane	224.016	1
American 5300 Crane	225.009	1
Blue Iron Silent Piler	BlueIron01	1
CAT 312C Trackhoe	192.046	1
CAT 329E Trackhoe	193.138	1
HP 915 Air Compressor	109.905	1
IR 185CFM Air Compressor	104.169	1
IR 185CFM Air Compressor	104.182	1
IR 185CFM Air Compressor	104.201	1
Vibro Hammer	700.43	1
Wood Chipper 1	Bayou Tree 5	1
Wood Chipper 2	Bayou Tree 6	1
250T Liebherr	B&G 01	2
315 Excavator	192.019	2
6" Hydraulic Pump	422.042	2
6" Hydraulic Pump	422.043	2
6" Hydraulic Pump	422.048	2
6" Hydraul ic Pump	422.049	2
8" Hydraulic Pump	422.053	2
American Auger - Tri-State	Tri-State1	2
American HC 80 TERE X	225.083	2
American HC 110 TEREX	R226514002	2
Asphalt Milling Machine	482.012	2
Asphalt/MTV	451.016	2
Asphalt Paver	451.030	2
Asphalt Shuttle Buggy	451.028	2
Bobcat	Bayou Tree 7	2
Bobcat BXT	192.047	2
Bobcat Cold Planer	482.011	2
BobCat E35i	10276274	2
Bobcat Skidsteer	371.015	2
CAT 312 Excavator	192.046	2
CAT 312 Excavator	192.049	2
CAT 312 Excavator	192.056	2
CAT 314 Excavator	R192214002	2
CAT 325D Excavator	193.129	2
CAT 325 Excavator	193.130	2
CAT 329 Excavator	LA Rental 00001	2
CAT 329E Excavator	PLW135	2
CAT 345B Excavator	195.035	2
CAT 345c long stick excavator	195.041	2
CAT 312 Puddle jumper	192.048	2
CAT 420F Puddle Jumper	LA Rent 01	2
CAT 420 PJ Puddle Jumper	R191112011	2
CAT D4 Dozer	251.127	2
CAT Excavator	363.040	2
CAT CB-334E Roller	446.024	2
CAT Roller CS-433E	445.015	2
CAT Front-End Loader	520.029	2
Caterpillar Asphalt Paver	451.029	2
Caterpillar Asphalt Paver	451.030	2
Caterpillar Excavator	R193115006	2
Caterpillar Loader/Backhoe	191.445	2
Caterpillar Ldr/Bkh Forks	520.035	2
Deere 310 Puddle Jumper	191.309	2
Deere 310 Puddle Jumper	191.357	2
Deere Dozer	251.113	2
EC35C Mini Excavator	58332-189	2
Excavator	192.069	2
Generator	R471315001	2
Grove RT 500C	221.052	2
J-Star JD Puddle Jumper	JSTAR0001	2
JD 50D Mini Excavator	192.061	2
JD 270 Excavator	192.039	2
JD 270 Excavator	193.132	2
JD 270c LC Track Hoe	193.120	2
JD 450D Excavator	195.040	2
JD 275 Long Stick	193.131	2
JD 550 Dozer	251.110	2
JD 550 Dozer	251.124	2
JD Dozer	251.102	2
JD Dozer	251.120	2
JD Puddle Jumper	191.426	2
JD Puddle Jumper	191.451	2
JD Puddle Jumper 310SK	191.457	2
Puddle Jumper	191.358	2
Puddle Jumper	191.428	2

Equipment Description	Serial No.	Noise Type
JD Rubber Tire Backhoe	191.428	2
Jet Truck	425.005	2
John Deere 35D Mini-Excavator	JD35D	2
John Deere 50C ZTS Excavator	192.036	2
John Deere 134	192.032	2
John Deere Backhoe 135D	192.057	2
John Deere Dozer	251.119	2
John Deere Excavator	193.115	2
John Deere Excavator - 200C	193.118	2
John Deere 310SK Rubber tire	191.460	2
John Deere Rubber Tire Backhoe 310 SJ	191.409	2
John Deere 310 SK Rubber Tire Backhoe	191.451	2
John Deere Trackhoe 135c RTS	192.041	2
John Deere Trackhoe 135c RTS	192.043	2
Kobelco Crane 85 ton	CK850	2
Komatsu D21P Dozer	250.100	2
Komatsu Bull Dozer	250.101	2
Kubota Generator	471.126	2
Kubota SQ-33 Generator	471.130	2
Link-Belt 50T	224.027	2
Link-Belt 50T	224.026	2
Manitowoc Crane 3900	226.261	2
Manitowoc W 4000	227. 387	2
Offroad Forklift	569076	2
Offroad Forklift	RSC0001	2
Pump Truck (Schwing)		2
Pump Truck (Putzmeister)		2
Pump Truck	511.023	2
Pump	0.00000	2
Roller	446.030	2
Roller	466.031	2
Roller	446.035	2
Rubber Tire Backhoe	191.440	2
Rubber Tire Backhoe	191.434	2
Rubber Tire Backhoe	191.454	2
Rubber Tire Backhoe	R191114002	2
Street Sweeper	431.030	2
Street Sweeper	431.031	2
Street Sweeper	431.032	2
Street Sweeper	431.033	2
Street Sweeper	829313	2
SunBelt 18" Pump	Sun Belt	2
SunBelt 18" Pump	SunBelt1	2
SunBelt 18" Pump	SunBelt2	2
SunBelt 18" Pump	SunBelt3	2
Takeuchi Mini-Excavator TB016	UR849477	2
Takeuchi Mini Excavator	United Rental	2
Terex HC80	225.087	2
Volvo Backhoe Long Stick	EC 300DLR	2
Volvo Long Stick Excavator	EC300DLR-2	2
Volvo Roller	Volvo1	2
Volvo Track hoe	EC300D	2
XP-185 Air Compressor	104.161	2
8-15 Ton Asphalt Roller	446.029	3
10 Ton Fork Lift	rented-000	3
115' Fixed Leads	705.328	3
Bucket Truck	Bayou Tree 1	3
Bucket Truck	Bayou Tree 2	3
CAT Rubber Tire Exc	191.493	3
Caterpillar Fork Carriage	520.470	3
Cherry Picker	HTC0080-01	3
F350	Bayou Tree 8	3
F650	Bayou Tree 3	3
F650	Bayou Tree 4	3
Forklift JLG	569076	3
Fuel Tank 500-550 Gal Skid	711.040	3
JLG Manlift 6005 402116	263.012	3
J.L.G. Sky Trak forklift	521.048	3
Lincoln Welding Machine	163.111	3
Link Belt Cherry Picker - 40/60Ton	224.06	3
Linkbelt Cherry Picker	224.261	3
Linkbelt RTC 8050 50 Ton Cherry Picker	224.026	3
Mi-Jack MJ-40 Travelift	R240014001	3
NES Manlift 860SJ	N55838	3
Peterbilt Tack Truck	502.113	3
RTC 8050 Link Belt Series II Cherry Picker	224.027	3
Service Truck	506.115	3
Swinging Leads 26"X115'	705.001	3
Tool Trailers/Skid	631.180	3
Tool Trailers/Skid	631.184	3
Tool Trailers/Skid	631.208	3
Tool Trailers/Wheeled	631.253	3
Water/Service Truck	502.116	3
Welding Machine	164.421	3

Figure 12

Summary of construction equipment used during the course of the construction project. Source: Author.

19. VIBRATION MONITORING

Vibrations due to all construction activities including driving sheet piles will be monitored. The Contractor shall perform the work in a manner which will limit vibrations at the structure nearest to the work being performed to a maximum of 0.25 inch per second. Vibrations will be monitored by others at all structures, including buildings and pools. The Contractor will be informed when the vibrations from his operation have exceeded the 0.25 inch per second limit and the Contractor shall take immediate action to reduce the vibrations to acceptable limits. The Contractor shall give the [redacted] notice at least 15 days prior to beginning vibration-inducing construction operations, and shall coordinate the daily location of these operations with the government personnel at least 48-hours prior. The Contractor shall also be responsible for contacting the vibration monitoring firm to schedule the necessary vibration monitoring personnel.

Figure 13
Excerpt from the project specifications addressing vibration monitoring. Source: Discovery Docs.

Project Documentation — Vibrations

Documentation for the project generated during discovery was reviewed and included: the project plans and specifications; contractor submittals and RFIs; contractor daily field reports; and contractor photos. A review of the project specifications identified requirements for construction-induced vibrations as well as the vibration monitoring requirements. The project specifications (**Figure 13**) required the utility to contract with an independent company to monitor vibrations "at all structures, including buildings and pools."

A consulting engineering firm (vibration consultant) was retained by the utility. The vibration consultant used two alpha-seismite digital seismographs. These instruments were manually monitored in lieu of more rapid and reliable automated reporting arrays.

The author notes that for a project as extensive as this, automated arrays provide far superior data collection and alert systems as they can be installed at the beginning of the project and used as a basis for interpolating across the project site. Empirically based 2D propagation maps can be generated to better manage construction-induced ground vibrations and overcome manually placed monitors too far from the construction work in order to characterize vibrations at the "structure nearest the work being performed," as required by the project specifications.

Reports were prepared daily by the on-site vibration consultant personnel that listed the maximum PPV values recorded, a general description of the monitoring location (including a sketch by the vibration monitoring technician), and notations of general construction activities in the vicinity of the vibration monitoring.

Noise Baseline Conditions

While the noise literature provides some guidance on noise levels, data was collected during the time forensic engineering analyses and reporting were underway by a specialty sound consultant. This work occurred after completion of the project, so results were inferred to be representative of pre-project conditions. Sound measurement devices were placed at select locations along the historic construction right of way (**Figure 14**). (Note: The construction right of way per the project drawings essentially terminated at the residential property lines along the sidewalk).

Continuous sound recordings were made over the course of one week across the former project site. An overlay, based on time period, is presented in **Figure 15**. Each color plot represents a different location along the construction route. Spikes in the time histories are typically the result of emergency response vehicles (police, fire, ambulance). The low bound ambient noise level during the course of the "work day" (8 a.m. to 5 p.m.) is approximately 55 dB and a high of approximately 67 dB. This range is consistent with the published literature of anticipated noise levels for an "urban residential area."

The measured ambient background noise closely matched the ranges reported in the published literature

Figure 14
Example configuration of a sound monitoring location set up at the historic construction right of way. Source: Sound consultant.

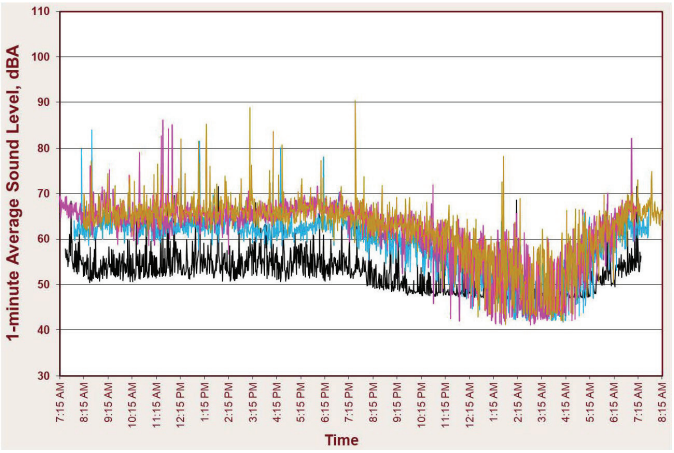

Figure 15
Representative ambient background sound levels along the construction route limits. Source: Sound consultant.

(**Figure 16**). The construction noise levels in excess of 85 dB result in a noise difference of 20 to 30 dB from baseline level at 60 dB, which, according to the published literature of community reaction (**Figure 3**), predicts strong reaction from the community. Community complaints were one of the plaintiff's claims against the utility. A-weighting was used, which is a standardized filter used to alter the sensitivity of a sound level meter with respect to frequency so that the instrument is less sensitive at low and high frequencies where the human ear is less sensitive — also written as dBA.

Construction Noise Analysis

The forensic noise analysis consisted of reviewing the inventory of equipment listed on each of the contractor's daily field report (**Figure 11**). Each piece of equipment was classified into one of three noise categories, based on the published literature identifying typical noise levels based on general equipment type:

- Red – more than likely in excess of 85 dB.
- Yellow – likely in the range of 85 dB.
- Green – likely less than 85 dB.

The maximum noise producing equipment on the project for each day was summarized and plotted on a calendar (**Figure 17**) to show the court the chronic and routine exceedance of the noise threshold (85 dB) at the construction easement.

A major challenge was documenting the specific locations of the equipment for each day to more precisely map the "noise zone" associated with the utilized equipment, but the documentation made available was insufficient to accomplish this in a reasonable manner. The contractor did provide a phased construction schedule for the project as a whole. This over-arching schedule was used to infer the general regions impacted by the equipment noise.

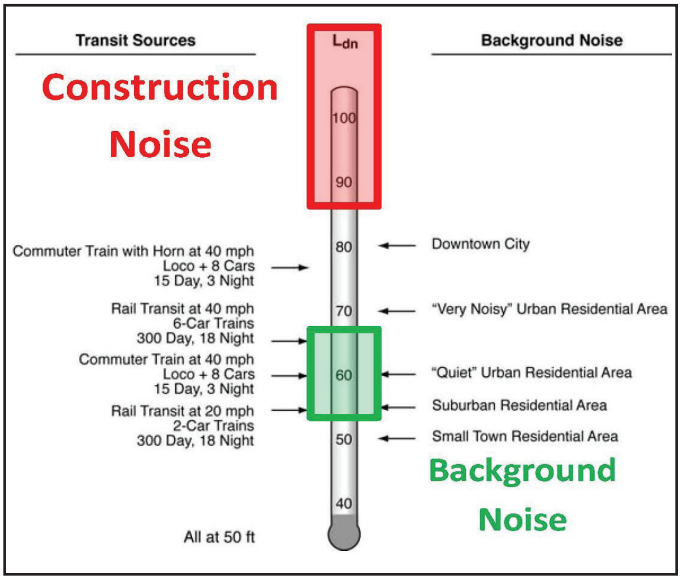

Figure 16
Comparison of construction noise levels relative to ambient background levels[17].

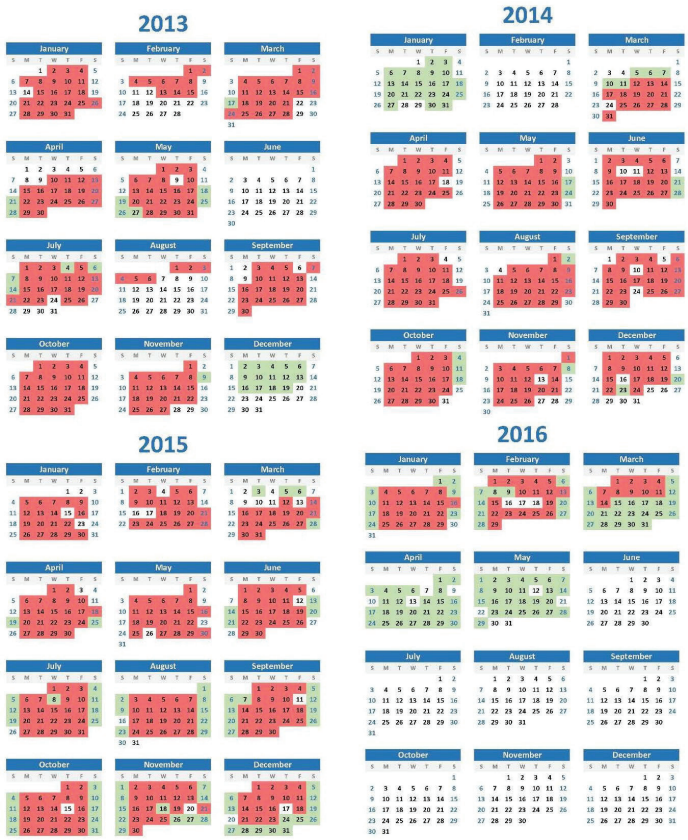

Figure 17
Summary of daily maximum noise level based on utilized contractor equipment over the course of the project. Source: Author.

The work varied spatially across the work area throughout the day and throughout the project duration. The width of the work limits was generally on the order of 85 ft. The typical distance of the residential structures and

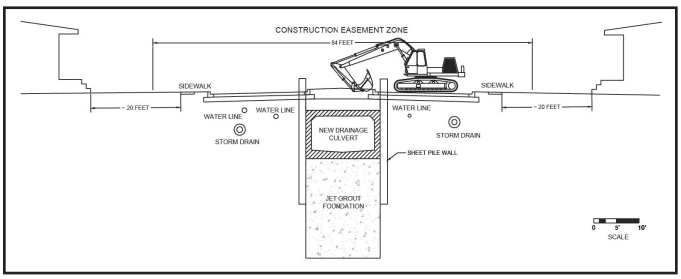

Figure 18
Typical configuration showing construction easement zone and proximity of adjacent residential structures. Source: Author.

the construction easement (**Figure 18**) was on the order of 25 ft.

Counter claims were made that the majority of the residents were away during the work day, and, as a result, were not inconvenienced by these exceedances. While an intriguing argument, it has no merit due to the fact that: (1) the project specifications clearly limit the maximum noise level to 85 dB at the construction easement irrespective of the time of day; (2) no effort was made by either the utility or the contractor to survey the adjacent residents if they were bothered by the noise; and (3) repeated complaints were made by the residents to a project complaint line regarding the construction noise and disruption of their use and enjoyment during the construction project.

It was also argued that the noise level inside the residential structures was likely less than 85 dB due to attenuation through the structure's framing. However, this argument also had no merit due to the fact that the project specifications restricted the noise to a maximum of 85 dB at the construction easement, not at the residential structure or inside the residential structure.

Courtroom Demonstrative — Noise

A courtroom demonstrative was developed to convey to the court the concepts of amplitude, frequency, and time pattern associated with noise, where[17]:

Amplitude — Loudness of a sound as a result of differences between the extremes of an oscillating sound.

Decibel — The standard unit of measurement for sound pressure level and vibration level. Technically, a decibel is the unit of level that denotes the ratio between two quantities that are proportional to power; the number of decibels is 10 times the logarithm of this ratio, also written as dB.

Frequency — The number of times that a periodically occurring quantity repeats itself in a specified period. With reference to noise and vibration signals, the number of cycles per second.

Time Pattern — Variation of noise over time.

The most important element of the demonstrative was communicating the relationship between amplitude and reported dB level. Because an increase of 1 dB is a tenfold increase in sound pressure levels, illustrating the sound levels was important to ensure there was an appreciation between a sound at 85 dB and 95 dB.

The demonstrative was configured so that speakers were oriented toward the judge, and sound levels were calibrated to reach the intended sound level (dB) at an offset distance of 20 ft (distance between the speakers and the judge). Sound meters were positioned at the judge's location to verify the intended dB level was achieved.

A portfolio of sounds was recorded from construction activities. Some recordings were based on current work in remaining areas of work for the drainage improvement project. Other recordings were based on video captured by residents during the course of the work. The recordings included (**Figure 19**):

- Ambient traffic noise (55 dBA & 65 dBA)
- Concrete breaker (85 dBA)
- Concrete saw (90 dBA)
- Roller compactor (95 dBA)
- Pile driver (100 dBA to 115 dBA)

While earplugs were made available to safely experience the full portfolio of recorded sounds, the court requested the demonstrative terminate upon reaching the 90 dBA example as the noise levels became very disagreeable.

Construction Vibration Analysis

Over the course of the construction project, 763 vibration reports were reviewed and tabulated. Of those reports, approximately 44% had daily maximum PPV values equal to or greater than 0.25 in./second (**Figure 20** and **Figure 21**) throughout the project area.

Figure 21 presents a spatial plot of setup locations of the vibration monitoring equipment and scaled circles are associated with each monitor location with a max PPV greater or equal to 0.25 in. per second. The recordings are representative of the ground vibrations observed at the unique vibration monitor location from all surrounding vibration sources.

Vibrations attenuate over distance. While the project specifications require monitoring "at the closest structure," the vibration monitors were frequently situated at more distant structures, with no monitoring at the "closest

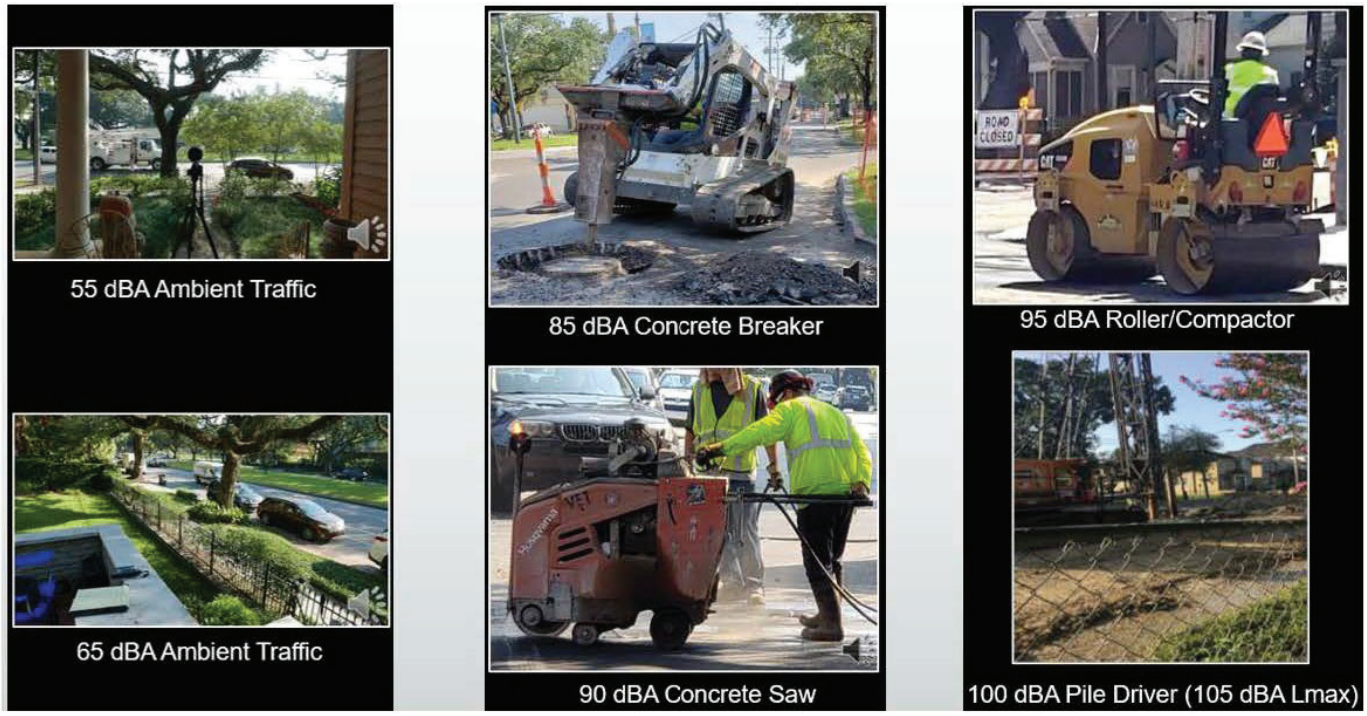

Figure 19
Overview of sounds included in the courtroom demonstrative. Source: Sound consultant.

structure" as required by the project specification.

The reported ground vibrations do not represent the maximum construction-induced vibration "the nearest structure" would experience. **Figure 22** shows a photo taken by the contractor during the course of the work where the vibration monitor was not situated in a position to represent construction-induced ground vibrations 'at the nearest structure. Additionally, numerous field reports note work occurring at significant distances from the vibration monitor, as shown in **Figure 23**.

These factors lead to "under-reporting," where the reported values do not satisfy the project specifications, which require reporting values at the "nearest structure," rather than "at the monitoring device."

The PPVref value was back-calculated to establish the ground vibration magnitude at a distance of 25 ft. Thus, if the vibration monitor was located more than 25 ft from the

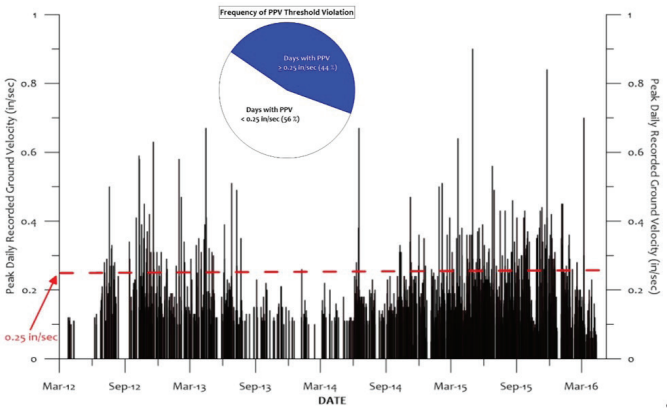

Figure 20
Vibration monitoring days where the maximum PPV exceeded the allowable threshold. Source: Author.

Figure 21
Plot of recorded maximum daily PPV values (in./second). Source: Author.

source, the equivalent PPV at 25 had to be back-calculated. Following establishment of the PPVref, vibration magnitudes based on distance were calculated and reported as PPVequiv. Results are illustrated in **Figure 27** through **Figure 30**.

The dashed blue line in **Figure 27** through **Figure 30** delineate the construction easement. As can be seen in the attenuation results, construction-induced ground vibrations exceeding the project threshold of 0.25 in. per second extend well beyond the project construction easement. As a result, the construction-induced ground vibrations were determined to be "substantial factors of harm" to the adjacent structures.

Figure 22
Example where vibration monitor was not situated at a location representative of vibrations experienced "at the nearest structure." Source: Discovery Docs.

VIBRATION MONITORING REPORT

Page 1 of 6

PROJECT NO.	21689	DATE	Friday 3/22/13
TECHNICIAN	Jonathan McCrory	PROJECT LOCATION	Claiborne Avenue Phase 1 (SELA 24a)
EQUIPMENT	White Seismology # 208		Monticello Avenue to Leonidas Street
MONITOR NO.	1 of 1		

High PPV at 50 ft

TIME	LOCATION	DISTANCE FROM SOURCE	MAXIMUM PPV (IN./SEC)	DESCRIPTION AND COMMENTS
0709 - 0729	#1	50'	(A) .78	Komatsu excavator moving construction materials
0729 - 0849	#1	50'	(B) .10	Komatsu excavator moving construction materials
0849 - 0909	#1	200' to 240'	negligible	
0909 - 0939	#1	200' to 240'	negligible	Komatsu excavator grading and excavating work area
0939 - 1009	#1	200' to 240'	negligible	site work / low activity
1009 - 1039	#1	200' to 240'	negligible	Komatsu excavator grading and excavating work area
1039 - 1109	#1	200' to 240'	negligible	site work / low activity
1109 - 1139	#1	200' to 240'	negligible	site work / low activity
1139 - 1209	#1	200' to 240'	negligible	site work / low activity

Low PPV at >200 ft

VIBRATION SOURCE	5 Komatsu excavators / Komatsu bulldozer / link-belt crane / Bottom line Jack hammer / Vibro forcefire
SCALE	0.00 to 1.2 IPS
REMARKS	location #1 is 25' east of monticello ave. 176' south of Nelson St. 240' to 240' North of the work area. work was also performed 50' east of location #1 while work was being performed in this area the work required above .85 Jpers Crane with the Army Core was installed

Figure 23
Example daily vibration monitoring report. Source: Discovery Docs; notes by author.

Location (I)			Location (J)			Location (K)		
PPVref	D	PPVequip	PPVref	D	PPVequip	PPVref	D	PPVequip
0.66	25	0.66	1.26	60	0.34	0.93	60	0.25
0.66	5	7.38	1.26	5	14.13	0.93	5	10.39
0.66	30	0.50	1.26	30	0.96	0.93	30	0.71
0.66	35	0.40	1.26	35	0.76	0.93	35	0.56
0.66	40	0.33	1.26	40	0.62	0.93	40	0.46
0.66	45	0.27	1.26	45	0.52	0.93	45	0.38
0.66	50	0.23	1.26	50	0.45	0.93	50	0.33
0.66	60	0.18	1.26	60	0.34	0.93	60	0.25
0.66	70	0.14	1.26	70	0.27	0.93	70	0.20
0.66	80	0.12	1.26	80	0.22	0.93	80	0.16
0.66	90	0.10	1.26	90	0.19	0.93	90	0.14
0.66	100	0.08	1.26	100	0.16	0.93	100	0.12
Dist to 0.25 ips	*48*	0.25	*Dist to 0.25 ips*	*74*	0.25	*Dist to 0.25 ips*	*60*	*0.25*

Figure 24
Construction-induced ground vibration attenuation calculation. Source: Author.

Conclusion

A lawsuit was filed by residents situated adjacent to a major urban drainage improvement construction project in a historic district against the utility owner (utility) for damages, including physical distress and loss of use as a result of the construction activities. This study performed

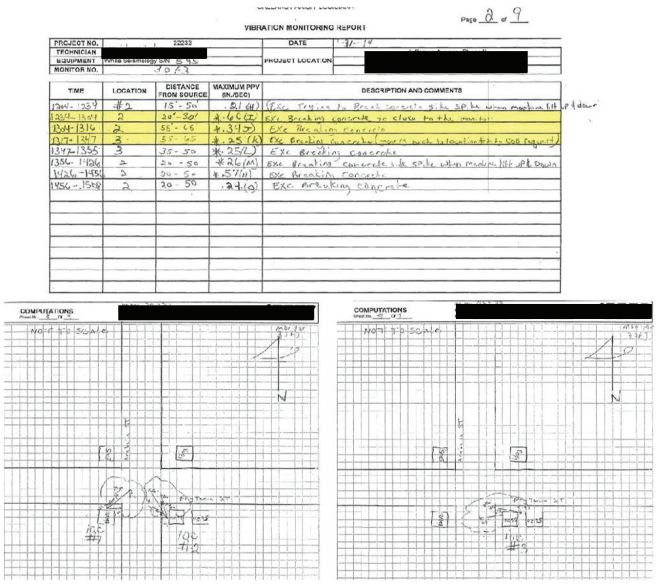

Figure 25
Calculation of vibration attenuation from January 31, 2014. Source: Discovery Docs.

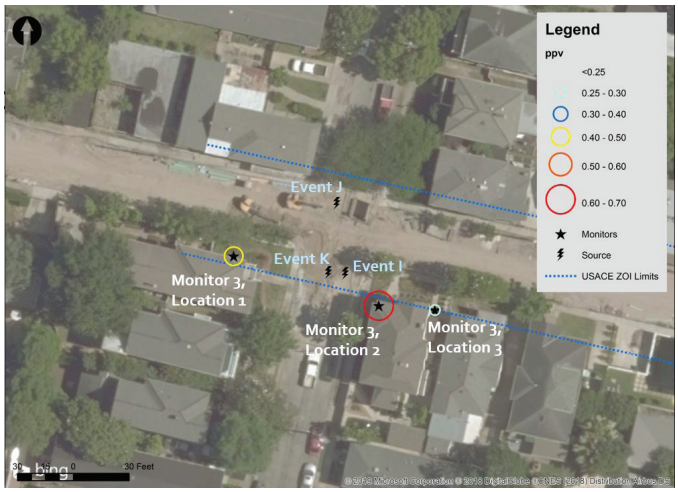

Figure 26
Location of construction-induced ground vibration attenuation example with three monitor setup locations and three exceedance events. Source: Author.

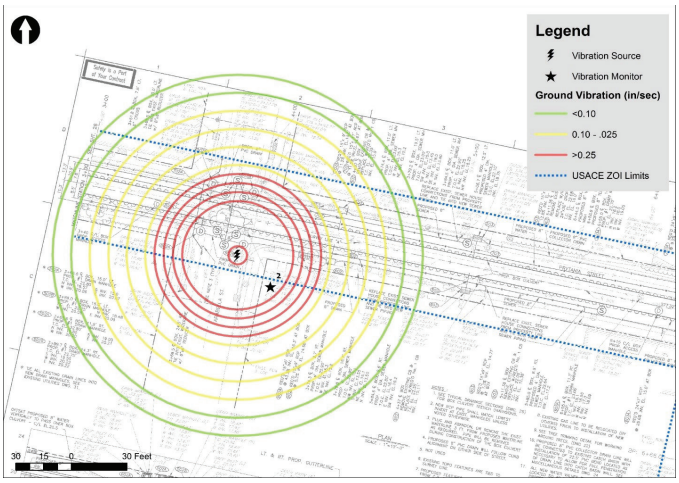

Figure 27
Attenuation of Event "I" with project plan overlay showing event origin relative to planned work. Source: Author.

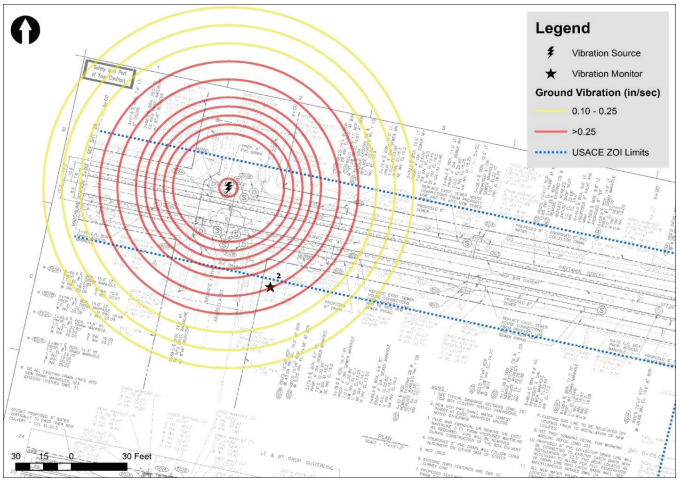

Figure 28
Attenuation of Event "J" with project plan overlay showing event origin relative to planned work. Source: Author.

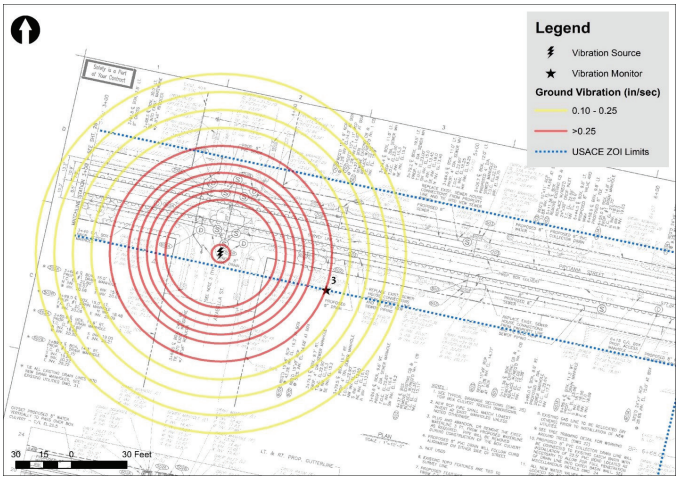

Figure 29
Attenuation of Event "K" with project plan overlay showing event origin relative to planned work. Source: Author.

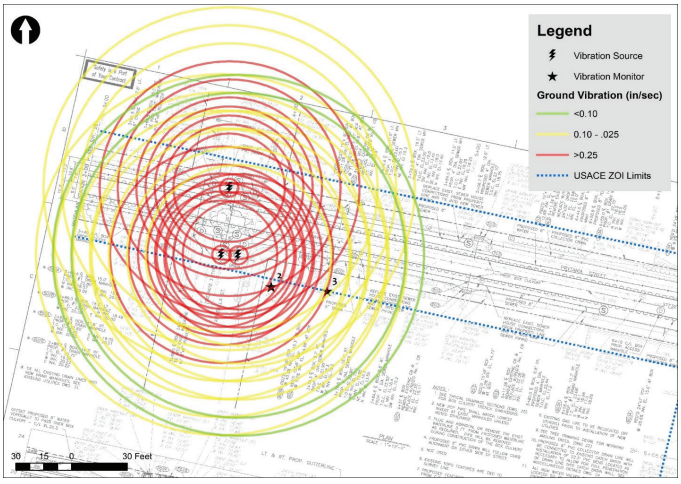

Figure 30
Overlay of attenuation of all three events (I, J, and K). Source: Author.

an FE of construction-induced noise and ground vibrations impacting residents near the construction activities.

Noise data collected during the course of the drainage project were used to create a "time history" of daily maximum noise levels. These maximum noise levels were contrasted with the maximum allowable per the project specifications. The FE found significant deviations from the required data collection protocols and routine violation of the maximum allowable thresholds specified for the project.

Attenuation relationships were used to delineate ground vibration extents and magnitudes propagating from the source to adjacent receptors (i.e., structures). The FE found significant deviations from the required data collection protocols and a high degree of "under-reporting." Construction-induced ground vibrations were determined to be "substantial factors of harm" to the adjacent structures.

The case was tried in state court via bench trial. The court's decision mirrored the findings of the forensic analyses.

References

1. E. P. Agency, "Information on Levels of Environmental Noise Requisite to Protect Public Health and Welfare with an Adequate Margin of Safety; Report No. 550/9-74-004," Washington DC, 1974.

2. F. I. C. o. U. Noise, "Guidelines for Considering Noise in Land Use Planning and Control; a joint publication of the Environmental Protection Agency, the Department of Transportation, the

Department of Housing and Urban Development, the Department of Defense, and the Veterans," Washington DC, 1980.

3. D. o. H. a. U. Development, "Environmental Criteria and Standards of the Department of Housing and Urban Development, 24 Code of Federal Regulations Part 51; 44 Federal Register 40861," Washington DC, 1979.

4. A. N. S. Institute, "American National Standard: Compatible Land Use with Respect to Noise, Standard S3.23-1980," New York, 1980.

5. A. N. S. Institute, "American National Standard: Quantities and Procedures for Description and Measurement of Environmental Sound – Part 5. Sound Level Descriptors for Determination of Compatible Land Use, Standard S12.9-1998/Part 5," New York, 1998.

6. T. J. Schultz, "Noise Rating Criteria for Elevated Rapid Transit Structures, U.S. Department of Transportation Report No. UM-TA-MA-06-0099-79-3," U.S. Department of Transportation, Washington DC, 1979.

7. T. J. Schultz, "Synthesis of Social Surveys on Noise Annoyance," Journal of the Acoustical Society of America, vol. 63, no. 8, August 1978.

8. S. Fidell, D. S. Barber and T. J. Schultz, "Updating a Dosage-Effect Relationship for the Prevalence of Annoyance Due to General Transportation Noise," Journal of the Acoustical Society of America, vol. 89, no. 1, 1991.

9. S. Fidell, "The Schultz Curve 25-years Later: A Research Perspective," Journal of the Acoustical Society of America, vol. 114, no. 6, 2003.

10. E. W. West, "Technical Guidance for Assessment and Mitigation of the Effects of Traffic Noise and Road Construction Noise on Bats," Caltrans, Sacramento, 2016.

11. U. D. o. T. (USDOT), "Highway Traffic Noise Analyses and Abatement," U.S. Department of Transportation, Federal Highway Administration, Office of Environment and Planning, Noise and Air Quality Branch, Washington DC, 2011.

12. Federal Transit Administration, "Transit Noise and Vibration Impact Assessment." Prepared by C. E. Hanson, D. A. Towers, and L. D. Meister, Burlington, MA. Prepared for Office of Planning and Environment, Washington, DC., 2006.

13. Wilson, Ihrig & Associates, Inc., ICF International and Simpson, Gumpertz & Heger, Inc., "NCHRP 25-25/Task 72, Current Practices to Address Construction Vibration and Potential Effects to Historic Buildings Adjacent to Transportation Projects," 2012.

14. American Association of State Highway and Transport, "Standard Recommended Practice for Evaluation of Transportation Related Earthborne Vibrations, AASHTO R8-96," Washington, DC, 2004.

15. California Department of Transportation, "Transportation- and Construction-Induced Vibration Guidance Manual, Prepared by Jones & Stokes, Sacramento, CA.," 2004.

16. Esrig, M. I., and A. J. Ciancia., "The Avoidance of Damage to Historic Structures Resulting from Adjacent Construction," American Society of Civil Engineers, New York, NY, 1981.

17. Federal Transit Administration, "Transit Noise and Vibration Impact Assessment." Prepared by C. E. Hanson, D. A. Towers, and L. D. Meister, Burlington, MA. Prepared for Office of Planning and Environment, Washington, DC., 2006.

18. International Organization for Standardization, "Mechanical Vibration and Shock; Vibration of Buildings: Guidelines for the Measurement of Vibrations and Evaluation of their Effects on Buildings." Second edition. ISO 4866-2010., 2010.

19. Kelley, P. L., S. J. DelloRusso, and C. J. Russo., "Building Response to Adjacent Excavation and Construction." Pp. 80-97., Boston, 1998.

20. Konon, W. and J. R. Schuring., "Vibration Criteria for Historic and Sensitive Older Buildings.," vol. 111, no. 3.

21. Whiffin, A. C., and D. R. Leonard., "A Survey of Traffic-induced Vibrations. Road Research

Laboratory Report LR418.," 1971

22. Caltrans, "Transportation and Construction Vibration Guidance Manual; CT-HWANP-RT-13-069.25.3," Sacramento, 2013.

23. J. E. Bowles, Foundation Analysis and Design, Fourth Edition, New York: McGraw-Hill Book Company, 1988.

24. S. L. Kramer, Geotechnical Earthquake Engineering, Upper Saddle River: Prentice-Hall International, 1996.

25. USACE, USACE Engineering Manual 1110-1-1904, Washington, DC: USACE, 1990.

26. H.-Y. Fang, Foundation Engineering Handbook, 2nd Edition, New York City: Chapman & Hall, Inc., 2004.

Forensic Engineering Analysis of Fatal Overhead Crane Accident

By Richard M. Ziernicki, PhD, PE, (NAFE 308F) and Ricky Nguyen, MS, PE

Abstract

This paper outlines the forensic procedure and techniques used in the reconstruction and safety assessment of a fatal overhead crane accident. The decedent (a subcontractor) was working as a pipe fitter at a manufacturing plant. At the time of the accident, the decedent had climbed up onto an overhead crane rail to move existing pipework when the crane struck and killed him. This paper presents the application of various techniques/methodologies to reconstruct the complex accident, including 3D HD scanning, drone video imaging, and 3D modeling/principles of photogrammetry to understand how the incident occurred and provide visualizations of the construction project. Safety analysis was conducted by analyzing crane maintenance and operation as well as the duties/responsibilities of the different employers and comparing industrial standards and practices such as OSHA, ANSI, and safety principles.

Keywords

Overhead crane, 3D high-definition scanning, drone video imaging technology, 3D modeling, visualization, safety, OSHA, ANSI, safety, forensic engineering

Introduction

In 2012, the decedent was working as a pipe fitter with laborers from other contractors in the installation of new and large manufacturing equipment at a paper mill plant in Virginia.

On the day of the accident, one of the contracted companies asked the construction manager for pipework to be relocated so the scaffolding could be installed. The construction manager, who was contracted by the plant owner to supervise the new installation of the equipment, directed the decedent's employer (another contractor involved with the construction project) to relocate the pipework. A cross-beam attached to a structural column was interfering with the relocation of the pipework. The cross-beam, which was located approximately 36 ft above the main floor of the plant, was adjacent to one of the travel tracks/rails of an overhead bridge crane (**Figure 1**). The cross-beam needed to be removed for the pipework to be relocated (**Figure 2**). On the same day, another contractor was operating the crane to move around other equipment/materials in the plant.

As the overhead crane was being operated, the decedent was in the process of removing the cross-beam. As the crane was traveling down the plant on the track/rails, it apparently struck the decedent and dragged him in between the crane and the column that the cross-beam was attached to, crushing him in the process. Witnesses to the accident started yelling at the crane operator to stop the crane. The operator momentarily stopped the crane by

Figure 1
Accident location. Cross-beam to be removed pointed out with a green arrow. Overhead crane in the background pointed out with a blue arrow. Overhead crane rail pointed out with a red arrow.

Richard M. Ziernicki, PhD, PE, 7185 S. Tucson Way, Centennial, CO 80112, 303-925-1900, rziernicki@knottlab.com

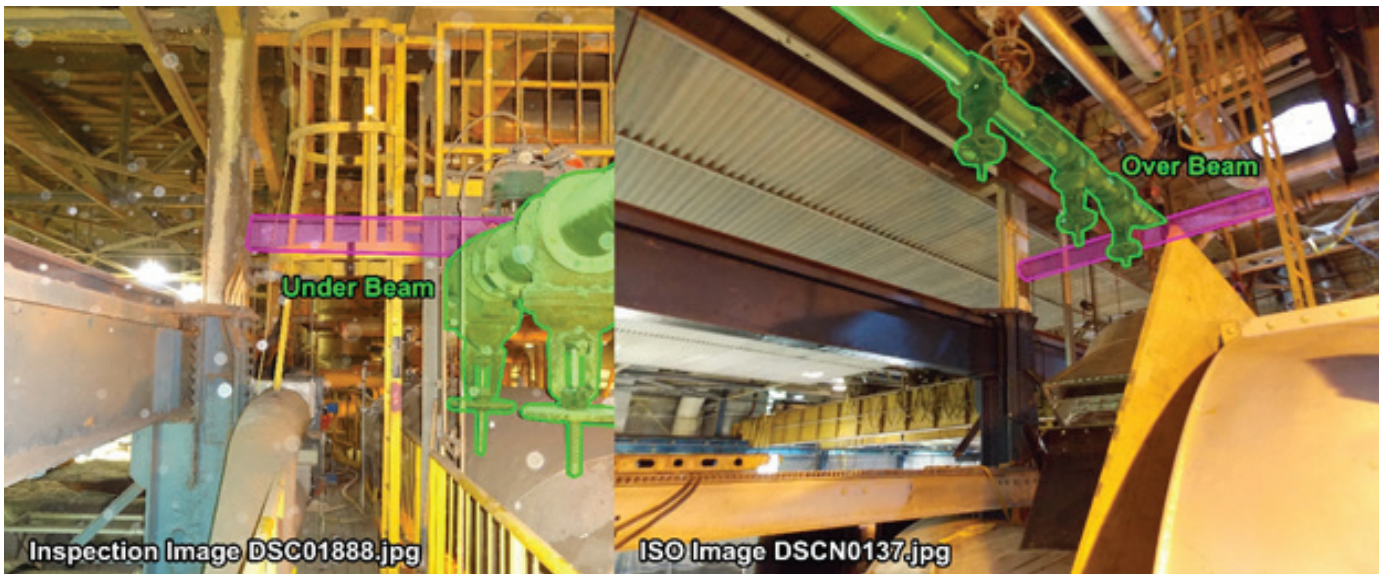

Figure 2
Photographs comparing the location of the pipework and cross-beam after the pipework was relocated (left) and before the pipework was relocated (right). Cross-beam is highlighted in pink; pipework is highlighted in green.

letting go of the controls and was intending to reverse the crane away from the decedent. However, he inadvertently moved the crane forward again instead, further crushing the decedent, who later succumbed to his injuries.

The Virginia Occupational Safety and Health Administration (VOSH) investigated the accident, had the crane tested, and determined that it had too much "drift" after the brakes were applied. The VOSH official determined that based on the testing of the crane's brake system, it should have been taken out of service, and cited the crane/plant owner for operating a crane with a defective brake system. Furthermore, the official found that the parts to fix the brakes were in the plant for some time before the accident, but the plant owner decided to not fix the brakes. The official also found the crane's alarm, which sounds during movement of the crane, was difficult to hear and was ineffective.

In addition, the VOSH official found that the operator was not trained on the crane in question at the time of the accident and was not authorized to operate the crane. Therefore, the crane operator's employer was cited for allowing the operator to operate the crane. The VOSH official also cited the crane operator's employer for failing to properly inspect, notice the brakes were defective, and take the crane out of service for the brake problems.

The plaintiff was the estate of the decedent, and the defendants included the owners of the plant/crane, construction manager, crane operator, and his employer. The purpose of the forensic investigation was to determine whether or not the plaintiff had any contributory negligence in the accident. Virginia law recognizes the pure contributory negligence rule, "which says that a damaged party cannot recover any damages if it is even 1% at fault[1]".

The defendants made claims that the decedent should not have been where he was at the time when he was struck by the crane, that he should have heard and seen the crane coming, and/or that he should have stopped his work and locked out/tagged out the crane from operating before beginning his work.

Methodologies used for this forensic engineering analysis included:

1. Using 3D HD scanning, drone video imaging, analysis of accident scene photographs and 3D modeling of the plant to reconstruct the position of equipment at the time of the incident.

2. Determining the impact location based on physical evidence.

3. Conducting a line-of-sight study to determine whether or not the crane operator could have seen the decedent prior to the accident.

4. Evaluating the maintenance and operation of the crane and the duties/responsibilities of the different contractors by comparing industrial standards

and practices such as from Occupational Safety and Health Administration (OSHA), American National Standards Institute (ANSI), and safety principles.

Reconstructing the Renovation Project in the Plant

It was the manufacturing plant's policy, the crane's operator manual, and the ANSI B30.2 safety standard, "Overhead and Gantry Cranes," that the crane operator must keep the crane's travel track/rails clear of all personnel[2]. The ANSI standard states:

2-3.3.4 Before the lift. Crane Operators shall verify that no worker is on or adjacent to the crane before closing the main switch (Crane Disconnect).

The overhead crane in question was controlled with a remote pendant that extends down from the crane (**Figure 3**) and allows the operator to control the crane from the floor of the plant (also referred to as a "floor-operated" crane). Since the pendant is directly connected to the crane, the operator is required to walk with the crane as the crane is traveling inside the plant. At the same time, the decedent was working 36 ft above the floor.

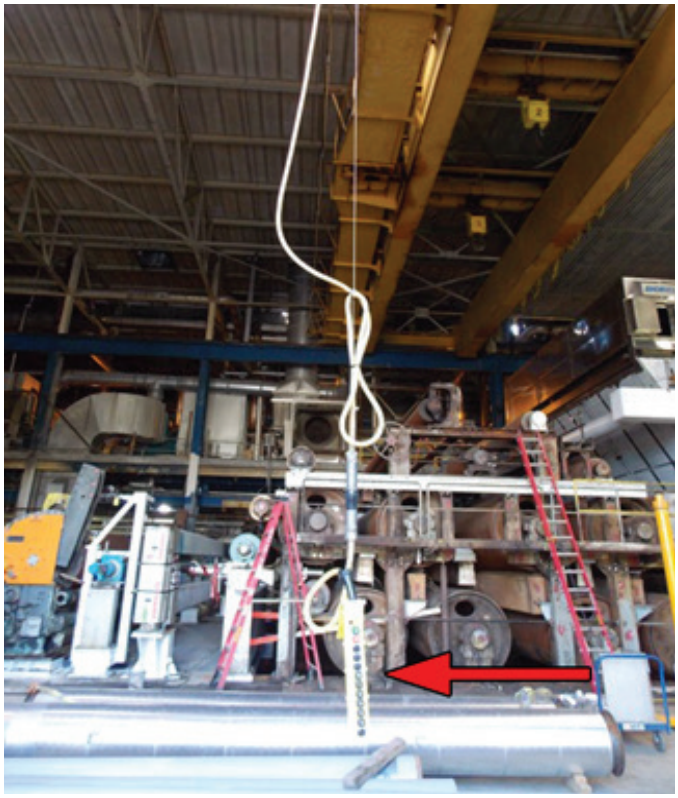

Figure 3
Provided photograph of the overhead crane and remote pendant (pendant point out with a red arrow).

In analyzing this accident, an understanding of the conditions and construction phase of the equipment in the plant at the time of the accident was necessary to determine whether the decedent was observable from the crane operator's point of view. As part of the investigation, the plant was inspected, photographed (**Figure 4**), and was scanned with a high-definition, 3D laser scanner to capture millions of points to define the geometry of the plant and all of the equipment inside the plant. The collected data points were later used to create a 3D point-cloud model of the plant. Due to the size of the plant, the various large machinery/equipment, and limited physical accessibility to various parts of the plant, an aerial drone was flown inside the plant to image and document the equipment. The aerial drone imagery provided information, views, and details that would not be easily accessible to people.

The 3D point cloud model of the plant was then put into a computer-generated virtual 3D space. Since the construction of the large equipment had already been completed at the time of the authors' inspection (years after the accident), photographs taken immediately after the accident by the VOSH official and the construction manager (**Figure 5**) were analyzed to determine which pieces of

Figure 4
Photograph taken during the inspection of the plant.

Figure 5
Provided photograph of the plant taken immediately after the accident.

equipment and construction were present at the time of the accident (such as certain ladders, rails, incomplete ductwork, and pipework, etc.). The equipment and materials, which did not exist at the time of the accident, were then removed from the 3D model of the plant. **Figure 6** demonstrates a 3D model of the plant during the inspection — with the pieces of equipment that did not exist or was constructed at the time of the accident highlighted in green. The photographs were also analyzed to determine which equipment and construction existed at the time of the accident but did not exist at the time of the inspection. Computer-generated 3D models of the equipment and construction were then digitally generated. The placement of the modeled equipment in the 3D virtual space was established using principles of photogrammetry, in conjunction with the 3D point cloud model as a reference[3,4,5,6,7,8]. **Figure 7** shows the added computer-generated 3D models of the equipment and construction, placed in the 3D virtual model of the plant, highlighted in red. **Figure 8** is a graphic of the 3D virtual model of the reconstructed accident scene, matching the conditions and phase of the construction at the time of the accident.

Figure 6
Computer-generated 3D virtual model of the plant at the time of inspection. Equipment and construction, which was not present at the time of the accident, is highlighted in green.

Location of the Crash

After reconstructing the accident scene, the location where the decedent was crushed was determined by analyzing evidence found in photographs and the plant's building plans. Photographs taken immediately after the accident showed evidence of blood on the support column. The location of the support beam in photographs taken immediately after the accident and during the forensic inspection were analyzed to determine the location in the building plans. Principles of photogrammetry were then used to determine the location of the decedent in the 3D virtual model of the reconstructed accident scene (**Figure 9**).

Line-of-Sight Study

After reconstructing the accident scene and determining the location where the decedent was crushed, a line-of-sight study was then performed to determine whether or not the operator would have been able to observe the decedent working near the crane's rail before and during the crane operation. The study spatially analyzed at what points in time the decedent was observable to the crane operator as he was walking with the traveling crane.

Figure 7
Computer-generated 3D models of the equipment and construction that was present at the time of the accident, highlighted in red, added into the accident scene virtual model.

Figure 8
Graphic of the computer-generated, reconstructed accident scene, matching the condition and phase of construction at the time of the accident.

Figure 9
The location where the decedent was crushed, highlighted in red in the reconstructed accident scene.

Figure 10 demonstrates the position of the crane operator and crane, relative to the decedent at a specific point in time. From the line-of-sight study, it was determined that the crane operator would have been able to see the decedent, had the crane operator checked for personnel near the crane's travel tracks/rail before and during crane operation, as required by the ANSI B30.2 standard, the crane operator's manual, and the plant policies.

Figure 11 is a graphic of the reconstructed accident scene from the point of view of the crane operator, showing the decedent was visible to the operator before he operated the crane and for at least 21 seconds before the decedent got crushed, assuming the operator was traveling at an average walking speed. From the line-of-sight study, it was determined that had the crane operator checked for personnel near the crane's travel track/rail, he would have seen the decedent near the crane's travel track/rail,

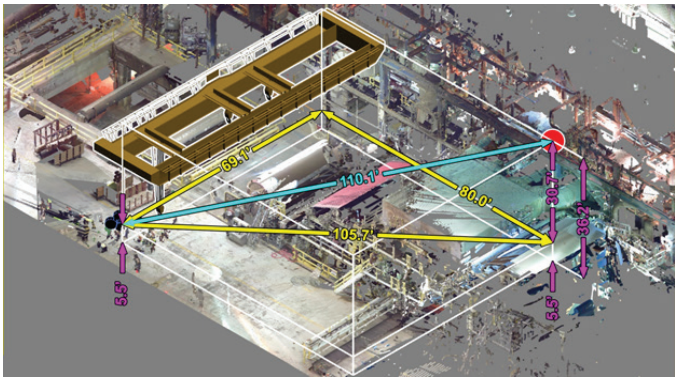

Figure 10
Graphic showing the spatial analysis for the line-of-sight study at a specific point in time. Analysis to determine where the crane operator was spatially located to the decedent.

Figure 11
Graphic showing the reconstructed accident scene from the point of view of the operator 30 seconds before the decedent got crushed. The decedent circled in green.

he would not have operated the crane until the decedent was no longer near the crane rail, and the accident would not have occurred.

Safety Analysis

A safety analysis was conducted by analyzing crane maintenance and operation practices as well as the duties/responsibilities of the different contractors and comparing industrial standards and practices such as OSHA, ANSI, and safety principles.

Improper Work Procedure/Control of Work

The construction manager was the person in charge of the construction project and was (or should have been) aware of all the work that was being done on the day of the accident.

The construction manager tasked the decedent with relocating pipework, knowing that the pipework was near the crane's path of travel and foresaw that the cross-beam that was adjacent to the path of the crane, was going to be removed for the pipework to be relocated. The construction manager also knew the crane was being operated that day. Therefore, knowing that the decedent was working near a crane that was operating that day, the construction manager should have prevented the accident from occurring by using lockout/tagout procedures to prevent the crane from being used, as required by the plant polices and the ANSI B30.2 safety standard, which states:

2-3.8.1(a) A lockout/tagout policy and procedure shall be developed, documented and implemented by the owner

or user of the overhead crane. (c) The policy shall give consideration to the following areas: (7) work to be done other than on a crane but within the path of a crane where its movement creates a hazard.

Furthermore, there was no evidence that the decedent was aware the crane was going to be used that day — and there was no discussion from the construction manager or other contractors in pre-job "toolbox" meetings that the crane was going to be used that day.

Failing to Put Crane Out of Service

The VOSH official tested the crane after the accident, determined the crane had defective brakes, and concluded the crane should have been taken out of service. The plant/crane owner was aware of the crane's brake problems for months. Two months before the accident, the company that was hired to perform monthly inspections of the crane reported to the plant owner that its brake assembly needed to be replaced. Furthermore, the parts to fix the brake assembly were delivered and were in the plant for some time before the day of the accident. However, the plant owner decided to not put the crane out of service until the renovations work was completed — a violation of Title 29, Section 1910.179 of the *Code of Federal of Regulations* (CFR)[9], which states:

(f)(4)(vii) Brakes for stopping the motion of the trolley or bridge shall be of sufficient size to stop the trolley or bridge within a distance in feet equal to 10 percent of full load speed in feet per minute when traveling at full speed with full load.

and the ANSI B30.2 safety standard, which states:

2-1.12.4(a) A power-driven bridge shall be equipped with either a braking means or have a bridge drive frictional characteristics that will provide stopping and holding functions, under conditions where the rails are dry and free of snow and ice, as follows: (1) have torque capability to stop bridge travel within a distance in feet (meters) equal to 10% of rated load speed in ft/min (m/min) when traveling with rated load.

Furthermore, plant owners were also aware (a month before the incident) that the brake's emergency brake system (E-stop) was not working at the time of the accident. The inoperable E-stop is also a violation of section 1910.179 of the CFR, which states:

(f)(6)(iii) On all floor, remote and pulpit-operated crane bridge drives, a brake of noncoasting mechanical drive shall be provided.

And ANSI B30.2 safety standard, which states:

2-1.12.5(k) When provided an emergency brake shall stop trolley or bridge travel in accordance with the requirements of para. 2-1.12.3(a)(1) or para, 2-1.12.4(a)(1)

Had the crane been taken out of service for the defective brake systems, as required by the CFR and ANSI standard, the crane would not have been in operation — and the accident would not have occurred.

Crane Operator Responsibility

At the time of the accident, the crane operator was not trained nor was he authorized to operate the crane, as required by Section 1910.179 of the CFR, ANSI B30.2 safety standard and the plant policies. The crane operator's unfamiliarity with the crane in question is based upon the several fatal errors he made, which resulted in the death of the decedent. The errors included:

- He did not make sure the crane's track/rail was clear as required by ANSI B30.2 and the plant policy.
- He stopped the crane by letting go of the controls, instead of using the E-stop or plugging (by reversing) to more effectively stop the crane.
- After personnel yelled at him to stop the crane and move it back, he moved the crane forward, toward the decedent, instead of reversing it away from the decedent.

Furthermore, the crane operator's employer did not properly inspect the crane before using the crane as required by section 1910.179 of the CFR, which states:

(j)(2) Frequent inspection. The following items shall be inspected for defects at intervals as defined in paragraph (j)(1)(ii) of this section or as specifically indicated, including observation during operation for any defects which might appear between regular inspections. All deficiencies such as listed shall be carefully examined and determination made as to whether they constitute a safety hazard: All functional operating mechanisms for maladjustment interfering with proper operation. Daily.

Had the crane been properly inspected before the

crane was operated as required by CFR, the problems with the crane's brake system would have been observed, and the crane would have been taken out of service. Had this occurred, the crane would not have been used, and the accident would not have occurred.

Decedent's Contribution

The defendants made claims that the decedent should not have been where he was at the time when he was struck by the crane. As discussed earlier, the construction manager put the decedent in a dangerous location by tasking him to work near the crane's path of travel and allowing the crane to be used at the time of the accident. Furthermore, there was no evidence that the decedent was aware the crane was going to be used that day. There was no discussion from the construction manager nor from other contractors in pre-job "toolbox" meetings that the crane was going to be used that day.

The defendants claimed that the decedent should have heard and seen the crane coming. The VOSH official found the crane's travel alarm was ineffective for the decedent to hear the approaching crane. In addition, the decedent was doing the job he was tasked to do and was not aware that the crane was going to be in operation that day.

The defendants claimed that the decedent should have locked out the crane from operating before beginning his work. However, the decedent was not a trained crane operator and had never used the crane in question. Furthermore, he was not aware that the crane was going to be used that day. In summary, the authors concluded that the decedent had no contribution to the accident.

Conclusion

The case study presents an analysis and investigation of a complex accident at a manufacturing plant that had significant changes to its conditions and construction years after the accident occurred. The case study presents techniques/methodologies to reconstruct the accident site using the following technologies and techniques:

1. Reconstruction of the accident scene

To reconstruct the accident scene, 3D high-definition laser scanning and aerial drone imagery were used to document the manufacturing plant. This data was then used to create a computer-generated 3D model of the plant. Photographs taken immediately after the accident were analyzed, and principles of photogrammetry were used to determine which equipment and construction materials did not exist at the time of the accident, so the objects could be removed from the 3D model of the plant. 3D modeling and principles of photogrammetry were then used to create a digital 3D representation of equipment and the phase of construction at the time of the accident.

2. Line-of-sight study

After the accident scene was reconstructed, a line-of-sight analysis was performed to determine that the decedent was visible to the crane operator before and during the operation of the crane.

3. Safety analysis.

A safety analysis was conducted by analyzing crane maintenance and operation practices as well as the duties/responsibilities of the different employers and comparing industrial standards and practices such as OSHA, ANSI and safety principles. Based on the analysis, it was determined the plant owner, construction manager, the crane operator and his employer all contributed to the accident and the decedent had no contribution to the accident.

In closing, the plaintiff's attorneys held three mock trials with jury focus groups. The focus group members soundly rejected the contributory negligence and lack of primary negligence and causation defenses, which helped with the mediation in the case. The focus group also found the 3D visualizations to be especially helpful as it provided a complete and accurate visual account of the accident scene and how the accident happened. One month before trial was scheduled to commence, the case ended with a non-confidential out-of-court settlement for $4.7 million. Furthermore, details of the case were published in an article for the *Virginia Lawyer Weekly*[10].

References:

1. G. Wickert, "Understanding Comparative Fault, Contributory Negligence, and Joint and Several Liability", Matthiesen, Wickert & Lehrer S.C., 2013. [Online]. Available: https://www.mwl-law.com/understanding-comparative-fault-contributory-negligence-and-joint-and-several-liability/. [Accessed: 07- Jun- 2019].

2. Overhead and Gantry Cranes, ANSI B30.2. 2011.

3. K. Breen and C. Anderson, "The Application of Photogrammetry to Accident Reconstruction," SAE Technical Paper Series, 1986, Paper no. 861422.

4. M. Callahan, B. LeBlanc, R. Vreeland, and G.

Bretting. “Close-Range Photogrammetry with Laser Scan Point Clouds,” SAE Technical Paper Series, 2012, Paper no. 2012-01-0607.

5. C. Coleman, D. Tandy, J Colborn, and N. Ault, “Applying Camera Matching Methods to Laser Scanned Three Dimensional Scene Data with Comparisons to Other Methods,” SAE Technical Paper Series, 2015, Paper no. 2015-01-1416.

6. S. Fenton and R. Kerr, “Accident Scene Diagramming Using New Photogrammetric Technique,” SAE Technical Paper Series, 1997, Paper no. 970944.

7. R. Ziernicki and D. Danaher, “Forensic Engineering Use of Computer Animations and Graphics.” Journal of the National Academy of Forensic Engineers, Vol. 23, No. 2, pp. 1-9. Dec. 2006.

8. D. Danaher and R. Ziernicki, “Forensic Engineering Evaluation of Physical Evidence in Accident Reconstruction,” Journal of the National Academy of Forensic Engineers, Vol. 24, No. 2, Dec., pp. 1-10, 2007.

9. Code of Federal Regulations Title 29 Part 1910 Section 179 (29CFR1910.178), Overhead and gantry cranes.

10. “Family of man killed in plant conversion settles for $4.7M – $4.7 Million Settlement”, Virginia Lawyers Weekly, 2019. [Online]. Available: https://valawyersweekly.com/2018/10/09/family-of-man-killed-in-plant-conversion-settles-for-4-7m-4-7-million-settlement/. [Accessed: 20-Jun- 2019].

Metallurgical and Mechanical Failure Analysis of an Aftermarket Flywheel

By Nikhil Kar, PhD, PE (NAFE 1095M)

Abstract

A failure analysis investigation was performed on the remnants of an aftermarket gray cast iron flywheel that catastrophically fractured during operation in a vehicle after 24 miles of operation. Light microscopy, 3D X-ray micro-computed tomography (micro-CT), scanning electron microscopy (SEM), metallography, and hardness/tensile testing techniques were utilized to characterize manufacturing quality, mode(s) of failure, microstructural variation, fracture surfaces, and mechanical properties of the failed component. Light microscopy examination of the remnant surfaces showed that the flywheel shattered with signs of radial heat checking fissure cracks. A metallurgical examination of the flywheel showed that it was manufactured from cast gray iron, with evidence of microstructural changes near heat-affected zones from graphite flakes in a ferrite/pearlite matrix to needle and lath formations similar to bainite or martensitic phases. The CT scan slices and fracture surface examination in the SEM showed signs of porosity and dendritic formations along a fracture surface believed to be the crack initiation location. The analysis suggests manufacturing flaws found within the flywheel were a likely contributing factor leading to premature failure during service. A review of original equipment manufacturer (OEM) flywheel material specifications showed that the OEM flywheel was manufactured out of ductile nodular iron with significantly higher tensile strength and ductility, an indication that the failed aftermarket flywheel product was not manufactured to meet or exceed OEM specifications.

Keywords

Gray cast ion, fissure cracks, porosity, dendrites, manufacturing flaws

Introduction

Due to ease and low price of manufacturing cast parts, many companies look overseas to various foundries for reverse engineering and aftermarket product development for replacement components that are to be used in classic U.S. muscle cars. This is primarily because U.S. car manufacturers (such as Ford and Chevrolet) no longer support or manufacture OEM parts for these vehicles, and they do not make OEM specifications available (as their designs are considered proprietary and not available to the general public).

Gray cast iron is used in many automotive applications, including camshafts, spring gears, and flywheels. While there are a number of publications related to failure analysis of various vehicle components and flywheels that have been in service for an extended period of time, this paper analyzes the failure of a cast gray iron flywheel that occurred only after 24 miles, using forensic metallurgical and mechanical techniques including microscopy, metallography, 3D X-ray computed tomography, and scanning electron microscopy.

A review of the literature has shown that Dellinger et al. analyzed a cracked plain carbon steel flex plate from a 1978 Oldsmobile custom cruiser station wagon that had been driven in excess of 200,000 miles and found evidence of a fatigue failure[1]. Becker and Shipley identified microporosity as a major contributing factor in the cracking of a cast gray iron cylinder head[2]. Casting stresses have also been found to cause premature cracking in gray cast iron crank cases[3] due to excessive or rapid cooling during the casting process. Hou and Jiang performed an investigation on an engine crankshaft that suddenly fractured, and they concluded the failure occurred in the ductile iron due to fatigue from bending and twisting with

Nikhil Kar, PhD, PE, 2528 W. Woodland Dr., Anaheim, CA 92801-2636, 714-527-7100, nikhil.kar@karslab.com

Figure 1a
Overall photograph of fractured flywheel showing side that would mate to crankshaft. Note crankshaft seal outline near center hub.

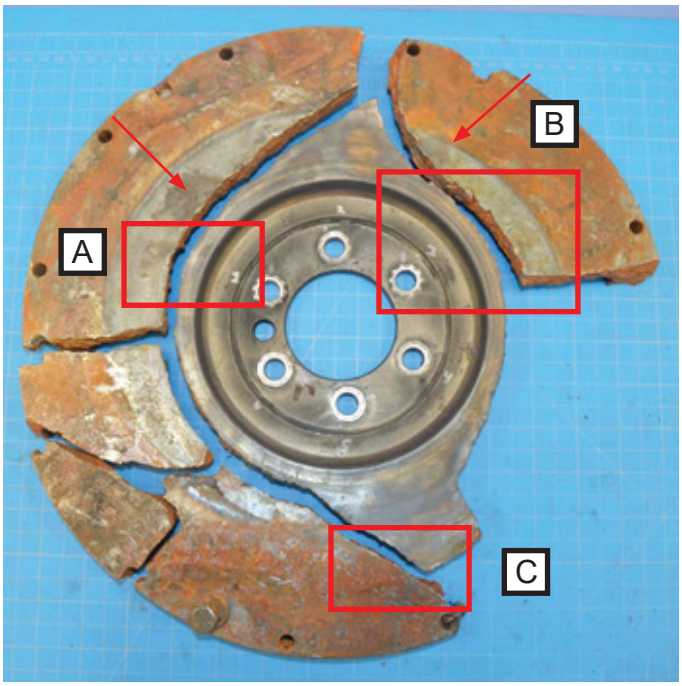

Figure 1b
Overall photograph of fractured flywheel showing side that would mate with clutch disk surface. Note heat damage to areas A, B, and C.

cracks originating at subsurface shrinkage[4]. Computed tomography has been used to characterize defects in castings[5], and has been shown to have excellent sensitivity in revealing casting defects.

Background

An aftermarket replacement flywheel that was advertised as meeting or exceeding OEM specifications was used in a vehicle conversion from an automatic transmission to a four-speed manual transmission. The transition and installation occurred over a period of a week, and the vehicle was driven for 24 miles prior to catastrophic fracture and failure of the flywheel based on a forensic investigation. The flywheel fractured into multiple components when the vehicle was in neutral, and the engine was being revved to 3,500 rpm for 3 to 5 seconds.

Figure 1 shows two photos of the remnant portions of the flywheel that were collected after the incident occurred. **Figure 1a** shows the side of the flywheel that would face the crankshaft; **Figure 1b** shows the side that would make contact with the clutch disk when the clutch pedal is disengaged in neutral or in gear. The flywheel was manufactured at an overseas foundry using a casting process with appropriate dimensions for the application and was routinely sold at automotive retailers that provide aftermarket parts to older vehicles when OEM parts are not available.

Findings

Fractography

Macroscopic inspection photographs of the fracture surface are shown in **Figure 2** at locations A, B, and C as indicated in **Figure 1**. These surfaces show heat tinting, discoloration, and radial fissure cracks on the side of the flywheel that would make contact with the clutch pad disk. The central portion of the remnant flywheel containing the bolt holes for mounting the flywheel to the crankshaft had a complete circumferential fracture surface that was examined in detail using visual examination, optical microscopy, and scanning electron microscopy techniques. Location C was unique, as it was the only area that contained both radial and circumferential fracture surfaces, as shown in **Figure 2c**.

An end-on photograph of the circumferential fracture surface at location C is shown in **Figure 3a**. The majority of the fracture surface appears dull, with a small band of a shiny fracture surface near the lower left and lower right region. SEM examination in the dull location as shown in **Figure 3b** shows that the dull surface was comprised of dendrites, porosity, and material that was not fractured, but rather it was liquid that solidified and did not fuse with any other material when casting of the flywheel occurred. The figure shows the surface contains dendrites, an indication that this entire surface separated and contained porosity; a

Figure 2a
Close-up photomicrograph in location A shows heat tinting and fissure cracks.

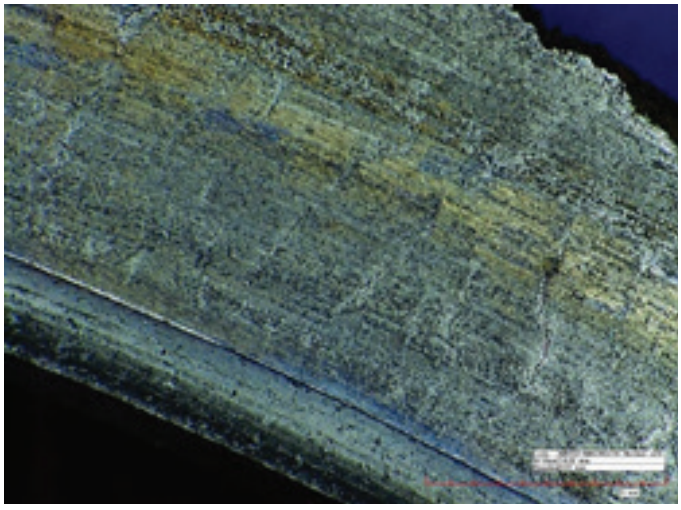

Figure 2b
Close-up photomicrograph in location B shows heat tinting and fissure cracks.

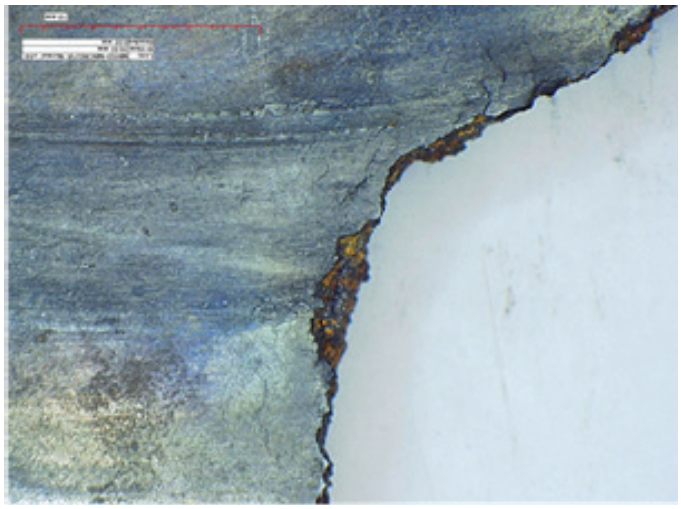

Figure 2c
Close up photomicrograph in location C shows heat tinting and fissure cracks.

Figure 3a
End on view of location C shows dull fracture surface.

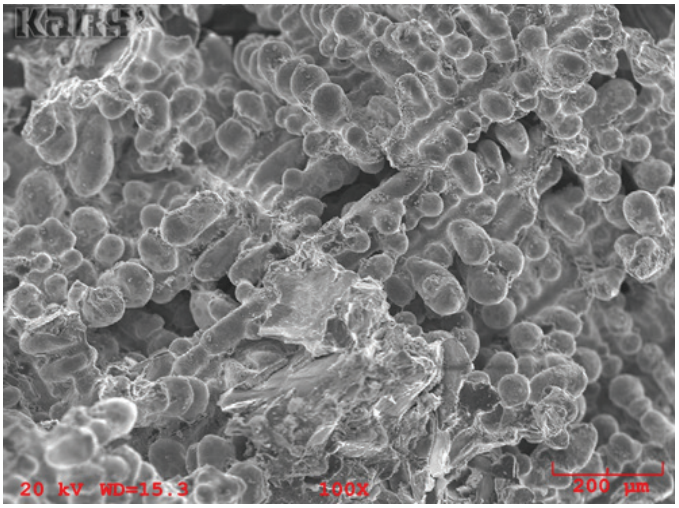

Figure 3b
High magnification SEM image in dull fracture surface area shows dendrites and solidified droplets that were not fractured.

likely initiation site that led to catastrophic failure of the entire flywheel. While all castings may contain some level of porosity that is generated due to internal gas entrapment and material shrinkage during solidification, it is important to identify and quantify the amount of porosity from a manufacturing quality standpoint.

Computed Tomography

The location and appearance of porosity and dendrites where fracture initiation occurred was suitable for 3D X-ray computed tomography, as it could be used to understand the distribution and location of the porosity. 3D X-ray computed tomography is a non-destructive inspection technique that uses high-energy X-rays to create thousands of radiographic images of a sample as it rotates about a central axis. A computer algorithm is then used to combine the radiographic images that generate a 3D model that can be sliced in software to reveal internal structural details of

any material.

Figure 4a shows the location of area C in the flywheel and the reference CT slice data in **Figure 4b**. **Figure 5**, a magnified CT slice view of area C, indicates that the porosity envelopes the entire width of the fracture surface, which is 1.6 in. in length.

Figure 6 shows a CT slice transverse view of location C, an indication to the depth of the porosity, which was measured to be 0.4 in. deep. The slices provide information regarding the amount of porosity and proximal location to the fracture surface, which cannot be seen using visual microscopic techniques. The CT analysis of this area shows casting flaws, and metallography was performed in this area to understand the microstructural differences in the flywheel at such locations.

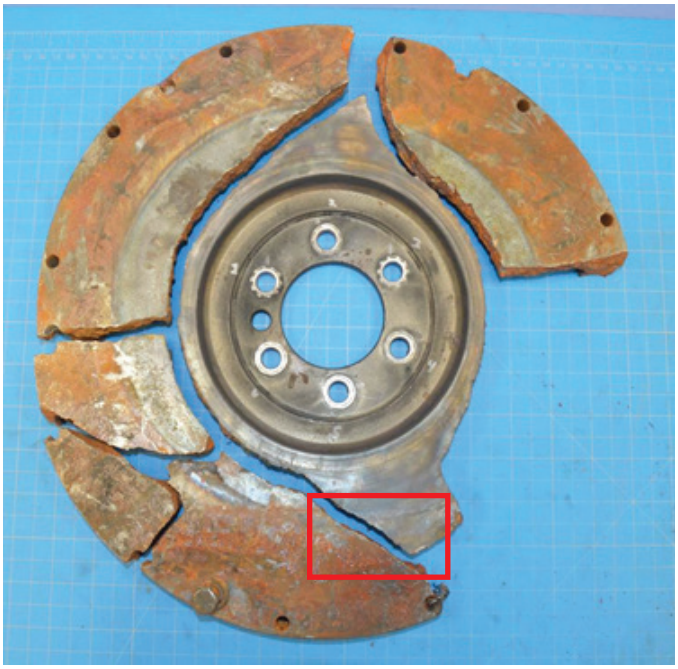

Figure 4a
Overall view of flywheel remnants and location for computed tomography.

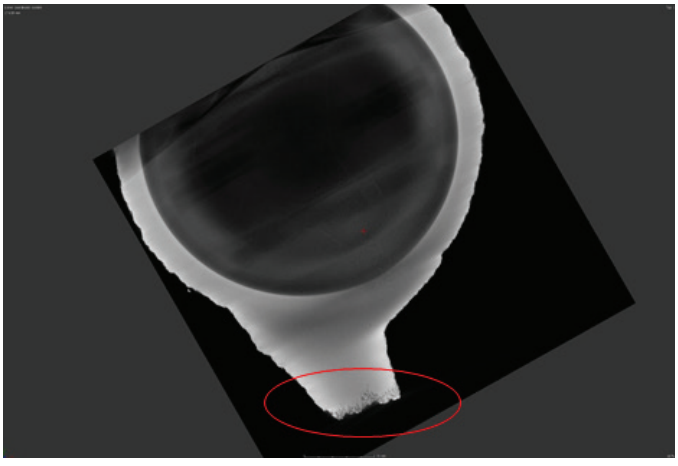

Figure 4b
CT slice shows no porosity except near fracture surface as indicated.

Metallography and Microstructure

Figure 7 contains three photomicrographs obtained from representative areas in the flywheel that characterize the base cast gray iron microstructure, microstructural changes due to heat/temperature exposure, and metallurgical deficiencies due to casting. **Figure 7a** shows that the base microstructure is consistent with gray cast iron, containing graphite flakes in a matrix of ferrite and pearlite grains. **Figure 7b** shows that in the heat-affected zone, the gray cast iron has transformed into different phases of needle and lath type structures similar to bainite or martensite. Metallurgical deficiencies in the form of dendrites

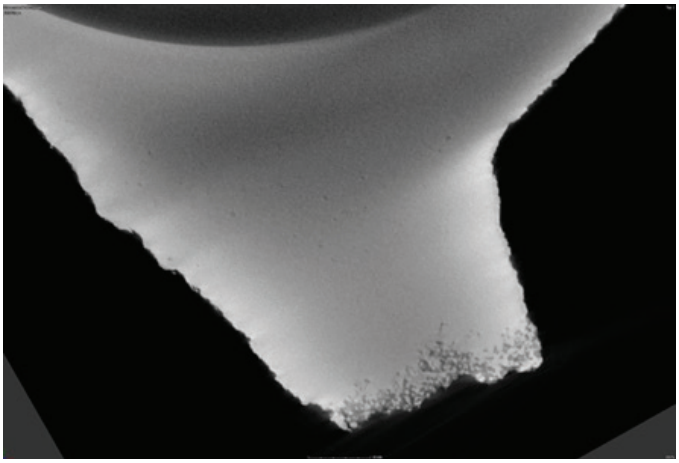

Figure 5
High magnification CT slice shows porosity and dendrites along fracture surface location.

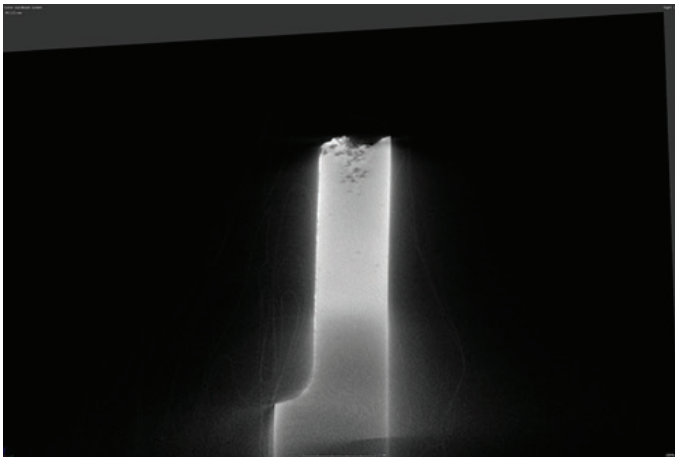

Figure 6
High magnification transverse CT slice shows porosity depth and dendrites along fracture surface.

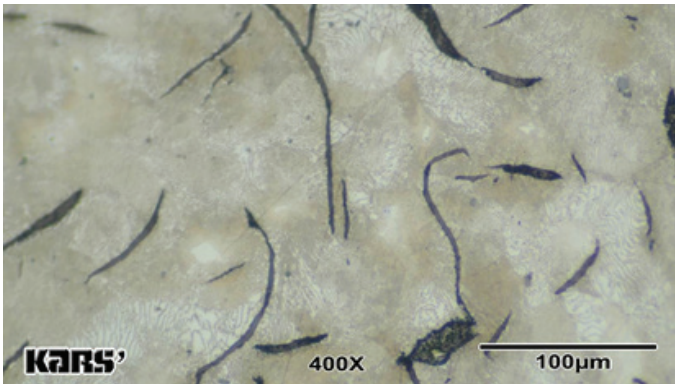

Figure 7a
Photomicrograph of base cast gray iron microstructure shows ferrite pearlite matrix with graphite flakes.

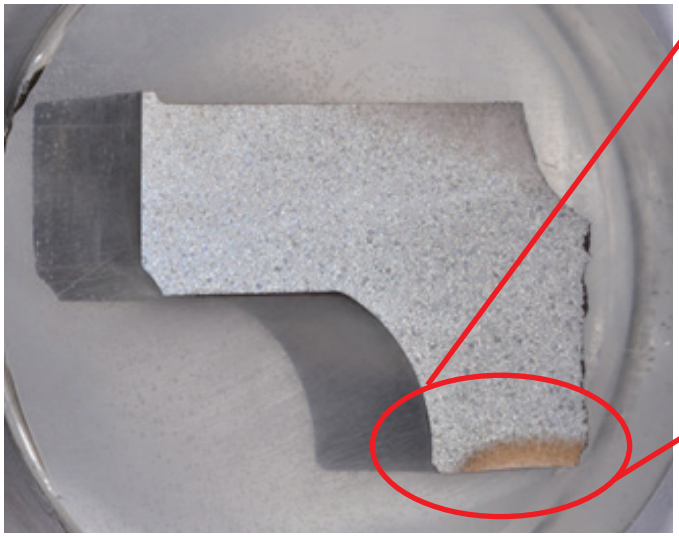

Figure 7b
Photomicrograph of heat-affected zone shows fissure cracks and microstructural changes to include needle and lath features similar to bainite or martensite phases. Photomicrograph of base cast gray iron microstructure shows ferrite pearlite matrix with graphite flakes.

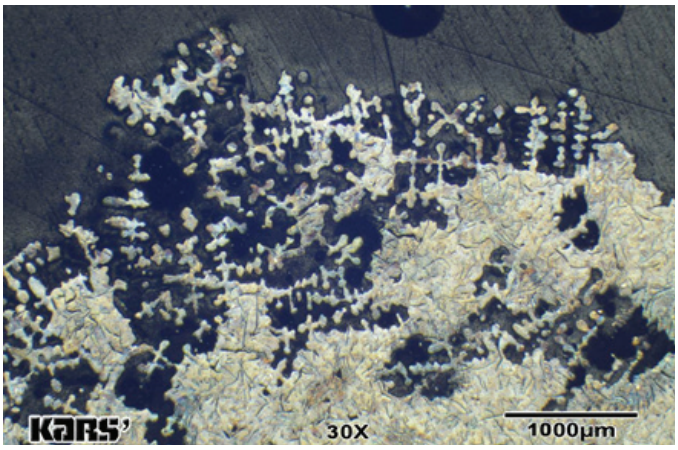

Figure 7c
Photomicrograph shows casting porosity and dendrites, indicating poor casting procedures.

and porosity due to rapid solidification and shrinkage during casting are shown in **Figure 7c**. This cross section was taken from area C as discussed in **Figure 3** and **4**. These areas were found on, and within the radial and circumferential fracture surface (Area 3), where it is believed the failure initiated.

Mechanical Testing

Sub-specimen flat dogbone tensile coupons consistent with ASTM E8 were machined away from the heat-affected zone in the subject flywheel to determine mechanical properties, the results of which are shown in **Figure 8** and **Figure 9**. These results confirm that the material was manufactured from gray cast iron with a tensile strength similar to that of SAE G3500 (35 KSI) and

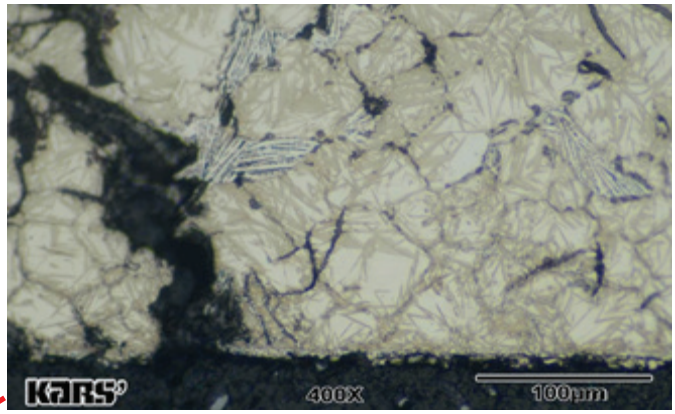

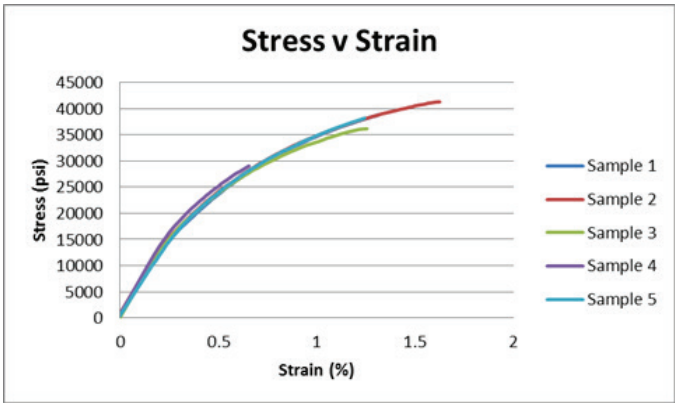

Figure 8
Tensile stress versus elongation of five tensile coupons machined from failed flywheel away from heat affected zone.

hardness of 215 HRB. Similar testing was performed on an OEM flywheel, and the testing results showed the OEM flywheel was manufactured out of ASTM A536 ductile iron with a tensile strength of 80 KSI, a yield strength of 55 KSI and an elongation of 6%. Gray cast iron materials are brittle, and — when subject to metallurgical defects — heat and substantive stresses rapid and catastrophic fracture can occur.

Sample	Gage Length (in)	Width (in)	Thickness (in)	Area (in^2)	Maximum Load (lbf)	UTS (psi)	Elongation at Fracture (%)
1	1	0.1322	0.0644	0.00851368	338.77	39791.25	1.422499958
2	1	0.1272	0.062	0.0078864	325.74	41304.02	1.62499994
3	1	0.1309	0.061	0.0079849	288.73	36159.5	1.25500001
4	1	0.1289	0.063	0.0081207	315.55	38857.49	1.397500001
5	1	0.1339	0.0643	0.00860977	350.1	40663.11	1.489999983
						39355.07	1.437999979

Figure 9
Tabulated stress strain data.

Discussion

The failure analysis investigation on the fractured flywheel showed three important metallurgical and material factors contributed to the catastrophic failure shortly after installation. Evidence of heat and temperature generated microstructural changes led to the formation of radial surface fissure cracks along a circumferential area where the clutch disk engaged the flywheel.

While the formation of heat check cracks can occur in flywheels, the rapid propagation and growth of the surface generated cracks is more susceptible in cast gray iron flywheels due to its inherent brittle nature due to graphite flakes in the microstructure, low ductility and low toughness. Localized porosity was found along the fracture surface. Rapid propagation and growth of the surface cracks allowed for catastrophic fracture of the flywheel.

Testing data shows that the fractured flywheel did not meet or exceed OEM specifications, lacking sufficient yield strength, had 60% lower tensile strength when compared to the OEM product and had 1% elongation versus 6% elongation of the OEM product. The lack of performance and sub-standard material selection of cast iron grade flywheels is noted in the racing industry, as SFI Foundation Inc. – Quality Assurance Specifications Specification 1.1 indicates no racing flywheel can be manufactured out of cast iron due its low strength, ductility and toughness.

Had the fractured flywheel been adequately designed or manufactured without casting deficiencies, or alternate material selection, it would have been able to resist crack propagation and growth of the heat fissure cracks generated due to clutch engagement. If the failed flywheel were manufactured out of ductile iron like the OEM flywheel, it is likely that a different mode of failure would have occurred where deformation or significant warping of the flywheel would have given the vehicle operators an indication that a failure was occurring, and catastrophic fracture would likely not have occurred.

Conclusion

An investigation was performed on an aftermarket replacement flywheel that failed after 24 miles of use. The author's findings suggest significant metallurgical deficiencies in the form of porosity and dendrites contributed to the premature failure of the flywheel when exposed to temperature loading during use. Microstructural changes and heat tinting occurred in the cast gray iron material, and a review of the literature has shown that OEM specifications for this vehicle application call for a ductile nodular iron grade of material.

References

1. D. Dellinger, "Case C: A Cracked Automobile Flywheel Flex Plate," Failure Analysis of Engineering Materials, pp 483 – 491, 2002.

2. W. Becker and R Shipley, "Example 1: Cracking in a Gray-Iron Cylinder Head Caused by Microporosity," in ASM Handbook Volume 11 Failure Analysis and Prevention. ASM International, 2002, pp. 112-113.

3. E. Unterweiser, "Example 11: Cracking in a Gray-Iron Cylinder Blocks Caused by Casting Stresses," in ASM Handbook Volume 11 Failure Analysis and Prevention. ASM International, 2002, pp. 134-135.

4. X. Hou, Y. Li, and T. Jiang, "Fracture Failure Analysis of Ductile Cast Iron Crankshaft in a Vehicle Engine," Journal of Failure Analysis and Prevention, vol. 11-1 pp. 10-16, 2011.

5. R. Bossi, J. Cline, E. Costello, and B Knutson, "X-ray Computed Tomography of Castings," Wright Research and Development Center, Interim Report fr Period April 1989- September 1989.

Acknowledgements

I acknowledge and thank the technical staff at Kars' Advanced Materials, Inc. for their discussions and assistance.

Forensic Engineering Investigation of a Pipe Joint Tester Explosion

By William Keefe, PE, (NAFE 481M)

Abstract

A construction laborer was killed while operating a pipe joint tester, which was used to test joints between sections of newly installed sewer pipe. The joint tester contained a donut-shaped rubber bladder, which was inflated with compressed air to seal against the inside of the pipe joint during the test. During a pipe joint test, the pipe joint tester bladder exploded without warning. The joint tester operator was fatally injured when he was struck by pipe joint tester components and the air blast. A forensic engineering investigation was conducted to determine the role of the design and construction of the pipe joint tester in the cause of the incident.

Keywords

Forensic engineer, pipe joint tester, compressed air hazard, stored energy, safety hierarchy, air pressure regulator, pressure relief valve

Pipe Joint Tester

The pipe joint tester involved in this incident was intended to leak test pipe joints by applying pressurized air to the interior side of the pipe joint. The joint tester could also be used to test pipe joints with pressurized water instead of pressurized air. The pipe involved in this incident was a glass-fiber-reinforced polymer mortar pipe meeting ASTM D3262 – 16 *Standard Specifications for "Fiberglass" (Glass-Fiber-Reinforced Thermosetting-Resin) Sewer Pipe*[1]. The test procedure was similar to the procedure contained in ASTM C1103-14, *Standard Practice for Acceptance Testing of Installed Precast Concrete Pipe Sewer Lines*[2]. There was no equipment specific standard for the pipe joint tester.

The joint tester consisted of an aluminum cylindrical frame with an externally mounted rubber bladder. The aluminum frame was equipped with wheels to permit it to be moved through the interior of a pipe from joint to joint. The wheels were adjustable and arranged to position the joint tester frame at the center of the pipe diameter.

The inflatable rubber bladder was a donut-shaped component. When inflated with compressed air, it expanded to fill the space between the joint tester frame and the inside diameter of the pipe. This was intended to create a seal around the entire inner circumference of the pipe joint. The compressed air inlet connection for the bladder was located on the inside diameter of the joist tester frame near the bottom of the frame. This connection was a female quick-disconnect fitting.

Two telescoping air supply pipes extended from the inner diameter of the joist tester frame to the outer circumference of the bladder. This allowed a separate source of compressed air to be introduced into the annular space at the pipe joint between the outer surface of the pressurized bladder and the inner surface of the pipes. This annular space was referred to as the test cavity. One test cavity air supply connection was located at the upper center of the joint tester; the other was located at the lower center of the joint tester. The upper connection was used to supply compressed air or water to the test cavity and was equipped with a male quick-disconnect fitting. The lower connection was equipped with a ball valve and was used to bleed air out of the test cavity (**Figure 1**).

The outer diameter of the pipe joint tester frame was 44 in., and the frame was 24 in. long (parallel to pipe axis). This model tester was intended to be operated in a pipe with an inside diameter ranging from 48 in. to 54 in. Two pairs of transport wheels were mounted on steel channels attached to the lower portion of the inner diameter of the frame. The weight of the joint tester with the transport wheels was about 340 lb. **Figures 2** and **3** show end and side views of the pipe joint tester positioned in a 54-in. diameter pipe.

William Keefe, PE, 1144 Ensell Road, Lake Zurich, IL 60047, 847-922-3646, keefe@hkleng.com

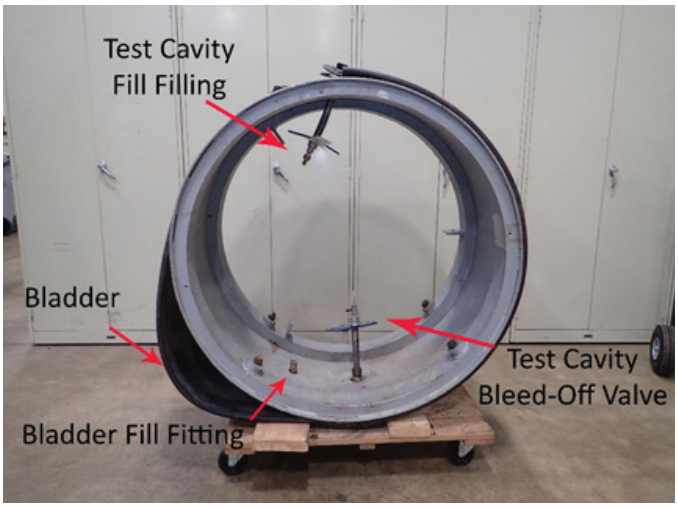

Figure 1
Damaged pipe joint tester (post-incident).

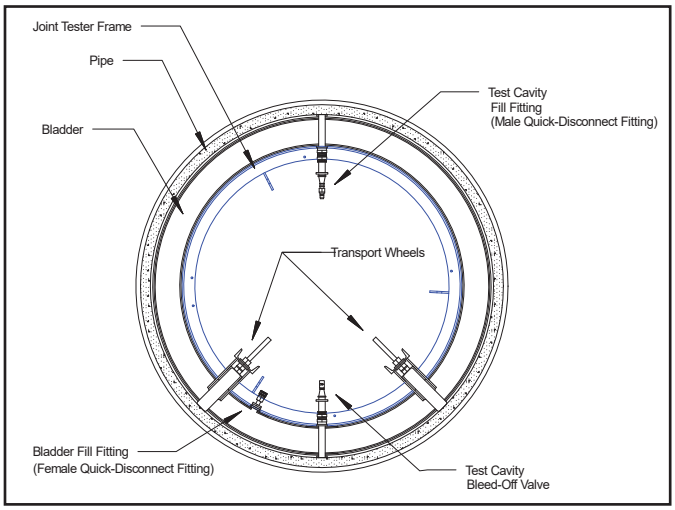

Figure 2
End view of joint tester in 54-in. pipe.

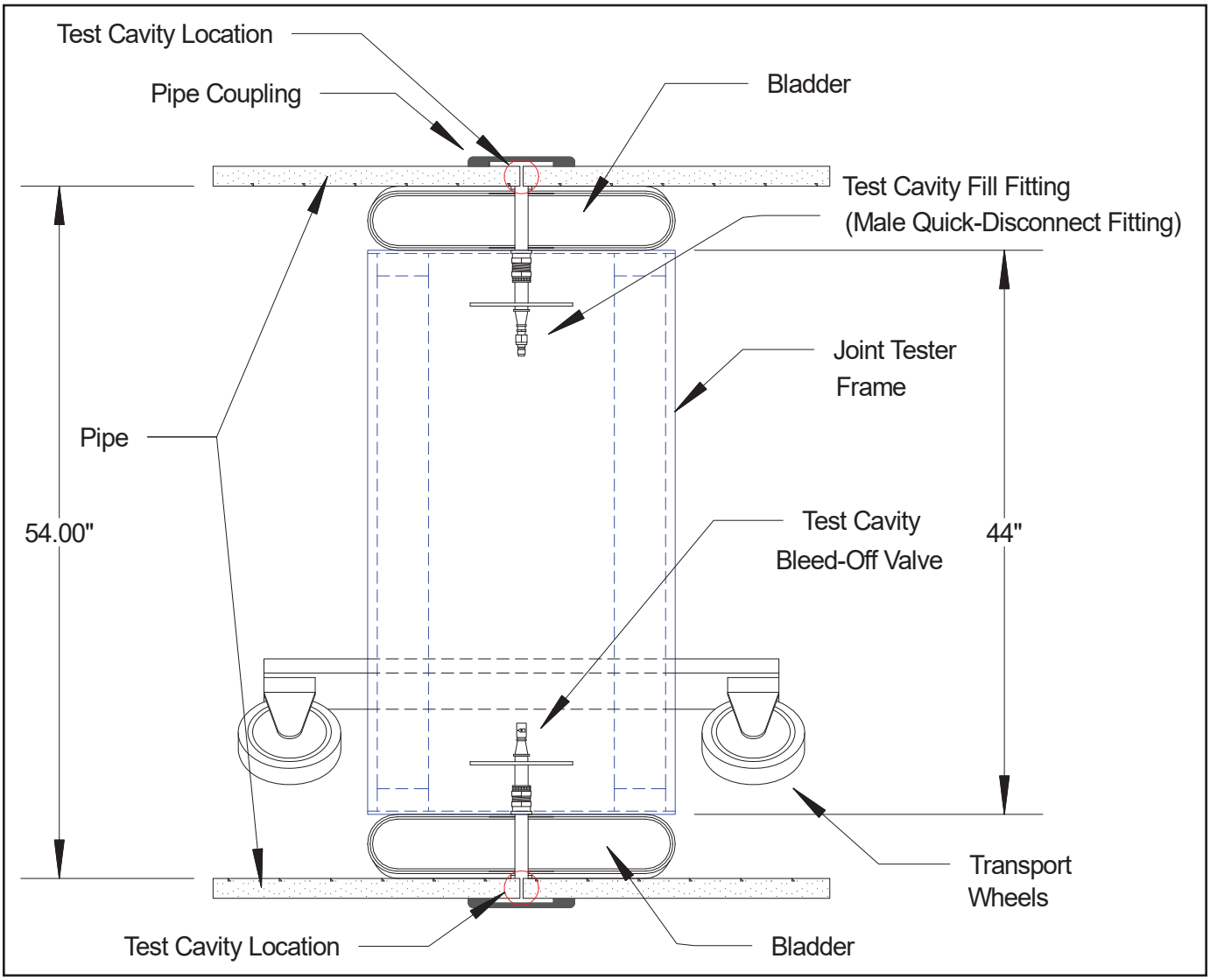

Figure 3
Side view of joint tester in 54-in. pipe.

Figure 4
Control panel.

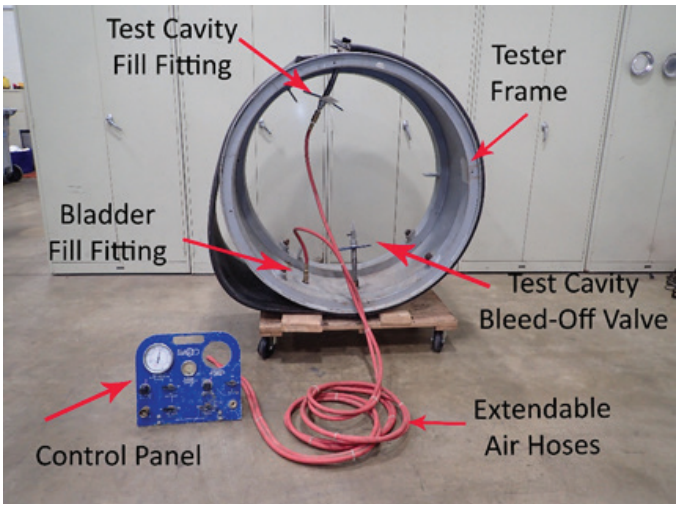

Figure 5
Control panel attached to tester (post-incident damaged condition).

The joint tester was operated from a portable control panel assembly (**Figure 4**), which contained separate control circuits for the bladder and test cavity. The bladder control circuit included a bladder air pressure regulator, an adjustable pressure relief valve, a three-way control valve (fill/off/out), and a bladder air pressure gauge. The test cavity control circuit included a test cavity air pressure regulator, a three-way control valve (fill/off/out), and a test cavity air pressure gauge. The test cavity control circuit did not contain a pressure relief valve. The test cavity circuit also contained controls utilized for the water testing.

When set up for operation, a source of compressed air was attached to a male quick-disconnect fitting on the control panel. That single source of compressed air served both the bladder and test cavity circuits. Separate air hoses extended from the control panel to the joint tester. Each hose was about 20 ft long, and the outlet ends were equipped with quick disconnect fittings to connect to the joint tester. The outlet of bladder supply hose contained a male disconnect fitting, and the outlet of the test cavity supply hose contained a female disconnect fitting. This prevented incorrect connection of the control panel to the tester. The two air hoses were grouped together with plastic wire ties (**Figure 5**). The hoses permitted the bladder and test chamber to be inflated and emptied with the control panel up to about 17 ft away from the tester frame. **Figure 6** shows the joint tester air control schematic.

The test chamber pressure required for a pipe joint test was obtained from the project specifications. When performing the test, the manufacturer of the pipe joint tester recommended inflating the bladder to 50 psi over the desired test chamber pressure not to exceed 150 psi. The bladder and test chamber pressures were adjusted using the control panel pressure regulators. The step-by step procedure used to test pipe joints was generally as follows:

1. After placing the pipe joint tester in the pipe, the transport wheels were adjusted to center the pipe joint tester frame within the pipe.

2. The pipe joint tester was rolled into position over a pipe joint and positioned so that the circumferential centerline of the pipe joint tester was aligned with the pipe joint.

3. The bladder was inflated to the required pressure.

4. The test cavity was then pressurized to the required test pressure. In order to verify that the tester was centered over the pipe joint, the operator would momentarily open the test cavity bleed-off valve.

5. After closing the bleed-off valve and the test cavity air supply valve, the test cavity pressure was monitored over a short time interval. The pipe joint test was successful when the test chamber pressure drop was less than the maximum permitted within the specified time interval. The manufacturer's specification sheet for the pipe joint tester stated: "If the pressure in the cavity holds or drops less than 1 PSIG in 5 seconds, the pipe joint shall be found to be acceptable."

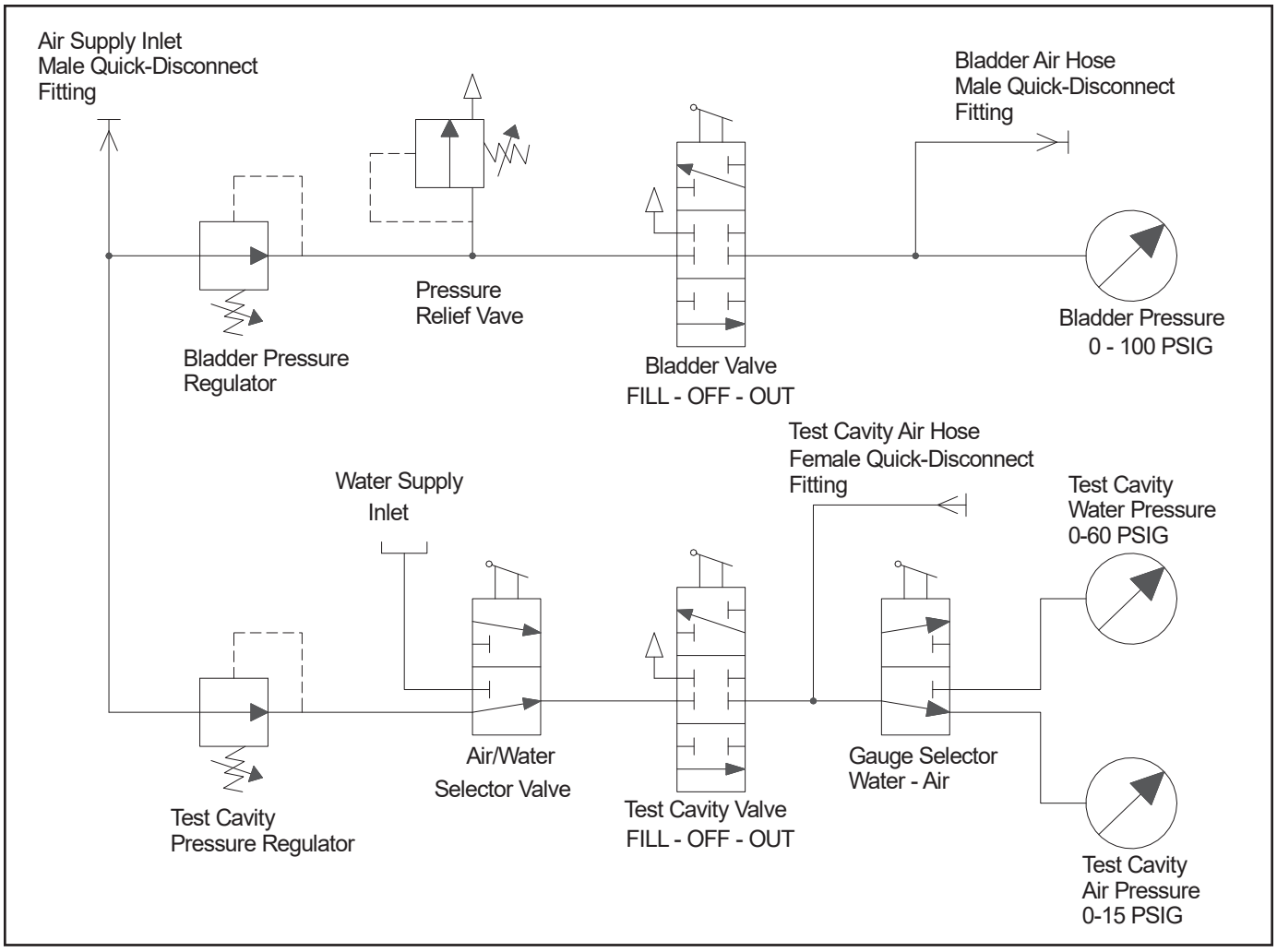

Figure 6
Joint tester control schematic.

6. The test chamber and bladder were then deflated, and the pipe joint tester was moved to the next pipe joint.

The subject pipe joint tester was manufactured in 2001 or 2002. It remained in the possession of the manufacturer and was leased to various contractors over its lifespan. When originally manufactured, the control panel was mounted directly on the tester frame and was intended to be used by an operator positioned immediately adjacent to the tester. In about 2011, the pipe joint tester design was changed by removing the control panel from the tester frame and adding hoses between the tester and control panel. This permitted the operator to perform some operations with the control panel at the limit of the hose extension.

Records provided in discovery indicated that the joint tester was repaired on two occasions prior to the incident. An August 2008 record indicated that the joint tester was returned to the manufacturer in a damaged condition, and the bladder was replaced. An April 2012 record indicated repairs to four spots on the bladder as well.

The only documentation provided to users of the pipe joint tester was a single laminated printed sheet of paper titled "Joint Tester Equipment Specifications." The content of the specification sheet was inconsistent with the configuration of the equipment. The specification sheet failed to provide the necessary instructions and warnings required for the safe assembly, inspection, operation and maintenance of the joint tester. This can be summarized as follows:

- The equipment specifications referenced a steel multi-section frame. The subject joint tester frame was a single piece aluminum frame.

- The specification sheet referred to the bladder as the "element." The labels on the control panel

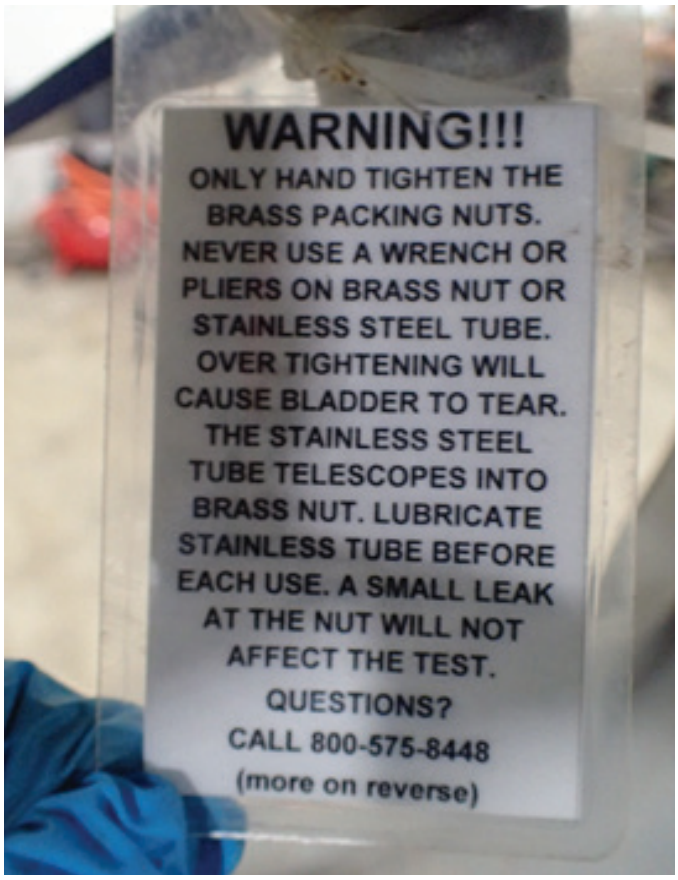

Figure 7
Warning tag (front).

Figure 8
Warning tag (rear).

refer to the bladder as the bladder.

- The specification sheet stated that the control panel was mounted on the frame. The subject control panel was not attached to the frame.

- The equipment specification stated that the control panel was equipped with one pressure regulator whereas the subject tester had two pressure regulators.

- The equipment specification stated that the bleed-off valve was located on the top of the joint tester assembly. On the subject tester the test cavity fill fitting was located on the top and the bleed-off valve was located on the bottom of the joint tester.

Two identical laminated warning tags were attached to the telescoping test cavity fill port and the telescoping test cavity bleed-off port. One side of each tag contained a warning regarding overtightening of the packing nut. The other side contained a warning against using the tester with bent telescoping tubes (**Figures 7** and **8**).

The maximum pressure rating of the pipe joint tester was documented at multiple locations. Those pressure ratings were inconsistent and contradictory. Step 2 of "Joint Air Testing" on the manufacturer's specification sheet stated that the maximum permitted bladder pressure was 150 psi. A label on the control panel stated "Bladder Pressure 80 psi MAX." A label molded into the bladder surface stated "75 PSI MAX."

During discovery in this case, engineering and technical documentation was requested from the manufacturer. It was determined that minimal documentation existed. No engineering documentation for the construction of the pipe joint tester was provided. There was no evidence that any analysis or testing had ever been performed by the manufacturer to determine the maximum permitted operating pressure or failure pressure for the bladder.

The Incident Project

The incident project involved constructing improvements to a municipal wastewater treatment facility. Part

Figure 9
Pipe with external coupler.

of the project involved installation of underground pipe. The general contractor subcontracted with a mechanical contractor to install various systems, including the underground pipe. The mechanical contractor, in turn, subcontracted with an excavation contractor who provided labor and heavy equipment to assist in setting the pipe.

The pipe involved was fiberglass reinforced polymer mortar pipe meeting ASTM D3262-14. When installed, the pipe joints were sealed with external compression couplings. The couplings contained an elastomer seal and a two-piece stainless steel clamp secured with external bolts. The pipe involved in the incident was 54 in. in diameter (**Figure 9**). The project specifications required testing of the pipe joints.

The mechanical contractor leased the subject joint tester from the manufacturer specifically for this project. It was delivered to the work site and was available for use the day before the incident. The project specifications required the pipe joints to be tested at 25 psi. The maximum permitted pressure drop in 1 minute was 1 psi or less.

The day before the incident, the pipe joint tester was assembled by two journeymen plumbers who were employees of the mechanical contractor. The first, Plumber A, was foreman on the incident project. He had no previous experience with the pipe joint tester. The second, Plumber B, had previously used a similar pipe joint tester at a different project. He was brought to specifically to help assemble the tester and start the pipe joint testing process. The sequence of events leading up to the incident generally unfolded as described below:

- Plumber A and Plumber B assembled the pipe joint tester, and then lowered it into the pipe with a crane to start testing pipe joints. They initially thought that they had to achieve zero pressure drop during the test; they also had trouble getting the bladder to seal against the inside of the pipe. Plumber A made two separate calls to the pipe joint test manufacturer asking for instructions.

- The president of the pipe joint tester manufacturer acknowledged that he spoke to someone at the project twice. He told them to clean the pipe surface, increase the bladder pressure to 100 psi, and increase the setting on the bladder pressure relief valve. He did not specify what the pressure relief valve setting should be.

- An engineer from a consulting firm was also present to observe the pipe joint testing and record test results. He clarified with a supervisor that the required test pressure was 15 psi — and that a pressure drop of 1 psi or less in 1 minute was acceptable. The engineer stayed at the site through all of the testing to observe and record data.

- Testing of pipe joints then proceeded. Plumber A and Plumber B completed successful tests on five or six pipe joints. Plumber B left the site to return to his original assignment at about 1 p.m.

- Plumber A then directed another employee of the mechanical contractor to assist in pipe joint testing. This was also a journeymen plumber (Plumber C). Plumber A trained Plumber C in the operation of the pipe joint tester that afternoon, and they completed about five successful pipe joint tests. They also used a laborer employed by the excavation subcontractor (Laborer 1) to clean the pipe joints ahead of testing and to assist in moving the equipment within the pipe.

- On the day of the incident, Plumber C continued to operate the pipe joint tester with the assistance of Laborer 1. They completed testing on about eight pipe joints prior to lunch. One of the pipe joints tested did not hold pressure.

- Due to a prior commitment, Plumber C was scheduled to leave the work site early. Plumber A directed a second employee of the excavation contractor, Laborer 2, to work with Plumber C to learn how to operate the pipe joint tester.

- After lunch, Plumber C and Laborer 2 completed two pipe joint tests together. Plumber C then observed Laborer 2 operate the pipe joint tester on a third pipe joint. Plumber C then left the work site, and Laborer 2 continued to operate the pipe joint tester. Laborer 1 continued to provide assistance, and the engineer continued to observe and record data.

- Near the end of the day, they returned to the pipe joint, which had failed the test earlier in the day. They set up the joint tester and proceeded with the test. During the test, Laborer 2 was seated on a board that extended across the lower portion of the pipe on one side of the joint tester. The engineer was seated on a board about 4 ft behind Laborer 2. Laborer 1 was on the other side of the joint tester collecting equipment. Laborer 1 estimated that he was 10 to 12 ft away from the pipe joint tester. During the test, the bladder exploded without warning. Laborer 2, who was operating the tester, was fatally injured when he was struck by components of the pipe joint tester and the air blast. Laborer 1 and the engineer were not injured.

Site Investigation

Photographs of the pipe joint tester and some ancillary components inside the pipe were taken by contractors and the police shortly after the incident. The pipe joint tester was then removed from the pipe interior.

The incident occurred in a section of 54-in. pipe near a concrete post-aeration structure. The pipe joint being tested was the second joint away from the structure (**Figure 10**). The operator (Laborer 2) and the engineer were positioned on the side of the joint tester closer to the aeration structure. Laborer 1 was positioned 10 to 12 ft from the opposite side of the tester. Information observed in the photographs included the following (see **Figures 11** through **13**):

- The photographs were taken from the side of the tester where Laborer 2 and the engineer had been positioned. A large amount of blood was present on the lower portion of the pipe adjacent to the tester frame.

- After the incident, the side of the joint tester frame equipped with lifting lugs was facing away from Laborer 2's position.

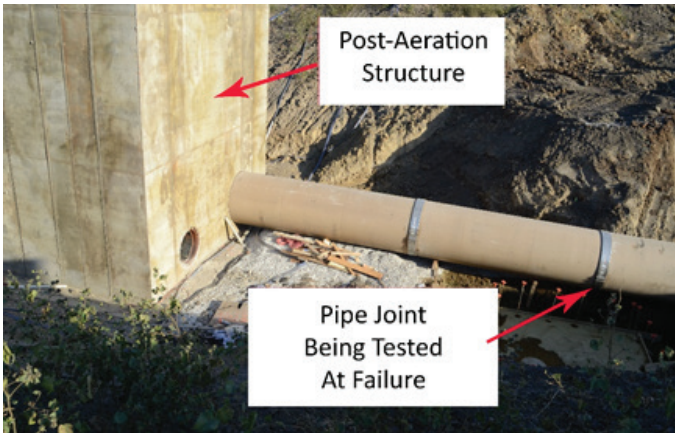

Figure 10
Incident location.

Figure 11
Pipe joist tester in pipe after incident.

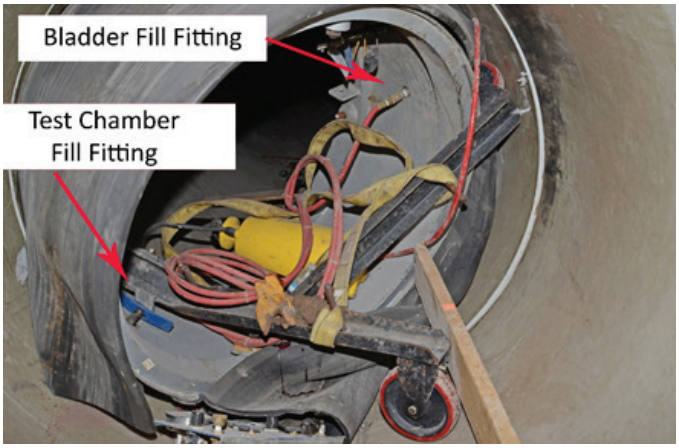

Figure 12
Pipe joist tester in pipe after incident.

Figure 13
Joint tester control panel.

- The axis of the tester frame was not parallel with the pipe axis. The frame was rotated slightly counterclockwise about a vertical axis (viewed from above) and slightly clockwise about a horizontal axis (viewed from the left).

- The test chamber fill fitting, which had originally been positioned at the 12:00 position was located at about the 7:30 position. The bladder fill fitting, which had originally been located at about the 7:00 position, was located at about the 2:30 position.

- The bladder contained a rupture parallel with the pipe and pipe tester axis. The rupture appeared to extend the entire width of the bladder. The bladder was partially separated from the frame.

- Both transport wheel frames were completely separated from the tester frame and were resting partially within the inner diameter of the frame. One steel channel wheel frame contained significant deformation. On the other frame, one wheel was wedged between the tester and the pipe wall.

- The control panel was resting on the lower pipe surface directly in front of the tester. The paired bladder and test cavity supply hoses were partially wrapped around the wheel frames. The air supply hose was not connected to the control panel and appeared to be wrapped around the right side of the joint tester.

- Some of the controls on the control panel were visible. The test media selector valve was positioned slightly clockwise from the AIR position. The test cavity valve was positioned slightly clockwise from the FILL position. The test gauge valve was positioned slightly counterclockwise from the AIR position.

- The interior of the pipe surface around the pipe tester appeared to contain black colored scuff marks.

At the time of the incident, air was being supplied to the pipe joint tester from a portable diesel-powered air compressor positioned on the ground surface adjacent to the pipe. This compressor was rated to supply 185 cubic feet per minute of compressed air at 125 psi. About one year after the incident, the maximum outlet pressure of the compressor was determined to be 122 psi.

A multi-party examination of the site was conducted several weeks after the incident. Photographs of the pipe joint tester control panel taken at that time showed that some of the controls had been moved after the control panel was photographed on the date of the incident. At the conclusion of that inspection, the pipe joint tester was shipped to the investigator's facility for additional evaluation.

Pipe Joint Tester Inspection and Testing

A non-destructive multi-party examination of the joint tester was conducted. Information obtained during this examination included the following:

- The damaged bladder was loosely attached to the tester frame. The bladder was held in place by the telescoping tubes of the test cavity fill fitting and the test cavity bleed-off fitting, which extended from the bladder through the frame. The bladder fill fitting was wedged between the bladder and the outer surface of the frame.

- The bladder was ruptured along a line parallel with the axis of the joint tester frame. The rupture was roughly centered on the test cavity fill fitting tube. This would have been located at the 12:00 position when the joint tester was set up for use in the pipe. The rupture extended almost completely through the entire bladder. A 1¼-in.-wide strip of material still connected the two sides of the rupture (**Figure 14** and **Figure 15**).

The construction of the bladder was similar to a flattened tube. In its uninflated condition, it lay flat against

the outer surface of the frame and extended the full 24-in. width of the frame. The bladder wall appeared to contain two distinct "rubber" layers with a layer of reinforcing fiber cords between the two rubber layers. The combined thickness of the two rubber layers on the inner wall was about $^{3}/_{8}$ in. Additional material had been added to the outer surface of the bladder, which increased the thickness of the outer wall to about $^{5}/_{8}$ in. The reinforcing cords were positioned around the circumference of the bladder cross-section, parallel to the axis of the joint tester frame and the pipe. The rupture was parallel to the reinforcing cords (**Figures 16** and **17**).

- The telescoping test cavity tubes extended through the inner side of the bladder, adjacent to the aluminum frame, and through the outer side of the bladder, which would be adjacent to the pipe wall. The bladder wall contained a reinforcing disc at each location where the telescoping tube extended through the bladder. These reinforcing discs were about 5 in. in diameter, and each was sandwiched between the two layers of rubber material of the bladder wall adjacent to the reinforcing cords. At the site of the rupture, the disc in the inner wall was still partially connected to one side of the bladder rupture. At the outer wall, the reinforcing disc had completely separated from the bladder (**Figures 18** and **19**).

- The test cavity fill tube was bent. A male quick-disconnect fitting was attached to the inlet end of

Figure 14
Top of joint tester showing ruptured bladder.

Figure 15
Ruptured bladder showing test cavity supply tube connection.

Figure 16
Bladder cross-section.

Figure 17
Bladder reinforcing cords.

Figure 18
Bladder rupture at test cavity fill tube.

the tube (**Figure 20**).

- The test cavity bleed-off tube did not appear to be bent. A ball valve was attached to the inner end of the tube. The valve was in the closed position (**Figure 21**).

Figure 19
Bladder rupture at test cavity fill tube.

Figure 20
Test cavity fill tube.

Figure 21
Test cavity bleed-off tube and valve.

- A label molded into the exterior surface of the bladder indicated a maximum pressure of 75 psi (**Figure 22**).

- Both transport wheel frames had separated from the joint tester frame. Each wheel support frame consisted of a 4-in.-wide steel channel with an 8-in. diameter wheel mounted on each end. Each wheel frame had been attached to the inner diameter of the joint tester frame with two ¾ in. nominal diameter acme thread bolts. Each wheel frame was positioned at a 45-degree angle from vertical. One of the wheel frame channels contained a severe bend extending from the end to the connecting bolt. The end of the channel was bent upward about 5 in. from the bolt and was twisted to the side. The other channel was bent upward about ½ in. All four of the ¾-in. connection bolts for both channels had fractured just below the adjusting nuts on the underside of the channel (**Figures 23** and **24**).

Figure 22
Label embossed on outer bladder surface.

Figure 23
Damaged wheel frame.

- The wheel frame connection bolts had been threaded into four cylindrical extensions on the inner diameter of the tester frame. The fractured ends of the ¾-in. bolts remained in the tester frame. Comparison of the fracture surfaces indicated that the deformed ends of the wheel frames had extended out the side of the joint tester frame equipped with the lifting lugs (**Figure 25**).

- The bladder pressure regulator was located at the right center portion of the control panel. This was a Norgren Model R07-200-RNLA regulator with a rated inlet pressure of 300 psi and a rated outlet pressure of 125 psi.

- The test cavity pressure regulator was located at the left center portion of the control panel. This pressure regulator was the same model and pressure rating as the bladder pressure regulator.

- A pressure relief valve was located on the rear side of the control panel. This pressure relief valve was connected with a tee fitting to the air line extending out of the bladder pressure regulator. This pressure relief valve was adjustable, and the relief valve manufacturer's specifications indicated that the adjustable range was 50 to 100 psi (**Figure 26**).

Figure 24
Damaged wheel frame.

Figure 25
Wheel frames repositioned in tester frame.

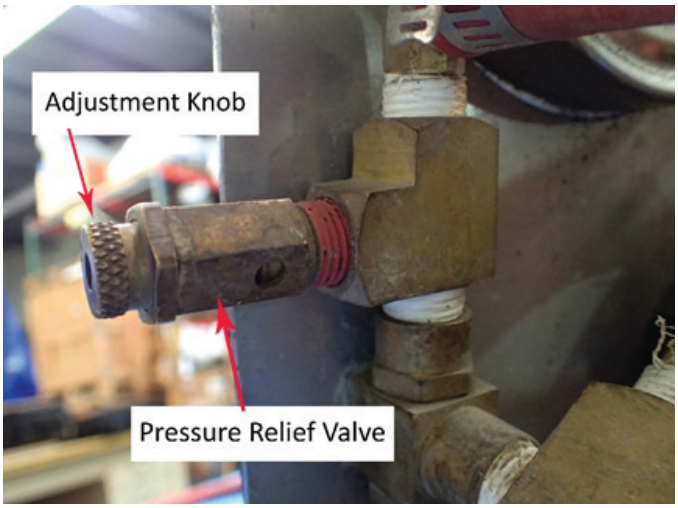

Figure 26
Bladder pressure relief valve.

- Separate air hoses extended from the bladder test circuit and from the test cavity circuit. The hoses were bundled together with plastic zip ties. The hoses extended about 19½ ft from the control panel.

After the non-destructive examination of the pipe joint tester was completed, a protocol was developed for testing of the pipe joint tester controls by the forensic engineer with agreement from other parties. An objective of the protocol was to determine the settings of the bladder pressure regulator, the test cavity pressure regulator and the bladder pressure relief valve. This testing was performed by the forensic engineer during an additional multi-party examination of the pipe joint tester. The following information was learned during this testing:

- No leaks were found in the control panel air lines and valves.

- The bladder three-way valve and the test cavity three-way valve functioned correctly to fill, shut off and exhaust the bladder and test cavity.

- The bladder pressure regulator was set at 104 psi.

- The test cavity pressure regulator was set at 126 psi.

- When first tested the pressure relief valve leaked at 89 psi and popped full open at 93 psi. On two subsequent trials, the valve leaked at 84 psi and popped full open at 90 psi.

Previous Incident

In 2011, a worker operating the same model pipe joint tester from the same manufacturer was fatally injured. Information regarding the previous incident was obtained from documents and deposition testimony created during the litigation of that previous incident. The pipe joint tester involved in the 2011 incident was a larger version of the same model pipe joint tester involved the subject 2015 incident. In the 2011 incident, the pipe joint tester rotated violently in the pipe, and the operator was struck by the pipe joint tester frame. However, the bladder on that tester reportedly did not rupture. The manufacturer concluded that the rotation of the pipe joint tester occurred because the test chamber pressure exceeded the bladder pressure. Pressurized air escaping from between the bladder and pipe caused the tester to rotate in the pipe.

As a result of that incident, the manufacturer changed the design of the pipe joint tester by removing the control panel from its mounted position on the tester frame and providing 20-ft-long extension hoses to connect the control panel. This permitted an operator to perform some of the operating tasks from just over 15 ft away from the tester.

Discussion

The subject pipe joint tester created a significant stored energy hazard when used as instructed by the manufacturer. An estimate of the available stored energy can be made using an equation for the isentropic expansion of the compressed gas as follows[3,4,5]:

$$E = \frac{P_1 V_1}{k-1}\left(1 - \left(\frac{P_0}{P_1}\right)^{\frac{(k-1)}{k}}\right)$$

where:

E = Work Energy

k = Ratio of Specific Heats

P_1 = Initial Pressure

P_0 = Ambient Pressure

V_1 = Initial Volume

For the subject tester, when positioned in a 54-in. diameter pipe and inflated to 75 psi (the maximum pressure listed on the bladder), the volume of compressed air was about 6.6 cubic feet, and the stored energy in this compressed air was about 86,000 lbf-ft. The stored energy will increase with increased pressure. A failure of the bladder will release this energy with explosive force. The effects of the explosion include violent rotation of the tester frame, violent displacement and projection of components/debris and an air blast. All these effects have the potential to seriously injure or kill personnel.

A comparison can be made of the pipe joint tester to an inflated semi-truck tire. In fact, a patent for a pipe joint tester by the manufacturer compared the bladder to a tire mounted on a truck wheel. A common size truck tire, such as an 11R22.5 all position tire, has a volume of about 3.4 cubic feet. When inflated to 75 psi, the available stored energy would be 44,500 lbf-ft.

A study prepared for the U.S. Department of Energy set a threshold value for the stored energy in a pressure hazard. The threshold value determined was 1,000 ft-lb. Pressure hazards with stored energy above the threshold value require additional consideration for factors, including design, fabrication, testing inspection and maintenance. The study also presented the following comparison of stored energy in real-world applications (**Figure 27**).

It was known to the manufacturer that operators and other personnel would be positioned near the joint tester during operation. Prior to the 2011 design changes implemented to the joint tester, the control panel was mounted on the joint tester frame, and it was intended that the operator be positioned immediately adjacent to the joint tester during operation. While the addition of 20-ft-long extension hoses between the control panel and the tester permitted an operator to move away from the joint tester during operation, those hoses did not require that action by the operator or other personnel.

Personnel were likely to be in close proximity to the tester to prevent shifting of the joint tester during inflation. This was particularly true when testing joints in sloped pipe runs. Operating personnel used the test cavity bleed-off valve to verify that test air was applied to the joint. No instructions or warnings were provided with the subject joint tester regarding a requirement to maintain a safe distance from the joint tester. No warnings were provided with the joint tester regarding the risk of severe injury or death during use of the joint tester.

Examination of the subject pipe joint tester after the incident showed that the bladder ruptured at the top of

Item	Volume ft^3	Gas	Pressure (psig)	Stored Energy (lbf-ft)	Method
Compressed Gas Cylinder	1.42	Air	2500	982,500	Stored Energy Spreadsheet
Standard Air Compressor, 50 gal	6.68	Air	125	159,000	Stored Energy Spreadsheet
Standard Air Compressor, 20 gal	2.67	Air	125	64,000	Stored Energy Spreadsheet
Propane Tank (grill, compressed gas expansion only)	0.63	Propane	200	35,000	Stored Energy Spreadsheet
Paint Ball Tank (20 oz)	0.02	Air	3000	21,300	Stored Energy Spreadsheet
M-80 (2.5 grams of powder)	N/A	N/A	N/A	17,000	See Appendix A
State Limit for Third Party Inspection of ASME Coded Vessel	5	Air	15	9,700	Stored Energy Spreadsheet
Car Tire	0.97	Air	35	5,100	Stored Energy Spreadsheet
Mountain Bike Tire	0.2	Air	65	2,230	Stored Energy Spreadsheet
CO2 2L Pop Bottle Bomb	0.05	CO2	150	1,750	Stored Energy Spreadsheet and Appendix A
Typical CO2 Cartridge (16 gram)	0.0047	CO2	900	1,263	Stored Energy Spreadsheet
STORED ENERGY LIMIT				**1,000**	
BMX Bike Tire	0.11	Air	50	915	Stored Energy Spreadsheet
Road Bike Tire	0.04	Air	110	820	Stored Energy Spreadsheet
Typical CO2 Cartridge (12 gram)	0.0058	CO2	420	650	Stored Energy Spreadsheet
Typical Firecracker (50 mg powder)	N/A	N/A	N/A	340	See Appendix A
Dust Spray Can	0.02	Mix	85	335	Stored Energy Spreadsheet
Soccer Ball	0.215	Air	12	320	Stored Energy Spreadsheet
Party Balloon	2.42	Air	1	255	Stored Energy Spreadsheet
Basketball	0.26	Air	8	250	Stored Energy Spreadsheet

Figure 27
Comparative stored energy[3].

the tester where the telescoping test cavity tube extended through the bladder. The rupture was parallel to the axis of the joint tester frame and extended along the entire 24-in. width of the bladder. The rupture was also parallel to the reinforcing cords. It is well known that holes, grooves, notches, and other discontinuities in any material alter the stress distribution in the material and create stress risers. The manufacturer had knowledge and previous experience with failures at the location of the test chamber fill and bleed-off fittings. Instruction tags on the pipe joint tester indicated that overtightening of the packing nut at the telescoping tube could create a delamination of the steel fixture inside the bladder and cause the bladder to rupture. However, there was no way for the user to examine that assembly to determine its condition.

The manufacturer produced no test data, calculations, or other information to indicate that it ever reliably determined the safe operating pressure for the bladder. The manufacturer produced no information to indicate that it had ever studied, analyzed, or determined what effect repeated use and aging has on the integrity of the bladder and the continued safe operating pressure.

After the subject 2015 incident, the manufacturer implemented additional changes to the design of the pipe joint tester and to the instructions provided with the tester. The manufacturer designed a device intended to prevent the joint tester from rotating inside the pipe in the event of bladder failure or test cavity overpressure. Instruction sheets were created that referenced the potential for injury or death during the operation of joint testers. The modified instruction sheets also instructed users to stay 15 ft away from the tester. There was no evidence that any objective analysis was used to select the length of the hoses between the pipe joint tester and the control panel. There was no indication that any analysis or testing was performed to select that length.

The joint tester controls permitted the maximum rated pressure of the bladder to be exceeded and the test cavity pressure to exceed the bladder pressure:

- The label for maximum pressure molded into the bladder was 75 psi. However, the pressure regulator was rated to supply air at a pressure of 125 psi. After the incident, the bladder pressure regulator was found set at 104 psi.

- The bladder pressure relief valve was adjustable

and could be adjusted above 75 psi. After the incident, the pressure relief valve was found set at about 90 psi.

- The maximum pressure for the test cavity was 25 psi. The test cavity pressure regulator was rated to supply air at 125 psi. After the incident, the test cavity regulator was found set at 126 psi.

- The test cavity was not equipped with a pressure relief valve.

- Operation of the test cavity bleed off valve required an operator to reach into the tester frame while the bladder was under pressure.

The standard of care for designing, manufacturing and installing a product includes identifying the hazards associated with that product and determining methods to minimize those hazards. A well-established and accepted methodology is used by engineers and designers to minimize the hazards (or maximize the safety level) of their product. This procedure has been outlined in a number of similar forms, all of which define a list of priorities (in descending order of effectiveness) known as a safety hierarchy or risk reduction hierarchy of controls (**Figure 28**)[6,7,8,9]. Under this system, the designer first identifies hazards associated with the system arising from many aspects of the product use including installation, operation, inspection, maintenance, repair, troubleshooting and reasonably foreseeable misuse. Once the hazards are identified, the designer must take appropriate steps to reduce those hazards. This methodology has been in use for decades in a wide spectrum of industries, applications, and products.

All the above formats list actions in decreasing order of effectiveness, and it can be seen that warnings, instructions, and safety procedures are not a substitute for eliminating the hazard, reducing the hazard or providing warning devices to address a hazard. Warnings and instructions can be used in combination with other measures and can be used alone when other measures are not feasible. This methodology applied to and should have been used on the design of the subject pipe joint tester.

In the hierarchy of controls shown in **Figure 28**, the actions described in the first through fourth levels are more effective because they rely the least on human behavior and the performance of personnel. Actions described in the fifth through seventh levels are inherently less reliable because they rely on the performance of personnel for their effectiveness[6].

Numerous feasible alternative designs were available when this pipe joint tester was designed and manufactured, which would have reduced the risks to personnel created by the design of the pipe joint tester. These alternative designs improved the safety of the pipe joint tester without a negative effect on the utility of the pipe joint tester. The risk reduction measures in the order of the preferred hierarchy include the following:

Elimination

- Use a two-bladder system on the tester. This eliminates the highly stressed mounting connections between telescoping test chamber air supply tube and the bladder

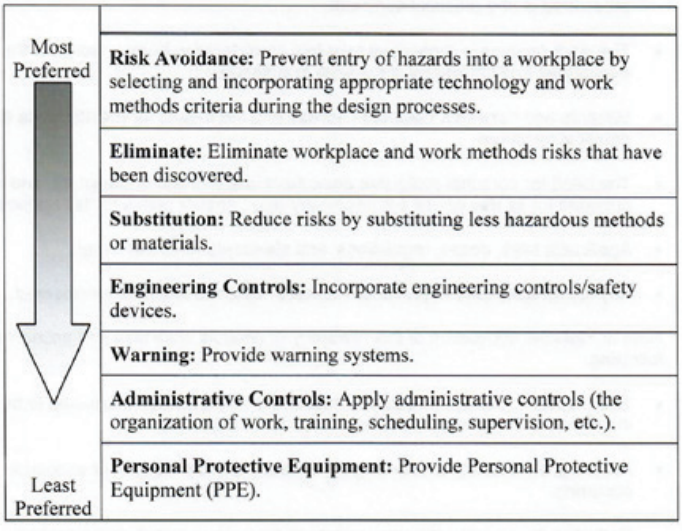

Figure 28
Risk reduction hierarchy of controls[6].

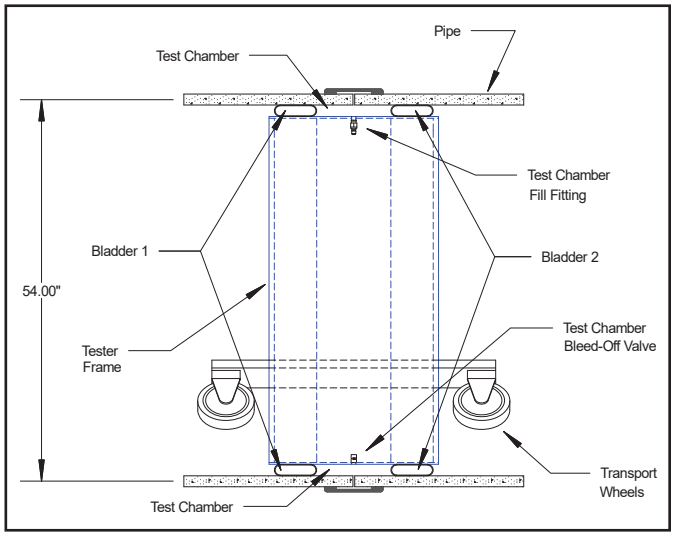

Figure 29
Side view of two-bladder joint tester in 54-in. pipe.

walls (**Figure 29**). The failure on the incident unit occurred at this connection and the manufacturer previously determined that this connection was a source of bladder failures.

Substitution

- Reduce the compressed air volume and stored energy by using a two-bladder system on the pipe joint tester. The volume of both bladders combined would be less than the single bladder. In the event of bladder failure, it is unlikely that both bladders would fail at the same time (**Figure 29**).

- Reduce the compressed air volume and corresponding stored energy by designing the tester to fit a single size of pipe more closely matched to the pipe joint tester diameter. In addition, the clearances with a single size tester would not permit the tester frame to rotate within the pipe.

Engineering Controls

- Replace the adjustable pressure relief valve with an appropriately sized non-adjustable pressure relief valve.

- Supplied air to the test cavity circuit from downstream of the bladder pressure regulator. This would prevent the test cavity pressure from ever exceeding the bladder pressure.

- Use a test cavity pressure regulator with a lower rated outlet pressure.

- Provide an appropriately sized non-adjustable pressure relief valve in the test cavity circuit.

- Provide a third air hose extending from the test cavity bleed-off port back to a valve at the control panel. This would eliminate the need for personnel to reach into the test cavity frame to operate the bleed-off valve.

- Use hoses of the appropriate length to adequately separate operating personnel from the pressurized pipe joint tester.

- **Figure 30** shows a modified air control schematic.

Administrative Controls

- Provide complete and accurate instructions and warnings for the safe assembly, inspection, operation and maintenance of the pipe joint tester.

- Provide appropriate warning labels on the control panel and on the pipe joint tester frame. As an example, use a safety sign in the format from the ANSI standard for Product Safety Signs and Labels[10] and a hazard alerting symbol from the ANSI standard for Safety Symbols[11], as shown in **Figure 31**.

Conclusions

- The pipe joint tester created a significant stored energy hazard when used as instructed by the manufacturer and presented a risk of serious injury or death to personnel.

- The design of the pipe joint tester required the operator and other personnel to be in close proximity to the pipe joint tester when it was pressurized.

- A maximum pressure rating of the pipe joint tester was at shown at multiple locations. Those pressure ratings were inconsistent and contradictory.

- The joint tester controls permitted the maximum rated pressure of the bladder to be exceeded.

- The joint tester controls permitted the test cavity pressure to exceed the bladder pressure.

- The bladder failed under pressure at the location where the test cavity supply tube passed through the inner and outer bladder walls. The manufacturer had previous knowledge of bladder failures at that location.

- The manufacturer failed to provide the necessary instructions and warnings for the safe assembly, inspection, operation and maintenance of the pipe joint tester.

- No inspection procedure was available to the user to evaluate the condition of the bladder test cavity connections.

- While the addition of 20-ft-long extension hoses between the control panel and the tester permitted an operator to move away from the joint tester during operation, those hoses did not require that action by the operator or other personnel.

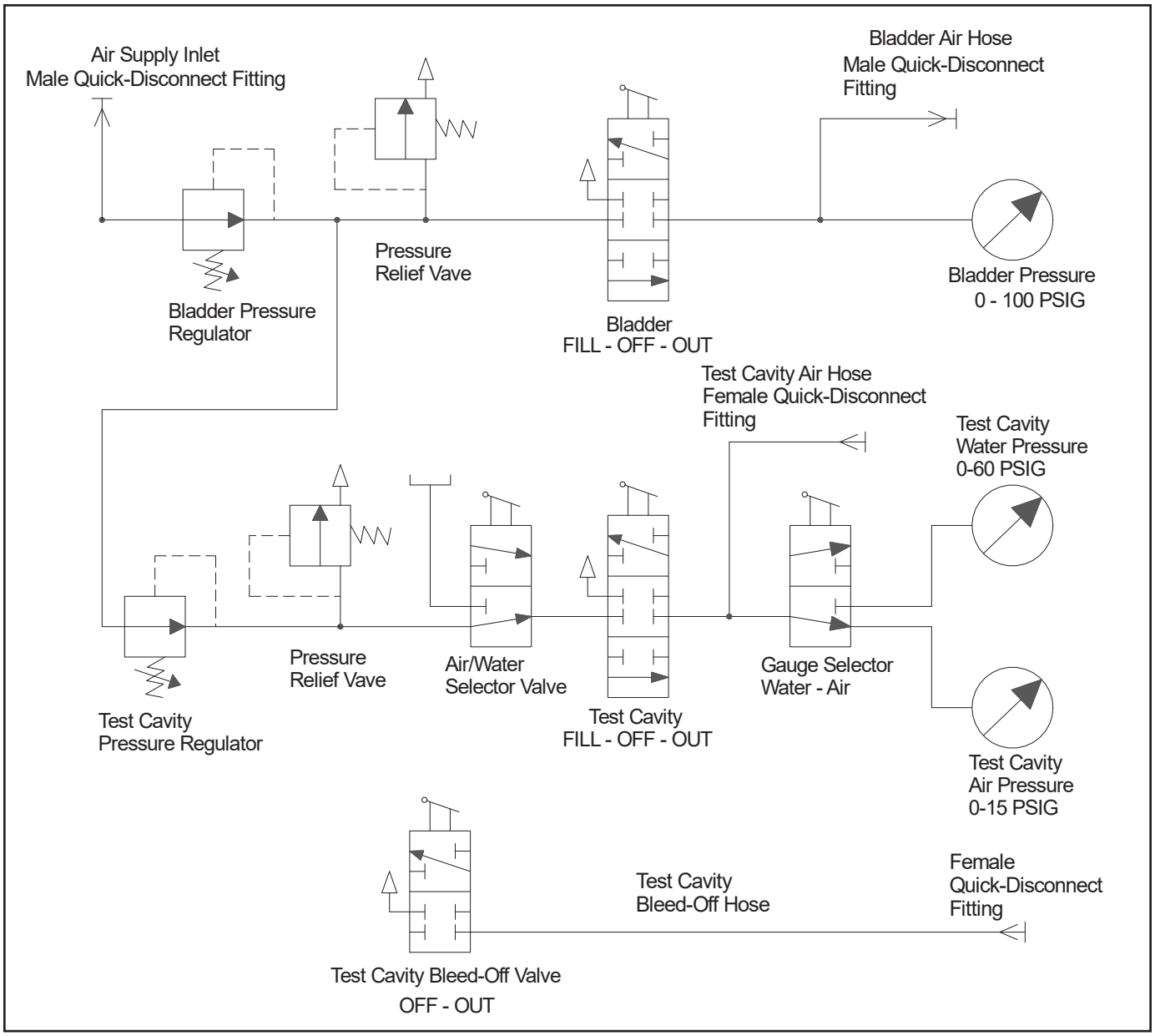

Figure 30
Modified control schematic.

Operating tasks still required personnel to work in close proximity to the pressurized joint tester. No instructions or warnings were provided with the subject joint tester regarding a requirement to maintain a safe distance from the joint tester. No warnings were provided with the joint tester regarding the risk of severe injury or death during use of the joint tester.

- Feasible alternative designs were available to the manufacturer when the pipe joint tester was initially manufactured up through the time it was

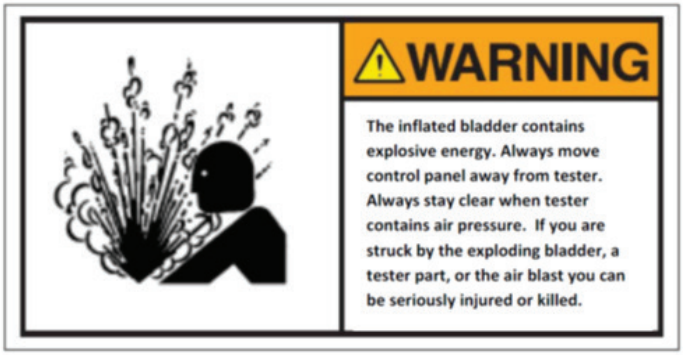

Figure 31
Proposed warning label.

leased for the incident project.

- Appropriate warning labels must be placed on the pipe joint tester frame and control panel.

References

1. ASTM D3262-16, Standard Specification for "Fiberglass" (Glass-Fiber-Reinforced Thermosetting-Resin) Sewer Pipe, West Conshohocken: ASTM, 2016.

2. ASTM C1102-14, Standard Practice for Joint Acceptance Testing of Installed Precast Pipe Sewer Lines, West Conshohocken: ASTM, 2014.

3. Pressure Systems Stored-Energy Threshold Risk Analysis, Richland, Washington: U.S. Department of Energy, 2009.

4. General Physics Corporation, "A Review of Energy Release Processes from the Failure of Pneumatic Pressure Vessels," Eastern Space and Missile Center, Patrick Air Force Base, 1988.

5. D. Crowl, Understanding Explosions, New York: American Institute of Chemical Engineers, 2003.

6. ANSI/ASSE Z590.3-2011 Prevention Through Design - Guidelines for Addressing Occupational Hazards and Risks in Design and Redesign Process, Des Plaines, IL: American Society of Safety Engineers, 2011.

7. An Instructional Aid For Occupational Safety and Health in Mechanical Engineering Design, New York: The American Society of Mechanical Engineers, 1983.

8. MIL-STD-882D - Department of Defense Standard Practice for System Safety, Washington: United States of America Department of Defense, 2000.

9. ANSI B11.TR-2000 - Risk Assessment and Risk Reduction - A guide to Estimate, Evaluate and Reduce Risks Associated With Machine Tools, McLean: The Association for Manufacturing Technology, 2000.

10. National Electrical Manufacturers Association, ANSI Z535.4-2007 - American National Standard for Product Safety Signs and Labels, New Yotk: National Electrical Manufacturer's Association, 2007.

11. National Electrical Manufacturers Association, ANSI Z535.3-2011 - Criteria for Safety Symbols, New York: National Electrical Manufacturers Association, 2011.

Forensic Engineering Evaluation of Excessive Differential Settlement on Compressible Clays

By Rune Storesund, DEng, PE, GE (NAFE 474S) and Alan Kropp, PE, GE

Abstract

This forensic engineering (FE) study evaluated root cause errors associated with excessive differential settlements on a housing project constructed on top of a variable thickness layer of highly compressible clays. The structures were reported to have experienced differential settlements on the order of 2 to 10 in. across 40 ft. The FE study examined fundamental assumptions, granularity/resolution of the settlement and differential settlement analyses, and finalized grading plan vs. the conceptual grading plan used as a basis for the differential settlement predictions. The FE study found numerous discrepancies between the "idealized site" used as a basis of analysis and the "actual site" as constructed.

Keywords

Consolidation settlement, foundations, settlement, differential settlement, compressible clays, root cause errors, time-rate effects, geotechnical, site development, forensic engineering

Introduction

This FE study evaluated root cause errors associated with excessive differential settlements on a housing project constructed on top of a variable thickness layer of highly compressible clays. These compressible clays are subject to volumetric strain as a result of loads applied changing the stress distribution.

Soil deformations, manifested primarily through vertical displacements or "settlement," occur via changes in stress, water content, soil mass, or temperature. These soil deformations are classified[1] into the following types:

- *Elastic Deformations* — Small deformations that occur nearly immediately following changes in stress state;
- *Primary Consolidation* — Time-delayed settlement by volumetric reduction as a result of reduction in water content. Due to the very low permeability of fine-grained clayey soils, consolidation settlement can take a very long time to occur as a result of the very slow drainage of water out of the soil matrix. Excess pore pressures are dissipated by the gradual expulsion of fluid from voids in the soil leading to the associated compression of the soil skeleton. Excess pore pressure is pressure that exceeds the hydrostatic fluid pressure. The hydrostatic fluid pressure is the product of the unit weight of water and the difference between the given point and elevation of free water (phreatic surface);
- *Secondary Compression/Creep* — The compression and distortion at constant water content of compressible soils. This phenomenon occurs at a much slower rate than consolidation settlement.
- *Dynamic Forces* — Dynamic loads can cause settlement from rearrangement of particles, particularly in cohesionless soils (i.e., sands and gravels), resulting in a decrease of void space (air or water).
- *Expansive Soil* — Expansive soils contain colloidal clay minerals, such as montmorillonite, that experience heave and shrinkage with changes in the soil water content.
- *Collapsible Soil* — Typically cohesive silty sands with a loose structure or large void ratio. The cohesion is usually caused by the chemical bonding of particles with soluble compounds such as

Rune Storesund, DEng, PE, GE, 154 Lawson Road, Kensington, CA 94707, 510-526-5849; rune@storesundconsulting.com

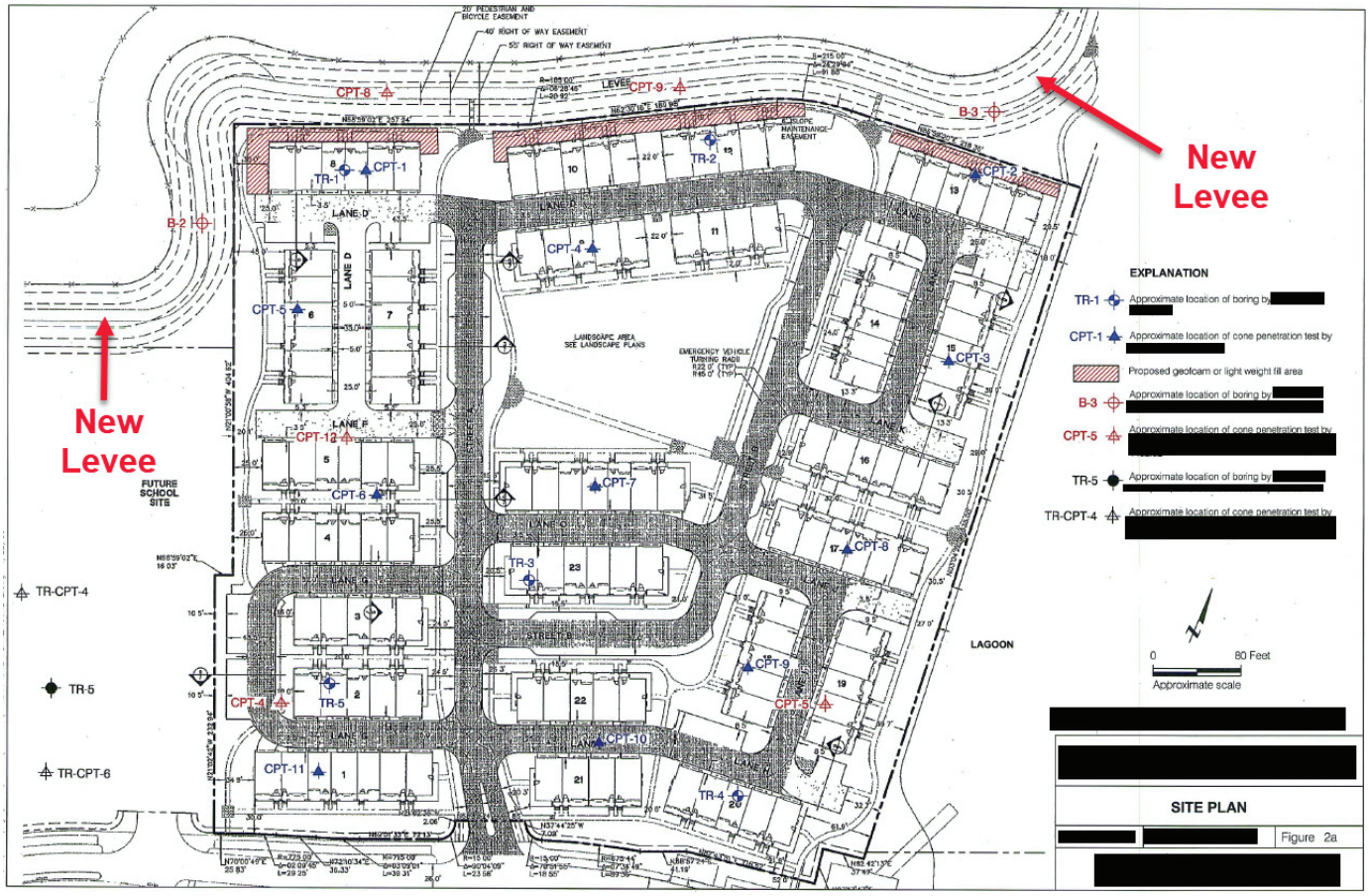

Figure 1
Overview of development features, which included a perimeter levee, site grading, multi-unit structures, and streets/utilities. Source: Discovery Docs.

cancerous or ferrous salts. Collapse occurs when the bonds between particles are dissolved.

The soil deformation mode being address in this paper is consolidation and the heterogeneity of vertical settlements across a spatially diverse deposit of highly compressible clays.

The authors were retained as experts by the plaintiffs. The case settled during mediation. The findings and opinions were subject to critique by defense experts as well as experts for both the plaintiff and defense being subject to depositions by opposing counsel. The mediation concluded in a settlement offer to the plaintiffs, which was accepted. The settlement was of a sufficient magnitude to compensate the plaintiffs for damages and fund mitigation efforts.

Project Overview

This project comprised the construction of a residential development and perimeter levee on a highly compressible non-uniform clay deposit with variable thickness (**Figure 1**). The potential for large and variable settlements were identified early in the planning process. **Figure 2** shows an overlay of an aerial image of the project area before initiation of construction. The area is situated in a bay margin with wetlands and sloughs. Interpolated contours of compressible clay are shown. The clay thickness varies

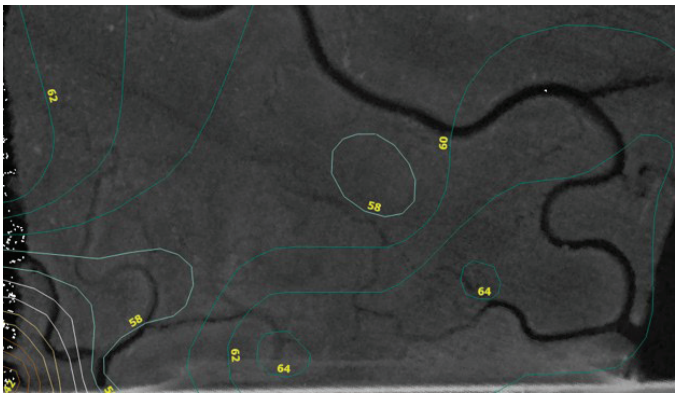

Figure 2
Overlay of compressible clay thickness and aerial image showing sloughs traversing the project area. Source: Author.

Figure 3
Overlay of compressible clay thickness and planned rough grading for the residential development and perimeter levee within the project area. Source: Discovery Docs; contours by author.

from about 58 ft to 64 ft, based on the available subsurface information. **Figure 3** shows the same overlay, but with the planned site rough grading.

Several approaches to confront the potential settlement were identified and evaluated prior to initiation of construction. These approaches included: deep foundations for the structures bypassing the compressible soils; conventional surcharge loading by placing soil stockpiles and waiting for the site to realize the expected settlements prior to construction of the structures; and use of wick drains to increase the rate of consolidation and reduce the waiting period between site loading and realization of the full magnitude of anticipated settlements.

Deep foundations were eliminated as a feasible foundation type due to the very high costs associated with the quantity and length of foundation elements required. The long wait time required for conventional surcharge loading precluded that as an option to mitigate projected consolidation settlements within the desired development time period.

To accomplish the project in a shortened construction period, wick drains were used along with staged fill placement to accelerate consolidation settlement (**Figure 4**).

Figure 4
Installation of wick drains at select locations to facilitate “rapid” consolidation settlement. Source: Discovery Docs.

Wick drains facilitate acceleration of the consolidation settlement process by reducing the drainage path of the water to evacuate the soil skeleton. By reducing the distance, the water has to travel before evacuating the soil mass, the time rate of consolidation is accelerated.

For example, without wick drains and a clay thickness of 60 ft, the water may have to travel a distance of 30 ft before it can be fully evacuated from the soil mass. With wick drains installed at a spacing of 6 ft (and driven the full depth of the clay layer thickness), the water now only needs to travel 6 ft before being evacuated. Thus, the reduced travel distance directly reduces the time required to achieve the anticipated settlement magnitude.

Figure 5 shows an overview of the wick drains installed in the slough areas (yellow highlight) that traverse the residential development. This limited treatment zone resulted in some buildings having wick drains installed in portion of the building pad area and no wick drains in the other areas. It is inferred that the design assumption was the majority of settlement would occur during the rough grading and phased fill placement stage of the project and after construction of the building pads, the magnitude of remaining settlement would be negligible, and thus the use of wick drains in limited areas would have insignificant impact on differential settlements.

The use of wick drains was selected for the areas of the project to receive the greatest quantities of import fill. These areas included the new levee as well as the historic sloughs. Settlement plates and pore pressure transducers were installed at select locations to allow the engineering team to evaluate the degree of pore pressure dissipation following placement of the fill. Once the magnitude of pore pressure dissipation reached the calculated stress from fill placement, it was assumed that the consolidation settlement was complete — and site work could continue with minor future settlements as a majority of the settlements had already occurred.

Figure 6 shows a conceptual rendering of the proposed residential units. The units were anticipated to be

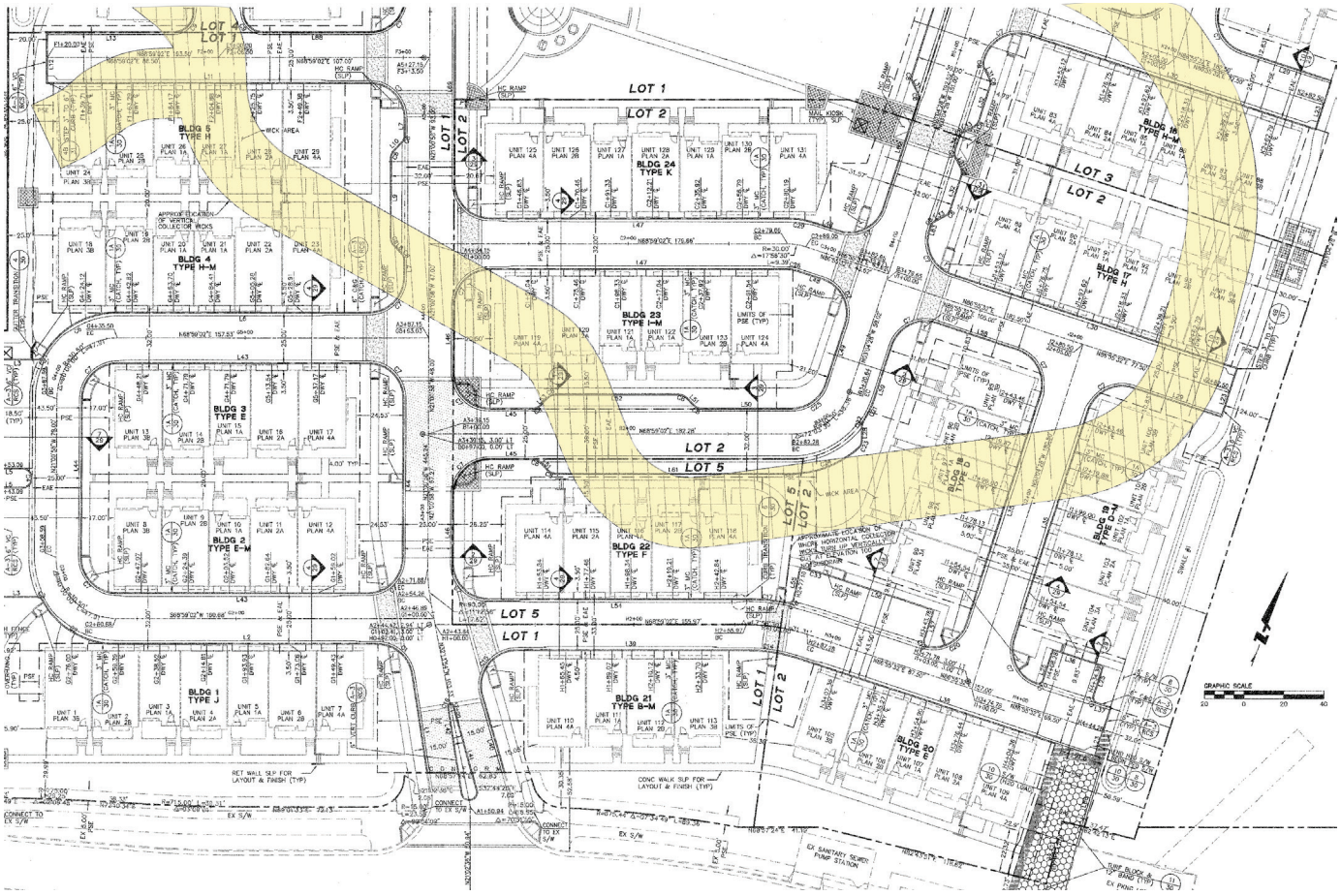

Figure 5
Location of historic slough relative to new building footprints. Source: Discovery Docs.

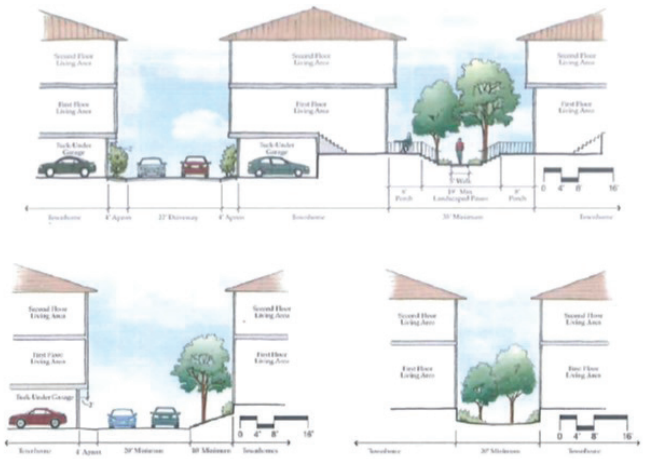

Figure 6
Architectural rendering of the multi-unit structures showing the micro-topography and variable site grade elevations across the project area. Source: Discovery Docs.

three stories tall, with the parking garage situated facing the street and the main entrance on the opposite side of the structure. All units had a stepped entrance with staircases to the front door elevated several feet above the surrounding grade. Some units were configured to have an elevated walkway (called a paseo), some units had slightly elevated landscaping area, and some units had porches with steps leading up from street level.

The project construction timeline spanned a period of approximately three years and consisted of the following :

- Month 0: Start construction/clear and grub.
- Month 1: Rough grade and wick drain installation.
- Month 3: Start Phase 1 rough grading fill placement.
- Month 5: End of Phase 1 rough grading fill placement; start consolidation wait period #1.
- Month 9: Start Phase 2 rough grading fill placement.
- Month 10. End Phase 2 rough grading fill placement, start consolidation wait period #2.
- Month 13: Start Phase 3 rough grading fill placement.
- Month 15: End Phase 3 rough grading fill placement; start consolidation wait period #3.
- Month 18: Start finish grading, streets/sidewalks, utilities.
- Month 20: Building Group 1 construction starts.
- Month 30: Building Group 1 construction complete, start Building Group 2.
- Month 34: Building Group 2 construction complete; start Building Group 3.
- Month 36: Building Group 4 initiated.
- Month 40: Construction complete.
- Month 64: Approximately two years following completion of construction, first complaints were submitted to builder about difficulty closing doors/windows.

There were no deviations or problems flagged during the course of construction and all as-built documentation indicated that the project had been constructed as specified and within the delineated tolerances.

Documented Structure Distress

The triggering of structure distress conversations between the homeowners and the builders initiated a couple years after completion of construction when the homeowners had problems opening/closing doors and windows.

Floor level surveys were commissioned by the Homeowners Association (HOA) to document the distribution of elevation differences across the structures. **Figure 7** shows an example floor level survey within a structure. Note that each structure has a number of sub-units. Typically, each structure associated with this project had five to seven sub-units.

The magnitude and distribution of realized differential settlements launched a development-wide inquiry (and subsequent litigation) as to the cause of these differential settlements, the acceptability thresholds of differential settlement for the structures and individual units, and ultimately identification of solution(s) available to mitigate the unacceptable realized settlements.

FE Evaluation

The FE study presented in this paper is focused on identification of root causes for the excessive differential settlements as well as an understanding of the potential

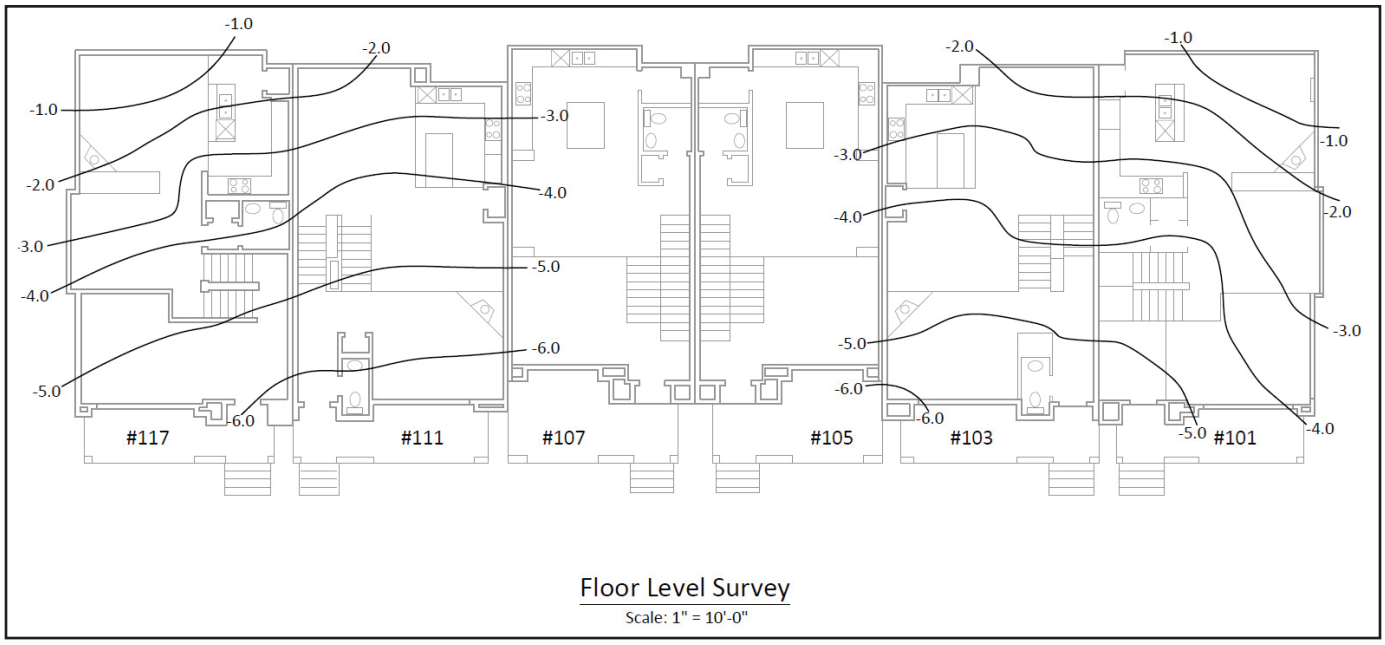

Figure 7
Example floor level survey showing differential settlement trends across the multi-unit structure. Source: Discovery Docs.

for additional differential settlement in the future. The FE study does not address mitigation efforts. The FE approach used to ascertain the root causes of the unintended differential settlements consisted of the following steps:

1. Review design calculations and associated assumptions;
2. Review project plans and specifications (construction bid package);
3. Review available construction documents; and
4. Compare/contrast the design details communicated via the construction bid package with the as-constructed conditions.

The discovery documentation made available for this case was fairly comprehensive, thus allowing for a reasonable evaluation of both the design calculations and the as-constructed conditions.

Idealized Conditions

The engineering analyses were centered about settlements for the perimeter levee. Few calculations were developed for the interior rough/finish grading associated with the building pads. In the building pad areas, analyses were performed assuming uniform fill. The placed fill was assumed to have a representative unit weight of 120 lb per cubic ft (pcf).

Based on these design assumptions, estimates were developed for total settlement, differential settlement, as well as settlement time-rate curves. The maximum settlement was anticipated to be approximately 2 ft over a 50-year period, with about ½ to 1 ft occurring in the first two years following completion of fill placement and the remaining 1.5 ft occurring fairly slowly over a 48-year period (**Figure 8**).

The maximum design differential settlement was documented by the project geotechnical engineer[2] to be "less than 2 in. in 40 ft," as shown in **Figure 9**.

Location	Fill Requirement (feet)	Approximate Settlement 2 Years After Fill Placement (feet)	Approximate Settlement 50 Years After Fill Placement (feet)	Approximate Settlement between 2 and 50 years (Design Settlement in feet)
Areas without sloughs	4	Less than ½	1½	1.5
Sloughs	7	1	2½	1.5

Figure 8
Predicted total settlements across the project site with development of housing units (Source: Project Geotechnical Report)[2].

The rate of settlement in the wick and non-wicked areas will be slightly different; therefore, although the total settlement between 2 and 50 years is about the same for areas with and without sloughs, there could be some differential settlement between the two areas over time. We estimate these differential settlements should be less than 2 inches in 40 feet. A profile through the slough, which shows our estimated settlements through the slough is presented on [redacted]. The above settlement estimates in Table 4 are based on 4 feet of fill over most of the site and 7 feet in slough areas. Our settlement analysis should be revised if these assumptions.

Figure 9
Identification of the expected differential settlement for the development (Source: Project Geotechnical Report)[2].

Figure 10 shows the general trend of settlement over time, with the majority of the settlement occurring in the first two to four years. The plot shown in **Figure 10** was prepared for the perimeter levee. No equivalent plots were developed for the interior residential development.

Findings (Actual Conditions)

The FE study found two major deviations from the design assumptions and over-simplification of analytic models: very heterogeneous fill materials used at the project site that were much larger than the assumed soil density; and highly variable fill thicknesses around the residential structures which exacerbated the magnitude of differential settlement experienced by the structures compared with the very linear and uniform site grading assumed as part of the design analyses.

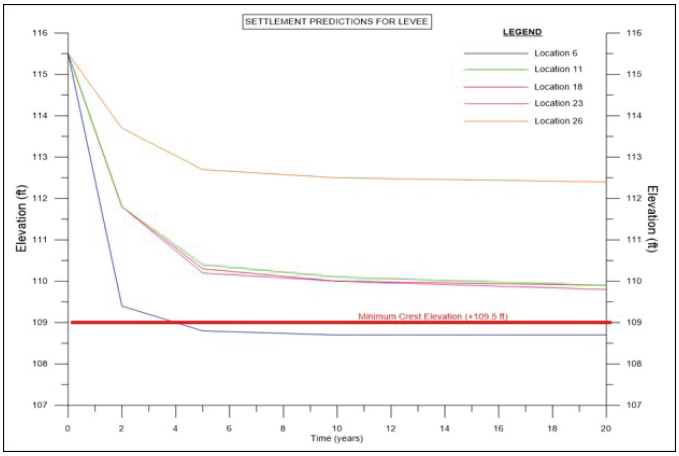

Figure 10
Plot of estimated site settlements at select locations for the first 20 years after levee grading. Settlement for the interior residential development would have a similar shape, but different ultimate magnitude 2 ft as predicted by the geotechnical engineer. Source: Author.

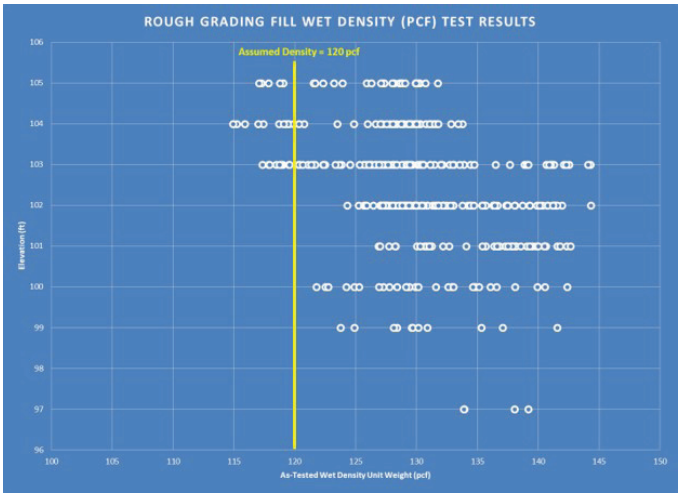

Figure 11
Distribution of actual in-place soil densities as a result of differing import sources and compaction effort. Source: Author.

Figure 11 shows a plot of measured soil densities during fill placement. The assumed density of 120 pcf is highlighted in yellow. The white circles are individual test results and span a density range of about 115 pcf to just under 145 pcf. Of the 359 soil density tests, 330 tests were in excess of 120 pcf, which is approximately 92% of all the tests. Additionally, the spatial distribution of the varying soil densities was not uniform, resulting in heterogeneous distributions of differing soil densities across the spatial footprint of the development. In addition to the large skew between assumed soil density and actual soil density, the complexity of the finish grading for the development further exacerbated the magnitude of realized differential settlements.

Figure 12 shows a simplified numerical model to examine the effects of small variations in fill thicknesses as a result of micro-topography. The micro-topography included levee fill on the left side of the houses and sloping landscape fill on the right-hand side of the houses. The analyses were not intended to directly replicate the realized differential settlements as the subsurface conditions and associated soil material properties were not sufficiently established. The model, however, was generally calibrated to the range of vertical settlements observed as part of the site response following fill placement and construction of the residential units.

The results of the numerical modeling of Building B-B are illustrated in **Figure 13**. The model evaluated the impact on differential settlement across the building. Point "A" is situated on the street side of the building with site grade at approximately El. +102 ft. Point "B" is located on the opposite side of the building, with site grade at approximately El. +106 ft. The numerical analyses of the simplified model show the impact of this fill thickness differential has the ability to increase the magnitude of differential settlement by a factor of two to three. Thus, the project geotechnical engineer's predicted differential settlements of 2 in. in 40 ft, would increase, as a result

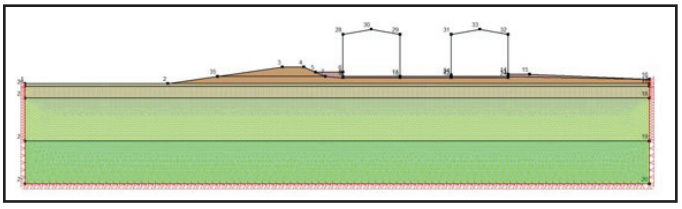

Figure 12
Simplified numerical model to explore implications of micro-topography. Source: Author.

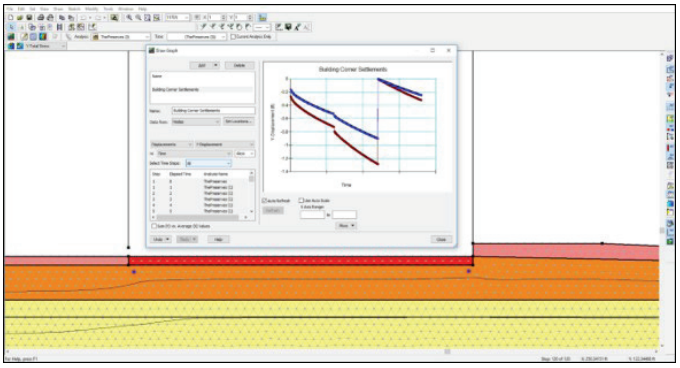

Figure 13
Calculated settlements at building edges
with micro-topography effects accounted for. Source: Author.

of the different fill thicknesses, to 4 in. in 40 ft or 6 in. in 40 ft. This simplified analysis illustrates the non-uniform fill results in differential settlements which are in excess of the maximum design differential settlement of 2 in. in 40 ft.

Conclusion

This FE study evaluated root cause errors associated with excessive differential settlements on a housing project constructed on top of a variable thickness layer of highly compressible clays. The soil deformation mode being address in this paper is consolidation and the heterogeneity of vertical settlements across a spatially diverse deposit of highly compressible clays.

This project comprised the construction of a residential development and perimeter levee on a highly compressible non-uniform clay deposit with variable thickness. The potential for large and variable settlements were identified early in the planning process.

The triggering of structure distress conversations between the homeowners and the builders initiated several years after completion of construction when the homeowners had problems opening/closing doors and windows.

The FE approach used to ascertain the root causes of the unintended differential settlements consisted of reviewing design calculations and associated assumptions; reviewing project plans and specifications (construction bid package); reviewing available construction documents; and comparing/contrasting the design details communicated via the construction bid package with the as-constructed conditions.

The FE study found two major deviations from the design assumptions and over-simplification of analytic models: very heterogeneous fill materials used at the project site that were much larger than the assumed soil density; and highly variable fill thicknesses around the residential structures that exacerbated the magnitude of differential settlement experienced by the structures compared with the very linear and uniform site grading assumed as part of the design analyses.

Reference

1. U.S. Army Corps of Engineers. “Engineering and Design, Settlement Analysis,” EM 1110-1-1904, dated September 30, 1990.

2. Geotechnical Design Report prepared for project and presented in disclosure documents.

A Forensic Engineering Approach to Documenting and Analyzing Domestic Plumbing Failures

By Stephen Knapp, PE (NAFE 891S), Henry V. Mowry, PE, and Dave Neidig

Abstract

Forensic engineering analysis of residential plumbing components can be a daunting task, particularly due to the manner in which they may be handled from the onset of a failure event. Usually, a water loss is discovered by a homeowner or tenant of a building where the source of the leak is easily determined. Remediation of a plumbing loss is likely to begin quickly and often compromises the investigation (i.e., the condition of the failed component changes, connections to the plumbing system are removed, etc.). Under most circumstances, the evidence is handled and collected by people without forensic training, such as the occupant or plumber, making spoliation a significant concern. This paper will discuss the scientific processes and evidence handling techniques utilized by forensic engineers to determine whether a product defect, installation defect, environmental condition, maintenance, or wear and tear were contributory factors to a plumbing loss.

Keywords

Plumbing, product failure, causation, spoliation, nondestructive, destructive, pressure testing, evidence collection, leaking, regulations, subrogation, product defect, design defect, installation, environment, corrosion, dezincification, freezing, insulation, piping, support, mechanical damage, chain of custody, forensic engineering

Introduction

The smallest of plumbing components can cause large monetary claims by damaging properties, displacing occupants, and causing loss of income. Plumbing losses are often the result of a defect in manufacturing or installation in which an insurance company could make a claim against the manufacturer or installer of the failed plumbing component, a process known as subrogation. Additionally, the cause of some losses may be attributed to the product's environment, maintenance, or wear-and-tear — factors that could potentially change what entity has liability for the plumbing loss. Therefore, it becomes important early on in an investigation to evaluate and consider all relevant factors of a plumbing loss to determine why a plumbing component failed and who is ultimately responsible for the loss.

Documentation of Evidence

Unlike most forensic investigations, remediation of plumbing-related losses is almost always immediate with a significant potential for the scene to be altered — and the evidence mishandled by the occupants, claim responders, or restoration companies. The origin of the plumbing failure will be obvious to initial responders to the property, and the failed product will likely be handled or manipulated in an effort to stop water leakage or even removed to restore the integrity of the plumbing system, potentially changing the state of the failed product. The people most likely to unintentionally change or alter evidence once the plumbing failure is discovered include, but are not limited to:

- Occupants of the property.
- Property maintenance personnel.
- Insurance representatives.
- Plumbers.
- Remediation and restoration personnel.

Once the insurance claim process begins, the individuals best suited for controlling the evidence and documenting the loss should be considered. Under ideal

Stephen Knapp, PE, 9249 S. Broadway #200-808, Highlands Ranch, CO 80129, 720-854-5533, sknapp@cgellc.net

circumstances, all parties interested in investigating and evaluating the cause of the loss should be contacted and put on notice before removing or altering plumbing components. Such parties can include insurance representatives (insurance adjuster, forensic engineer) as well as the installer and manufacturer of the failed plumbing component. Each involved party is expected to have a slightly different protocol/agenda when it comes to collecting evidence from the property for his or her representative's benefit.

Many times, relevant parties are not available to attend the inspection and collection of evidence. However, such parties may request that certain protocols are followed in an effort to preserve evidence. Professionals that would be expected to be qualified for preserving evidence and documenting the scene include, but are not limited to:

- Trained investigators or forensic engineers on behalf of the insured(s) or their insurance carrier(s).
- Trained investigators or forensic engineers on behalf of the original installer and manufacturer.
- Representatives from the manufacturer and/or distributor.

In most plumbing failure cases, it is expected that the scene documentation and evidence handling will not be initially conducted by trained and experienced professionals as recommended above. Therefore, it is necessary to research the background and establish important facts regarding the loss. A few key questions that help in establishing the basis of an initial investigation are:

- Who installed the failed part and when?
- Was the plumbing system recently modified?
- Was there adequate heat maintained to the property?
- Was the property water pressure regulated?
- What was the water pressure at the loss location and at the time of the loss?
- Were there any environmental issues such as the presence of corrosive chemicals or lack of insulation in the area of the failed part?
- When was the loss discovered, and when was the last time the plumbing component was observed without a failure prior to the loss?

The investigator should not take shortcuts to the origin and cause of the loss. The origin of the plumbing loss should be examined from the outside of the property in, documenting all pertinent information that could be a factor to the loss while working toward the origin of the loss. Following is a list of factors that should be in the investigator's mind when assessing the cause of a plumbing loss:

1) *Occupied*: It is not uncommon for plumbing failures to occur while a property is unoccupied. While the lack of occupancy may not be a direct causal factor, it can often explain the extent of damages sustained to a property following a loss, as well as potentially explain environmental factors that could be attributed to a loss. For example, if a property is unoccupied for an extended period, several factors can lead to a situation that could cause freeze failures.

A common occurrence with unoccupied properties is the failure to maintain heat during freezing weather conditions. Freeze failures would be expected to occur because the occupant failed to set the thermostat properly or because the property's source of fuel/electricity that allows the furnace/heat registers to function properly has been compromised. In addition, stagnant and empty refrigerators have been known to freeze internally mounted filter canisters during extended periods where they are not in use. Therefore, knowledge of the property's occupancy should be established and considered during a plumbing investigation.

2) *Weather*: When evaluating plumbing failures, it is important to investigate the weather conditions preceding a loss for an extended period. Plumbing system losses due to freezing often coincide with a large drop in temperature recorded at nearby weather stations. **Figure 1** demonstrates the weather data for a loss that occurred on December 10, 2012 (red dot). Here it was noted that the loss occurred on a date with -3°F weather conditions.

When outside temperatures drop significantly, any flaw in the property's ability to maintain heat can cause freezing or over pressurization of the plumbing system. When this occurs, the weak link in the plumbing system is often the first to decouple or fracture due to excessive stress. In some circumstances, freeze failures will not be discovered until ambient temperatures have returned to

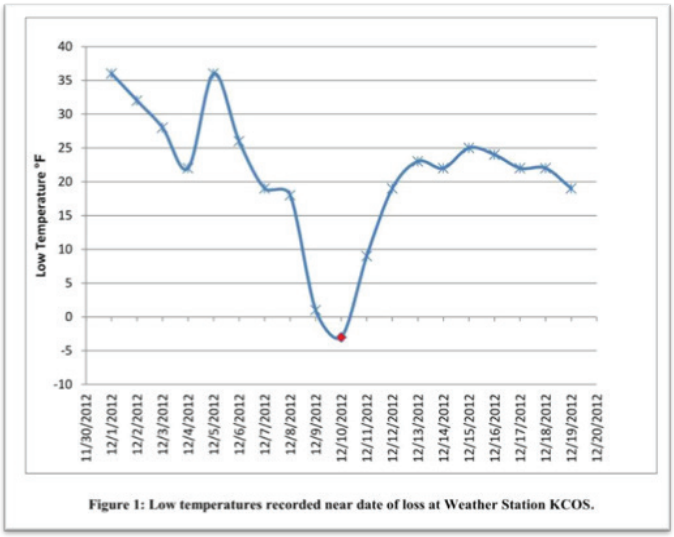

Figure 1
Freezing weather conditions corresponding to reported date of loss.

above freezing — and thawing of the plumbing components has occurred, allowing water to leak out and the plumbing failure to be discovered.

Upon first discovery of a failed plumbing component, it may appear that it failed due to a defect in the product or its installation; however, the weather conditions that were present close to the date of loss need to be evaluated in order to understand whether environmental conditions may have contributed to the loss due to freezing and over pressurization of the system.

When water freezes (changes its physical state from liquid to solid ice), it expands in volume by approximately 9%, according to the International Association for the Properties of Water and Steam. Therefore, any closed plumbing system that experiences freezing conditions will see significant increases in water pressure due to volumetric expansion created by the ice formation. The expansion of water to ice can rupture a plumbing component simply due to the change in volume increasing water pressure. A classic example of over-pressurization and failure due to excessive hoop stress is the copper pipe as shown in **Figure 2**. (Note: Hoop stress is the stress exerted circumferentially to the pipe cross section due to internal pressurization.)

3) *Water Main (domestic or well)*: Plumbing components are typically part of a plumbing system that begins at the water main. Therefore, the source of the water supply should be evaluated if it is suspected that any external factors may have contributed to a failed plumbing component. Interviewing the insured and neighboring properties can help to establish if any variance to the water pressure was observed prior to the loss event. If the building water supply lacks a water pressure reducing valve (WPRV), or other pressure regulation device, simple testing using a portable water pressure test gauge may be conducted to directly determine if the supply pressure is within the operating limits of the failed plumbing component.

4) *Water Pressure Reducing Valve*: The first plumbing component off the water main and into the property is typically a WPRV. The presence of a WPRV is an indication that the plumbing system is within a municipality providing water pressure above 80 pounds per square inch gauge (psig). A WPRV is typically required by the Authority Having Jurisdiction (AHJ) when the watermain pressure exceeds 80 psig, as it cannot be ruled out that elevated pressure will have damaging effects to plumbing system.

When investigating a property with a WPRV installed, the inlet and outlet pressures of the WPRV should be checked to ensure it is regulating the water supply pressure. In addition, when conducting pressure testing, the residence should be allowed to "dwell" for a period of time to determine if the WPRV allows the residence's pressure to slowly rise. A test that results in an immediate pressure reading of 60 psig may show pressures exceeding 80 psig after a sufficient amount of time has elapsed. In some instance, the property's WPRV may not be adjusted properly or possibly defeated by over-tightening of the adjustment screw on the WPRV. If the WPRV is malfunctioning, disassembly and examination of the valve's internal components for damage, wear, and contamination should be performed.

5) *Expansion Tanks*: Thermal expansion tanks are required in systems having a check valve or backflow preventor to regulate thermal expansion. Expansion tanks are equipped with a pressurized air bladder that allows room for thermal expansion of the water within the plumbing

Figure 2
Failed copper pipe "fish mouth."

system and prevents the water pressure from increasing when the water is heated. These devices are becoming more common as AHJs adopt more recent versions of the Uniform Plumbing Code[1]. Thermal expansion tanks are typically mounted on the cold (inlet) side of boilers and water heaters If a thermal expansion tank bladder loses its air pre-charge, the tank may become water solid and cease to perform its function of protecting against thermal expansion. This allows the water pressure in the residence to spike when heated, and could cause the weak link in the plumbing system to decouple or fracture due to excessive stress.

6) *Exterior Construction (thermal barrier)*: The exterior of the property should be checked for integrity, especially if freezing is suspected as a potential cause of the loss. A thermal imaging camera or infrared thermometer can aid in finding deficiencies in property insulation and/or construction and will also help identify structures that are affected by moisture from the water loss. Often when failed plumbing components are contained within walls and not readily visible, a thermal imaging camera can pinpoint the origin of the outdoor air infiltration intrusion while identifying the cause of the water loss.

7) *Identifying and Documenting the Origin of the Water Loss*: As mentioned above, the origin of the plumbing failure in many cases will be obvious to the initial responder(s), as leaking/spraying water is often easy to detect and trace to the failed component of the plumbing system. If you are not the initial responder (and the origin of the failed plumbing components has not been determined), the system can be cycled back on for detection of the water leak (with proper authorization). As an alternative, pressurized air can be substituted into the plumbing system for leak detection as a method to minimize additional water loss to the property. Once the origin of the water loss has been determined, many factors should be considered to fully document the operating environment of the failed component, such as:

- Documentation of the installation to ensure that it meets the AHJ's code requirements. Code compliance will depend on the adopted code that was in place at the time of the installation.

- Documentation of the service environment for factors that could be causal to the loss. Nearby stored chemicals and harsh working environments can accelerate the failure of many plumbing components.

8) *Preservation of Evidence*: Every effort should be taken to minimize alteration of the evidence. If undocumented evidence is altered, the integrity of the investigation is compromised. For example, a residence's WPRV is to be removed because of concern about over pressurization of a plumbing system, ensuring the position of the adjustment screw as unaltered is critical. Therefore, photographs, measurements, and indexing the head of the adjustment screw with a marker would ensure that the evidence has not been altered from its original position. Guidance for preservation of evidence is provided in many industry guides and standards. Below is a partial list of references that offers guidance on the collection and preservation of evidence:

a. National Fire Protection Association (NFPA) 921, "A Guide to Fire and Explosion Investigations[2]."

b. American Society for Testing and Materials (ASTM) E 1492, "Receiving, Documenting, Storing, and Retrieving Evidence in a Forensic Science Laboratory[3]."

c. ASTM E 860 "Standard Practice for Examining and Preparing Items That Are or May Become Involved in Criminal or Civil Litigation[4]."

d. ASTM E 1188, "Collection and Preservation of Information and Physical Items by a Technical Investigator[5]."

e. ASTM E 1459, "Standard Guide for Physical Evidence Labeling[6]."

Sometimes, it is not possible to maintain the site or preserve evidence as it may become inherently altered through the actions of collecting it. Therefore, it is important to put all potential liable parties on notice and obtain an agreement among parties on a protocol for evidence collection.

An investigator faced with this situation must use thorough and careful documentation of the configuration, position, and installation condition of the evidence to allow for accurate reconstruction and testing at an external facility. Methods can be implemented to document the as-found condition for use in later reconstruction. One example would be the use of "witness marks." For example, a paint pen or other marking device may be used to document cut locations on piping or to document thread engagement on a threaded connection. Tape measures,

rulers, and other measuring devices may also be used in photographs and/or video to document conditions such as thread engagement, spacing between components, gaps, component sizes, handle positions, etc.

Thoughtful collection of the evidence is also a key factor. If the evidence is to be later tested, consideration must be given to the requirements of the testing. Often, evidence is collected in a manner that provides insufficient material to connect exemplar components for testing. In this case, the engineer or technician performing the testing may be unable to test the component or may face spoliation concerns as a result of further alteration to adapt the component to the testing environment.

A common example is pipe length — when a component is removed from a plumbing system, enough pipe must be available on either side of the subject component and adjacent fittings (approximately 4 to 6 in.) to allow joining of the evidence to the test environment without disturbing the existing connections that may be related to the loss. ASTM E1492: "Receiving, Documenting, Storing and Retrieving Evidence in a Forensic Science Laboratory" provides valuable guidance for preservation and collection of evidence.

Testing

It is common to test plumbing components to determine specific information related to the mode of failure. Testing the component can be done in the field or in a lab environment and may help to determine where a leak is occurring and at what volume for a given water pressure. Testing can also assist in determining whether the mode of the failure was related to a product defect, installation defect, environmental condition, maintenance, or wear and tear. Testing falls into two main categories: non-destructive and destructive.

1. *Non-Destructive Testing*: When a component suspected of causing a plumbing loss is collected, the immediate cause of the component failure may not be obvious. Non-destructive testing is conducted to help identify the point of failure and assist in determining the mode of failure. Investigators must be careful to maintain non-destructive practices during their work.

ASTM E 860-07, "Standard Practice for Examining and Preparing Items That Are or May Become Involved In Criminal or Civil Litigation" established guidelines for examination and testing of items that "are or may be reasonably expected to be the subject of civil or criminal litigation." As discussed in the standard, the individual conducting the examination should document "the nature, state, and condition of the evidence by descriptive, photographic, or other suitable methods…" This work may utilize methods that do not require physical manipulation of the evidence, such as taking notes, drawing diagrams, taking photographs, etc. With tablet computers becoming increasingly common, it is often possible to take photographs and annotate them directly during the initial inspection.

If destructive testing, which is discussed in the subsequent section, were to take place without the appropriate parties being notified and having a chance to witness said testing, spoliation of the evidence may be considered to have taken place — and the investigation may be compromised. As defined in ASTM E 860, spoliation of evidence is "the loss, destruction, or material alteration of an object or document that is evidence or potential evidence in a legal proceeding by one who has the responsibility for its preservation. Spoliation of evidence may occur when the movement, change, or destruction of evidence or alteration of the scene significantly impairs the opportunity of other interested parties to obtain the same evidentiary value from the evidence as did any prior investigator."

2. *Destructive Testing*: Non-destructive examination and testing of evidence may result in undetermined conclusions as to the cause of the plumbing failure. If the cause of the failure cannot be determined through non-destructive means, it may be necessary to progress to destructive testing. As discussed in ASTM E 860, if destructive testing is determined to be necessary, the investigator should notify the client, recommend the client of notification of other interested parties, and recommend to the client that other interested parties be given the opportunity to participate in the testing.

When conducting destructive examination, a written protocol should be established beforehand that clearly lays out the steps to be performed and how they are to be performed. A clear, detailed protocol removes ambiguity and provides all interested parties with a clear understanding of what to expect at the time of the examination.

The protocol should include all steps anticipated to be conducted, including photographing of the evidence and chain of custody forms, dimensional measurements, functional testing such as pressurization (and what pressures will be used), etc. The protocol should be circulated to all interested parties in advance of the testing to allow for

careful consideration and potential alteration of the protocol (if mutually agreed upon). During destructive testing, deviation from the proposed protocol may be necessary, depending on the progression of the testing.

If deviation from the protocol is identified, all parties should be involved in discussing and documenting the change in protocol. All dissenting opinions — and the reason for the dissention — should be documented and given careful consideration. It may be necessary to cease the destructive examination and reconvene at a later date for continuation if a deviation or alteration is not agreed upon or if additional equipment is determined to be necessary. Additionally, the destructive exam may be ceased if it is determined that another potentially interested party, such as a subcomponent part manufacturer, is identified during the initial examination. Exclusion of an involved party is likely to raise spoliation issues during a destructive examination if the involved parties are not allowed the opportunity to participate in the exam.

Engineering Analysis

Once the investigation is complete and all testing and examination has reached its conclusion, it is time to determine the cause of the loss as it relates to the product failure. It is important to remember that just because the "why" of the product failure has been determined, the "who" may not be determined. It is not enough to determine the physical reason for the failure; the investigator must also determine what actions (or lack of actions) led to the failure. The causes of a product failure may be attributed to:

1. *Product Defect*: A plumbing component may be defective in many ways but can generally be categorized as either a "design defect" or "manufacturing defect."

   a. A design defect is a defect within the design of the component that resulted in the product failure. For example, dezincification is a well-known and well-understood phenomenon where a brass plumbing component with high-zinc content may fail due to the zinc being preferentially leached from the brass. The leaching of the zinc results in voids and brittleness where the zinc is now absent. If the design of the component was to use high-zinc brass alloy, the product defect would be attributable to a design defect because it is well known that high-zinc brass alloys may undergo dezincification. Plumbing components manufactured in large quantities with a "design defect" should experience systemic failures with multiple instances of failure occurring throughout the product's distribution.

In some cases, the design defect may be related to lack of critical warnings that would help prevent misuse or improper installation of a product. Toilet supply lines with polymer ballcock nuts are an example of a product design that evolved over the years from having no warnings, to having a "Hand Tight Only" warning imprinted on the face of the nut as shown in **Figure 3**. Due to the low strength of the polymer nut, over-tightening can cause the ballcock nut to fail over time at the last thread root. Even with the warning "Hand Tighten Only," it is not uncommon to see tool markings on the exterior of the polymer nut, indicating an improper installation (i.e., an "installation defect" discussed later) where the nut was potentially overtightened. Witness marks indicating that a tool was used on the polymer ballcock nut is also shown in **Figure 3**.

   b. A manufacturing defect is simply an imperfection within the component that was the result of the manufacturing process. For example, if the design of the brass product discussed above specified a low-zinc brass alloy but high-zinc alloy was utilized during manufacturing, then the product defect is considered to be a "manufacturing defect" because the part was not manufactured to its design specification.

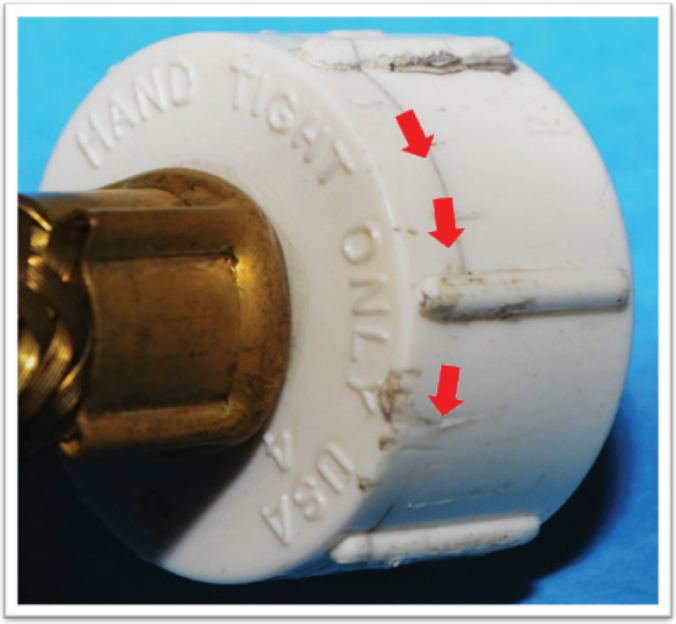

Figure 3
Failed ballcock nut. Warning: "Hand Tight Only."

2. *Installation Defect*: Installation defects are common and relatively self-explanatory. An installation defect is a defect in the installation of the component that directly leads to the loss. For example, toilet supply lines often use polymer ballcock nuts that explicitly state that they are to be hand-tightened only and to not utilize tools as a tool may overtighten the fitting. If the fitting is overtightened, initiation cracks may develop that will be affected by creep stress during service and ultimately result in rupture of the ballcock fitting. Tool marks on the ballcock nut may be a good indicator that the nut was tightened more than "hand-tight." If it can be determined that a tool was used, it may support fractography of the fracture surface to investigate the cause of the loss as an installation defect resulting from the installer's failure to follow the manufacturer's published requirements.

3. *Environmental Conditions*: Component failures due to environmental considerations are often referred to as "an act of nature" or "an act of God." An example of a failure due to environmental conditions may be corrosion of a steel or iron fitting due to proximity to the ocean and salt-laden air. However, the investigator must not be too quick to deem a product failure "an act of nature."

If it is foreseeable that component may be used in the subject environment and that component failed because of said environment, then the component failure may be attributed to a "design defect" as previously discussed. For example, polybutylene tubing was the subject of a class-action lawsuit that resulted in the stoppage of all production of polybutylene piping in 1995. Polybutylene was used in many residences in lieu of copper; however, polybutylene became embrittled due to common water treatment chemicals, such as chlorine. Due to the embrittlement, polybutylene began to fracture and resulted in many water losses throughout the country. The failure of polybutylene was considered a design defect because polybutylene was susceptible to chemicals that were known to be present in the environment for which it was intended.

4. *Lack of Maintenance*: Lack of maintenance, or lack of care, indicates the product failed due to the absence of expected and/or routine action. Similar to environmental conditions, an investigator must not be too quick to deem a product failure "an act of nature" or "long-term wear-and-tear" if the loss was due to a lack of expected maintenance activities. A common example of lack of maintenance is water heater failure due to a consumed or depleted anode rod. Anode rods are installed in traditional tank water heaters to provide corrosion protection. The anode rod is typically made of zinc and is preferentially degraded by residential water chemistries. Once an anode rod is depleted, corrosion of the water heater itself may progress at an accelerated rate. Because of this, water heater manufacturers provide maintenance instructions on inspection and replacement of the anode rod.

5. *Long-Term Wear-and-Tear*: Sometimes, a component fails because it has reached the end of its designed useful life. In this situation, the component that failed is considered to not have any defects, did not fail due to environmental conditions, and did not fail due to a lack of maintenance. For example, boilers have a finite life expectancy, even when routinely maintained and kept in good working order. The American Society of Heating, Refrigeration, and Air-Conditioning Engineers (ASHRAE)[7] lists the average life expectancy of an electric boiler as 15 years. A water loss that takes place with an electric boiler that is 25 years old may have failed as a result of degradation of non-replaceable or non-maintainable components that are beyond their published service life.

Conclusions

The forensic investigation of plumbing failure events involves more than just a visual examination and testing of a failed component. The investigation should go beyond a simplistic analysis and consider the system in which the failed component was installed, the environmental factors that may have affected the failure mode, as well as consideration for the age and maintenance provided to the failed plumbing component.

Failure to perform a complete and thorough analysis will ultimately hinder or prevent a determination of the proper root cause of the loss. Furthermore, the lack of a complete and thorough analysis serves to make this analysis vulnerable to arguments that the appropriate burden of proof has not been properly established. Once all factors of a plumbing failure have been carefully reviewed and analyzed, the forensic investigator should develop appropriate testing protocols based upon scientific principles to properly analyze the subject plumbing component(s) and to arrive at determining the root cause of the loss.

References

1. Uniform Plumbing Code. 2018. Section 608.3. Expansion Tanks, and Combination Temperature and Pressure-Relief Valves.

2. National Fire Protection Association. 921. 2017.

Chapter 17. Guide for Fire and Explosion Investigations. Physical Evidence

3. American Society for Testing and Materials. E 1492. 2017. Standard Practice for Receiving, Documenting, Storing, and Retrieving Evidence in a Forensic Science Laboratory.

4. American Society for Testing and Materials. E 860-07. 2013. Standard Practice for Examining and Preparing Items That Are or May Become Involved in Criminal or Civil Litigation.

5. American Society for Testing and Materials. E 1188-11. 2017. Standard Practice for Collection and Preservation of Information and Physical Items by a Technical Investigator.

6. American Society for Testing and Materials. E 1459-13. 2018. Standard Guide for Physical Evidence Labeling and Related Documentation

7. American Society of Heating, Refrigeration, and Air-Conditioning Engineers. 2015. HVAC Applications. Table 4. Comparison of Service Life Estimates.

FE Evaluation of Landowner Dispute Following Retaining Wall Failure

By Rune Storesund, DEng, PE, GE (NAFE 474S)

Abstract

This forensic engineering evaluation addressed a dispute between two neighboring landowners regarding cost-sharing associated with the repair of a failed retaining wall dividing the two properties. Qualitative forensic analyses considered both demand-based (i.e., lateral earth pressures, pore pressures, surcharge) and capacity-based (i.e., materials, configuration, drainage) factors to illustrate influence both parties had on the magnitudes of these loads. This paper outlines the qualitative forensic analyses that aided in resolution of the dispute before trial.

Keywords

Lateral earth pressure, property line, retaining wall, soil movement, forensic engineering

Setting/Context

This case involves a dispute between two neighboring property owners regarding costs associated with replacement of a compromised retaining wall. The orientation and location of the retaining wall relative to the two properties is shown in **Figure 1**. The two properties are situated near the top of a gradually sloping topographic knoll. The defendant's parcel is situated up-slope of the plaintiff's property.

The original retaining wall was constructed from pressure-treated lumber. A chain link fence was also physically attached to the wooden retaining wall. The retaining wall, which is approximately 3.5 ft in height, is situated immediately adjacent to the property line between the two neighboring properties (**Figure 2**). The area in front of the retaining wall and behind the retaining wall were used primarily as parking areas — both before and after the replacement of the retaining wall. No design documentation or as-built information was available for the original retaining wall. Additionally, the retaining wall had been fully removed and replaced prior to the forensic engagement. Some photographic information was available, but no photographic information was available relative to the foundation conditions of the original retaining wall, which precluded meaningful structural analyses of the wall.

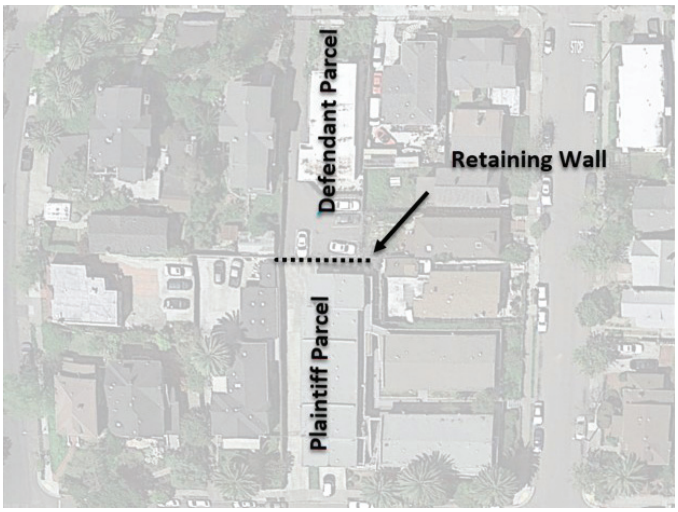

Figure 1
Site plan showing the location of the retaining wall in question relative to the plaintiff and defendant parcels.

Extension cracks were visible in the defendant's parking area (**Figure 3** and **Figure 4**). These cracks formed as a result of translation/rotation of the retaining wall, with the top of the retaining wall displacing away from the defendant's property toward the plaintiff's property. Drain

Figure 2
Photographs of the original wood retaining wall (2017).

Rune Storesund, DEng, PE, GE, 154 Lawson Road, Kensington, CA 94707, 510-526-5849; rune@storesundconsulting.com

holes to prevent hydrostatic pressure behind the wall were also observed at the base of the retaining wall (**Figure 5**).

Figure 6 shows the exposed soil conditions following removal of the distressed retaining wall in 2018. These soils appear to consist primarily of cohesive clayey soils, which have the ability to "stand" with a near vertical cut.

Figure 3
Extension cracks were visible in the defendant's parking area as a result of rotation of the retaining wall toward plaintiff's property.

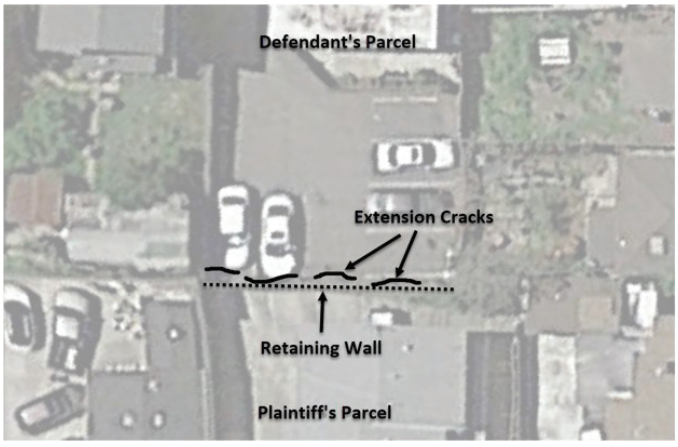

Figure 4
Location of extension cracks relative to the location of the retaining wall.

Figure 5
Drain holes in the original retaining wall to facilitate drainage behind the wall and mitigate potential for hydrostatic pressure loads on the wall.

The retaining wall was flagged as needing repair/replacement by the plaintiff's insurance company during a routine property inspection. The plaintiff made several attempts to contact the defendant, but no response was received. Under pressure to complete the repairs to satisfy the insurance company's concern, the plaintiff initiated demolition of the original retaining and installation of a new, reinforced masonry concrete block, retaining wall.

The plaintiff did not get a building permit for the construction of the replacement retaining wall. As a result, during the course of construction, the City Building Department visited the site and issued a notice of violation for performing work without a permit. The plaintiff then retained an engineer to develop plans and obtained a building permit to bring the work up to (and in compliance with) the local building code. The work started in late 2017, and was completed in 2019.

Approximate Timeline

A timeline of significant events is presented below. The structures on the two parcels were constructed at approximately the same time (early 1960s). The properties were more recently acquired by the defendant (early 2000s) and plaintiff (late 2000s).

- Early 1960s: Structures constructed on both the plaintiff and defendant's parcels with associated site grading.
- Early 2000s: Defendant purchases parcel and rental complex.

Figure 6
Exposed soil conditions following removal of the distressed retaining wall in 2018. Steel posts are bollards.

- 2005: Building department records indicate replacement of a 3-ft-tall retaining wall
- Late 2000s: Plaintiff purchases parcel and rental complex.
- 2016: Plaintiff's insurance company flags condition of retaining wall; plaintiff attempts to contact defendant to cost-share new retaining wall construction cost.
- Late 2017: Plaintiff initiates construction of new retaining wall without co-operation by defendant after multiple failed contact attempts. Plaintiff requests cost-sharing of the costs associated with the new retaining wall as it is located on the property line and benefits both parties.
- Early 2018: Construction of new wall halted by local building department due to lack of building permit.
- Mid 2018: Engineering completed and building permit obtained.
- Late 2018: Construction resumes.
- Early 2019: Construction completed. Lawsuit filed against defendant.
- August 2019: Expert retained by plaintiff.
- September 2019: Case settles two days after plaintiff expert deposition.

Plaintiff Contentions

The primary motivation for the plaintiff was to cost-share in the construction of the new retaining wall as it offered benefits for both parties. The plaintiff also noted that there were visible signs of distress that were unaddressed by the defendant and exacerbated the deterioration of the retaining wall. For the purposes of the litigation, the following claims were made by the plaintiff in formal court filings:

- In or around March 2016, the land and soil on the defendant's property moved, cracked the parking lot, opened a large hole that ran the rear boundary with plaintiff's property, damaged the fence, and resulted in a landslide onto plaintiff's property;
- At the aforementioned time and place, defendants negligently maintained, controlled, and managed their property and knew (or should have known) that the landslide resulted in an unreasonable risk of harm to plaintiff's property, to persons on plaintiff's property, and to those persons' personal property if not properly corrected or controlled.
- Defendants negligently failed to correct or control the landslide and soil subsidence, all of which caused the damages to plaintiff as described above.
- As a proximate result of the negligence of defendants, plaintiff's property was damaged and plaintiff incurred construction costs to repair the landslide and replace the rear fence and retaining wall that separates plaintiff's property from defendant's property.
- Pursuant to civil code, defendants are presumptively liable for at least 50% of the reasonable costs to construct the new fence and retaining wall.

Defendant Contentions

No formal rebuttal was provided by the defendant; however, the general response provided by defendant's counsel was that the defendant was "in no way responsible for" or owed any obligation to replacement of the retaining wall. The retaining wall was likely poorly constructed and provides benefit to the plaintiff. As such, the plaintiff should bear the full cost of the retaining wall, with no financial contribution from the defendant.

Forensic Evaluation

Following engagement by the plaintiff, the author initiated a forensic evaluation to understand and assess the merits of the contentions from both the plaintiff and defendant. The evaluation consisted of the following steps:

1. Collect and review the available discovery documentation;
2. Site visit to observe the site context and location of the retaining wall in question;
3. Review available historic aerial imagery to discover site changes (if any);
4. Characterize the suite of demands imposed on the

retaining wall that impact performance;

5. Evaluate factors impacting the capacity of the retaining wall; and

6. Develop opinions with regards to retaining wall performance and merit of plaintiff and defendant contentions.

Following completion of the forensic evaluation, the author participated in a deposition where the forensic evaluation process was outlined as well as the findings. These outcomes are discussed in more detail below.

Available Discovery

The available discovery consisted primarily of photographs taken of the distressed retaining wall in 2017, prior to start of construction and photographs taken during the course of construction of the replacement retaining wall in 2018 and 2019. The full inventory of discovery documents included:

- Pre-construction retaining wall photographs;
- Photographs taken during the course of the construction;
- Plaintiff property building permit history from local building department (Report of Residential Building Record);
- Plaintiff's Notice of Violation for the 2018 retaining wall work;
- Copies of engineering plans and calculations in response to the 2018 Notice of Violation; and
- Construction Formwork Certification by licensed land surveyor, which included formal delineation of property boundaries.

Figure 7
Example "street view" image available from Google Maps (note available timeline of photos in upper left).

Site Visit

A site visit and meeting with the plaintiff, the plaintiff's contractor, and the plaintiff's property manager occurred immediately following engagement in the case. This site visit allowed for a visual inspection of the topographic setting between the two properties, a verbal accounting of the sequence of interactions between the plaintiff and the defendant by the plaintiff, and description of conditions encountered by the contractor during the course of construction. Additionally, available imagery (aerial and "street view" on Google) were ground-truthed.

Available Imagery

Aerial imagery was available via Google Earth's "History" tool, which provided select aerial images between 2019 and 1993. Supplemental aerial images were obtained from a commercial aerial imagery company, which had images for the area between the 1950s and 2019.

In addition to aerial images, "street view" images (**Figure 7**) were also available from Google Maps, which allowed views of the retaining wall by looking from the street down the driveway toward the retaining wall in question. While this data is fairly recent, extending back to about 2010, it provides a valuable high-resolution perspective that is not available with conventional aerial imagery.

Retaining Wall Imposed Loads

The performance of a retaining wall can be characterized by a number of factors. For this forensic evaluation, lateral displacement (either through translation or rotation) was the primary performance metric considered. Lateral displacements of retaining wall can occur as the result of demands (or loads) applied. The greater the applied load, the greater the potential for lateral displacements.

Figure 8 shows a conceptual overview of typical loads imposed on retaining walls that impacts lateral

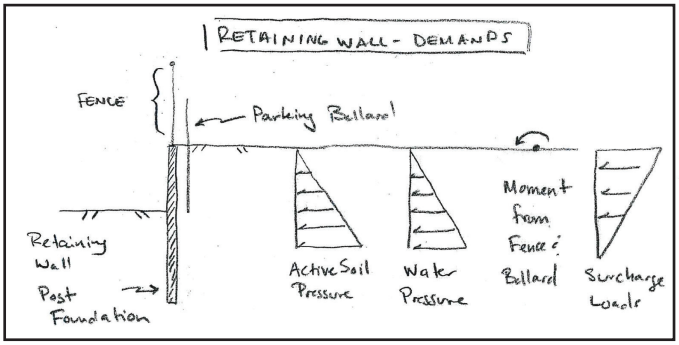

Figure 8
Conceptual overview of loads imposed on a retaining wall impacting lateral displacement (sketch by author, conceptual only).

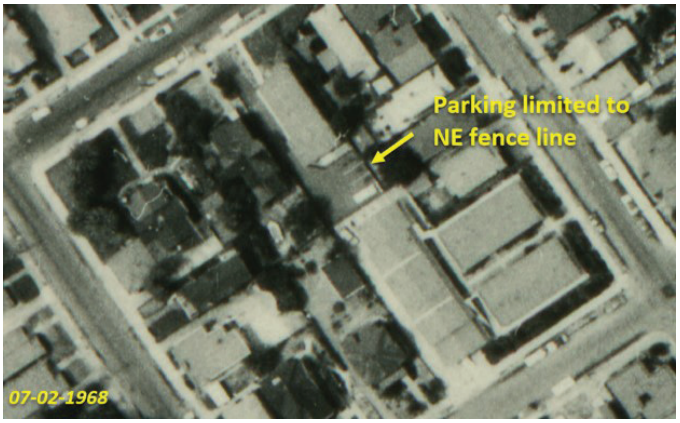

Figure 9
Original configuration of parking spaces based on aerial imagery from July 1968.

displacement(s) and include lateral earth pressures from retained soils and water (hydrostatic) pressures. Additionally, for this setting, the presence of a parking lot and fence attached to the retaining wall adds surcharge loading to the wall from parked vehicles and a moment load to the top of the wall from the fence when the fence is perturbed by either wind or lateral loading from vehicles. Note for this particular case, the configuration of the retaining wall results in all the imposed loads or "demands" being initiated on the defendant's parcel.

A review of the aerial imagery as well as the street view photos established that the area immediately behind the retaining wall was delineated as parking area on the defendant's property. The aerial imagery establishes the original (early 1960s) parking configuration (four parking spaces) as being limited to the northeast (NE) fence line (**Figure 9**). By the early 2000s, additional parking stalls were observed in the aerial images. **Figure 10** shows an

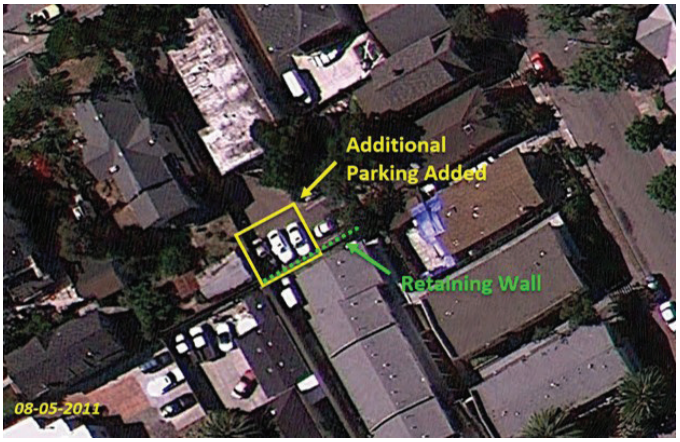

Figure 10
Additional parking spaces added on the defendant's parcel immediately adjacent to the retaining wall.

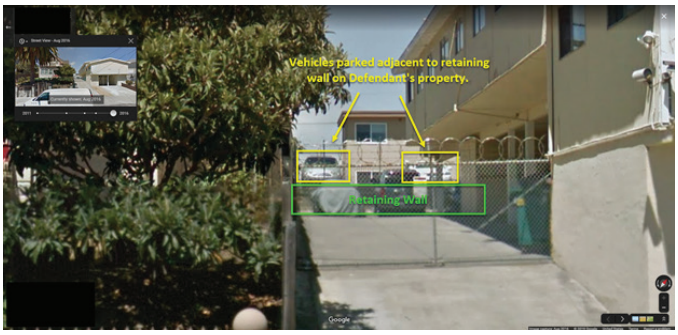

Figure 11
Vehicles parked immediately adjacent to the retaining wall exerting a surcharge load.

aerial image from 2011 with a total of four vehicles parked adjacent to the retaining wall on this particular day. **Figure 11** documents vehicles parked immediately adjacent to the retaining wall from a street view perspective.

Vehicles have the ability to "bump" into both the bollards along the alignment of the retaining wall as well as the fence secured to the retaining wall, resulting in moment loads on the wall. These moment loads directly impact the lateral displacements of the retaining wall. A review of the available photos (such as **Figure 6**) did not reveal the presence of any curb stops in the parking spaces that would have limited the ability for vehicles to accidentally bump into the bollards or fence as well as imposing a "setback" between the parked vehicle and the retaining wall, thereby reducing the magnitude of the surcharge load from the vehicle and the retaining wall.

In addition to the surcharge and moment loading onto the retaining wall from the defendant's property, the observed expansion cracks enabled water to infiltrate the asphalt concrete paving and increase the hydrostatic loading on the wall. While the hydrostatic loading was likely not significant, the cohesive/clayey soils would be subject to increased volumetric expansion as a result of increased moisture content. This volumetric expansion results in a direct increase in lateral earth pressures on the wall.

Retaining Wall Capacity

The ability to resist the imposed loads is the capacity of the retaining wall. The resistance is comprised of both the structural integrity of the retaining wall as well as the passive and soil bearing pressures (**Figure 12**).

Due to the lack of information, it was not possible to ascertain the actual structural integrity of the wall in 2016/2017. The available photographs suggest that the retaining wall had sufficient integrity to behave as a "unit."

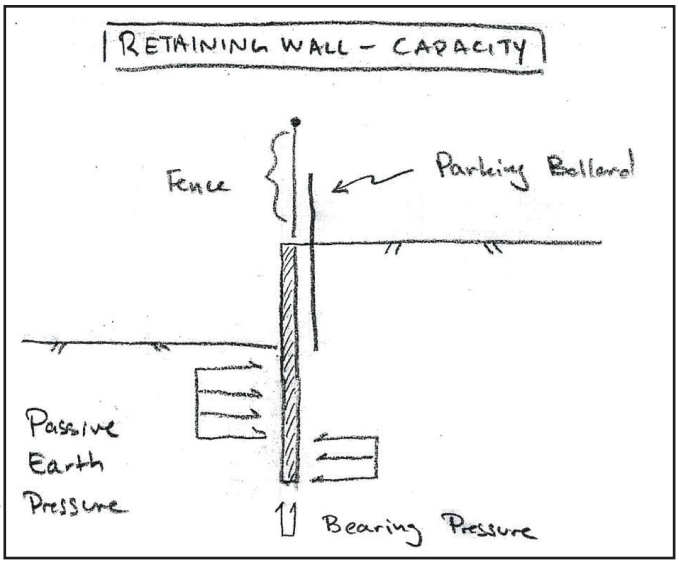

Figure 12
Primary retaining wall capacity elements include passive earth pressure, bearing pressure, and structural integrity of the wall (sketch by author, conceptual only).

However, for the purposes of this qualitative evaluation, the actual condition of the wall is ultimately not important. The inquiry here is to illustrate the contribution both parties have to the actual performance of the wall and that both parties receive benefit from the structure.

Unlike the retaining wall demands, the soil passive and bearing pressures are largely derived from the Plaintiff's parcel. A review of the available aerial and 'street view' images revealed no site modifications that may have altered the capacities of the retaining wall from the Plaintiff's parking area. Additionally, discussions with the property owner and property manager confirmed no known site modifications in the plaintiff's parking area adjacent to the retaining wall.

FE Opinions

The presence of the retaining wall provides a grade separation between the plaintiff's and defendant's properties. While offering some benefit to the plaintiff, and counter to the defendant's claim of the retaining wall offering no benefit, the retaining wall, in fact, offers significant benefit is provided to the defendant. Without the retaining wall, the defendant would actually lose parking area as a "stable" slope would need to be graded, sloping up from the plaintiff's parcel to the defendant's parcel at a slope on the order of 2.5 horizontal to 1 vertical (**Figure 13**). Thus, a significant benefit is provided to the defendant.

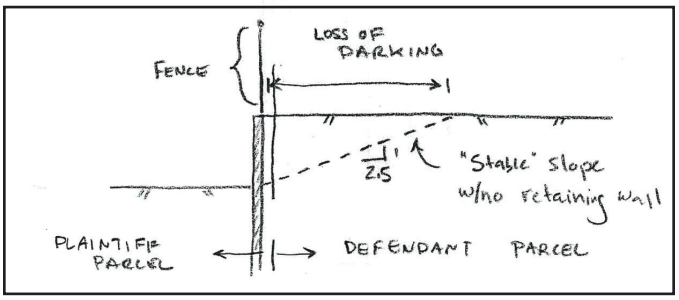

Figure 13
Retaining wall provides the defendant the benefit of parking space that would be "lost" if the retaining wall were removed and the transition graded to a "stable" slope (sketch by author, conceptual only).

The retaining wall is situated on the property boundary between the plaintiff and the defendant (**Figure 14**).

The majority of the demands imposed on the retaining wall originate from the defendant's parcel. The plaintiff has no ability to moderate these loads as they are not situated on his property.

As a result of the retaining wall demands being situated on the defendant's property, there were a number of measures available to the defendant to minimize degradation of the retaining wall integrity. These measures include:

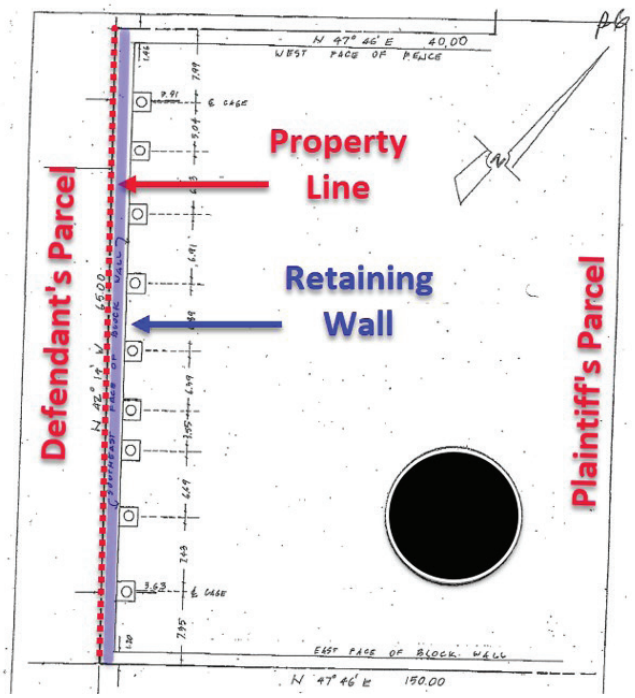

Figure 14
Copy of construction formwork survey showing the retaining wall relative to the property line.

- The observed expansion cracks were indicators of potential loss of wall integrity, requiring a heightened level of mindfulness, monitoring, and care by the defendant to ensure additional loss of integrity from excessive demands does not occur;

- The observed expansion cracks allow for the infiltration of water into the soils behind the retaining wall. These expansion cracks could have been sealed by the defendant to limit the quantity of water infiltrating the soils, which in turn, would limit the potential for increased hydrostatic pressures and the potential for increased lateral soil pressures due to swell of the cohesive clayey soils;

- The observed expansion cracks were an indicator of lateral displacements of the retaining wall. The defendant had the ability to limit the magnitude of surcharge loading on the retaining wall by eliminating or offsetting the parking stalls;

- The defendant had the ability to eliminate 'bumping' of the parking bollards and/or fence on the retaining wall by installing curb stops to enforce a suitable offset between vehicles and the fence/bollard;

The plaintiff, in their complaint, referred to "landslide[1] and soil subsidence[2]." These terms have specific technical meanings. A landslide is "the movement of a mass of rock, debris, or earth down a slope." Subsidence is settlement as a result of lowering the groundwater table. Neither of these mechanisms were applicable in this case. Rather, this was the result of the plaintiff's attorney not being familiar with these technical terms and attempting to describe the observed phenomena.

In summary, the forensic engineering evaluation found that the plaintiff's allegation that actions (or inactions) by the defendant exacerbated the distress of the shared retaining wall is valid and supported by the case facts. As a result, the defendant does receive benefit from the shared retaining wall and — from the perspective of received benefits — should cost share in the replacement of the retaining wall.

It was determined costs associated with the Notice of Violation by the local building department should not be shared and should be the responsibility of the plaintiff. All other costs, including engineering design, building permit fees, inspection fees, and construction costs are eligible for cost-sharing.

Conclusion

This case involves a dispute between two neighboring property owners regarding costs associated with replacement of a compromised retaining wall. The retaining wall was flagged as needing repair/replacement by the plaintiff's insurance company during a property inspection.

The plaintiff made several attempts to contact the defendant, but no response was received. Under pressure to complete the repairs to satisfy the insurance company's concern, the plaintiff initiated demolition of the original retaining and installation of a new, reinforced masonry concrete block, retaining wall. Litigation for cost-sharing of the incurred construction costs initiated immediately following completion of construction in early 2019.

The forensic engineering evaluation was initiated several weeks prior to trial and considered both demand-based (i.e., lateral earth pressures, pore pressures, surcharge) and capacity-based (i.e., materials, configuration, drainage) factors.

Prior to forensic engagement, the opposing party was unwilling to settle. Following completion of these forensic analyses, the case settled in less than two days, due to the clear delineation of causative factors.

References

1. Crudent, D.M. 1991. A Simple Definition of a Landslide. Bulletin of the International Association of Engineering Geology, No. 43, pp. 27-19.

2. Peck, Ralph, B., Walter E. Hanson, Thomas H. Thornburn. Foundation Engineering. Second Edition. John Wiley & Sons. Toronto. 1974.

Use of the Repairability Assessment Method for Evaluating Asphalt-Composition Shingle Roof Repairs

By Chad T. Williams, PE (NAFE 937A)

Abstract

Each year, wind and hail cause billions of dollars in damage to asphalt shingle roofs of residential and commercial buildings. In some instances, the damage is clearly apparent to justify replacement of the entire roof surface. In other instances, the damage is more difficult to ascertain, leading to divergent opinions on whether the roof should be fully replaced or have more economical, localized repairs conducted. Historically, methods used to evaluate whether localized shingle repairs can be successfully and adequately performed have been done using a variety of approaches that rely on inconsistent and subjective analysis. This paper offers an alternative approach — the Repairability Assessment method. In this approach, the repairability of the roof is determined by evaluating whether repair actions will propagate damage. Evaluators using this method can calculate a damage rate and damage ratio that will provide them with a quantitative and repeatable means to guide their repairability assessment.

Keywords

Asphalt-composition shingles, roofing, repairability assessment, forensic engineering

Introduction

Every year since 2008, thunderstorms generating tornadoes, large hail, and damaging straight-line winds result in public and private insurance payments that top $10 billion annually[1]. These damaging wind and hail conditions can wreak havoc on the asphalt-composition shingle roofs of residential and light commercial buildings. The challenge for owners and the insurance industry is understanding to what extent these types of roofing surfaces have been compromised. In some instances, the damage is clearly apparent to justify replacement of the entire roof surface. In other instances, the damage is more difficult to ascertain, leading to divergent opinions on whether it is more feasible to do localized repairs or if (based on the asphalt-composition shingles' condition) the roof's surface needs to be removed and replaced in its entirety.

This decision on whether to repair or replace the asphalt-composition shingle roof surfaces commonly involves a licensed professional engineer, who will have the expertise to properly evaluate, assess, and recommend whether a repair is feasible. Depending on the roofing system, type and condition of the asphalt-composition shingles, material availability, and other local or environmental factors, the engineer can determine the effectiveness of repair actions versus a full replacement.

A repair to an asphalt-composition roof, if feasible, may provide a cost-effective means to bring the roof to full functionality while ensuring it remains durable and reliable through its original intended service life. However, the ease with which such repairs can be accomplished and still be in compliance with manufacturer specifications, building codes, or other applicable requirements is often misjudged. Thus, determining the repairability of the roof requires a thorough evaluation of the structure, the condition of the existing materials, the impact of the repair process, and the complexity of the reconstruction task.

Asphalt-composition shingle roofs, while durable and long lasting, can be challenging to repair, especially as they age. However, even newer and tighter adhering seal strips can also present challenges when repairing relatively new roof surfaces. The bottom line is that simply removing and replacing damaged shingles in the area appearing to need repair does not necessarily return the roof's functionality or service life. Asphalt-composition shingles are essentially separate pieces that are interwoven into a

Chad T. Williams, PE, PO Box 783 Jenks, OK 74037, 855-918-5111, chad.williams@valorfes.com

mat of material that overlays and protects the roof from the natural elements. Each shingle relies on and, in turn, supports the integrity of the surrounding shingles. Therefore, the roof must be evaluated as a system — not just as individual shingles.

Since asphalt composite shingles overlap and interweave into each other, the removal of a single shingle requires that several surrounding shingles also be disturbed and or disengaged in order to accomplish a repair. When the shingles are new, they are flexible and pliant. However, as they age, they lose elasticity and become more brittle and prone to cracking when stressed. In these situations, a more extensive repair is usually necessary to increase the integration area between the old and new material in order to assure a proper, secure connection and overlay. **Figure 1** provides a visual example that demonstrates the results of a failed asphalt-composition shingle repair. In this example, the new material was not properly integrated with the existing shingles. In addition, the older shingles had lost their pliability; therefore, the stress of the repair caused extensive cracking and breakage, resulting in a failure at the junction between the old and new shingles.

Depending on the integrity of the existing roofing system and materials, it may not be feasible or possible to execute a localized repair. As discussed above, asphalt-composition shingles will degrade with time. In addition, depending on the location of the shingles on the roof, it has been observed that certain areas of shingles will degrade at different rates. For example, south-facing areas of the roof experience higher ultraviolet exposure, while north-facing sections may experience a higher wind or ice load. Therefore, prior to executing repairs, it may be necessary to delineate the unique conditions of the shingles based on their location in the overall roof system.

Figure 1
Failure of shingles along the perimeter of a previous repair. This represents a typical result of a nondurable and unreliable repair to a three-tab-style asphalt-composition shingle roof surface.

Common Construction and Types of Asphalt-Composition Shingles

Asphalt-composition shingles are generically constructed with a fiberglass mat that serves as the structural backing or support for the shingle. Older shingles may include mats made of organic fibers or other materials The next layer surrounding the core is an asphalt mix. The primary purpose of this layer is to prevent water incursion. It coats the fiberglass core and provides a layer of waterproofing protection on the upper and lower side of the fiberglass. This mix is typically made of a bituminous material similar to that used in asphalt road construction.

The topmost layer typically consists of ceramic covered granules that are overlaid on an adhesive mix and then pressed into the asphalt mix (**Figure 2**). The ceramic coating is designed to protect the granule's mineral core and prevent it from degrading. These granules not only provide vital protection to the asphalt mix against the sun's ultraviolet radiation, but they also reflect the sun's light away from the roof, thereby decreasing the temperature of the roof and the spaces below it (**Figure 3**).

Asphalt-composition shingles are primarily manufactured in two distinct styles: the "three-tab" style and the "laminate-style" (also often referred to as "architectural" or "dimensional"). Certain manufacturers may have additional styles boasting additional thickness or

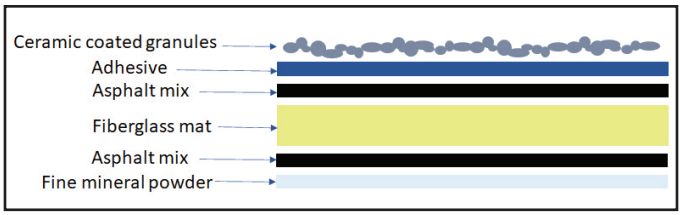

Figure 2
Generic construction of an asphalt-composite shingle.

Figure 3
Magnified view of shingle granules.

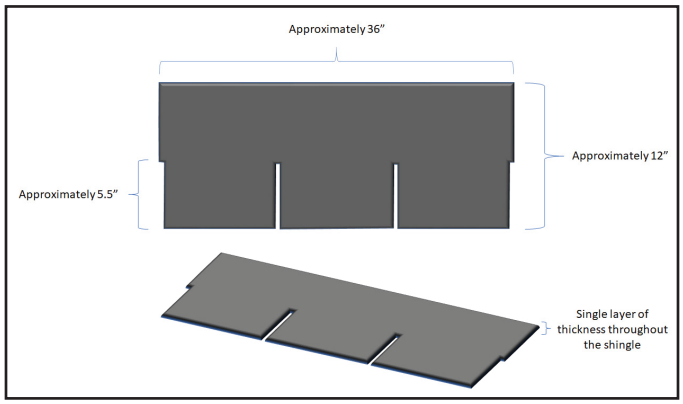

Figure 4
Typical three-tab style asphalt-composition shingle construction and dimensions.

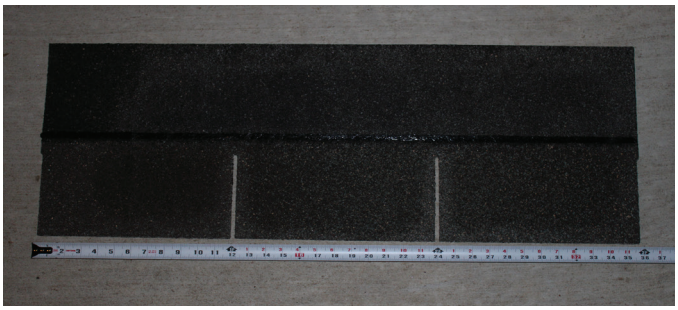

Figure 5
Photograph of a typical three-tab style asphalt-composition shingle.

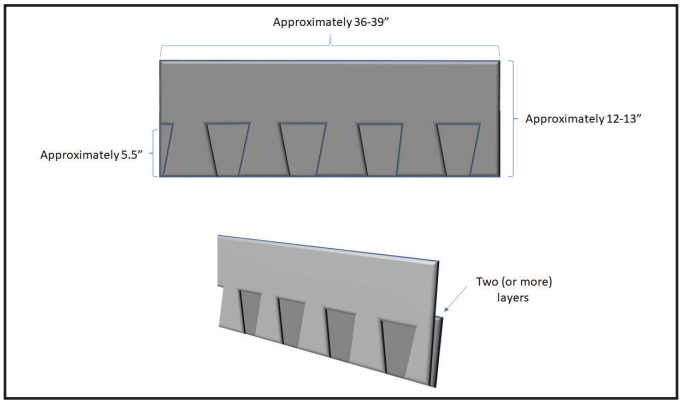

Figure 6
Typical laminate style asphalt-composition shingle construction and dimensions.

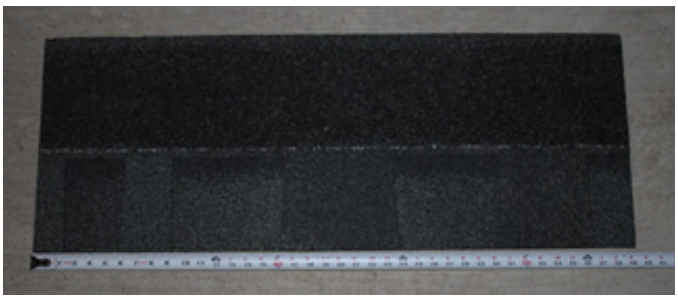

Figure 7
Photograph of a typical laminate-style asphalt-composition shingle

layers; however, the focus of this paper is on these two types, which are used predominantly throughout the industry.

Three-tab-style shingles are constructed of a single layer of the matrix of materials depicted in **Figure 2**. This type of shingle is approximately 36 in. long by 12 in. wide (although sizes may vary slightly by manufacturer). The top half of the shingle is solid, and the bottom half has three cutouts or "tabs" — hence the reason they are referred to as three-tab shingles (**Figures 4** and **5**).

Laminate shingles, on the other hand, are typically constructed of two or more layers of material. The top layer has a solid, uncut section on its top half with cutout tabs on the bottom portion. These tabs will vary in shape and width based on the aesthetic desire of the manufacturer. The bottom layer will be a solid piece with no cutouts. The top layer's tabs are then adhered to the bottom layer with an asphalt sealant to prevent movement and flexing during wind events (**Figures 6** and **7**). In some cases, manufacturers will have additional internal layers. These are usually for aesthetic purposes. For example, they will have a middle layer that also has cut out tabs of varying shapes and sizes that provide additional visual enhancements to the roof surface.

A very generic laydown for these types of shingles consists of an underlayment of plywood and roofing felt or other synthetic materials, with the asphalt-composite shingles being the topmost layer (**Figure 8**). It is important to note, however, that this underlayment will vary by region and manufacturer specifications. This paper will not address the specifications of the underlayment, as each layer in the roof structure has specific requirements based on the type of shingles being installed, geographic

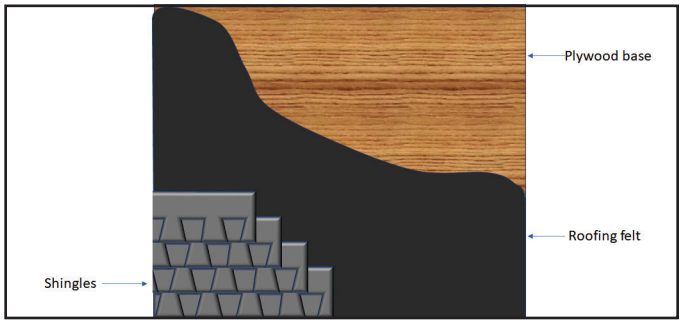

Figure 8
Example of a shingle and underlayment configuration.

location of the structure, material's location and purpose within the roof system, and other local or environmental considerations.

Shingles are typically attached to a roof substructure by galvanized steel nails, with 1¼ in. being one of the more common sizes. Again, the size and type of nail may vary by manufacturer and other considerations. However, the nailing process is an important factor in the performance and life expectancy of the shingles. Some of the more common issues associated with the nailing of shingles are:

- *Over-driven nails* — A nail is over-driven when it is hit too hard and is driven too far into or even through the shingle. The obvious issue in this situation is that it leaves a gap around the nail where water can now migrate through.

- *Using the correct number of nails per shingle* — Depending on the manufacturer and the climate the roof will be in, there is a specified number of nails that should be used. This can range from about four to six nails per shingle, with more nails being required in areas that experience higher wind loads.

- *Incorrect nail placement* — Not only do manufacturers specify the number of nails that should be used, but they also have specific locations designated on their shingles for placing these nails. Usually, there is some type of marking on the shingle that highlights this location. **Figure 9** is an example of a laminate shingle where the manufacturer used white lines to indicate the boundaries in which the nails should be placed. Typically, this marked nail strip location is also where all the layers of the shingle merge. Therefore, nails that are errantly placed above the top line or below the bottom line may result in lower shingle performance, as they are subject to tearing or the nails being over-driven.

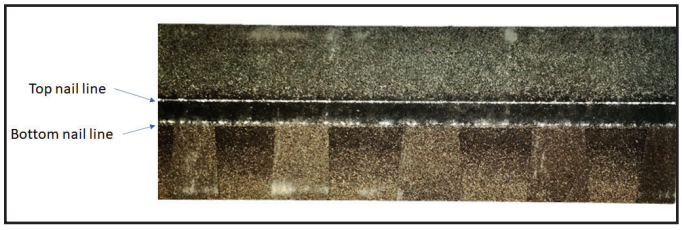

Figure 9
Nail location for a typical laminate asphalt-composite shingle.

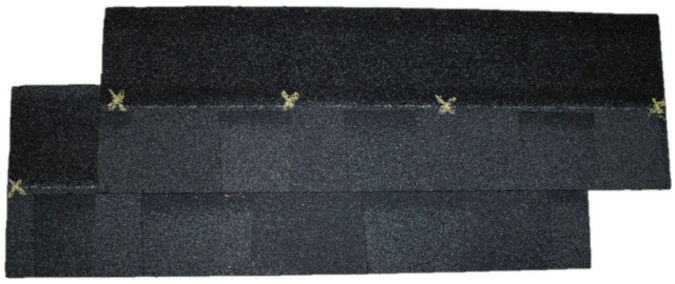

Figure 10
Typical shingle overlap, indicating the nail placement.

Due to how shingles are overlaid on top of each other during installation, individual shingles will also have a second set of nails that is above the nail strip of the underlying shingle. An example highlighting this is demonstrated in **Figure 10**. Here the "x"s on the top shingle mark nail locations within the shingle's nailing strip. These nails will also penetrate the top portion of the underlying shingle, thereby enhancing the overall strength of the shingle matrix.

Review of Historical Methods Used to Determine Repairability

In order to decide if a repair is even possible, the first challenge of a repair/replace decision is to establish the condition of the remaining or existing shingles. Asphalt-composition shingles typically have their greatest flexibility when they are new and ready to be applied to a roof surface. Over time, the asphalt within the shingles age and degrade, resulting in the individual shingles becoming less flexible. In addition, the seal strips located along the lower edges of the shingles also tend to weaken over time (**Figure 11**). As mentioned at the beginning of this paper, the natural aging of the shingles increases the potential for additional damage during repair or maintenance activities. The challenge then becomes determining whether the roof must be completely replaced or if it is possible to repair only the damaged areas.

The roofing industry has relied on a number of different methods to determine asphalt-composition shingle

Figure 11
Typical seal strip location on the back side of a laminate asphalt-composite shingle.

condition. However, these historical investigative methods are subjective and lack a consistent method for guiding repair versus replacement determinations. This inconsistency leads to improper roof repairs, failed repairs, repairs that potentially further compromise the roofing system, or the need for future repairs resulting from the damage created by the original repair itself.

One of the more common methods employed examines the pliability or brittleness of the existing shingles. Known colloquially as the "brittle test," this involves the evaluator observing and documenting the ability of the existing shingle to bend with or without further damage (e.g., cracking or breaking). Another method evaluates the cost benefits of repair versus replacement. (e.g., the "DURA" formula). Finally, other methods may use mathematical calculations, models, or even internal company-based policies or methods. Some of these techniques are described in further detail below. Upon review, it is easy to see the challenges these methods present when using them to make reliable and repeatable repair determinations.

Brittle Test Method

The "brittle test" was originally developed as a method for determining whether three-tab shingles had enough flexibility to allow for replacement and repair without cracking or breaking. There is no known or industry-accepted standard for how the "brittle test" should be conducted. As such, it is subject to variation, depending on the personnel conducting the assessment.

In general, the brittle test begins with the unsealing of the seal strip along the lower edge of a shingle tab. The shingle tab is then lifted to an angle between 45 degrees or 90 degrees, relative to the roof deck. In some cases, this lifting of the tab is repeated several cycles. Failure is commonly identified by the displacement of granules where the tab creases, cracks, or breaks.

Aside from the lack of a standardized industry protocol for executing this test method, other complaints include its expanded use on laminate-style asphalt-composition shingles for which it was not intended and its evaluation of only the shingle bending and not the entire repair process.

Economic Feasibility Method

The economic feasibility of repairing shingles versus replacing roof slopes has historically been determined using mathematical equations and/or models. In these types of assessments, the cost of repairs is factored in as part of the repairability consideration. One of the most common variants of this method is the "repair cost formula" presented in the "Protocol for Assessment of Hail Damaged Roofing" paper by Tim Marshall and Richard Herzog[2]. Commonly referred to as the "DURA" equation, this method attempts to estimate the potential cost of a repair by multiplying a unit price variable to an area of existing shingle damage and then applying a weighting factor. The equation is:

$RC = D \times U \times R \times A$ where:

RC = The cost to repair the entire slope (in dollars)

D = The number of damaged shingles or shakes per roofing square

U = The unit cost to repair a shingle or shake (in dollars)

R = The repair difficulty factor

A = The actual area of the slope (in roofing squares)

Note: A "roofing square" is equal to 100 square feet.

The weighting factor (R) is an attempt to quantify how difficult a roofing repair would be to implement. Marshall and Herzog provide the following guidance in selecting a value for "R":

"The repair difficulty factor is based on the age and condition of the roofing and is assigned values ranging from 1 to 2. Roof coverings in good, fair, or poor condition can be assigned repair difficulty factors 1, 1.5, and 2, respectively, which effectively adjusts the unit cost of repair. The repair difficulty factor considers that roof coverings become brittle with age and are broken more easily during the repair process; therefore, difficulty factors of 1.5 or 2 account for the additional breakage that may occur or extra care needed in the repair process. The repair difficulty factor is a subjective determination based on the inspector's experience in assessing and/or repairing roofs."

By including this variable in the calculation, it provides evaluators with a means to adjust the cost based on the potential ease or difficulty a repair might entail. However, the variable is somewhat subjective and open to interpretation by the evaluator. A lack of specific parameters to determine what values should be used for R has led to disagreements about the validity of the formula in evaluating a roof repair. In addition, there is a lack of consensus

in the industry as to whether the maximum value of 2 for R can provide a sufficient enough weighting factor to capture extremely challenging or deteriorated conditions. Finally, the value for "D" is calculated based on a roofing section selected by the evaluator. While Marshall and Herzog provide guidance on how these areas should be selected, it is still up to the evaluator on what part of the roof they choose to use for this part of the calculation. So, while the DURA formula attempts to inject a quantitative means to measure a roofing condition, it still is affected by subjectivity and individual interpretations.

Shingle Age Method

Another common approach for determining the repairability of asphalt-composition shingles is based on the "age" of the shingles (i.e., the length of time since their original installation). The assumption is that an older shingle will be more difficult to repair due to its deterioration and fragility.

As with the brittle test, this method also lacks standardized protocols. In this situation, however, there is no consistent means to identify at what age a shingle can or should no longer be repaired. Additionally, this method makes the erroneous assumption that younger shingles are less susceptible to damage. While this may be true for the shingle material itself, the problem is that the sealant on the backside of the shingle (**Figure 11**) that secures the top shingle to the one beneath it is quite robust on newer shingles. Therefore, when shingles are "unsealed" or pried apart during a repair, this bonded strength can override the latent strength of the shingle material, resulting in tears and chipping. This can exacerbate damage to the roof's shingles as repair actions propagate new damage on adjacent shingles during the process.

Repairability Assessment Method

To address the concerns and limitations presented with other assessment methods, it is necessary to develop a protocol that reduces the subjectivity inherent in those methods. While subjectivity will always be a factor when humans are required to exercise any sort of evaluation, there are ways to minimize its overall impact on the final results. The repairability assessment method was developed to help reduce this subjectivity by expanding the scope of the assessment to include the evaluation of repair actions.

As discussed previously, the removal and replacement of an asphalt-composition shingle has the potential to directly damage the surrounding shingles. For example,

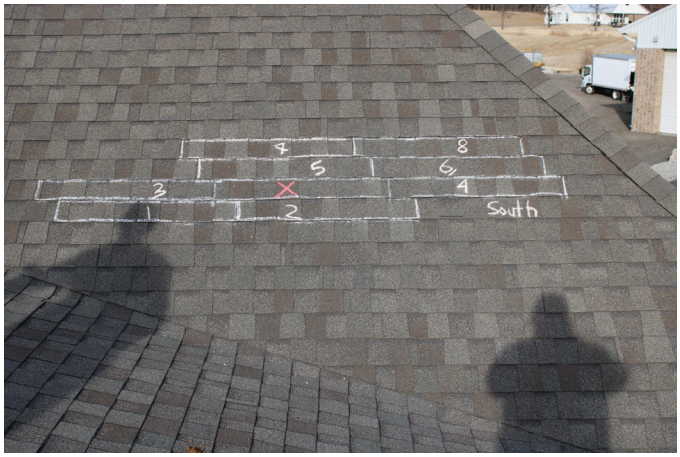

Figure 12
Outline of the primary damage assessment area.

in **Figure 12**, the shingle marked with an "X" represents a single damaged shingle. In order to remove and replace this shingle, approximately eight other shingles surrounding this one would be impacted.

- The sealant on the bottom of the damaged shingle, "X," is adhering to the top surfaces of shingles 1 and 2. Therefore, there is potential to damage shingles 1 and 2 as the sealant is pried open in order to loosen the bottom edge of the damaged shingle.

- Conversely, the same thing exists for shingles 5 and 6, except in this case the sealant strip on the bottom edges of these shingles is bound to the top surface of shingle "X." Again, there is potential to damage these shingles when prying the sealant loose.

- Because of the nailing pattern previously discussed (**Figure 10**), the underlying shingles, 1 and 2, would be subjected to additional damage during the nail removal process. In these cases, the nail often strips through the shingle material, leaving tears and unsealed holes.

- The nails placed in the nail strip area of shingles of 5 and 6 also go through shingle "X" and therefore also require removal. Again, there is potential for damaging these shingles when removing these nails.

- In order to access the nailing strips of shingles 5 and 6, the bottom sealed edges of shingles 7 and 8 must also be pried loose.

- Finally, shingles 3 and 4 are also susceptible to damage, resulting from the unsealing of the seal strips for shingles 5 and 6 above.

This example highlights the potential cascading repair effects and why it is important to take into consideration the possible damage that might be imparted upon these adjacent shingles during the repair. The repairability assessment method offers a means by which these outlying shingles are integrated into the evaluation. By taking into consideration the amount and type of damage caused to these surrounding shingles, the evaluator is able to get a measurable sense of the impact the repair process may have on the overall roof's surface. One note of caution, however. The repairability assessment is intended to supplement a damage assessment of these surfaces and is not to be used in place of a conventional damage evaluation. Only by conducting a damage assessment will the evaluator be able to confirm existence of actual wind, hail, or other damage to the roof surface to know if a repair assessment is necessary.

It is important to note that because of construction inconsistencies during the initial installation of the original shingles, there may, in fact, be damage that extends beyond the eight shingles used in this example. Therefore, while not specifically part of the repairability assessment process, the condition of the shingles around the assessment area or areas of recent repairs should also be visually evaluated and documented.

Repairability Assessment Procedures

The following sections provide details on conducting a repairability assessment. While the emphasis of the discussions primarily focuses on the technical aspects of conducting the assessment, practical considerations are offered as well to provide additional context when appropriate.

Initiating the Assessment

There are eight shingles that constitute the primary damage assessment area and form the basis of the repairability assessment (**Figure 12**). These shingles are specifically selected to capture the potential impact of repair actions. As outlined in the previous section, each of these eight shingles must be disturbed in order to remove a damaged shingle.

Since the repairability assessment is designed to simulate the conditions that would occur during the repair process, the location of the test area should be established on a section of the roof that is most representative of where the repairs are to be performed. In addition, as this assessment involves the removal and replacement of individual shingles, it should be obvious that this may potentially undermine the existing integrity of the roof in that area. Therefore, the evaluator should first obtain the approval of the building owner prior to conducting the assessment and have the ability and materials available to complete a larger repair — or, if necessary, have the means to temporarily tarp the roof.

The repairability assessment method should be performed in the months when normal roofing construction activities are usually conducted, such as late spring, summer, and early fall. Performing a repairability assessment "off season" risks providing an inaccurate perspective of the shingle's ability to withstand repair actions. For example, shingles tested during the cold weather may prove to be more fragile than if the same assessment was conducted during warmer months when the repair might actually be performed. However, there are situations that may occur that drive such an assessment to be performed off season. In these cases, the assessment should be conducted under conditions that mirror the potential repair activity.

Roles and Responsibilities of Repairability Assessment Personnel

The repairability assessment typically requires the minimum participation of two personnel. It includes a licensed and insured roofing contractor (per state requirements as applicable) to remove and replace the individual shingles in a careful and workmanlike manner and an independent and knowledgeable evaluator, such as a qualified forensic engineer (licensed in the state in which the building is located). The roofing contractor selected to assist with the repairability assessment should be independent and not under contract for the repair or replacement of the shingle roof surfaces if possible.

Repairability Assessment Weather Conditions

As previously mentioned, removal and replacement of asphalt-composition shingles are ideally undertaken in environmental conditions that allow the shingle to flex without damage during the assessment and subsequent repair. Therefore, air temperatures should be between 40ºF and 90ºF. While the lower temperatures are not ideal when performing a repairability assessment, the 40-degree lower threshold is based on the minimum temperatures commonly present in manufacturer installation instructions. During periods of cooler weather, it is recommended that the shingles to be used for the assessment are on roof slopes that have been exposed directly to sunlight for at least two hours.

The 90ºF upper limit is also based on manufacturer recommendations regarding the maximum temperature for installing asphalt-composition shingles. This higher threshold is due to the potential for marring of the shingles. As shingles soften with the increase in temperature, they become more susceptible to scratches, dents, or the sliding or moving of granules on the shingles' surface. This type of damage can happen when the roof is walked upon or tools/other equipment are placed on the softened shingles. Evaluators should take care during these higher temperatures to avoid further damaging the roof beyond what is necessary as part of the repairability assessment.

For safety of the evaluators — and to minimize unnecessary damage to the roof and shingles — the following additional weather considerations should be followed:

1. Conduct assessments during weather without an immediate forecast of precipitation. This is done in order to avoid slippery conditions and the potential to expose the roofing underlayment to rain during the assessment.

2. Ensure that the roof surfaces are dry at the time of the assessment. Again, this is to protect the evaluator and any other personnel from slippery conditions and potential falls.

3. Wind gusts should be less than 25 miles per hour. This is a typical safety measure taken by industry roofers and personnel working on exposed, elevated surfaces.

Repairability Assessment Shingle Selection Criteria

When conducting a repairability assessment, it is important to select an appropriately representative area for laying out the primary damage assessment area. This area should be centered away from edges and protuberances as much as possible, located in an area of the roof that is safe to access, and minimize the impact on the outlying shingles (e.g., walking, ladder marks, unnecessary tool marks, etc.). The subject shingle for the repairability assessment, marked as an "X" in **Figure 11**, should meet the following criteria:

1. It should be of full length and uncut.

2. Be at least two rows above any eaves.

3. Be at least a full shingle length from any rakes or hips.

4. Be at least a full shingle length away from valleys.

5. It must not contain any vents, structural irregularities, or other roof appurtenances within the primary damage assessment area.

6. It should be in an area that is representative of the overall roof (i.e., not sheltered by trees, other roof surfaces, or building elements that would alter the natural weathering of the roof surfaces).

When possible, the repairability assessment should be performed on shingles where wind and/or hail damage has already been identified. In cases where it is not possible to utilize storm damaged shingles, the testing should be performed on the slopes where damage has been identified. If the roof surfaces include shingles of different types, styles, manufacturers, or dates of manufacture or installation, it will be necessary to perform a repairability assessment for each type of damaged shingle.

Protocol for Conducting the Repairability Assessment

Once the location of the primary damage assessment area has been identified, the following steps outline the process to be undertaken when conducting the repairability assessment. **Figure 13** provides an expanded shingle layout of the primary damage assessment area. In this graphic, the shingles are drawn unlayered to aid in identifying the specific shingles used in this process.

1. The first step is to mark the subject assessment shingle. This is the individual shingle to be removed and replaced as part of the repairability assessment. **Figure 12** has denoted this shingle with an "X" and pink outline. In some cases, more than one shingle can be used, depending on the area required to perform the assessment. However, for clarity, the steps and process provided below will use the layout described above.

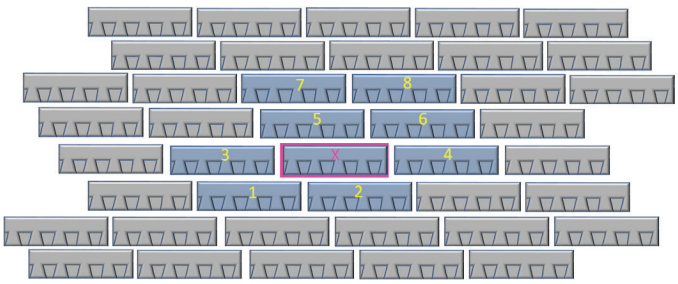

Figure 13
Expanded, unlayered perspective of the shingles to be used in the primary damage assessment area.

2. Mark and number the other eight perimeter shingles used in the primary damage assessment area following the location and numbering sequence provided in **Figure 13**. For clarity, the markings for shingle X should be distinctive from the other eight perimeter shingles. For example, in **Figure 13**, shingle X is marked using pink while the perimeter shingles are numbered in yellow. The specific choice of colors is not important. The only imperative is that the colors and markings must be distinguishable from one another in photographs and video. Once the markings and outlines are complete, digital images of the entire primary damage assessment area should be taken.

3. Any preexisting damage to the asphalt-composition shingles in the primary damage assessment area should be marked and documented with digital images. While the method for marking or highlighting damage can vary from one evaluator to another, it is important to provide a legend or reference that explains the markings used for that particular investigation. Additionally, since the existing damage should be easily distinguishable from the damage caused during the assessment, it is wise to select distinguishing colors for each type of damage (e.g., pre-assessment versus post-assessment damage).

4. Use a flat pry bar, crowbar, "five-in-one" painter tool (or similar) to gently pry open the seal strips securing shingle X in order to access its nails or fasteners. Document any damage (e.g., splits. cracks, tears, etc.) to the eight-perimeter shingles resulting from this action. Also document the condition of the seal strips as well as the condition of the shingles and fasteners where the shingles have pulled past the original nail head or shaft.

5. Again, using a flat pry bar (or similar tool), remove the nails, securing both the middle of shingle X as well as the nails in the middle of shingles 5 and 6 that are also penetrating through the top of shingle X (i.e., the mid nails on the far right of shingle 6 will not need to be removed since they do not penetrate through shingle X). Once both rows of nails securing shingle X have been removed, shingle X can then be removed.

6. Visually assess the condition of all the shingles within the primary damage assessment area for damage. Any shingle that sustained damage as part of the removal actions of shingle X must be appropriately marked. The shingle on which the damage occurred will then have the number stricken through for tracking purposes. It is important to note that preexisting damage to the shingles that was annotated and marked as part of Step 3 above is excluded; only the additional damage sustained during the repairability assessment determines if the shingle's number is crossed out.

7. While shingle X is removed, visually assess the exposed underlayment (e.g., roofing felt, moisture barrier, etc.) for indications of damage resulting from the removal process. Document and record any findings.

8. A new asphalt-composition shingle (compliant with the manufacturer's instructions) should then be inserted and secured. The new shingle X will first require a series of nails in the manufacturer specified nail strip. Next, shingles 5 and 6 will need to be secured with nails in their nail strip area as well. The nails from this action should also penetrate through the top portion of the new shingle X. In addition, it will likely be necessary to supplement the now weakened seal strips on all the disturbed shingles with additional adhesives. Follow the guidance and instructions of the shingle manufacturer when applying these adhesives. Finally, ensure all surfaces are properly and adequately re-secured.

9. Any additional damage that occurs during the installation of the new asphalt-composition shingle and the placement of the fasteners should be documented. Again, as noted in step 6 above, if a shingle sustains damage during this process, cross out the shingle number for tracking purposes. If it was already crossed out, then no additional action is required.

10. Of the eight perimeter shingles, count the number of shingles where the number was stricken through or crossed out. This is the total number of shingles that were damaged as a result of the removal and replacement process.

Damage to shingles is reported on a "per shingle" basis, regardless of the types of damage present or the number of times that specific type of damage occurs. The

Figure 14
View of a narrow tear along the bottom edge of an asphalt-composition shingle.

Figure 15
View of a tear along the bottom edge of an asphalt-composition shingle.

Figure 16
Shingle pulled past the nail head during the repairability assessment.

subject assessment shingle (i.e., shingle "X") is already considered to be damaged. Therefore, any additional damage to this shingle from the assessment process is excluded from the assessment count. An evaluator may find damage to the subject assessment shingle resulting from the repairability assessment noteworthy. In these cases, the damage may be documented and reported; however, this damage will not alter the resulting damage calculations.

As part of the damage assessment process, the evaluator may deem it necessary to remove a shingle for identification purposes. The subject assessment shingle removed as part of the repairability assessment may be retained or otherwise documented to assist with separate identification processes.

Reporting Repairability Assessment Findings

Damage to the asphalt-composition shingles within the primary damage assessment area resulting from the repairability assessment process is reported as follows:

1. The damage rate provides a single-digit, whole number that represents the number of shingles damaged in the assessment. This value will be from 0 to 8.

2. The damage ratio is the damage rate divided by the total number of shingles used in the primary damage assessment area (not including the subject assessment shingle). For example, the damage ratio would be presented as "1 to 8" for a situation — where one shingle was damaged during repairability assessment and eight shingles were located within the primary damage assessment area.

Common Types of Damage to Asphalt-Composition Shingles

The potential for damage to the shingles within the primary damage assessment area is usually associated with the necessary breaking of the seal strips and the removal/replacement of fasteners. Damage will commonly present as tears, gouges, holes, or chipping. In some cases, the sealant will strip away the underlying shingle's granules and asphalt binder, leaving the fiberglass mat exposed.

The following list outlines a variety of types of damage often seen as part of a repairability assessment. It is not an exhaustive list, and other types of damage may be seen.

1. Tearing or cracking of the asphalt-composition shingles (**Figures 14** and **15**).

2. Pulling of a shingle past the nail head or fastener resulting in a hole or tear. (**Figure 16**).

3. Hinging or fracturing of the granule surface. In some cases, the fracture may extend into or through the asphalt binder or fiberglass mat.

4. The displacement or stripping of granules and binder, resulting in exposed fiberglass mat of either the overlying or underlying shingle (**Figures 17** and **18**).

5. The chipping of a shingle as pieces of it remain bonded to the surface of an underlying or overlying shingle (**Figure 19**).

6. Impact damage to the lower edges or sides of shingles resulting from the placement of the new nails. Since the shingle no longer has the flexibility to be lifted out of the way in order to have the new nails inserted, the hammer cannot get the clearance it needs to set the nails. The supporting roofing contractor should take extra care in these situations to limit the potential for this type of damage while replacing the test subject's assessment shingle.

7. Laminate-style shingles may also experience delamination between the top cut sheet and the lower continual sheet. This separation of sheets on a multi-sheet shingle should also be noted on a repairability assessment as either preexisting damage or damage resulting from the assessment process.

Repairability Assessment Findings and Damage Propagation

A roof surface is considered to be repairable when individual damaged shingles can be removed and replaced without causing additional damage to the surrounding shingles. However, when adjacent shingles are weakened or unable to maintain their integrity during the repair action, it is likely that any subsequent repairs to fix these newly damaged shingles will result in a continued propagation of damage. **Figure 20** shows an 8-ft by 8-ft demonstration area that underscores this repair issue.

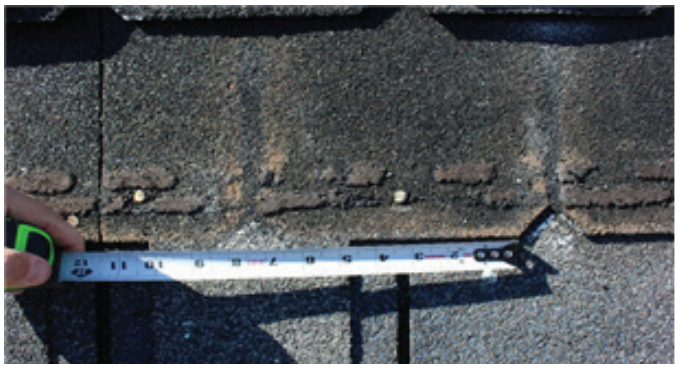

Figure 17
Transfer and accumulation of asphalt from the overlying shingle.

Figure 18
Displaced sections of granules at the lower seal strip. In this case, the granules and binder asphalts were transferred to the overlying shingle.

Figure 19
Shingles torn, and sections remained bonded to the underlying shingle.

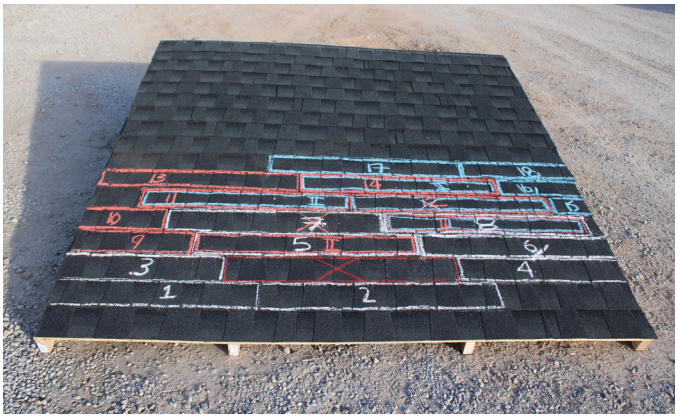

Figure 20
Initial area of influence located within a demonstration roof section.

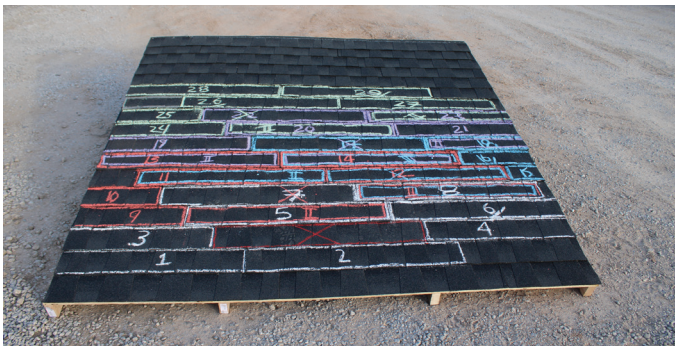

Figure 21
Fifth iteration highlighted with green chalk.

In this example, the shingle marked with a red "X" demonstrates a shingle undergoing a repair by replacement, and the shingles outlined in white represent the area of influence for this repair. In this case, assume that shingle 7 was damaged during the repair process. The damage rate would be "1," and the damage ratio would be "1 to 8." While a 1 to 8 damage ratio sounds nominal, it has the potential to cascade. Since shingle 7 was damaged during the repair process of shingle X, it must now also be replaced. Thus, the repair process must now be repeated and moves into its second iteration.

This iterative repair process will continue to potentially damage additional shingles with each follow-on repair. Continuing with the 1 to 8 damage ratio, **Figure 21** shows an enlarging area of influence after five iterations of repair. The colors indicating the specific iterations are as follows:

1) Iteration 1 – White

2) Iteration 2 – Orange

3) Iteration 3 – Blue

4) Iteration 4 – Purple

5) Iteration 5 – Green

At the completion of the fifth repair iteration, 29 shingles have been disturbed, and five additional shingles have been damaged. Additionally, several times throughout these series of repairs, certain shingles were disturbed two or more times, resulting in a higher potential of damage to those shingles.

Additional Factors Limiting the Repairability of Asphalt-Composition Shingles

Aside from the ability to adequately conduct a repair, there are other considerations that need to be taken into account when deciding if a roof can be repaired. While these factors may or may not affect the performance of the repair, they are, nonetheless, important aspects that can ultimately impact an evaluator's repairability decision.

- *Material obsolescence* — Manufacturers must continue to make changes to their shingle inventory. These types of changes include altering shingles' sizes and shapes. Older roofs, therefore, may have shingles that are no longer being manufactured and thus can no longer be replaced in kind.

- *Visual incompatibility* — In these cases, the roofing color or style can no longer be matched. For example, a faded roof with new shingle patches will likely have a color mismatch and be aesthetically undesirable.

- *Manufacturing defects* — Over the years, there have been a number of recalls on asphalt-composition shingles. Typical problems include, but are not limited to, premature cracking, curling, loss of granule, failed seal strips, and thermal splitting. The reason for the failures can stem from a number of causes; substandard source material, improper construction, or logistics and storage issues.

- *Installation errors* — Typically, these types of errors include not following manufacturer's installation recommendations, not applying proper underlayment materials or techniques, not using the correct type or number of fasteners, not placing fasteners in the correct area of the shingle, etc.

- *History of previous repairs* — Previous repairs can be an indication of an underlying problem, or because of improper actions or materials be a source of water incursion.

- *Deterioration related to age or materials* (e.g., deterioration of the asphalt binder) — Weather, sunlight, shade, and trees can accelerate the deterioration of the shingles and shorten their lifespan.

- *The presence of roof vents, turbines, solar panels, or other devices* — These types of appurtenances have the potential to undermine the shingle system by permitting water incursion through poorly formed flanges or seals.

- Code or manufacturer installation requirements may have changed, or there may be defects found in the roof decking, ventilation, etc. (e.g., existing roof decking may not be acceptable for the installation of new shingles). This most commonly occurs for plank decking.

While beyond the scope of this paper, these considerations and others may be relevant in the broader determination of the repairability of asphalt-composition shingles. The licensed professional engineer responsible for making the recommendations will need to consider such additional factors in concert with the results of the repairability assessment.

Determining a Repairability Assessment Score

The decision to repair or replace asphalt-compositions shingles using the repairability assessment method is based on the conditions of the roof as observed during the damage assessment survey, and the damage rate resulting from the repairability assessment. **Figure 22** provides a guide for calculating the total repairability assessment score. In the

REPAIRABILITY ASSESSMENT SUMMARY

GENERAL CONDITIONS BY TYPE	Not Present (0 pts)	Present (1 pt/Condition)	Limiting (2 pts/Condition)
Deterioration Related to Age/Materials			
Installation Errors [1]			
History of Previous Repairs			
Manufacturing Defects			
Material Obsolesce (due to size)			
Visual Incompatibility			
TOTAL:	**0**	**0**	**0**

DAMAGE RATE [2]

Number of shingles damaged during field replacement efforts (1-Point per damaged shingle)	**0**

TOTAL REPAIRABILTY ASSESSMENT [3]	**0**

0-2: Localized repair may be feasible depending on the overall conditions present and the availability of suitable and compatible materials.
2-4: Repairability is limited but may be feasible on a case by case situation depending on the availability of suitable and compatible materials.
4 or More: Repairability is limited and localized repair is not recommended.

Notes:
1 - The following provides a guide on scoring for this
Present - Installation errors present to 0 to 10% of shingles
Limiting - Installation errors present to more than 10% of shingles
2 - Based on the removal and replacement of a test shingle.
3 - Sum of "General Conditions" and "Damage Rate".

Figure 22
Repairability assessment calculation guide.

top portion of the guide, the evaluator will enter the roof's condition data. This data comes from the evaluator's visual inspection of the roofing surface and shingles. For this part of the calculation the evaluator will identify the appropriate category for each condition. It is divided into three damage categories: not present, present, and limiting. If a condition is not present, a "0" (zero) will be entered into the field. Only the deterioration and installation conditions offer the option for the evaluator to assess the condition as being "present." Finally, for conditions being assessed as a damage category of "limited," the evaluator will place a "2" in the corresponding field. These values are then totaled and added to the repairability assessment's damage rate.

Total repairability assessment values between 0 and 2 indicate that local repairs may be feasible, keeping in mind the potential for repair damage propagation. Total values falling between 2 and 4 may be possible on a case by case basis, depending on the availability of suitable and compatible materials. Total values of 4 and higher indicate that the ability to repair the roof is limited, and a localized repair is not recommended.

Conclusion

Historically, methods used to evaluate whether localized shingle repairs can be successfully and adequately performed have been done using a variety of approaches that rely on inconsistent and subjective analysis. This paper offers an alternative approach: the repairability assessment method.

It provides an improved process for analyzing whether an asphalt-composition shingle roof can be effectively repaired by taking into consideration the possible impacts the repair actions will have on the surrounding shingles. Evaluators using this method are able to track and report any damage as a total repairability assessment score that is based on the condition of the roof and shingle and repairability damage rate. Together, these values provide a quantitative and repeatable means to measure the potential for shingle damage to be propagated as a result of the repair process. While no processes that depend on human intervention or observations are infallible, when compared to other historical methods used to determine whether an asphalt-composition shingle roof is repairable or not, the repairability assessment method offers the most comprehensive physical assessment method to date.

Definitions

Area of influence — shingles requiring repair and their immediate, adjacent shingles.

Damage rate — the number of shingles damaged during a repairability assessment in the primary damage assessment area. The value will be 0 to 8.

Damage ratio — the damage rate divided by 8 (the total number of shingles evaluated for damage in the primary damage assessment area). It is reported as "(damage rate) to 8."

Evaluator — Licensed professional engineer conducting the repairability assessment.

Primary damage assessment area — The nine shingles used in a repairability assessment.

Subject assessment shingle — The shingle that will be replaced as part of the repairability assessment and is the center most shingle in the primary damage assessment area.

References

1. Aon, "Weather, Climate & Catastrophe Insight: 2019 Annual Report", p 27, 2020.

2. T. P. Marshall and R. F. Herzog, "Protocol for Assessment of Hail-Damaged Roofing," Proceedings of the North America Conference on Roofing Technology, p 40-46, 1999.